UNIVERSIDADE DE SANTIAGO DE COMPOSTELA

DEPARTAMENTO DE ENXEÑARÍA QUÍMICA

Bioenergetics-based modelling of microbial ecosystems for biotechnological applications

Memoria presentada por

Rebeca González Cabaleiro

Para optar ó grado de Doutor pola
Universidade de Santiago de Compostela

Santiago de Compostela, abril de 2015

USC
UNIVERSIDADE
DE SANTIAGO
DE COMPOSTELA

UNIVERSIDADE DE SANTIAGO DE COMPOSTELA

DEPARTAMENTO DE ENXEÑARÍA QUÍMICA

Bioenergetics-based modelling of microbial ecosystems for biotechnological applications

Rebeca González Cabaleiro

Santiago de Compostela

Abril 2015

USC
UNIVERSIDADE
DE SANTIAGO
DE COMPOSTELA

UNIVERSIDADE DE SANTIAGO DE COMPOSTELA

DEPARTAMENTO DE ENXEÑARÍA QUÍMICA

Don Juan M. Lema Rodicio, Catedrático de Enxeñaría Química da Universidade de Santiago de Compostela e Don Jorge Rodríguez Rodríguez, Profesor Titular de Enxeñaría Química e Ambiental en Masdar Institute of Science and Technology (Abu Dhabi, UAE).

Informan:

Que a presente memoria titulada "*Bioenergetics-based modelling of microbial ecosystems for biotechnological applications*" presentada por Dona Rebeca González Cabaleiro, para optar ó grado de Doutor en Enxeñaría Química, Programa de Doutoramento en Enxeñaría Química e Ambiental, foi realizada baixo a nosa inmediata dirección no Departamento de Enxeñaría Química da Universidade de Santiago de Compostela.

E para que así conste, firman o presente informe en Santiago de Compostela, abril de 2015.

Juan M. Lema Rodicio

Jorge Rodríguez Rodríguez

USC
UNIVERSIDADE
DE SANTIAGO
DE COMPOSTELA

USC
UNIVERSIDADE
DE SANTIAGO
DE COMPOSTELA

Abstract

The bioenergetics analysis and mathematical modelling of several bioprocesses with industrial interest aiming for waste materials recovery, is conducted in this Thesis. The objective is to mechanistically understand the physical limits of the processes together with the ecological interactions established in their different microbial ecosystems. This new knowledge could lead towards an improvement of the bioprocesses control increasing their efficiency. Three mathematical models have been developed based on bioenergetics and minimizing the empirical information necessary.

Firstly, a novel metabolic energy-based model has been developed that accurately predicts the experimentally observed changes in product spectrum with pH variations when glucose is fermented in acidogenic conditions. The results are mechanistically explained analysing, under different environmental conditions, the impact that variable proton motive potential and active transport energy costs have in terms of energy harvest over products yielding.

Secondly, several bioenergetics analyses to investigate the potential reversibility of specific anaerobic pathways of interest (more reduced products yielding with higher energy density) have been developed. Thermodynamics of the different steps in biochemical pathways are analysed and combined with assumptions concerning kinetic and physiological constraints to evaluate if the pathways are potentially reversible by imposing changes in process conditions.

And thirdly, a last model is presented based on the assumption that mixed cultures are composed by undefined species competing for the energetic resources available and limited by the fundamental trade-off between yield and rate of energy harvest per unit of substrate. In this model, the competition between existing and non-experimentally reported microbial catabolic activities**,** is simulated. Successful ecological relations of competition or collaboration are predicted under the hypothesis of maximum energy harvest rate and in line with experimental observations.

Keywords: Bioenergetics; Thermodynamics; Microbial ecology; Bioprocesses; Anaerobic fermentation.

USC
UNIVERSIDADE
DE SANTIAGO
DE COMPOSTELA

Resumen

En esta Tesis se analizan y describen matemáticamente, utilizando conceptos de bioenergética, diferentes bioprocesos que fundamentalmente pretenden la recuperación de productos con mayor contenido energético a partir de residuos. El objetivo de este trabajo es generar nuevo conocimiento, investigando los límites de las biotecnologías estudiadas y las interacciones ecológicas entre los microorganismos responsables de las biotransformaciones consideradas. Pare ello se han desarrollado y validado tres modelos matemáticos todos ellos basados en conceptos de termodinámicos.

En primer lugar, se presenta un nuevo modelo que permite predecir la influencia del pH de operación sobre la distribución de productos generados en la fermentación anaerobia de glucosa. El modelo permite explicar los resultados experimentales obtenidos al modificar las condiciones operativas en el reactor en base a las variaciones de los costes energéticos debidos al transporte activo de productos a través de la membrana celular y a la fuerza protón motriz.

A continuación se presenta un análisis bioenergético de diversas rutas catabólicas anaerobias pretendiendo evaluar la posibilidad de revertir el sentido de estas rutas, con el objetivo de generar productos con una mayor densidad energética. Se parte de la hipótesis de que al tratarse de procesos que transcurren con una muy limitada variación de energía libre, puede ser viable conseguir un cambio de sentido de la reacción siempre y cuando se impongan las condiciones ambientales adecuadas.

Por último, se simula una competición hipotética entre especies que catalizan tanto reacciones observadas experimentalmente, como otras posibles aunque no observadas pero considerando rutas catabólicas conocidas. Este modelo permite predecir las actividades microbianas capaces de sobrevivir en ecosistemas particulares. Los resultados permiten explicar las observaciones experimentales, y concluir que los procesos catabólicos efectivos resultan ser aquellos que maximizan la velocidad de generación de energía para el crecimiento y el mantenimiento de la población microbiana.

Palabras clave: Bioenergética; Termodinámica; Ecología microbiana; Bioprocesos; Fermentación anaerobia.

USC
UNIVERSIDADE
DE SANTIAGO
DE COMPOSTELA

Resumo

Nesta Tese analízanse e descríbense matematicamente, utilizando conceptos de bioenerxética, diferentes bioprocesos que fundamentalmente pretenden a recuperación de produtos con maior contido enerxético a partir de residuos. O obxectivo de este traballo é xerar novo coñecemento, investigando os límites das biotecnoloxías estudadas e as iteracións ecolóxicas dos microorganismos responsables das biotranformacións consideradas. Para isto, nesta Tese desenroláronse e validáronse tres modelos matemáticos todos eles baseados en conceptos termodinámicos.

Nun primeiro lugar, preséntase un novo modelo que permite predicir a influencia do pH de operación sobre a distribución de produtos xerados na fermentación anaerobia de glicosa. O modelo permite explicar os resultados experimentais obtidos o modificar as condicións operativas no reactor en base as variacións dos custes enerxéticos debidos o trasporte activo de produtos a través da membrana celular e a forza protón motriz.

A continuación preséntase un análise bioenerxético de diversas rutas catabólicas anaerobias que pretende a avaliación da posibilidade de reverter o sentido destas rutas, perseguindo o obxectivo de xerar produtos cunha maior densidade enerxética. Pártese da hipótese de que ó tratarse de procesos que transcorren cunha moi limitada variación de enerxía libre, pode ser posible conseguir un cambio de sentido da reacción sempre que se impoñan as condicións ambientais adecuadas.

Por último, simúlase unha competición hipotética entre especies que catalizan tanto reaccións observadas experimentalmente, como outras posibles pero non observadas pero considerando rutas catabólicas coñecidas. Este modelo permite predicir as actividades microbianas capaces de sobrevivir en ecosistemas particulares. Os resultados permiten explicar as observacións experimentais, e concluír que os procesos catabólicos efectivos resultan ser aqueles que maximizan a velocidade de xeración de enerxía para o crecemento e o mantemento da poboación microbiana.

Palabras chave: Bioenerxética; Termodinámica; Ecoloxía microbiana; Bioprocesos; Fermentación anaerobia.

USC
UNIVERSIDADE
DE SANTIAGO
DE COMPOSTELA

Resumen extendido

La implementación de nuevos procesos industriales que permitan la recuperación de productos con valor añadido a partir de residuos, puede reducir el coste de su tratamiento y, a largo plazo, la dependencia de recursos no renovables. Mediante procesos biotecnológicos basados en cultivos mixtos o indefinidos (en los cuales no es posible cuantificar la biota en detalle) se puede conseguir la recuperación de productos de interés comercial a partir de residuos orgánicos complejos. El uso de cultivos mixtos permite reducir la complejidad de los procesos, y por tanto los costes, poseyendo, como interés añadido, una flexibilidad que los hace adecuados para el tratamiento de residuos que pueden variar en su composición. En efecto, la presencia de especies muy diferentes en los cultivos mixtos, junto con la evolución del ecosistema microbiano, permite una adaptación del proceso a cambios en la operación o en la composición del sustrato, aumentando la resistencia del cultivo y mejorando de este modo la robustez y fiabilidad de todo el sistema. Sin embargo por contrapartida, resulta complicado predecir la respuesta de su actividad, ya que actualmente no es posible describir con detalle los mecanismos biológicos que controlan el proceso. Por esta razón, resulta necesario profundizar en estudios más básicos que permitan una mejor comprensión que, finalmente, posibiliten lograr la suficiente eficiencia necesaria para su implementación industrial.

Por otra parte, dado que el objetivo es la recuperación de productos con mayor contenido energético, deben considerarse como procesos de coste energético intrínseco mínimo, lo que limita notablemente las condiciones operacionales viables. Bajo este supuesto, se limita la velocidad y rendimiento de la actividad microbiana al reducirse la extensión de la degradación de la materia orgánica, condición imprescindible para que se puedan generar productos con una densidad energética suficiente para ser empleados como biocombustibles o como materias primas en la industria química. Los procesos de fermentación anaerobia, en donde no existe un aceptor de electrones externo, presentan estas características; el cultivo mixto bajo estas condiciones tiene un crecimiento limitado y, al mismo tiempo, es capaz de convertir corrientes residuales ricas en azucares, lípidos, carbohidratos, grasas, etc. en carbohidratos de cadena corta con valor potencial para la industria química y/o energética. Adicionalmente, una segunda

fermentación puede promover la elongación de estos componentes hacia productos con mayor valor añadido.

En esta Tesis se analizan varios bioprocesos empleando como base conceptos de bioenergética y bioquímica con el objetivo de entender los mecanismos de respuesta del cultivo ante cambios operacionales. Se han desarrollado varios modelos matemáticos que pretenden la descripción de estas biotecnologías utilizando la información disponible y proponiendo diversas hipótesis acerca de los mecanismos que los controlan. El objetivo es generar nuevo conocimiento que permita a posteriori incrementar la eficacia y la robustez de estos sistemas de cara a su implementación industrial. Adicionalmente a las potenciales aplicaciones prácticas, el estudio de ecosistemas complejos limitados energéticamente presenta interés científico en el ámbito de la ecología microbiana ya que se estudian las relaciones que se establecen entre microorganismos de diferentes especies presentes en un cultivo y los mecanismos bioquímicos que permiten la supervivencia de estos en condiciones medioambientales desfavorables. En esta Tesis, se presentan tres modelos matemáticos basados en conceptos de bioenergía y principios físicos fundamentales, pretendiendo minimizar la información empírica específica necesaria.

En el Capítulo 2, se analiza la importancia de una descripción minuciosa de los procesos fisicoquímicos que tienen lugar en la fase líquida de cualquier sistema y de forma concomitante a la actividad microbiana de cualquier cultivo. Si se pretende predecir la respuesta de un bioproceso ante cambios en las condiciones medioambientales, resulta necesaria una adecuada descripción de las condiciones operacionales existentes en el reactor y por tanto, de los procesos fisicoquímicos que tienen lugar. La precisión en la descripción de estos procesos dependerá del impacto que tengan sobre el sistema analizado (si existe precipitación, si la fuerza iónica del medio es elevada, etc.) y del grado de complejidad que se pretenda en el modelo desarrollado. En este Capítulo 2 por tanto, se valoran los posibles errores de precisión que se cometen al no considerar el comportamiento no ideal de cualquier fase líquida, lo que permite calibrar el esfuerzo necesario para la descripción fisicoquímica de un proceso concreto.

En el Capítulo 3 se presenta un modelo que pretende la descripción matemática de los procesos biológicos que tienen lugar en la fermentación acidogénica de glucosa por medio de cultivos mixtos. Este proceso biotecnológico es bien conocido cuando se emplean cultivos puros y es la base de muchos

procesos industriales, sin embargo hasta el momento, no se comprenden adecuadamente los mecanismos que controlan la fermentación cuando se emplean cultivos mixtos. En este caso, el proceso genera un amplio espectro de productos que resulta difícil de controlar y que por tanto hace que sea difícil explicar y predecir su respuesta frente a la modificación de las condiciones ambientales, lo que limita su aplicación industrial especialmente cuando el objetivo es la revalorización de residuos complejos.

El modelo asume la existencia de una única especie capaz de llevar a cabo los procesos catabólicos observados en la fermentación anaerobia de glucosa considerando que en un cultivo indefinido, todas las rutas metabólicas tendrán posibilidad de desarrollarse al estar conformado por un elevado número de diferentes microorganismos. La competición entre diferentes especies permite asumir que aquella ruta que permita un mayor crecimiento y por tanto una mayor producción de ATP, será la dominante. Para cada ruta catabólica estudiada, se estima la cantidad de ATP producida que luego se empleará en el proceso anabólico. La maximización del ATP producido es empleada como función objetivo para predecir las rutas catabólicas dominantes en el proceso bajo las condiciones ambientales impuestas. Se consideran los flujos bioenergéticos del proceso, se analizan los posibles catabolismos esperados y se estiman los límites de máximo crecimiento del cultivo mixto. En este modelo se describen las reacciones que ocurren en el citoplasma celular (y con ello las condiciones fisicoquímicas del mismo), las reacciones de transporte a través de la membrana y las que ocurren en la fase líquida del reactor (transferencia a la fase gas, reacciones ácido base).

De este modo, el modelo desarrollado permite predecir las tendencias observadas experimentalmente debido a la influencia del pH sobre la distribución de los productos obtenidos. Así, se predice y explica que el hidrógeno y el dióxido de carbono sean los productos mayoritarios a bajo pH mientras que su producción se reduce cuando la de fórmico se favorece en un medio alcalino; se predice y explica también que la producción de etanol se favorezca a pH altos mientras que la de butírico se observe en condiciones ácidas siendo ambos productos mayoritarios y acompañados por la producción de ácido acético; y asimismo, se predice y explica la producción de ácido propiónico en vez de butírico o etanol a pH intermedio.

La producción única de fórmico en vez de la producción conjunta de hidrógeno y dióxido de carbono que se observa en condiciones de pH básico se explica debido a la mayor solubilidad del carbono inorgánico. Esto reduce la energía disponible para la producción de ácido carbónico por parte del cultivo, favoreciendo así la producción de fórmico ya que, en estas condiciones, es capaz de generar más energía para crecimiento. De un modo análogo, se pueden explicar las tendencias a diferentes pH del resto de productos mayoritarios, relacionando los cambios de pH en el reactor con la reducción de la energía disponible del proceso para el transporte activo a través de la membrana celular, y con la variación de la fuerza protón motriz que se produce cuando varía el pH extracelular. Estos resultados, concordantes con los resultados experimentales, demuestran que la maximización de energía disponible para crecimiento y mantenimiento celular tiene un claro impacto sobre los productos producidos en fermentación anaerobia ya que los cambios en las condiciones ambientales provocan una variación de la energía de la que disponen los microorganismos al catalizar una u otra ruta posible en el proceso de fermentación de glucosa.

En el Capítulo 4 se ha desarrollado un segundo modelo centrado en el análisis de la bioenergética de diversas rutas metabólicas con interés en la revalorización de productos. Son rutas anaerobias y fermentativas (ocurren en ausencia de aceptores externos de electrones) y por tanto limitadas energéticamente. Al ser procesos con una variación de energía libre muy pequeña, se plantea como hipótesis la posibilidad de orientar las rutas del proceso hacia productos con densidades energéticas elevadas mediante la selección adecuada de las condiciones de operación. Fundamentalmente, se analiza la producción de alcoholes o ácidos de cadena media o larga al imponer condiciones reductivas en procesos de fermentación anaerobia, pero además, esta metodología podría ser empleada también para el desarrollo de nuevos bioprocesos de interés. De este modo, se analizan las rutas metabólicas que van desde la fijación del dióxido de carbono con la producción de ácido acético, hasta la elongación de la cadena de carbonos llegando a la producción de ácido caproico, considerado ya como un ácido graso de cadena media. El objetivo de estos procesos es producir componentes con mayor densidad energética que el sustrato introducido, por lo el objetivo es que la energía destinada al crecimiento de la población microbiológica sea mínima.

Para analizar la viabilidad de cada ruta, se asume que cada reacción ocurre en condiciones de equilibrio termodinámico y se calculan las concentraciones de los metabolitos intermedios. De este modo se determinan las concentraciones límite, es decir, las concentraciones mínimas de sustrato y máximas de producto necesarias para que cada reacción catabólica analizada se pueda llevar a cabo. Por tanto, el proceso será viable en el caso de que estas concentraciones límites se encuentren en el intervalo de concentraciones fisiológicamente posibles dentro del citoplasma celular (entre 1 μM y 10 mM). Además, se analiza si en alguno de los procesos de la ruta, se genera energía para mantenimiento y crecimiento, bien sea a través de la producción directa de ATP o a través de la translocación de protones en la membrana celular. Mediante este análisis, este trabajo permite demostrar que los microorganismos que catalizan estos procesos operan muy cerca del equilibrio termodinámico y disipan muy poca energía ya que de otro modo, el proceso no permitiría ninguna generación de energía para anabolismo y mantenimiento. Debido a esto se concluye que los mecanismos bioquímicos empleados por los microorganismos para generar energía para crecimiento (producción de ATP y fuerza protón motriz) deben ser altamente eficaces.

Se aplica la metodología en un primer caso a la ruta de consumo de ácido acético hacia la producción de hidrógeno y dióxido de carbono y se analiza su posible reversibilidad (homoacetogénesis). Además de comprobar que esta reversibilidad es termodinámicamente posible, en este trabajo se discute que la homoacetogénesis podría transcurrir con los mismos mecanismos bioquímicos que la ruta en sentido opuesto (producción de hidrógeno y dióxido de carbono desde acético). Además, esta hipótesis parece tener una base experimental fiable ya que se han observado microorganismos capaces de revertir rápidamente la homoacetogénesis en función de las condiciones ambientales. Sin embargo, cuando la reducción de acético a butírico fue analizada, se observó que no era posible considerando los mismos mecanismos de la ruta (demostrada factible) en sentido opuesto. En este caso, la termodinámica de las reacciones que conforman la ruta catabólica completa, predice una concentración extremadamente baja de uno de los metabolitos intermedios del proceso (acetoacetyl-CoA) lo que supone una limitación cinética del proceso, por ser este compuesto el sustrato de la siguiente reacción catabólica de dicha ruta. Así, aunque inicialmente el proceso pueda parecer perfectamente posible (con una energía de Gibbs negativa), el estudio detallado de la termodinámica de cada una de las reacciones que lo conforman, demuestra que es inviable. En este caso, es necesaria la participación

de otro donador de electrones diferente al hidrógeno para una reducción de acético a butírico en condiciones de fermentación anaerobia. De este modo en el siguiente análisis se demuestra la viabilidad del proceso con etanol o láctico como donadores de electrones del proceso, resultando incluso posible su elongación hacia la producción de ácido caproico. Por último, en este estudio también se analiza la reducción de ácido acético a etanol empleando elevadas presiones parciales de hidrógeno y se plantean hipótesis acerca de cómo los microorganismos son capaces de generar energía para crecimiento con este proceso que, aunque ha sido experimentalmente observado, requiere el consumo de un mol de ATP sin su regeneración.

Finalmente, el Capítulo 5 se enfoca hacia el estudio de las relaciones ecológicas que existen en cultivos mixtos complejos empleados en tratamiento de residuos (digestión anaerobia, tratamiento de aguas, etc.). El objetivo es analizar las causas que permiten explicar la dominancia de ciertos procesos catabólicos en estas condiciones ambientales. El modelo pretende analizar por qué en algunos casos en estos bioprocesos las transformaciones de sustratos son llevadas a cabo mediante relaciones sintróficas establecidas entre diferentes especies microbianas mientras que en otros, son efectuados por una única especie. Para investigar estas relaciones microbianas, se analiza el compromiso que existe entre la maximización de la velocidad o del rendimiento de producción energética para anabolismo por unidad de sustrato consumido en cualquier actividad microbiana.

Para ello, se desarrolla un modelo matemático que permite simular la competición entre diferentes actividades microbianas catalizando reacciones observadas e hipotéticas (no observadas experimentalmente) pero basadas en rutas metabólicas conocidas. En este modelo se asume que todas las especies tienen las mismas características fisiológicas y no están especialmente adaptadas a ningún ambiente, por lo que se considera que sus cinéticas pueden describirse con los mismos parámetros. Además, se simplifica el modelo considerando que los microorganismos son completamente eficaces, despreciando la disipación de energía en las rutas catabólicas estudiadas. Además, asumiendo que todas las enzimas que intervienen en las rutas analizadas tienen una capacidad similar, se consideró que la característica principal para estimar la velocidad de cada uno de los procesos analizados era el número de reacciones de oxidación y reducción necesarias para llevarlos a cabo. De este modo, en este modelo, la velocidad de

cada uno de los procesos catalizados por los microorganismos se considera proporcional al número de reacciones de la ruta considerada.

En la competición virtual entre especies que se simula con este modelo, las actividades microbianas predichas como dominantes coinciden con las observaciones experimentales. Como primer ejemplo se ha seleccionado un proceso de digestión anaerobia con glucosa como sustrato, y se observa que la estrategia que permite un mayor crecimiento es aquella en la cual un primer microorganismo degrada la glucosa a ácido acético y de forma sintrófica un segundo consume este acético produciendo dióxido de carbono y metano. Se comprueba que otros microorganismos catalizando potenciales procesos catabólicos (pero no observados experimentalmente) tales como la transformación directa de glucosa en metano y dióxido de carbono, no serían capaces de sobrevivir. A raíz de este análisis, se observó además que la velocidad de generación de energía para crecimiento de los diferentes microorganismos que producen ácidos de cadena corta y etanol en estas condiciones, es aproximadamente la misma, lo que podría explicar que una u otra ruta sea favorecida en función de las condiciones ambientales impuestas en el proceso. Por ello también se simula otra fermentación de glucosa pero esta vez cambiando las condiciones operacionales al considerar un pH ácido y una alta presión parcial de hidrógeno y se comprueba que el proceso favorecido cambia, siendo mayoritaria la producción de ácido propiónico en vez de la de ácido acético.

El segundo ecosistema estudiado es el que conforma el ciclo del nitrógeno con los procesos de nitrificación y denitrificación. En el proceso de nitrificación, se observa que la relación sintrófica que existe entre las bacterias amonio oxidantes y las nitrito oxidantes es el proceso que permite una mayor velocidad en la producción de energía para crecimiento. Por ello otros microorganismos hipotéticos considerados en el sistema no serían capaces de sobrevivir, tales como una especie capaz de realizar el proceso de nitrificación completo. Sin embargo, cuando se simulan las condiciones en las que se lleva a cabo la desnitrificación anaerobia, se detecta que en este caso no domina el proceso en varias etapas, sino que resulta más ventajosa la desnitrificación completa, tanto considerando una fuente de carbono como donador de electrones, como cuando se alimenta amonio favoreciendo así la ruta del proceso *anammox*.

De este modo, este trabajo parece apoyar la hipótesis que relaciona la maximización de generación de energía para crecimiento por parte del cultivo

microbiano con aquellas especies dominantes en él. Aunque los procesos catabólicos largos sean capaces de generar una mayor cantidad de energía para anabolismo, estos no serán dominantes si su velocidad no es competitiva, por lo que llevar a cabo otros procesos catabólicos más cortos pueden resultar una estrategia más eficaz ya que aunque generen menos energía para crecimiento por unidad de sustrato, pueden aumentar la velocidad global de generación de energía para crecimiento del conjunto de la población. Además, potencialmente, el modelo puede ser empleado no sólo para predecir el comportamiento de diversos ecosistemas microbianos conocidos, sino también para generar hipótesis sobre la existencia de otras posibles especies microbianas que catalicen procesos con interés industrial.

Globalmente, esta Tesis pretende incrementar el conocimiento que se tiene de diversos procesos biotecnológicos centrándose fundamentalmente en aquellos limitados energéticamente. El trabajo realizado apoya la hipótesis de que el proceso evolutivo que han sufrido los microorganismos de los diferentes ecosistemas estudiados, les ha permitido ser extraordinariamente eficaces en cuanto a sus capacidades para sobrevivir incluso cuando las condiciones del sistema no son favorables. Además, los análisis realizados permiten concluir que las relaciones ecológicas entre diversos microorganismos se establecen con el objetivo de lograr una mayor eficiencia del conjunto de la población en la generación de energía para crecimiento, asegurando así su mantenimiento. En esta Tesis se concluye asimismo que resulta viable el control de la distribución de productos obtenidos mediante la actividad de cultivos indefinidos en sistemas limitados energéticamente, seleccionando las condiciones medioambientales concretas que permitan promover la producción de un producto deseado y restringiendo de forma importante el crecimiento del cultivo para maximizar la generación de productos de interés.

Bioenergetics-based modelling of microbial ecosystems for biotechnological applications

USC
UNIVERSIDADE
DE SANTIAGO
DE COMPOSTELA

1

Introduction

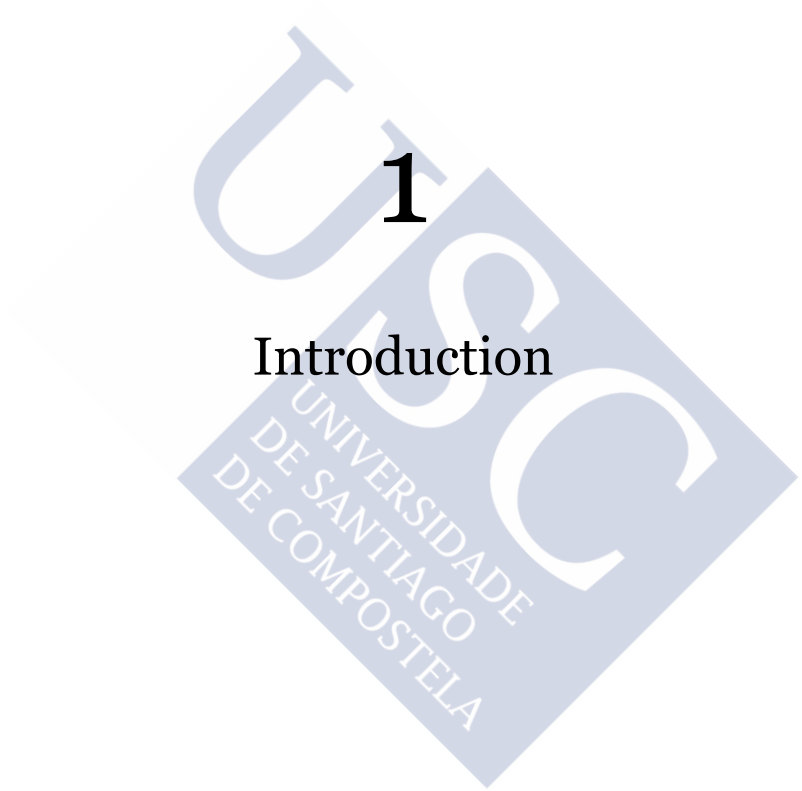

USC
UNIVERSIDADE
DE SANTIAGO
DE COMPOSTELA

1.1 From removal to resources recovery

The biobased industry to convert industrial and agricultural wastes and wastewaters into chemical components with added value, fuels or even electricity, is evolving (Figure 1.1). The global growing cost and dependence on fossil fuels together with the ever growing production of residues makes the valorisation of waste materials interesting however still in many instances their traditional treatment is involving energy consumption without recovery. Under specific conditions, microorganisms or enzymes are capable of catalysing with high specificity and low cost, the transformation of complex organic materials present in wastes into bioproducts, which opens an interesting avenue for new efficient and low cost valorisation processes [1-3].

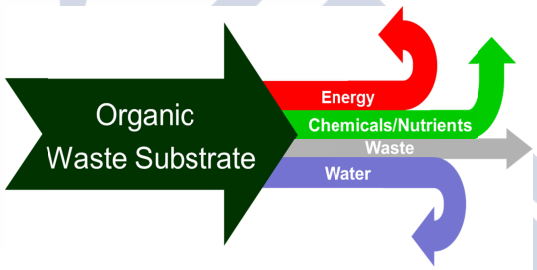

Figure 1.1 Energy and other valuable products can be recovered from organic (waste) substrates.

Among the long number of bioprocesses present in industry, only anaerobic fermentations, taking place in absence of external electron acceptors, are capable of yielding high energy density products, which are good candidates for fuels or valuable chemicals. This is opposed to the most commonly used aerobic bioprocesses in which an almost complete oxidation of the substrates (respiration) into non-value products (mainly CO_2 and H_2O) occurs together with the obstacle of large rapid biomass growth (Figure 1.2) (non-active biomass becomes a sludge which requires management). For this reason, whereas aerobic processes have been typically used for pollution removal (e.g. wastewater treatments), anaerobic fermentations are a promising avenue for resources recovery.

1.2 Anaerobic fermentation. Mixed culture fermentation

Since ancient times, anaerobic fermentations have been of interest. The production of fermented food and beverage were achieved employing microbial populations and incorporating them to the human collective knowledge. The evolution of these bioprocesses however, was slow because even if the biotechnological applications were exploited, no advance in the understanding of the mechanisms that control these processes was developed. Nowadays pure culture fermentations are widely used and their applications increased, not only for food or beverages production but also towards biodiesel, plastics, pharmaceutical and personal care products or chemical building blocks yielding. This evolution came together with a deeper understanding on biology, genetics and technology of the processes which permitted to achieve a higher efficiency towards the production of more interesting and necessary chemical compounds [5].

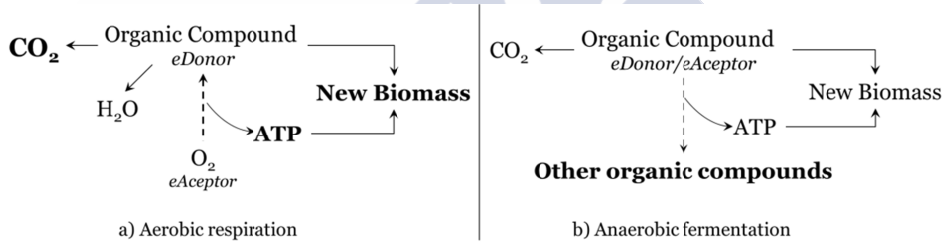

Figure 1.2 Graphic distribution of respiration and fermentation processes yielding products and biomass. Respiration leads to high amounts of biomass production whereas in fermentation energy remains in the organic compounds formed (Adapted from Madigan et al. [4]).

Focusing on waste recovery, fermentations are an option when carried out by mixed undefined populations. These bioprocesses could be conducted towards methane production that is a source of renewable energy or, alternatively, it is possible to stop the process at intermediate steps producing volatile fatty acids (VFAs) and/or other chemicals. Both strategies increase the possibilities of valuable resources recovery from wastes management which in one hand, reduces the incremental amount of wastes that are becoming a technological problem of higher social impact, and in other hand, could reduce in a close future and in an

important percentage the social dependence on the limited energy source that suppose the fossil fuels [1].

Mainly used as anaerobic digestion towards biogas production, fermentation has been included in many processes as a fundamental part of waste treatment industry (widely used for treating liquid wastes but also solids and gases) to recover energy from waste sources with high organic content [6]. The microbial consortium formed in anaerobic digestion is easily stabilized, for this reason the interest on the research of this system focuses on the improvement of the process efficiency (higher methane content in the biogas produced) with several different kinds of wastes (and co-digestion) [7].

Together with anaerobic digestion, H_2 production [8] and biological electricity production (microbial fuel cells) [9] have also been intensively investigated for energy recovery from wastes through mixed culture anaerobic fermentations. But the consideration that high valuable chemicals production is possible maintaining acidogenic conditions, raised the interest of this system increasing the investigation developed in order to optimize these processes aiming at economic feasibility [3].

1.3 The carboxylate platform

The variability and complexity of wastes composition is the first main challenge for their industrial processing and fermentation with undefined populations could be an option to handle broad changes in feed conditions. If a first acidogenic fermentation of the residues is conducted using a mixed culture fermentation, the output is a mixture of short carbon chain components, different VFAs and alcohols (Figure 1.3). This mixture of products is called typically the carboxylate platform, which could be used as first step from wastes towards the production of valuable chemicals [1]. A primary fermentation could be followed by a secondary fermentation with the objective of e.g. increasing the energetic density of the products obtained. A combination of several fermentation and separation steps can constitute an industrial biorefinery in which the value of the streams from complex wastes could be maximized, analogously way that for a traditional refinery from crude oil streams.

Several VFAs are principally formed in first step fermentation like formic, acetic, butyric, propionic, succinic, malaric, fumaric, lactic, valeric, oxaloacetic, acetoacetic acids, and other products like ethanol, acetone, butanol, isopropanol, glycerol or xylitol [10]. These products are themselves valuable [1] but from the undefined mixture formed, they are difficult and costly to isolate. While there have been some efforts to try to develop systems fed by direct mixture of fermentation products (which are until now unpredictable and highly variable) [11], the main industrial limitation still remains on the poor control of the product spectrum and on the difficulties for separation.

These organic compounds could be elongated increasing their value through a second fermentation [12,13]. Longer carbon chain products have higher hydrophobicity, simplifying product purification through phase separation. Thus, condensations of VFAs to produce medium and long chain fatty acids (MCFAs and LCFAs) allows for the valorisation of the products obtained from fermentation [14-16]. In addition to this option, reduction of VFAs to higher energy density products (e.g. alcohols) is also possible under reductive environments [17-19]. Secondary fermentations can be carried out by pure cultures (e.g. caproate production from ethanol and acetic or butyric acid [15], Figure 1.3 (h)) or by bio-electrochemical processes with whereas electrical power production (e.g. microbial fuel cells [9], Figure 1.3 (d)) or electrical power consumption towards the production of more reduced chemical components (e.g. microbial electrolysis cells [20]). In all the cases, the main objective of this second fermentation is the increase in energy density of the product obtained. However, the reduction of a product is not always easy. As the products are highly energetic, it implies that the energy available for the microbial population to grow becomes very limited as it occurs in the reduction of VFAs to alcohols (Figure 1.3 (c) never higher than 10 kJ per mol of substrate available at biological conditions and 37 ºC [1]).

Directing product formation in mixed culture fermentations (MCFs) is still a challenge [21] principally because the control of the operation is difficult as the impacts of changes in the operational conditions of the process remain unknown (e.g. it was experimentally observed that the changes in the pH of the operation modify the products spectrum obtained [10]). The influence of the operational conditions over the process could not be explained yet because the reactions performed have similar pathways which makes very difficult to elucidate which process and in which conditions would be favoured [10]. However, different

experimental results with different mixed cultures have reported important similarities in their trends [22-24] clearly suggesting that product yield changes seem to be more related with energetic or kinetic limitations of the metabolic pathways performed [21] than on the microbial community composition.

Deeper understanding of the microbial mechanisms which control the behaviour of the process, would lead undoubtedly to a better control and a higher efficiency. A better control in the primary fermentation that produces the carboxylate platform could imply an increment in the efficiency making the process industrially competitive. Under the premise that fermentations are systems where biomass is not able to harvest high amounts of energy for their own maintenance and growth, the analysis of the bioenergetics of the process provides a feasible approach to study them that could explain the mechanisms that control anaerobic MCFs [25].

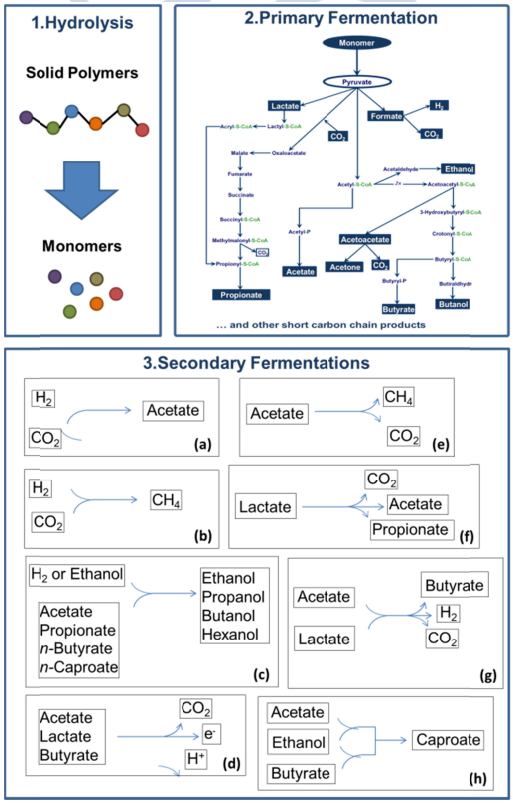

Figure 1.3 The carboxylate platform as a first step for more valuable products yielding. Adapted from Agler et al. [1]

1.4 Feeding on negative entropy

Living systems are well-organized organic structures associated to low entropy states. The natural evolutionary trend towards more robust species capable of surviving under diverse environments and of increasing their population size seems to have promoted the rise of living organisms with higher degrees of organization and lower entropy states. This is a tendency that might appear as violating the second law of thermodynamics.

This paradox was firstly approached when Schrödinger in 1944 using only well-known physical laws introduced the term of negative entropy [26]. He presented a living organism as a system capable of dispelling the thermodynamic equilibrium ($\Delta G = 0$) as opposite to non-animated systems which tend to it. Thermodynamic equilibrium implies no interchange of mater or energy between a system and its surroundings, which would imply death for any living organism. In thermodynamic equilibrium, the entropy of a system is the maximum, but living organisms delay this ultimate fate through highly organized mechanisms that prevent the disorder observed in the environment [26] and maintain its own state of low entropy while obeying the thermodynamic laws [27,28]. These mechanisms consist of reactions that living organisms use during the exchange of matter and energy with the surroundings (what we call growth, eat or move) [29]. These relations between the organism and its surroundings do liberate free energy, and increase therefore the total entropy of the overall system (Figure 1.4). The energy and matter harvested from the environment are used by the living organism for organizing itself lowering its own entropy.

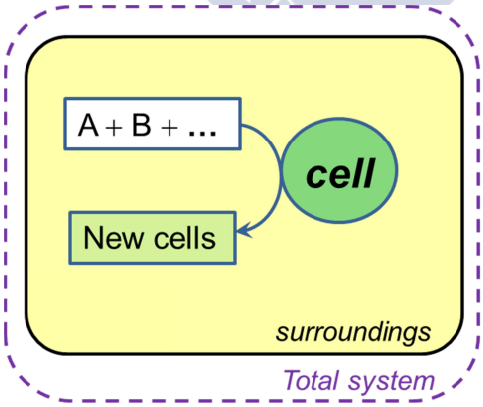

Figure 1.4 Representation of a system containing a living organism.

Indeed, for a system involving a living organism at constant pressure and temperature, it is easy to demonstrate that overall total positive entropy is generated when a reaction with energy liberation is occurring even if the entropy of the organism decreases.

The total entropy of the system (ΔS_{sys}) is the sum of the entropy in the living organism (ΔS_{org}) plus the surroundings (ΔS_{surr}).

$$\Delta S_{sys} = \Delta S_{org} + \Delta S_{surr} \quad 1.1$$

As the second law of thermodynamics must be obeyed, the entropy of the complete system has to be increased with the organism activity.

$$\Delta S_{surr} + \Delta S_{org} > 0 \quad 1.2$$

$$\Delta S_{surr} > -\Delta S_{org} \quad 1.3$$

Considering a close system at constant temperature (T) and pressure, it is possible to relate the variation of enthalpy coming from the activity of the organism (ΔH_{org}) with the variation of entropy of the surroundings by the equation 1.4.

$$\Delta S_{surr} = \frac{-Q_{org}}{T} = \frac{-\Delta H_{org}}{T} \quad 1.4$$

Therefore, the ΔG of the reaction carried out by the organism in the system could be expressed as in equation 1.5 and according to equation 1.2 it must be negative.

$$\Delta G_r = \Delta H_{org} - T\Delta S_{org} = -T\cdot(\Delta S_{surr} + \Delta S_{org}) < 0 \quad 1.5$$

This means that the reaction must be exergonic and therefore accompanied by energy liberation. In this way, exergonic reactions catalysed by living organisms while decreasing their own intrinsic entropy, increase the overall entropy of the whole system.

In summary, living organisms need to interact with their surroundings to generate disorder (positive entropy) in order to maintain their own order (negative entropy). This is analogous to say that to maintain its own order they have to dissipate free energy to the environment by catalysing exergonic reactions.

The dissipated energy of these reactions is the driving force, which makes them possible [30]. At the same time, it is its intrinsic organization what allows living organisms to harvest the necessary energy from the environment to fuel their decreasing entropy reactions.

Under this broad perspective, some limits could be established of what living organisms are able to do under a given environment [31] by taking into account also physiological mechanisms [32]. The thermodynamic analysis of a living organism in a closed system (e.g. Figure 1.4) can potentially provide valuable information especially when the environment is energy limited (like in anaerobic environments) and when considerable information is available about the physiology of the organism.

1.5 Catabolism to fuel anabolism

Although the microbial metabolism is made up of all the reactions catalysed by a cell, it can be represented as two processes only linked by bioenergetics considerations: catabolism and anabolism (Figure 1.5) [33].

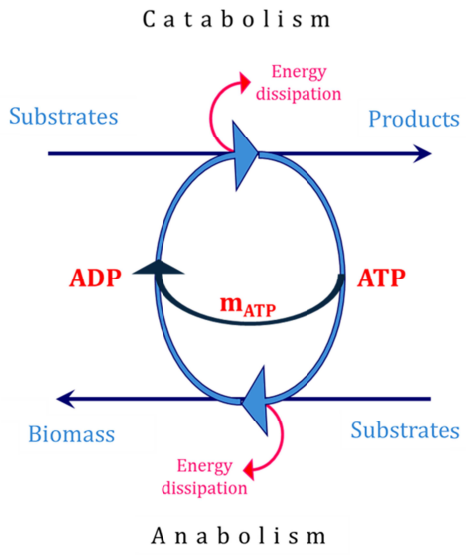

Figure 1.5 Energetics cycle of the cell metabolism. ATP molecules produced in the catabolic process are invested into fuel anabolism and fulfil the maintenance requirements together with the inevitable energy dissipation. Adapted from Heijnen and van Dijken, 1992 [36].

Catabolism is made up of the overall exergonic reactions that harvest energy from the environment, while anabolism is made up of the overall typically endergonic reactions that consume the energy harvested through catabolism to generate new biomass (growth) [34]. From the catabolic energy (ΔG_{cat}), part is used for so-called cell maintenance purposes (ΔG_m) and part must be dissipated to drive the overall metabolism as previously discussed (ΔG_{dis}) [35-37]. Cells use energy conservation mechanisms that are part of their physiology, to couple the energy from catabolism with anabolism (ΔG_{ana}) and maintenance (Figure 1.5). Thus, biomass growth yields (Y_{XS}) could be estimated analysing the bioenergetics fluxes (equation 1.6).

$$Y_{XS} \cong \frac{\Delta G_{cat}}{-(\Delta G_{ana} + \Delta G_{m} + \Delta G_{dis})} \qquad 1.6$$

In the overall metabolism, it is mainly ATP the energy carrier linking both anabolism and catabolism. Therefore, a living organism could be described by accounting for the energy yields obtained from its environment that are directed to growth, maintenance and other products formation (Figure 1.6).

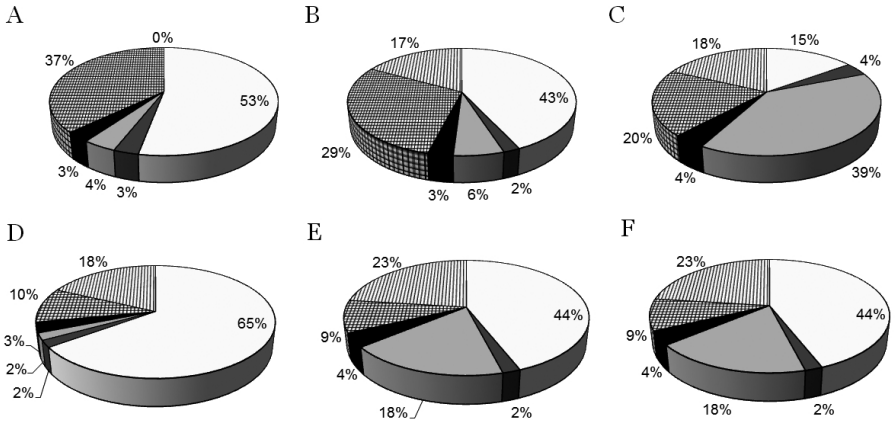

Figure 1.6 ATP balances of B. subtitlis chemostat cultures. The following processes were considered (in clockwise orientation): biomass formation (white); riboflavin biosynthesis (dark grey); overflow metabolism (light grey); metabolic shifts from optimal pathway usage (black); maintenance metabolism (grid); ATP excess (hatched) ATP balances under carbon limited (A and D), nitrogen limited (B and E), or phosphate limited (C and F) conditions at (D, dilution rate) D = 0.1 h^{-1} (A to C) and D = 0.4 h^{-1} (D to F). Balances are based on the total cellular energy flux in each culture. Adapted from Dauner et al. [38].

The energy that is directed to growth is reduced by the energetic cost of specific maintenance tasks that the organism is forced to carry out in order to survive under the given environmental conditions [38] (e.g. production of a secondary metabolite), however, assuming that the overall system tends to a maximum of entropy, it could be hypothesized that growth maximization is generally pursued. This leads to the conclusion that the evolutionary adaptation of organisms to the environment may be through the selection of those able to maximize growth, maximizing the energy harvest under specific environmental conditions [29,39,40].

1.6 Following the energy path

Prokaryotes, by remaining the simplest living organisms on earth, have retained key evolutionary advantages that make them capable of surviving in extreme environments and under very high energy scarcity [39]. Their simplicity could allow for versatility as their energetic demands have been reported as lower than those of other more complex organisms [41]. This characteristic could have apparently improved the ubiquitous presence of these microorganisms in almost all environments (Figure 1.7) [42-44].

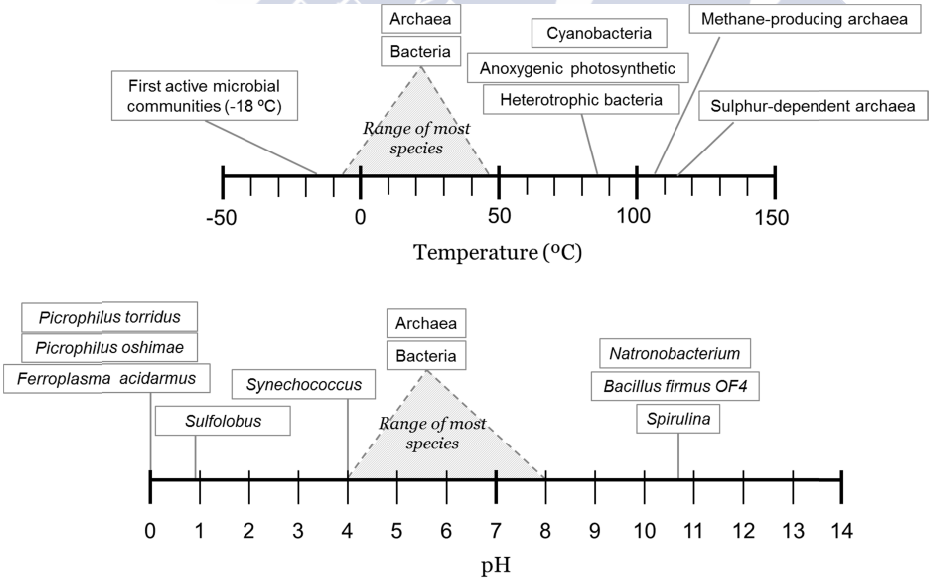

Figure 1.7 Broad range of pH and temperature tolerance for the microbial activity of archaea and bacteria. Adapted from Rothschild and Macinelli 2001 [42].

Because microorganisms evolved to become specialized survivors in all the broad spectrum of conditions, the study of the microbial diversity is an enormous task [45,46] (Figure 1.7). However, this analysis reduces complexity by looking at the energy available in a given environment as their diversity relates directly to their capacity of being the most efficient energy scavenger [47]. The simplicity related to prokaryotes and archaea physiology, reduces the minimum energy needed for these microorganisms increasing their chances to survive. Indeed, the minimum catabolic energy threshold for bacteria remains undefined as several experimental reports have indicated that anaerobic fermentations proceed at the edge of thermodynamic equilibrium [48,49]. They occur closer than the 20 kJ per mol of substrate consumed, considered until recently, as the minimum energy dissipation required to drive a reaction [50] (Table 1.1).

Table 1.1 Experimental minimum free energy changes observed in anaerobic fermentations. Data from Kleerebezem and Stams, [30]

SUBSTRATE	MICROBIAL CULTURE	$\Delta G^{(*)}_{min}$
Ethanol	3 *Pelobacter* sp.	-10.6
	2 *Desulfovibrio* sp.	-27.8 and -36.8
	In situ measurements	-14
Propionate	Enrichment culture	-3
	Digesting sludge	-5.8
	In situ measurements	+4
Butyrate	Defined triculture	-4
	NSF-2 & *M. hungatei* PM-1	-3.8
	NSF-2 & *Desulfovibrio* PS-1	-17.0
	Digesting sludge	-3.2
	Syntrophomonas wolfei	-26.3
	In situ measurements	+2
Benzoate	SB & *Desulfovibrio* G-11	-30
	BZ-2 & *Methanospirillum* PM-1	-32
	Enrichment culture	-29

$^{(*)}$Different conditions depending on each experiment (reference Kleerebezem and Stams, [30])

In energy scarce environments, the identification of which metabolisms would be able to survive requires less physiological information and the identity and differences between microbial species become less important under the assumption that successful microbial activities will be limited to those conducted by the ones able to harvest sufficient energy. In this way, interesting conclusions of the ecosystem that most probably would succeed could be drawn by analysing the bioenergetics of the process.

1.7 Mechanisms of energy harvest

Mechanistically, the energy harvested by catabolism is stored in ATP molecules (called energy carriers). The total concentration of ATP, ADP plus phosphate is constant as these chemical components are part of a group often called conserved moieties [51] that do not cross the cell membrane and maintain their total cytoplasmic concentration constant. The ATP, ADP and phosphate ratio is controlled by cell homeostasis [52], as the cost of a mol of ATP production is presumed maintained close to constant as part of the cell homeostasis.

$$ADP + Pi + H^+ \rightarrow ATP + H_2O \qquad \Delta G \cong +50\ kJ/mol \qquad 1.7$$

The main mechanisms of energy harvest that cells have are the protons (or other charged molecules) translocations across the membrane, or the metabolic reactions associated to ADP phosphorylation (substrate level phosphorylation, SLP) [53] (Figure 1.8). Both mechanisms yield ATP that later energetically fuel anabolic or maintenance cell processes.

ATP formation via SLP occurs when highly exergonic metabolic reactions take place and the energy released is sufficient to form one molecule of ATP (> 50 kJ/mol ATP). In other cases the contrary occurs and an ATP is broken in ADP and phosphate when energy is needed to carry out what was in first instance an endergonic reaction. Thus, ATP is invested strategically by the cell: the loss of an ATP somewhere in metabolism is meant to be gained back in another part of the system.

Proton motive force is the second mechanism used by the cells to harvest energy from the environment and (in most cases) it is producing ATP as well. This mechanism, described first time by Mitchell in the chemiosmotic theory [54],

explains the semi-permeable membrane bioenergetics when protons (or other ions) are pumped across the membrane generating an electrochemical potential. This potential can be used to do work (i.e. driving endergonic reactions) while in the opposite direction (same potential direction) protons can cross the membrane dissipating energy [55] (Figure 1.9).

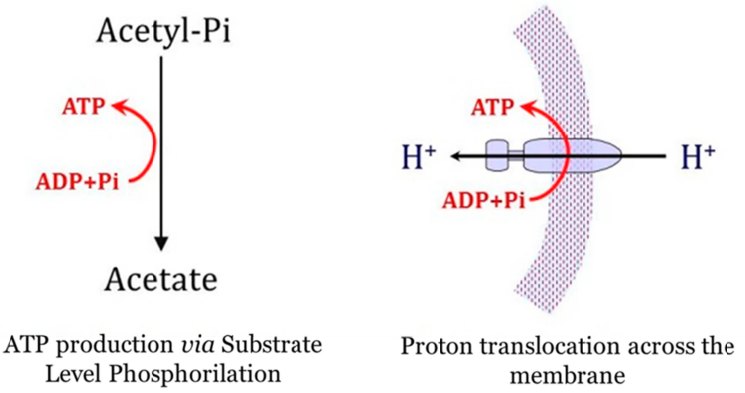

Figure 1.8 Mechanisms for energy harvesting. Left side represents ATP production coupled to highly exergonic metabolic reactions. Right side represents protons or other specific ions crossing the charged membrane through the ATP synthase complex yielding ATP.

In the external surface of the cell membrane, an accumulation of protons occurs which allows the membrane to act as an electrical capacitor. A current flow conducted by charged species movement [56] occurs between the inner and outer surfaces of the membrane which can in some cases lead to energy harvesting (i.e. ATP production). This is possible due to the semi-permeability of the cell membrane, which does not permit charged species to freely diffuse. Therefore, the concentration of the ions in the cytoplasm is controlled by the cell homeostasis and an accumulation of cations occurs in the external surface as the internal is negatively charged.

The gradient established between the concentration of protons in the cytoplasm and outside the cell generates a chemical potential (pH gradient) and an electrical potential (difference of charges) in the membrane. The bioenergetics of a membrane is typically defined by the electrochemical work that is performed when a proton crosses it (i.e. in the gradient favour, from outside to inside the

cell). It is the sum of the chemical potential ($(RT/F)\cdot\ln[H^+]_{in}/[H^+]_{out}$) and the electrical potential ($\Delta\psi$), called proton motive force.

$$\Delta p = {\Delta\mu_{H+}}/{F} = \Delta\Psi + \frac{R\cdot T}{F}\cdot\ln\left(\frac{[H^+]_{in}}{[H^+]_{out}}\right) \quad 1.8$$

Where $\Delta\psi$ represents the electrical potential difference between inner and outer cell membrane sides ($\Delta\psi = \psi_{in} - \psi_{out}$).

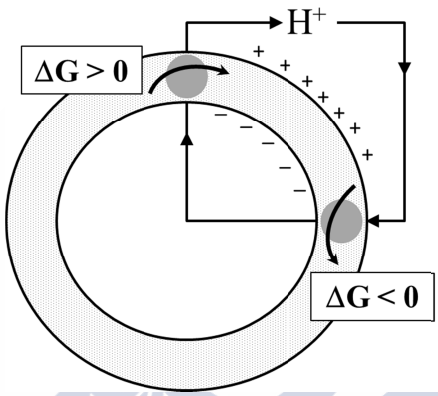

Figure 1.9 Proton translocations. When a proton cross the membrane from inside to the cell membrane surface, energy is needed for the process; it is coupled to an exergonic reaction to proceed. If the proton crosses from outside the cell to inside the cytoplasm, energy is released; this process could be coupled to an endergonic reaction (e.g. ATP production). Adapted from White et al. [58].

The Δp of the cell is controlled by the cell homeostasis [57] and could be adapted to the environmental conditions [58]. This mechanism allows for higher efficiency on the energy harvest by the cells as this proton motive force controlled by the cell homeostasis is less energetically demanding compared with ATP formation via SLP. Proton translocation has been described coupled with particular metabolic reactions [55] or to active transport mechanisms across the membrane [59] and it constitutes the minimum energy unit that the cell is able to harvest. Reactions that release lower energy than the necessary to make a proton to cross the membrane, would lead to energy dissipation. However, Δp is not only modified by proton translocation but by any other charged species that might cross the membrane modifying the chemical and/or the electrical potential [56].

These effects could require in some cases for additional protons extrusion to maintain the proton motive force, at ATP expense.

1.8 Thermodynamics to study energy limited systems

Knowing the mechanisms used by the cell to harvest energy, it is possible to approximate the energy available in a system for microbial growth. The initial feasibility of a specific catabolism can be assessed by accounting for the energy available. It is clear that a minimum amount of energy needs to be harvested through catabolism in order to maintain a microbial population.

$$\Delta G = \Delta G^0 + R_{th} \cdot T \cdot \ln \prod_i a_i^{\nu_i} \qquad 1.9$$

Equation 1.9 defines the total energy available for a given reaction in the given conditions. If the energy available is harvested, part can be invested in growth, part in maintenance and part must be dissipated to provide the overall driving force of the process [60,61]. By looking at microbial catalysed processes under this energy balance perspective, it is possible to preliminarily assess potential novel bioprocesses of interest and to theoretically analyse its viability [62]. The question of whether the available energy is sufficient to sustain a necessary microbial population can be computed.

Figure 1.10 shows an example of a tight energetic space in an anaerobic ecosystem. The butyrate oxidation into two acetic acids cannot proceed when high H_2 partial pressures are present in the system, because the reaction becomes endergonic. However, under the presence of a microorganism H_2 consumer, the process could be possible. There is a shared tight space of viability between butyrate oxidizers to acetic acid and reducers to butanol that at set operational conditions, both processes are feasible. In this space of conditions, the whole system could theoretically proceed if both strains are able to harvest enough energy for their maintenance.

Through thermodynamic analysis not only could be studied the limitations of a system but also the advantages of a set catabolism over others under specific conditions. Environmental conditions may constrain the possible catabolic activities that succeed in generating highly stable and specific populations [63]. In a mixed culture, where different microorganisms may conduct different activities,

energy boundaries are limiting which catabolism is successful under these given conditions [64] and which kind of synergies would be necessary for the whole microbial population survival.

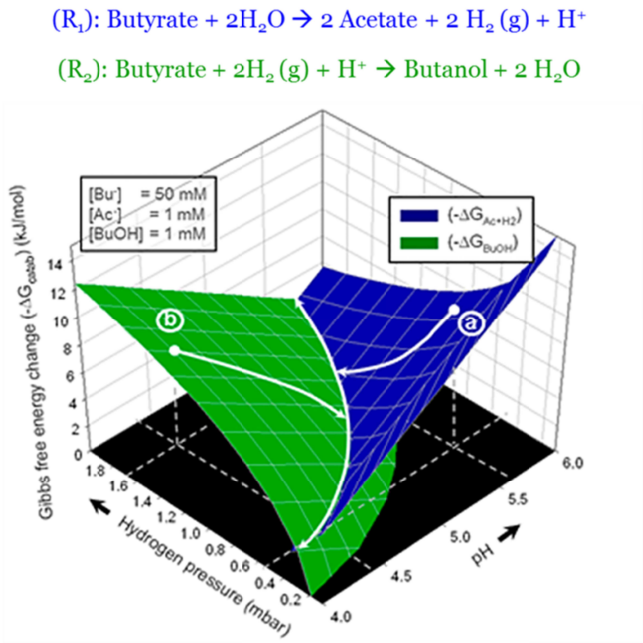

Figure 1.10 Space of feasible conditions for the synergy of two catabolic processes linked by consumption and production of H_2. Partial pressure of H_2 and pH are the variables analysed. Around the intersection, both reactions are feasible whereas in point (a) only reaction R1 is feasible and at point (b) only reaction R2. Adapted from Rodríguez et al. [25]

Microbial mixed cultures in bioreactors are highly dynamic and complex due to their fast evolution and multiple and complex interactions between species that can spring up [65]. The differences between species may become blurred in these systems in which the probability of mutations to occur is very high due to the fast reproduction of the microbial population [66]. Indeed, this increases the difficulty to establish the relation between species and functions but at the same time, it might increase the stability and resilience of the process [63]. For anaerobic acidogenic fermentation, DGGE based microbial community studies have been reported [67] trying to relate changes in metabolic functionality and microbial population composition but they do not lead to strong conclusions. More

advanced DNA sequencing based tools for microbial community characterization recently available might lead to stronger conclusions in the near future [63].

For this reason, by approaching a microbial ecosystem as a competition between catabolic activities instead of microbial species, some complexity might be avoided. The mixed population can be treated as a physical system in which all catabolic reactions, known to be possible under the given operational conditions and according thermodynamic laws are considered in competition [68].

This competition between species could be considered present in every mixed microbial ecosystem constrained by bioenergetics [41,69]. The competition for resources can be described as an energy harvest struggle [70] where the dominant microbial species would be the one capable of harvesting energy faster from the environment. Some microbial collaborative interactions can as well be explained by energetic considerations, as several microbial syntrophic examples are found in nature in which one species is not able to survive if another specific one is absent [50,71-73] (in a case analogous to the Figure 1.10). Thermodynamics analysis together with the cellular physiological information available could bring insights to explain the evolutionary course that specific microorganism activity follows in a specific environment towards the maximum energy harvest rate from the surroundings [41,69].

This approach could help to understand the ecological interactions between metabolisms and the dynamics that explain the behaviour of microorganisms [40,74]. It can also be used to seek for new theoretically possible microbial catabolic functionalities [75] that could have a potential industrial interest (similar as with the discovery of the *anammox* bacteria predicted by Engelbert Broda [76]).

1.9 Models for the understanding and control of bioprocesses: Previous models

Modelling could be used to simply control a well-known process for which the physical mechanisms that govern it can be mathematically described to predict future results. But also, modelling could be used for more fundamental objectives, to investigate the physical or biological mechanisms of systems not yet fully understood.

Models can be classified based on the applied knowledge and the data used [77,78]. A model which aims at mechanistically describing the physical and chemical processes of a system (white box model) [79] could imply a highly complex model with large difficulty for its development but as well, it could facilitate the fundamental understanding of the system. At the same time, mechanistic white box models allow, to some degree, for the extrapolation of results as the model is based on basic principles. Other models called phenomenological or empirical models (black box models) [80] are not based on a deductive process made from physical laws but on data obtained from experiments. These second type of models have difficult extrapolation and are used for interpolated prediction of the system response in set conditions. Nevertheless models could be between both approaches (grey box models) [81].

Mainly, the most interesting models for biotechnology are constructed with a core of derivative equations which try to predict the dynamics within a reaction vessel. Commonly, these derivative equations are mass balances of the different components considered and for which their dynamic behaviour is simulated. For example, the mass balance of a component inside a continuous well-mixed reactor corresponds to equations 1.10 and 1.11.

$$\text{Accumulation} + \text{Consumption} = \text{Input} - \text{Output} + \text{Reaction} \qquad 1.10$$

$$\frac{dS_i}{dt} = \frac{1}{V_{liq}} \cdot Q_{liq} \left(S_{i,inf} - S_i \right) + r_i \qquad 1.11$$

Q_{liq} is the flow that comes in and out of the reactor (L/h), V_{liq} the liquid volume (L), $S_{i,inf}$ and S_i the concentrations of the component i in the inflow and in the reactor respectively (gS_i/L) and r_i the rate of the reaction that could consume or produce the component i ($gS_i/L\ h$). By mathematically integrating the equation time course, concentrations for all components can be approximated (Figure 1.11).

Under this scheme, several models have been developed to describe the performance of different biotechnological systems. In the wastewater treatment field, the IWA developed models are up to date the most widely used [82-84]. Numerous implementations on different platforms, as well as adaptations and improvements [85-89] of these models have been published. In the specific case of anaerobic fermentation, other models have been reported [90-93] but it is the ADM1 model which is by far the most widely applied [83,94,95]. However, even if

the ADM1 has also been used at research level with several modifications, extensions and applications developed [95-98], it has specific limitations for its use to explain or predict several characteristics of fermentation processes [99,100].

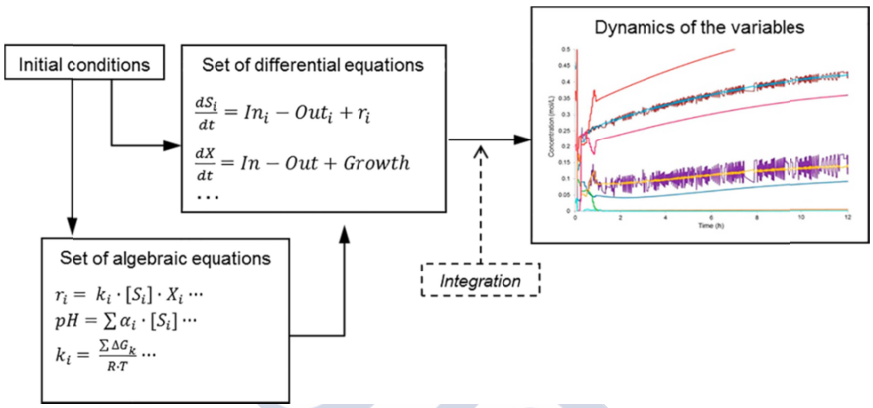

Figure 1.11 Schematic representation of a model with derivative equations

1.10 Kinetics-based models fail in describing acidogenic anaerobic fermentation

ADM1 and other models for anaerobic fermentation are based on a fixed stoichiometry. The rate of each biological reaction included is considered mainly controlled by the availability of substrates according to half saturation constants [83] and specific maximum uptake rates experimentally measured.

The inherent difficulty of identifying the large number of Monod-parameters posed a major first problem. Indeed, the application of ADM1 might require in some cases for the calibration of kinetic parameters for each specific case study [90,98,101,102] with an extrapolation of the model that is not direct and requires an important effort of analysis for each application. This aspect indicates that mechanistically, ADM1 is not offering fundamental answers about the microbial community performance. Indeed, no consensus on a clear explanation of what Monod-kinetic terms are representing has been reached to date [103,104].

The use of fixed stoichiometry for the acidogenic fermentation reactions remains the main hurdle for models such as ADM1 towards its application to non-methanogenic fermentations. Mosey (1983) [105,106], already demonstrated

how product formation from acidogenesis is function of the redox state of the system [102]. Thus, a variable stoichiometry is needed to predict the dynamics of the system in relation to the environmental conditions [107]. Nevertheless, the application of a variable stoichiometry able to predict changes happening in MCF requires a great improvement in the knowledge of the biological mechanisms of the cells that defines the microbial mixed culture. Indeed, mathematical equations able to describe the impact of environmental changes over the microbial population are needed to implement these new models. A higher prediction in MCFs response over environmental changes would indeed imply a direct improvement of the fermentation process control. This could have high impact on processes as the ones previously presented, fermentations which aim resources recovery from wastes, that produce short-chain carbohydrates or/and H_2 as first step to higher biofuels and chemicals production [1].

1.11 Bioenergetics based models for microbial bioprocesses

Thermodynamic conditions impose constrains to any process which together with the mass conservation laws, limit the possible reactions taking place in a system [25,108,109]. Besides these limitations, some bioenergetics-based models are also based on the main assumption that microbial populations tend towards growth maximization. This is a key hypothesis that allows for the connection of the reactions stoichiometry in the process with a metabolic optimization to maximum biomass growth.

When the relationship between stoichiometry and the maximization of growth is established, a variable stoichiometry able to describe changes in the catabolic yields of products when changes occur in operational conditions is possible. This approach has already been used for modelling product formation in anaerobic fermentations with moderate initial success [68,110]. These first models fell short in accurately predicting specific important shifts in product yields. A need has been identified for a more comprehensive description of the reactions which define the metabolic network analysed together with a more detailed account of the different electron carriers and the reactions coupled to proton translocations in order to achieve a superior prediction of experimentally observed distribution in products yielding as function of reactor operation conditions.

In Figure 1.12 a first step of a metabolic network for anaerobic fermentation is presented. However, there are many uncertainties related with it in order to accurately analyse the bioenergetics of the process. Some of them are detailed in the following paragraph.

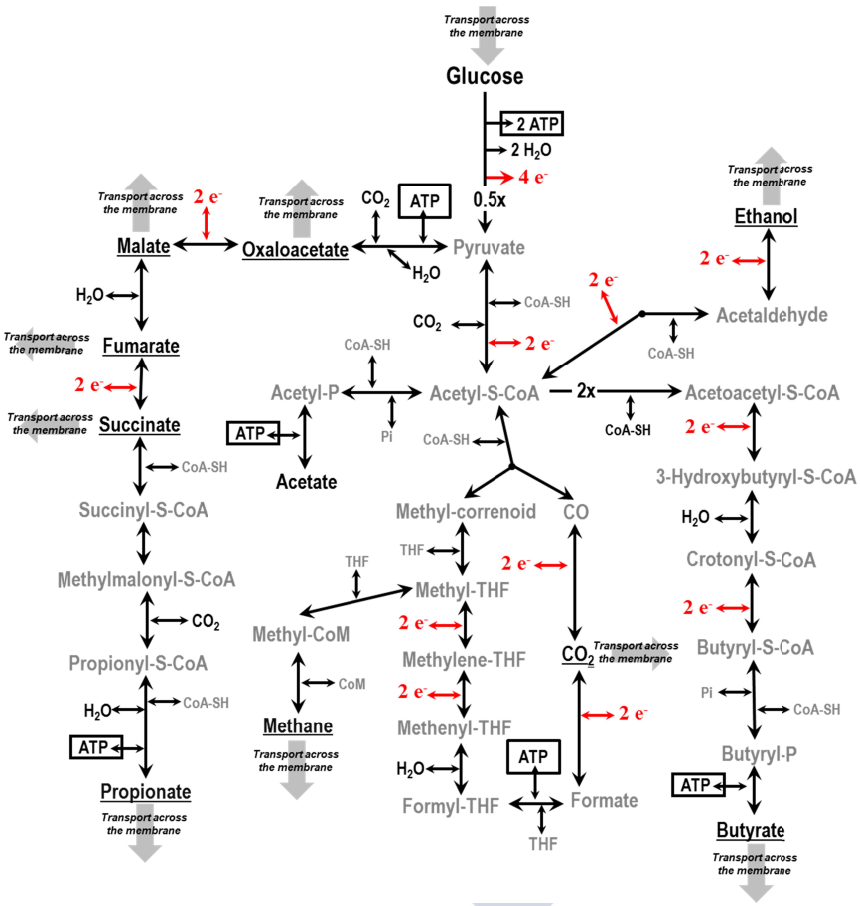

Figure 1.12 Schematic metabolic network to describe anaerobic fermentation of glucose until methane production using MCFs. The network is not complete but the main products are indicated as well the electrons transferred in oxidative/reductive reactions, the intermediate conservative moieties (-CoASH, -THF, etc.) and the ATP consumption/production.

1. *The chemical form of the chemical component that is acting as product or reactant in the metabolic reaction*: In most of the cases, the more abundant form in cytoplasmic conditions is the reactive one (e.g. for VFAs the deprotonated form is the reactive).

2. *The electron carriers involved in each oxidative or reductive reaction need to be identified*: In some cases, two or more different electron carriers could be related with only one metabolic reaction or the coupling of two different metabolic reactions could directly interchange electrons (or conserved moieties).

3. *The availability of the different conserved moieties*: Concentrations of -CoASH, -THF, electron carries, ATP, etc. should be a known parameter in order to compute the bioenergetics of the whole network.

4. *Which points of the network are linked to protons translocations across the membrane*: A thermodynamic analysis could reveal the most exergonic or endergonic reactions that are more likely to be coupled to proton translocations (to produce ATP or to energetically fuel them).

Rodríguez et al. [68] provided a first model under this approach with a simplified metabolic network, however in it is assumed that H_2 could be produced directly from NADH oxidation and that the reaction of the equation 1.12 was always close to equilibrium.

$$NADH + H^+ \leftrightarrow NAD^+ + H_2 \qquad 1.12$$

The analysis of the NADH relation with H_2 production was described in more detail in the model by Zhang et al. [110] but again, NADH/NAD^+ ratio remained assumed as fixed by the H_2 partial pressure.

These first models both assumed that H_2 could act as the external electrons sink to balance the oxidations taking place in glycolysis and therefore allowing for the prediction of known to be unfeasible reactions such as e.g. fermentation of glucose yielding only acetic acid, CO_2 and H_2 [111]. The oxidation of NADH towards H_2 production is assumed to occur in anaerobic digestion where exists the syntrophic relation with hydrogen oxidizing archaea that maintain very low H_2 partial pressure in the system [50]. However, in acidogenic fermentation there is no partner to consume hydrogen which leads to conditions of unfeasible values of ΔG for equation 1.12 [112-114] (Figure 1.13). At high concentrations of H_2 however, the reduction of NADH is indeed possible being a feasible method to yield reduced products like butanol or ethanol.

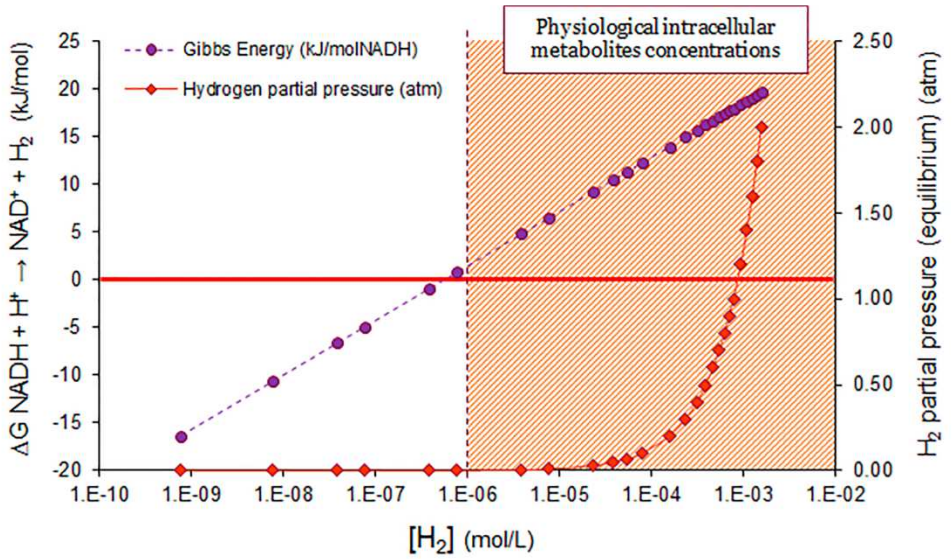

Figure 1.13 ΔG values for the NADH oxidation to H_2 at different H_2 dissolved concentrations for an NAD^+/NADH ratio of 1.

The total concentration of the conserved moiety NAD(H) (reduced plus oxidized forms) is constant inside the cytoplasm but the values for the ratio of NADH/NAD^+ are still not clearly defined. It could be hypothesized that this ratio is optimized and controlled by the cell to achieve a maximum energy harvest [115] while not limiting any important reaction for the cell. Payot et al. [116] reported that values of NADH/NAD^+ ratio higher than 1 would inhibit glycolysis in glucose fermentation in agreement with later results obtained by Canelas et al. [112]. In contrast, for aerobic conditions, a NADH/NAD^+ ratio between $3.12 \cdot 10^{-3}$ - $9.90 \cdot 10^{-3}$ have been reported.

Environmental conditions seem to clearly affect NADH/NAD^+ ratio but it remains difficult to determine. If upper limits of the NADH/NAD^+ ratio are established such that glycolysis remains feasible, ratios with a higher value than 1 would not be expected and the production of H_2 from NADH oxidation would remain thermodynamically very limited (Figure 1.13). At same time, the experimental observations by Temudo et al. [10] are consistent with the assumption that H_2 is produced only via oxidation of ferredoxin (an electron carrier with lower reduction potential than NAD(H) [113]) implying a maximum of 1 mol of H_2 produced per pyruvate to acetyl-CoA oxidation (one of the fermentation central steps, Figure 1.12). In conclusion, these uncertainties show

that a more detailed analysis of the interrelations between intermediate metabolites and electron carriers is missed from the existing models and this might be one of the limitations for the reported mathematical descriptions to predict the experimentally observed products more accurately.

The modelling of solute transport processes and their energy coupling appears to be another area in need for improvement in these bioenergetics-based models. ATP produced and consumed in the catabolism has to be accurately accounted for if the description of bioenergetics fluxes is aimed. For this reason, all the processes involved which imply consumption or production of energy must be accurately described. Active transport of molecules across the cell membrane (Figure 1.14) could suppose an energetic cost or profit, and they constrain the energy harvested for growth of a set microorganism [117].

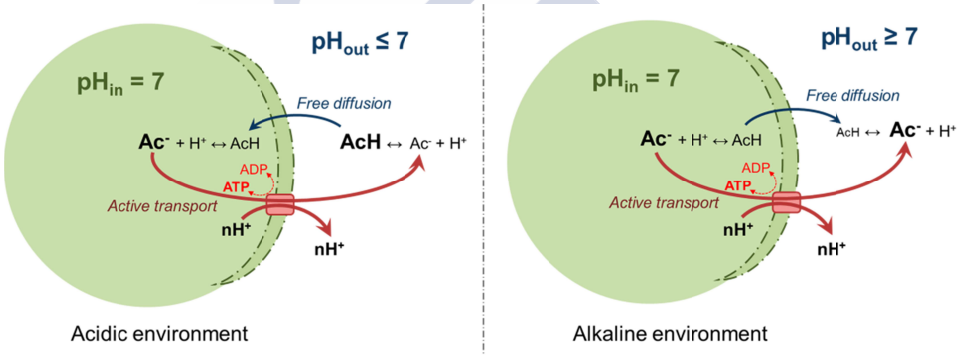

Figure 1.14 Transport of a weak acid. The fully protonated form is able to diffuse freely across the semi-permeable membrane whereas charged forms have to be extruded with active transport. Free diffusion and active transport have to be both considered to describe the dynamic evolution of the intra- and extracellular chemical components concentrations.

The so called recycling model [59,118,119], assuming thermodynamic equilibrium in active transports, constitutes a good approximation to account for the membrane proton translocations associated to the active extrusion of molecules, and therefore to approximate the global catabolic ATP production or consumption. However, its application requires an accurate description of the dynamics of the intra- and extracellular components concentrations which defines the energy available or needed in the active transports [120]. For this reason, it is important to highlight the semi-permeability of the cell membrane and allows for the diffusion of some molecules [121], fact has to be fully considered because it

impacts on the Gibbs energy terms of catalysed reactions of the cell (some reactions could become unfeasible), as well as in both, cytoplasmic and reactor physicochemical conditions.

1.12 Outline of this Thesis

The bioenergetics analysis and mathematical modelling of several bioprocesses of industrial interest (focusing on anaerobic fermentations processes towards waste materials recovery) is conducted in this Thesis. The aim is to mechanistically understand the physical limits of the processes and as well the ecological interactions established in the different microbial ecosystems. The new knowledge pursued by this research work, could lead towards an improvement of the bio-systems control increasing their efficiency towards the recovery of a desired product of value.

CHAPTER 2 analyses the models employed to describe the physicochemical condition of the liquid bulk of a reactor, i.e. pH, ionic strength and the calculation of the concentrations of all chemical species in solution. The impact of considering non-ideality corrections are analysed when describing different liquid media.

CHAPTER 3 is focussed on the development of a fully comprehensive mathematical model based on bioenergetics of the anaerobic acidogenic fermentation using mixed cultures. The objective is to predict the products spectrum of the process under controlled environmental conditions. The limitations of other models are addressed by rigours description of the intra- and extracellular physicochemical conditions of the system and all the metabolic reactions and transports across the membrane that could suppose energy generation or consumption by the cell catabolism.

CHAPTER 4 is presenting several bioenergetics analyses of different anaerobic processes towards production of reduced products. While typically these processes follow the direction of degradation (yielding products of lower energy density), they are potentially reversible because occur under energy scarcity. The analysis of their reversibility permits to formulate conclusions regarding its feasibility by imposing reductive operational conditions (e.g. high hydrogen

partial pressures). Moreover, this study permits to mechanistically understand the capacity of microorganisms to survive in energy limited conditions.

CHAPTER 5 investigates the ecological relations between the microorganisms of several undefined cultures, based on the assumption that mixed cultures are composed by different species competing for the energetic resources of a system and limited by the fundamental trade-off between yield and rate of energy harvest per unit of substrate. In the model presented in this chapter, competition between existing and not experimentally reported microbial catabolic activities (but possible) is simulated. Successful ecological relations of competition or collaboration are predicted under the hypothesis of maximum energy harvest rate and in line with experimental observations reported.

1.13 References

1. Agler MT, Wrenn BA, Zinder SH, Angenent LT (2011) Waste to bioproduct conversion with undefined mixed cultures: the carboxylate platform. *Trends in Biotechnology* **29**: 70-78.

2. Angenent LT, Wrenn BA (2008) Optimizing mixed-culture bioprocessing to convert wastes into bioenergy. In: Press A, editor. Bioenergy. Washington. pp. 181-194.

3. Angenent LT, Karim K, Al-Dahhan MH, Wrenn BA, Domíguez-Espinosa R (2004) Production of bioenergy and biochemicals from industrial and agricultural wastewater. *Trends in Biotechnology* **22**: 477-485.

4. Madigan MT (2012) Brock. Biology of microorganisms. San Francisco: Benjamin Cummings.

5. von Stockar U, Valentinotti S, Marison I, Cannizzaro C, Herwig C (2003) Know-how and know-why in biochemical engineering. *Biotechnology Advances* **21**: 417-430.

6. Verstraete W, Morgan-Sagastume F, Aiyuk S, Waweru M, Rabaey K, et al. (2005) Anaerobic digestion as a core technology in sustainable management of organic matter. *Water Science and Technology* **52**: 59-66.

7. Appels L, Baeyens J, Degrève J, Dewil R (2008) Principles and potential of the anaerobic digestion of waste-activated sludge. *Progress in Energy and Combustion Science* **34**: 755-781.

8. Hallenbeck PC, Ghosh D (2009) Advances in fermentative biohydrogen production: the way forward? *Trends in Biotechnology* **27**: 287-297.

9. Rabaey K, Verstraete W (2005) Microbial fuel cells: novel biotechnology for energy generation. *Trends in biotechnology* **23**: 291-298.

10. Temudo MF, Kleerebezem R, van Loosdrecht MCM (2007) Influence of the pH on (open) Mixed Culture Fermentation of Glucose : A Chemostat Study. *Biotechnology and Bioengineering* **98**: 69-79.

11. Levy PF, Sanderson JE, Kispert RG, Wise DL (1981) Biorefining of biomass to liquid fuels and organic chemicals. *Enzyme and Microbial Technology* **3**: 207-215.

12. Smith DP, McCarty PL (1989) Reduced product formation following perturbation of ethanol- and propionate-fed methanogenic CSTRs. *Biotechnology and Bioengineering* **34**: 885-895.

13. Spirito CM, Richter H, Rabaey K, Stams AJM, Angenent LT (2014) Chain elongation in anaerobic reactor microbiomes to recover resources from waste. *Current Opinion in Biotechnology* **27C**: 115-122.

14. Ding H-B, Tan G-YA, Wang J-Y (2010) Caproate formation in mixed-culture fermentative hydrogen production. *Bioresource Technology* **101**: 9550-9559.

15. Steinbusch KJJ, Hamelers HVM, Plugge CM, Buisman CJN (2011) Biological formation of caproate and caprylate from acetate: fuel and chemical production from low grade biomass. *Energy and Environmental Science* **4**: 216.

16. Agler MT, Spirito CM, Usack JG, Werner JJ, Angenent LT (2012) Chain elongation with reactor microbiomes: upgrading dilute ethanol to medium-chain carboxylates. *Energy and Environmental Science* **5**: 8189-8192.

17. Steinbusch KJJ, Hamelers HVM, Buisman CJN (2008) Alcohol production through volatile fatty acids reduction with hydrogen as electron donor by mixed cultures. *Water Research* **42**: 4059-4066.

18. Steinbusch KJJ, Hamelers HVM, Schaap JD, Kampman C, Buisman CJN (2010) Bioelectrochemical ethanol production through mediated acetate reduction by mixed cultures. *Environmental Science and Technology* **44**: 513-517.

19. Steinbusch KJJ, Arvaniti E, Hamelers HVM, Buisman CJN (2009) Selective inhibition of methanogenesis to enhance ethanol and n-butyrate production through acetate reduction in mixed culture fermentation. *Bioresource Technology* **100**: 3261-3267.

20. Rabaey K, Rodríguez J, Blackall LL, Keller J, Gross P, et al. (2007) Microbial ecology meets electrochemistry: electricity-driven and driving communities. *The ISME journal* **1**: 9-18.

21. Temudo MF (2008) Directing product formation by mixed culture fermentation. Delft, The Netherlands: T. U. Delft. 122 p.

22. Zoetemeyer RJ, Vandenheuvel JC, Cohen A (1982) pH influence in acidogenic dissimilation of glucose in an anaerobic digester. *Water Research* **16**: 303-311.

23. Horiuchi JI, Shimizu T, Tada K, Kanno T, Kobayashi M (2002) Selective production of organic acids in anaerobic acid reactor by pH control. *Bioresource Technology* **82**: 209-213.

24. Fang HHP, Liu H (2002) Effect of pH on hydrogen production from glucose by a mixed culture. *Bioresource Technology* **82**: 87-93.

25. Rodríguez J, Lema JM, Kleerebezem R (2008) Energy-based models for environmental biotechnology. *Trends in Biotechnology* **26**: 366-374.

26. Schrödinger E (1945) What is life? The physical aspect of the living cell. Cambridge Eng. New York: The University press; The Macmillan company. viii, 91 p.

27. Trevors JT (2010) Generalizations about bacteriology: thermodynamic, open systems, genetic instructions, and evolution. *Antonie van Leeuwenhoek Journal of Microbiology* **97**: 313-318.

28. Trevors JT (2010) Perspective: Researching the transition from non-living to the first microorganisms: Methods and experiments are major challenges. *Journal of Microbiological Methods* **81**: 259-263.

29. von Stockar U, Maskow T, Liu J, Marison IW, Patiño R (2006) Thermodynamics of microbial growth and metabolism: an analysis of the current situation. *Journal of Biotechnology* **121**: 517-533.

30. Kleerebezem R, Stams AJM (2000) Kinetics of syntrophic cultures: a theoretical treatise on butyrate fermentation. *Biotechnology and Bioengineering* **67**: 529-543.

31. Hoehler TM, Amend JP, Shock EL (2007) A "follow the energy" approach for astrobiology. Astrobiology **7**: 819-823.

32. Nealson KH, Tsapin A, Storrie-Lombardi M (2002) Searching for life in the Universe: unconventional methods for an unconventional problem. *International Microbiology* **5**: 223-230.

33. Heijnen JJ, Romein B (1995) Derivation of kinetic equations for growth on single substrates based on general properties of a simple metabolic network. *Biotechnology Progress* **11**: 712-716.

34. Desmond-Le Quemener E, Bouchez T (2014) A thermodynamic theory of microbial growth. *ISME Journal* **8**: 1747-1751.

35. Heijnen JJ (2001) Stoichiometry and kinetics of microbial growth from a thermodynamic perspective. In: Ratledge C, Kristiansen B, editors. Basic biotechnology. Second ed. Cambridge: Cambridge University Press.

36. Heijnen JJ, Van Dijken JP (1992) In search of a thermodynamic description of biomass yields for the chemotrophic growth of microorganisms. *Biotechnology and Bioengineering* **39**: 833-858.

37. Russell JB, Cook GM (1995) Energetics of bacterial growth: balance of anabolic and catabolic reactions. *Microbiological Reviews* **59**: 48-62.

38. Dauner M, Storni T, Sauer U (2001) Bacillus subtilis metabolism and energetics in carbon-limited and excess-carbon chemostat culture. *Journal of Bacteriology* **183**: 7308-7317.

39. Kempes CP, Dutkiewicz S, Follows MJ (2012) Growth, metabolic partitioning, and the size of microorganisms. *Proceedings of the National Academy of Sciences of the United States of America* **109**: 495-500.

40. Schuster S, Pfeiffer T, Fell DA (2008) Is maximization of molar yield in metabolic networks favoured by evolution? *Journal of Theoretical Biology* **252**: 497-504.

41. Lane N, Martin W (2010) The energetics of genome complexity. *Nature* **467**: 929-934.

42. Rothschild LJ, Mancinelli RL (2001) Life in extreme environments. *Nature* **409**: 1092-1101.

43. Curtis TP, Head IM, Lunn M, Woodcock S, Schloss PD, et al. (2006) What is the extent of prokaryotic diversity? *Philosophical Transactions of the Royal Society of London Series B, Biological Sciences* **361**: 2023-2037.

44. Uratani J, Kumaraswamy R, Rodríguez J (2014) A systematic strain selection approach for halotolerant and halophilic bioprocess development: a review. *Extremophiles* **18**: 629-639.

45. Curtis TP, Sloan WT, Scannell JW (2002) Estimating prokaryotic diversity and its limits. *Proceedings of the National Academy of Sciences of the United States of America* **99**: 10494-10499.

46. Ward BB (2002) How many species of prokaryotes are there? *Proceedings of the National Academy of Sciences of the United States of America* **99**: 10234-10236.

47. Hoehler TM, Jørgensen BB (2013) Microbial life under extreme energy limitation. *Nature Reviews Microbiology* **11**: 83-94.

48. Jackson BE, McInerney MJ (2002) Anaerobic microbial metabolism can proceed close to thermodynamic limits. *Nature* **415**: 454-456.

49. Hoehler TM (2004) Biological energy requirements as quantitative boundary conditions for life in the subsurface. *Geobiology* **2**: 205-215.

50. Schink B (1997) Energetics of syntrophic cooperation in methanogenic degradation *Microbiology and Molecular Biology Reviews* **61**: 262-280.

51. Reich JG, Selkov EE (1981) Energy metabolism of the cell: a theoretical treatise. Academic Press London. 345 p.

52. Elston T, Wang H, Oster G (1998) Energy transduction in ATP synthase. *Nature* **391**: 510-513.

53. Thauer RK, Jungermann K, Decker K (1977) Energy conservation in chemotrophic anaerobic bacteria. *Bacteriological Reviews* **41**: 809.

54. Mitchell P (1961) Coupling of phosphorylation to electron and hydrogen transfer by a chemi-osmotic type of mechanism. *Nature* **191**: 144-148.

55. Sapra R, Bagramyan K, Adams MWW (2003) A simple energy-conserving system: proton reduction coupled to proton translocation. *Proceedings of the National Academy of Sciences of the United States of America* **100**: 7545-7550.

56. White D (2007) The physiology and biochemistry of prokaryotes. New York: Oxford University Press. 628 p.

57. Toei M, Gerle C, Nakano M, Tani K, Gyobu N, et al. (2007) Dodecamer rotor ring defines H+/ATP ratio for ATP synthesis of prokaryotic V-ATPase from Thermus thermophilus. *Proceedings of the National Academy of Sciences of the United States of America* **104**: 20256-20261.

58. Tran QH, Unden G (1998) Changes in the proton potential and the cellular energetics of Escherichia coli during growth by aerobic and anaerobic respiration or by fermentation. *European journal of biochemistry FEBS* **251**: 538-543.

59. ten Brink B, Konings WN (1982) Electrochemical proton gradient and lactate concentration gradient in Streptococcus cremoris cells grown in batch culture. *Journal of Bacteriology* **152**: 682-686.

60. Heijnen JJ, Kleerebezem R (2010) Bioenergetics of microbial growth. Encyclopedia of Industrial Biotechnology: Bioprocess, Bioseparation and Cell Technology. pp. 1-24.

61. Kleerebezem R, van Loosdrecht MCM (2010) A Generalized Method for Thermodynamic State Analysis of Environmental Systems. *Critical Reviews in Environmental Science and Technology* **40**: 1-54.

62. Broda E (1977) Two kinds of lithotrophs missing in nature. *Zeitschrift für Allgemeine Mikrobiologie* **17**: 491-493.

63. Werner JJ, Knights D, Garcia ML, Scalfone NB, Smith S, et al. (2011) Bacterial community structures are unique and resilient in full-scale bioenergy systems. *Proceedings of the National Academy of Sciences* **108**: 4158-4163

64. McCarty PL, Bae J (2011) Model to Couple Anaerobic Process Kinetics with Biological Growth Equilibrium Thermodynamics. *Environmental Science and Technology* **45**: 6838-6844.

65. Wintermute EH, Silver PA (2010) Dynamics in the mixed microbial concourse. *Genes and Development* **24**: 2603-2614.

66. Covert MW, Famili I, Palsson BO (2003) Identifying constraints that govern cell behavior: a key to converting conceptual to computational models in biology? *Biotechnology and Bioengineering* **84**: 763-772.

67. Temudo MF, Muyzer G, Kleerebezem R, van Loosdrecht MC (2008) Diversity of microbial communities in open mixed culture fermentations: impact of the pH and carbon source. *Applied Microbiology and Biotechnology* **80**: 1121-1130.

68. Rodríguez J, Kleerebezem R, Lema JM, van Loosdrecht MCM (2006) Modeling product formation in anaerobic mixed culture fermentations. *Biotechnology and Bioengineering* **93**: 592-606.

69. Lane N, Martin WF, Raven JA, Allen JF (2013) Energy, genes and evolution: introduction to an evolutionary synthesis. *Philosophical Transactions of the Royal Society of London Series B, Biological Sciences* **368**: 20120253.

70. Pfeiffer T, Schuster S, Bonhoeffer S (2001) Cooperation and competition in the evolution of ATP-producing pathways. *Science* **292**: 504-507.

71. Seitz J, Schink B, Pfennig N, Conrad R (1990) Energetics of syntrophic ethanol oxidation in defined chemostat cocultures. *Archives of Microbiology* **155**: 89-93.

72. Schink B (2006) Syntrophism among Prokaryotes. The Prokaryotes, Vol 2. New York: Martin Dworkin. pp. 309-335.

73. Stams AJM, Plugge CM (2009) Electron transfer in syntrophic communities of anaerobic bacteria and archaea. *Nature Reviews Microbiology* **7**: 568-577.

74. Pfeiffer T, Bonhoeffer S (2004) Evolution of cross-feeding in microbial populations. *The American naturalist* **163**: E126-135.

75. van De Leemput IA, Veraart AJ, Dakos V, Klein JJMD, Strous M, et al. (2011) Predicting microbial nitrogen pathways from basic principles. *Environmental Microbiology* **13**: 1477-1487.

76. van der Star W (2008) Growth and Metabolism of Anammox Bacteria. Delft, The Netherlands: T. U. Delft. 162 p.

77. Roubos JA (2002) Bioprocess modelling and optimization. Fed-batch Clavulanic Acid production by Streptomyces clavuligerus. Delft, The Netherlands: T.U. Delft. 320 p.

78. Rodríguez J (2006) Modelling anaerobic mixed culture fermentations. Santiago de Compostela, Spain: U. Santiago de Compostela 236 p.

79. Karr JR, Sanghvi JC, Macklin DN, Gutschow MV, Jacobs JM, et al. (2012) A whole-cell computational model predicts phenotype from genotype. *Cell* **150**: 389-401.

80. Heijnen JJ, van Loosdrecht MCM, Tijhuis L (1992) A Black Box Mathematical Model to Calculate Auto- and Heterot rophic Biomass Yields Based on Gibbs Energy Dissipation. *Biotechnology and Bioengineering* **40**: 1139-1154.

81. te Braake HAB, van Can HJL, Verbruggen HB (1998) Semi-mechanistic modeling of chemical processes with neural networks. *Engineering Applications of Artificial Intelligence* **11**: 507-515.

82. Henze M, Gujer W, Mino T, van Loosdrecht MCM (2000) Activated sludge models ASM1, ASM2, ASM2d and ASM3. Iwa Task Group on Mathematical Modelling for Design. 128 p.

83. Batstone DJ, Keller J, Angelidaki I, Kalyuzhnyi SV, Pavlostathis SG, et al. (2002) The IWA Anaerobic Digestion Model No 1 (ADM1). *Water Science and Technology* **45**: 65-73.

84. Baek SH, Jeon SK, Pagilla K (2009) Mathematical modeling of aerobic membrane bioreactor (MBR) using activated sludge model no. 1 (ASM1). *Journal of Industrial and Engineering Chemistry* **15**: 835-840.

85. Vrecko D, Gernaey KV, Rosen C, Jeppsson U (2006) Benchmark Simulation Model No 2 in Matlab-Simulink: towards plant-wide WWTP control strategy evaluation. *Water Science and Technology* **54**: 65-65.

86. Smets IY, Haegebaert JV, Carrette R, Van Impe JF (2003) Linearization of the activated sludge model ASM1 for fast and reliable predictions. *Water Research* **37**: 1831-1851.

87. Keskitalo J, la Cour Jansen J, Leiviska K (2010) Calibration and validation of a modified ASM1 using long-term simulation of a full-scale pulp mill wastewater treatment plant. *Environmental Technology* **31**: 555-566.

88. Ostace GS, Cristea VM, Agachi PŞ (2011) Cost reduction of the wastewater treatment plant operation by MPC based on modified ASM1 with two-step nitrification/denitrification model. *Computers and Chemical Engineering* **35**: 2469-2479.

89. Petersen B, Gernaey K, Henze M, Vanrolleghem PA (2002) Evaluation of an ASM1 model calibration procedure on a municipal-industrial wastewater treatment plant. *Journal of Hydroinformatics* **3**: 15-38.

90. Siegrist H, Vogt D, Garcia-Heras JL, Gujer W (2002) Mathematical Model for Meso- and Thermophilic Anaerobic Sewage Sludge Digestion. *Environmental Science and Technology* **36**: 1113-1123.

91. Kalyuzhnyi SV (1997) Batch anaerobic digestion of glucose and its mathematical modeling. II. Description, verification and application of model. *Bioresource Technology* **59**: 249-258.

92. Angelidaki I, Ellegaard L, Ahring BK (1993) A mathematical model for dynamic simulation of anaerobic digestion of complex substrates: Focusing on ammonia inhibition. *Biotechnology and Bioengineering* **42**: 159-166.

93. Siegrist H, Renggli D, Gujer W (1993) Mathematical modelling of anaerobic mesophilic sewage sludge treatment. *Water Science and Technology* **27**: 25-36.

94. Batstone DJ, Keller J, Steyer JP (2006) A review of ADM1 extensions, applications, and analysis: 2002–2005. *Water Science and Technology* **54**: 1.

95. García-Gen S, Lema JM, Rodríguez J (2013) Generalised modelling approach for anaerobic co-digestion of fermentable substrates. *Bioresource Technology* **147**: 525-533.

96. Donoso-Bravo A, Mailier J, Martin C, Rodríguez J, Aceves-Lara CA, et al. (2011) Model selection, identification and validation in anaerobic digestion: A review. *Water Research* **45**: 5347-5364.

97. Penumathsa BKV, Premier GC, Kyazze G, Dinsdale R, Guwy AJ, et al. (2008) ADM1 can be applied to continuous bio-hydrogen production using a variable stoichiometry approach. *Water Research* **42**: 4379-4385.

98. Parker WJ (2005) Application of the ADM1 model to advanced anaerobic digestion. *Bioresource Technology* 96: 1832-1842.

99. Kleerebezem R, van Loosdrecht MCM (2006) Critical analysis of some concepts proposed in ADM1. *Water Science and Technology* **54**: 51-57.

100. Batstone DJ, Amerlinck Y, Ekama G, Goel R, Grau P, et al. (2012) Towards a generalized physicochemical framework. *Water Science and Technology* **66**: 1147-1161.

101. Blumensaat F, Keller J (2005) Modelling of two-stage anaerobic digestion using the IWA Anaerobic Digestion Model No. 1 (ADM1). *Water Research* **39**: 171-183.

102. Pavlostathis SG, Giraldo-Gomez E (1991) Kinetics of anaerobic treatment: A critical review. *Critical Reviews in Environmental Control* **21**: 411-490.

103. Snoep JL, Mrwebi M, Schuurmans JM, Rohwer JM, Teixeira de Mattos MJ (2009) Control of specific growth rate in Saccharomyces cerevisiae. *Microbiology* **155**: 1699-1707.

104. Liu Y (2007) Overview of some theoretical approaches for derivation of the Monod equation. *Applied Microbiology and Biotechnology* **73**: 1241-1250.

105. Mosey FE, Matter O (1983) Mathematical modelling of the anaerobic digestion process: Regulatory mechanisms for the formation of short-chain volatile acids from glucose. *Water Science and Technology* **15**: 209-232.

106. McCarty PL, Mosey FE (1991) Modelling of anaerobic digestion processes (a discussion of concepts). *Water Science and Technology* **24**: 17-33.

107. Rodríguez J, Lema JM, van Loosdrecht MCM, Kleerebezem R (2006) Variable stoichiometry with thermodynamic control in ADM1. *Water Science and Technology* **54**: 101-110.

108. Vallino JJ (2003) Modeling microbial consortiums as distributed metabolic networks. *The Biological bulletin* **204**: 174-179.

109. Rodríguez J, Premier GC, Guwy AJ, Dinsdale R, Kleerebezem R (2009) Metabolic models to investigate energy limited anaerobic ecosystems. *Water Science and Technology* **60**: 1669-1675.

110. Zhang F, Zhang Y, Chen M, van Loosdrecht MCM, Zeng RJ (2013) A modified metabolic model for mixed culture fermentation with energy conserving electron bifurcation reaction and metabolite transport energy. *Biotechnology and Bioengineering* **110**: 1884-1894.

111. Stams AJM (1994) Metabolic interactions between anaerobic bacteria in methanogenic environments. *Antonie van Leeuwenhoek Journal of Microbiology* **66**: 271-294.

112. Canelas AB, van Gulik WM, Heijnen JJ (2008) Determination of the cytosolic free NAD/NADH ratio in Saccharomyces cerevisiae under steady-state and highly dynamic conditions. *Biotechnology and Bioengineering* **100**: 734-743.

113. Kleerebezem R, Rodríguez J, Temudo MF, van Loosdrecht MCM (2008) Modeling mixed culture fermentations; the role of different electron carriers. *Water Science and Technology* **57**: 493-497.

114. Lee H-S, Krajmalinik-Brown R, Zhang H, Rittmann BE (2009) An electron-flow model can predict complex redox reactions in mixed-culture fermentative BioH 2 : Microbial ecology evidence. *Biotechnology and Bioengineering* **104**: 687-697.

115. Hoelzle RD, Virdis B, Batstone DJ (2014) Regulation mechanisms in mixed and pure culture microbial fermentation. *Biotechnology and Bioengineering* **111**: 2139-2154.

116. Payot S, Guedon E, Cailliez C, Gelhaye E, Petitdemange H (1998) Metabolism of cellobiose by Clostridium cellulolyticum growing in continuous culture: evidence for decreased NADH reoxidation as a factor limiting growth. *Microbiology* **144**: 375-384.

117. Jol SJ, Kümmel A, Hatzimanikatis V, Beard Da, Heinemann M (2010) Thermodynamic calculations for biochemical transport and reaction processes in metabolic networks. *Biophysical Journal* **99**: 3139-3144.

118. Otto R, Sonnenberg AS, Veldkamp H, Konings WN (1980) Generation of an electrochemical proton gradient in Streptococcus cremoris by lactate efflux. *Proceedings of the National Academy of Sciences of the United States of America* **77**: 5502-5506.

119. ten Brink B, Otto R, Hansen UP, Konings WN (1985) Energy recycling by lactate efflux in growing and nongrowing cells of Streptococcus cremoris. *Journal of Bacteriology* **162**: 383-390.

120. Maskow T, von Stockar U (2005) How reliable are thermodynamic feasibility statements of biochemical pathways? *Biotechnology and Bioengineering* **92**: 223-230.

121. Walter A, Gutknecht J, Carolina N (1986) Permeability of small non-electrolytes through lipid bilayer *Membranes* **217**: 207-217.

USC
UNIVERSIDADE
DE SANTIAGO
DE COMPOSTELA

2

Basis towards an accurate description of physicochemical reactions when modelling bioprocesses

Abstract

Even if mathematical models in biotechnology are rapidly evolving towards a better description of microbial activities, the physicochemical reactions mechanistically well-known occurring concomitantly and affecting all the system, are in many cases erroneously neglected or approached with not accurate empirical models. This work presents an implicit algorithm for simple implementation of a generalized model to calculate all the activities of all the forms of the chemical species in liquid solution as well as the pH and the ionic strength of the medium. B-dot and Davies equations have been used for the calculation of the different activity coefficients.

The model response is analysed for several cases such as a liquid solution of phosphates and an example of the typical anaerobic digestion liquid bulk considering pH as a variable or an input in the model. The conclusions obtained shows that in conditions when pH is known and/or the ionic strength and pH are low, the consideration of an ideal solution could be a well compromised description. In this case, ionic strength can still be approached and it correction could be applied when required (e.g. if Gibbs energy values calculations are needed). However, in cases where ionic chemical species are present in elevated concentrations in the liquid bulk (e.g. in a phosphate solution), the model has to strictly consider non-ideality in order to approximate a realistic pH, ionic strength and chemical species concentrations. Moreover, the non-ideality correction has been proven of importance when total and partial alkalinities calculation is of interest.

2.1 Introduction

Bioprocesses are typically characterized by different chemical reactions taking place at different rates and with components in different phases (solid, liquid, gas) [1]. The microbial activity of the culture modifies the environmental conditions in the reactor in interaction with physicochemical processes that at the same time might promote or inhibit the biocatalysed reactions.

Changes in physicochemical conditions can lead to major impacts on the process bioreactions [2]. A drop on pH leading to a fast accumulation of free acids inhibiting the activity of a microbial population, or a rise in pH leading to a sudden increase in free ammonia inhibitory effect for some microorganisms are examples of these effects [3]. Other processes such as precipitation of specific components could affect the microbial activity [4].

In recent years very comprehensive mathematical models to describe and control microbial bioprocesses have been developed and widely applied [5]. Many of the models have been however extensively focused on improving the description of different microbial activities while the physicochemical reactions occurring concomitantly might have been to some extent overlooked or described through rudimentary or largely empirical approaches [6].

Although many uncertainties and questions remain regarding the activity of microorganisms, physicochemical processes are well-known [7], and accurate models to describe them are available. However, assumptions as which physicochemical processes have low impact on the microbial activities, have led to the marginalisation of their detailed description in models where, on the other hand, big efforts on analysing microbial activity aspects have been applied. Recent coordinated works have started addressing this as well as the need for a consensual, accurate and useful framework to describe physicochemistry in bioprocesses [6].

The accurate description of any physical or chemical reaction taking place in a bioprocess and therefore the ability to quantify its overall impact on the system is a requirement of any mathematical model aiming at a reliable prediction of the behaviour of a particular system. The lack of such adequate physicochemical

modelling can lead often to wasted effort in calibration of microbial related parameters of an incomplete or inaccurate model structure.

This study contributes to the development of an accurate but simple physicochemical model by providing a generalised framework for the calculation of all acid-base related chemical speciation either including or excluding ion activity corrections in the context of different values of the ionic strength.

2.2 Modelling acid-base speciation in aqueous phase

Acid-base and hydration reactions (Figure 2.1) are comparatively much faster than biological reactions occurring concomitantly in a reactor. For this reason, the approximation that considers equilibrium of these processes as constant is in most of the cases appropriate. pH stabilizes around seconds, thus the dynamic modelling of the acid-base and hydrolysis processes could be only necessary for exceptional applications.

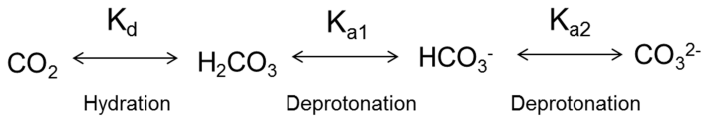

Figure 2.1 Equilibrium reactions for inorganic carbon in liquid solution as example.

Assuming that these aqueous equilibriums are instantaneous, an algebraic routine is consider for calculating the concentrations of all the chemical species present in the liquid solution. Thus, the concentrations of all the non-deprotonated and deprotonated forms are not time dependent.

In a similar way that presented in Batstone et al. [1], we advocate for assuming the dynamic variables of the model as the total sum of concentrations of the chemical components forms in the same phase. Therefore, the calculation of all the forms concentrations could be approximated in each step of simulated time through the algebraic routine. This permits to reduce the number of dynamic variables of the model and thereby, the number of differential equations and problems related to stiffness [8]. In Table 2.1 is presented as example, the chemical forms of the inorganic carbon in liquid phase.

Table 2.1 Different forms of total inorganic carbon state

STATE	FORMS			
Total Inorganic Carbon *(liquid phase)* $IC = \sum_{i=1}^{4}[Form_i]$	Not hydrated CO_2	Fully protonated H_2CO_3	1st deprotonation HCO_3^-	2nd deprotonation CO_3^{2-}

2.3 Acid-base constants from thermodynamic equilibrium

All the physicochemical reactions occurring in a process tend to thermodynamic equilibrium. When modelling these processes therefore, this equilibrium plays an important role as typically, kinetics of these processes should be controlled by the driving force available. The equilibrium constants (acid-base and hydrolysis equilibrium constants, Henry constants, precipitation constants) define this thermodynamic equilibrium and are used for modelling high number of physicochemical processes typically being necessary parameters in mathematical models. However, in this work is proposed their calculation through the Gibbs energy values of formation at standard conditions that are available for a high number of chemical components (equations 2.1-2.3).

$$\Delta G = \Delta G^0 + R_{th} \cdot T \cdot \ln \prod_i a_i^{\nu_i} \quad 2.1$$

$$\text{with} \quad \Delta G = 0 \qquad -\frac{\Delta G^0}{R_{th} \cdot T} = \ln \prod_i a_i^{\nu_i} = K_{eq} \quad 2.2$$

$$K_{eq} = e^{-\frac{\Delta G^0}{R_{th} \cdot T}} \quad 2.3$$

In equations 2.1-2.3, T refers to the temperature at standard conditions (298.15K) and R_{th} the universal constant of gasses in units of J/mol·K.

Equilibrium constants are dependent on temperature. The equation 2.3 permits its calculation at 298.15 K but when a correction for temperature is needed, van't Hoff approximation could be used directly over the equilibrium constants (equation 2.4) or correcting Gibbs values knowing the enthalpy and the entropy of the chemical components considered at standard conditions

(equation 2.5). Both corrections typically assume that enthalpy and entropy are constants with temperature as, in general, no data is available for all chemical components for all temperatures, and however, the impact of the approximation should be valued [6].

$$\ln\frac{K_{eqA/B(T1)}}{K_{eqA/B(T2)}} = -\frac{\Delta H^0}{R}\left(\frac{1}{T_1}-\frac{1}{T_2}\right) \quad 2.4$$

$$\Delta G^0{}_{(T)} = \Delta H^0{}_{(298.15K)} - T\cdot\Delta S^0{}_{(298.15K)} \quad 2.5$$

2.4 Implicit calculation of pH, ionic strength and species activities and concentration matrixes

Considering acid-base and hydration equilibria as instantaneous in solution, an algebraic routine is used for the calculation of species activities and concentrations, pH and ionic strength. The relation between these variables makes the calculation implicit; pH ($pH = \log_{10}(a_{H^+})$) depends on the concentrations of the chemical species in the solution because it is based on equilibria and the charge balance between the concentrations of all charged species in the liquid solution (equation 2.6).

$$C_{H^+} + \sum_{i=1}^{S} C_i\cdot z_i = 0 \quad 2.6$$

In equation 2.6, z_i is the charge and C_i is the concentration of the i component.

Generalised equations for any number of deprotonations (equations 2.7-2.13) have been derived to calculate the activity of the chemical species in solution (including all deprotonations) which is depending on pH, equilibrium constants (K_d for hydration and Ka_i for deprotonations), activity coefficients and total concentration of each chemical component.

Not hydrated form activity: $$a_{NotHyd} = \frac{K_d}{a_{H_2O}}\cdot\frac{C_T\cdot\left(a_{H^+}\right)^N}{A} \quad 2.7$$

Fully protonated form activity: $$a_{Hyd} = \frac{C_T\cdot\left(a_{H^+}\right)^N}{A} \quad 2.8$$

$$1^{st}\text{ deprotonated form activity: } a_1 = \frac{C_T \cdot Ka_1 \cdot \left(a_{H^+}\right)^{N-1}}{A} \quad 2.9$$

$$2^{nd}\text{ deprotonated form activity: } a_2 = \frac{C_T \cdot Ka_1 \cdot Ka_2 \cdot \left(a_{H^+}\right)^{N-2}}{A} \quad 2.10$$

$$3^{er}\text{ deprotonated form activity: } a_3 = \frac{C_T \cdot Ka_1 \cdot Ka_2 \cdot Ka_3 \cdot \left(a_{H^+}\right)^{N-3}}{A} \quad 2.11$$

$$k^{st}\text{ deprotonated form activity: } a_k = \frac{C_T \cdot \prod_{j=1}^{j=k} Ka_j \cdot (a_{H^+})^{N-j}}{A} \quad 2.12$$

$$A = \left(1 + \frac{K_d}{a_{H_2O}}\right) \cdot (a_{H+})^N + Ka_1 \cdot (a_{H+})^{N-1} + \frac{Ka_1 \cdot Ka_2}{\gamma_1} \cdot (a_{H+})^{N-2} + \frac{Ka_1 \cdot Ka_2 \cdot Ka_3}{\gamma_2} \cdot (a_{H+})^{N-3} + \sum_{k=4}^{k=N} \left(\prod_{j=1}^{j=k} \frac{Ka_j}{\gamma_{j-1}} \cdot (a_{H+})^{N-k} \right) \quad 2.13$$

γ_i is the activity coefficient for the i deprotonation, Ka_i the equilibrium constant for the i deprotonation, and C_T the total concentration of the chemical component including all protonated, partially and fully deprotonated and hydrated forms (e.g. total sum of inorganic carbon present in the liquid solution, Table 2.1).

Different equations to calculate the activity coefficients (γ_i) are available in the literature. Debye-Hückel equations are the most commonly used [9] although they become inaccurate at ionic strengths over 0.1 M [10]. For higher ionic strengths, Davies, B-dot or Pitzer equations must be used [7]. Davies equation (equation 2.14) is reasonably accurate at higher ionic strengths of 0.3 to 0.5 M [10]. B-dot equation (equation 2.15) has a wider range of accuracy considered as a good model at ionic strengths of 1 M but it requires the value of the molecule hard-core diameter or ion size (α_i), that is typically determined by fitting the equation to experimental data [10].

In this work the use of Davies and B-dot equations is proposed in line with the recommendations by Batstone et al. [6]. Pitzer equations are a more accurate option but their complexity and requirement of parameters is much larger than for B-dot equation [7].

$$\log_{10}(\gamma_i) = -A \cdot z_i^2 \cdot \left(\frac{\sqrt{Ic}}{1+\sqrt{Ic}} - 0.3 \cdot I_C \right) \quad 2.14$$

$$\log_{10}(\gamma_i) = -\frac{A \cdot z_i^2 \cdot \sqrt{Ic}}{1 + B \cdot \alpha_i \cdot \sqrt{Ic}} + \dot{B} \cdot I_C \quad 2.15$$

In Davies and B-dot equations, A, B and Ḃ are constants depending only on temperature. Moreover, B-dot equation includes a correction for neutral species ($z_i = 0$), however, for these species, an empirical approximation is typically used instead B-dot equation [7,10].

The use of B-dot equation implies that the approximation to non-ideal description of the solution is accurate but not always the ion size of all the molecules in solution is a known parameter. Figure 2.2 shows, the dependence of activity coefficients with ion size. The impact could be of importance in some cases, but the error seems to be restricted to no more of ± 0.4 units over the gamma value (Figure 2.2). In most cases, assuming an intermediate typical value for the ion size of the species in solution, the error committed could be assumable.

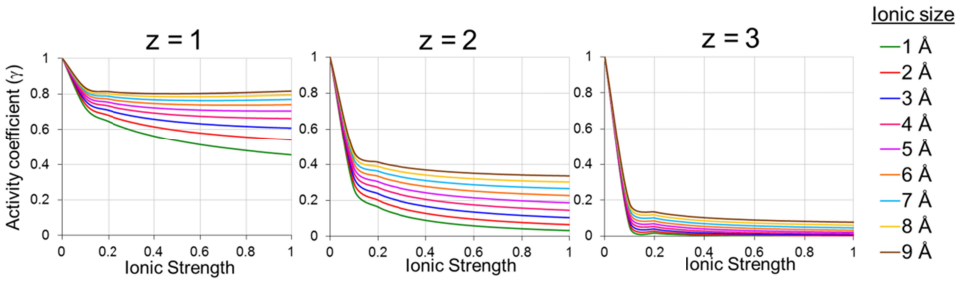

Figure 2. 1 Activity coefficient values (γ) estimated using the B-dot model as function of the ionic strength for and size, considering different ion charges (z).

The ionic strength I_C is calculated with equation 2.16 where C_i refers to the concentrations of the chemical species.

$$I_C = 0.5 \cdot \sum_i C_i \cdot z_i \qquad 2.16$$

In Figure 2.3 the implicit calculation method to solve pH, ionic strength, activity coefficients and activities for all chemical species in the liquid solution is presented. An implicit mathematical method is necessary to solve the algorithm with two nested loops of calculation.

A Newton-Raphson implicit method is highly efficient and simple to implement to resolve the algorithm of Figure 2.3 (it has quadratic convergence implementing the derivatives of equations 2.7-2.13). However, when the pH of the solution is found in the extremes of the feasible range (0-14), the

Newton-Raphson routine could fail due to the presence of non-feasible roots. In these cases, a robust method (the right solution is always found) like bisection method or a most efficient variation of it [11], could be implemented. These methods are slow (they have linear convergence), for this reason they are only recommended to mathematically solve those extreme cases in which Newton-Raphson might fail.

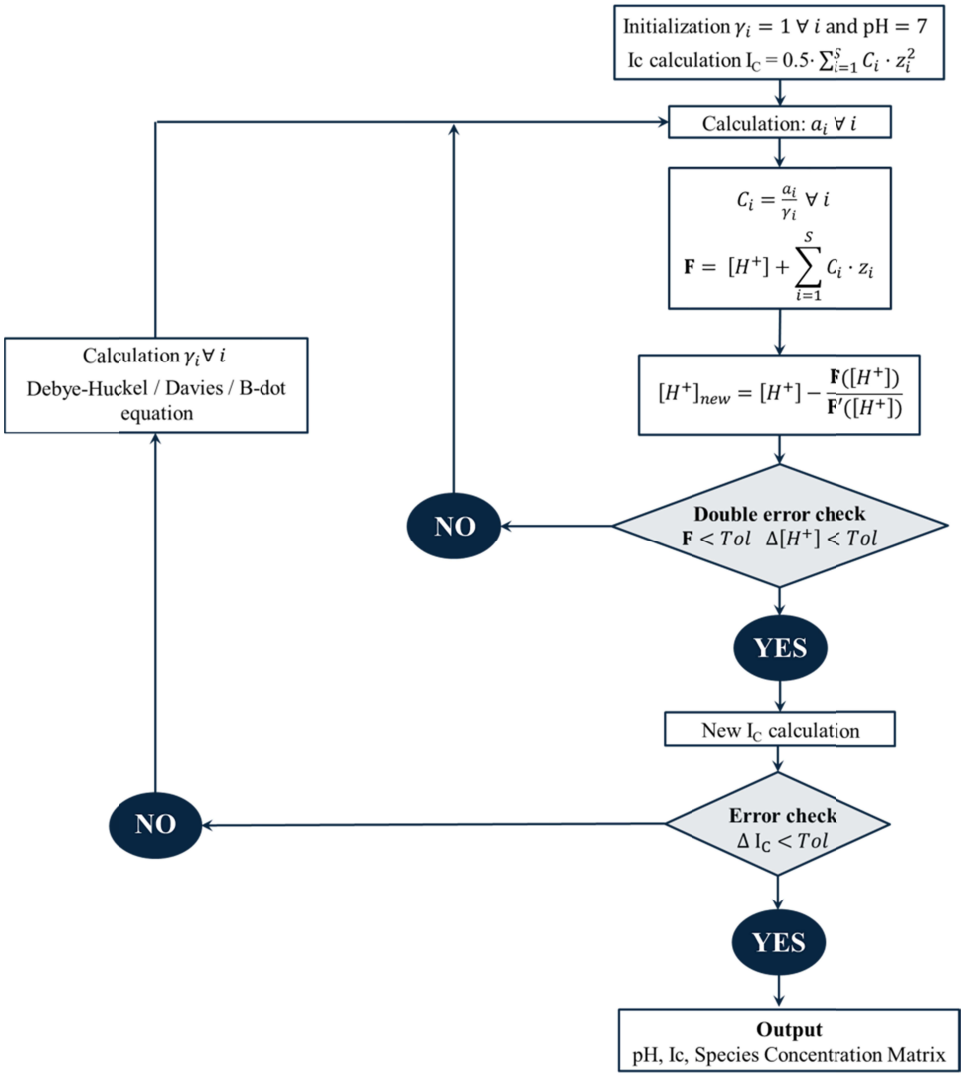

Figure 2.3 Proposed algorithm for the implicit solution of pH, ionic strength and concentrations of all chemical species in solution.

Equations 2.7-2.13 are generalized for all deprotonations and are simple to apply, although, for many applications, the scheme of Figure 2.3 could be reduced, assuming ideal solution. The decision of whether or not to include a description of non-ideal solution in a bioprocess model depends highly on the system and on the intended application of the model (Table 2.2). If the model is to be applied to the description of a system with a high ionic strength, non-ideality correction must be considered. This appears as much more important if a model aims at describing reactions taking place inside cells at intracellular cytoplasmic conditions due to the high concentration of charged species [12]. In most bioprocesses however at low ionic strength, it is recommended to save computing and programing effort assuming that the activity constants to be one [13]. In these cases, the algorithm of Figure 2.3 can be simplified in to one single loop for the solutions of the charge balance and pH leaving the ionic strength loop open.

Table 2.2 Recommended physicochemical modelling approach to different wastewater types in relation with their ionic strengths. Adapted from Batstone et al. 2012 [6].

IONIC STRENGTH (M)	TYPE OF WATER	RECOMMENDED APPROACH
< 0.001	Drinking water	Assumed ideal
< 0.1	Domestic and weak industrial wastewaters	Non ideal behaviour assumed but non-ideality correction for pH calculation is necessary
< 1	Sea water, anaerobic digesters	Non ideal behaviour assumed
	As above, with gas transfer	Non ideal behaviour assumed and non-valent ion correction of B-dot equation should be applied
< 5	Strong industrial, landfill leachate, reverse osmosis brine	Non ideal behaviour assumed and inclusion of specific ion pairs correction should be considered

2.5 Impact of ideal solution model on the bioprocesses description

The errors incurred in when ideal solution models are used, are assessed for a number of cases. From this analysis it becomes evident that depending on the conditions, non-ideality corrections must be incorporated to describe accurately the system.

Solution of phosphates

In Figure 2.4 the relative error incurred when considering ideal solution is presented for a solution of 10 mM total concentration of total phosphates when considering ionic strengths of 0.1, 0.5 and 1 M and pH values of 4, 7 and 9. The ionic strength and the pH considered are set through added concentrations of undefined single charge cations and anions.

The relative error is defined as the difference between the concentrations calculated as accurate as possible with the activity coefficients correction (considering the complete algorithm as per Figure 2.3) and those obtained assuming ideal solution. This difference is normalized over the values obtained considering the non-ideality corrections (equation 2.17).

$$\text{Relative error} = \frac{\aleph_{\text{Non-Ideal}} - \aleph_{\text{Ideal}}}{\aleph_{\text{Non-Ideal}}} \cdot 100\% \qquad 2.17$$

To calculate the values corrected by non-ideality, Davies equation is used for ionic strength of 0.1 M and B-dot equation for ionic strengths of 0.5 and 1. M. For B-dot equation, the values of the constants A, B and Ḃ are obtained from Bethke C.M. [10] at 25 ºC and an ionic size of 4 Å is considered for all species. For non-valent ions, an empirical correction as presented in Bethke C.M. [10] is used to apply the B-dot equation.

The solution analysed in Figure 2.4 containing only phosphates is very sensitive to changes in the charged species concentrations. For this reason, the assumption of ideal solution makes the errors in the concentrations very significant reaching 100% and more in most cases. Considering that the B-dot equation corrects for non-valent species, the error is also reflected in the

non-charged species. As expected, error incurred is much larger at higher ionic strengths and basic pH. Moreover, any errors in the calculation of ionic species concentrations have subsequently an impact on the calculation of the pH in the solution. In Figure 2.5, the pH values calculated considering ideal and non-ideal solution are compared for the three pH values and three ionic strengths.

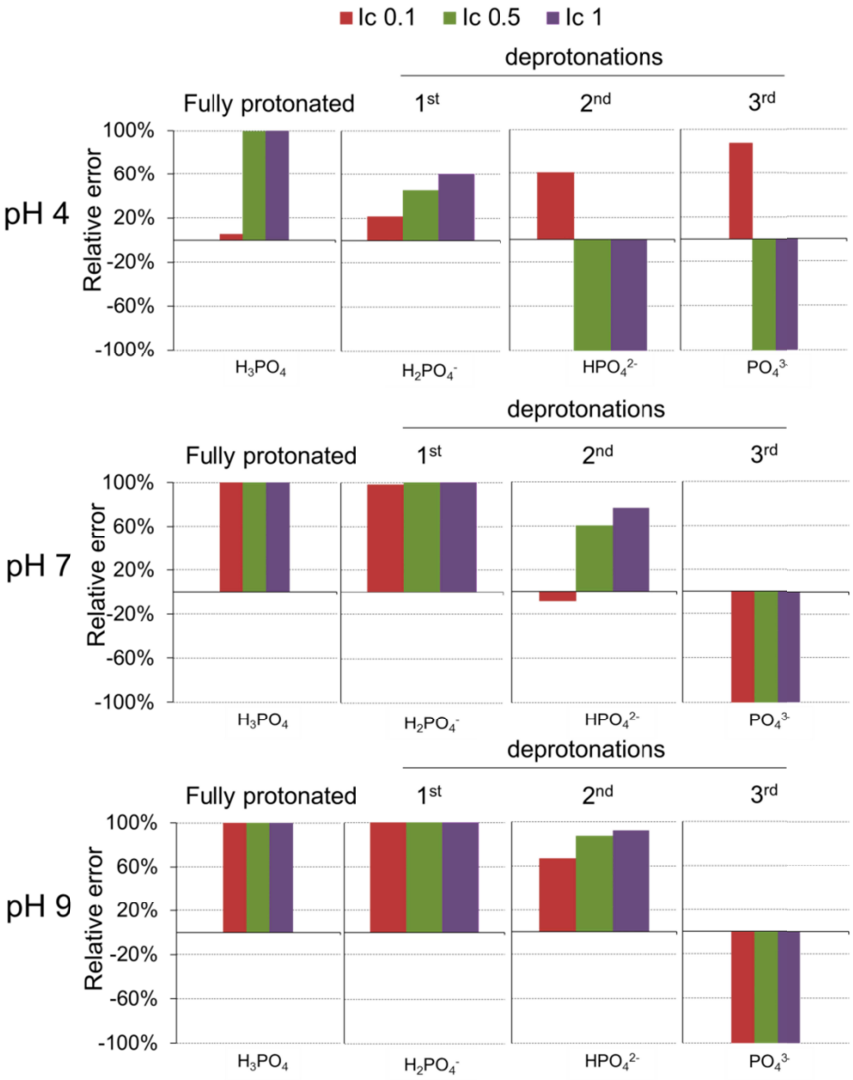

Figure 2.4 Relative errors incurred in the phosphate species concentrations at three different pH and ionic strengths when using the simplification of ideal solution vs. non-ideal solution.

The error clearly increases with a more basic pH of the liquid bulk (**F**igure 2.5). When the pH is acid, and the ionic strength is low, the error could be assumed in some cases but already, at neutral pH values and for any value of the ionic strength, pH calculated considering ideal solution appears to be very much deviated and therefore would not allow for a good physicochemical description of the system.

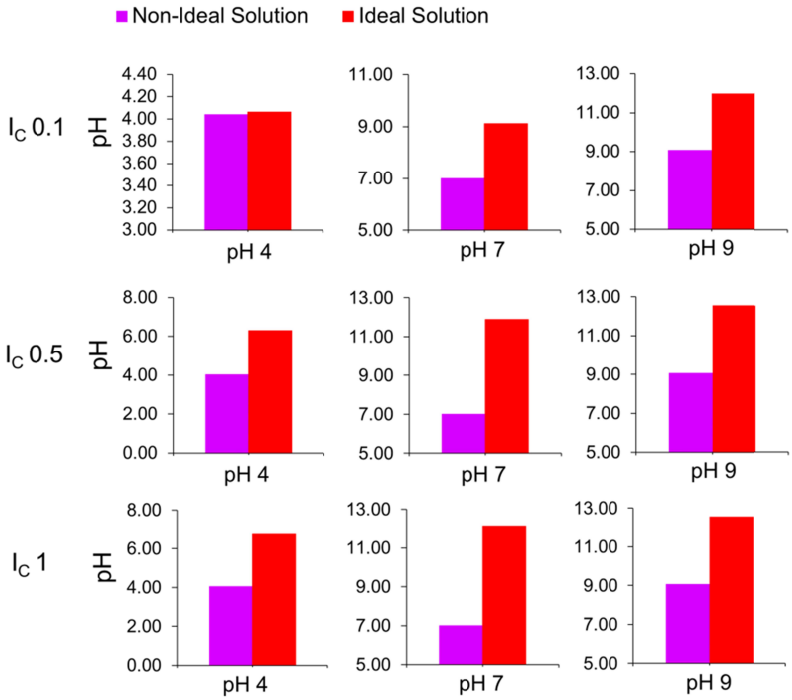

Figure 2.5 Comparison of calculated pH considering the ideal solution simplification vs. non-ideal solution at different ionic strength and pH values in the phosphate media example.

Anaerobic digestion media example

The above incurred errors appear to be smaller when solutions are considered with a lower concentration of highly deprotonated species. In Figure 2.6 the errors incurred between both simplified and non-simplified models are compared (analogously to Figure 2.4) for a water composition example system typical of anaerobic digestion bioreactor. This solution contains 10 mM of total

concentrations for acetic, butyric and lactic acids and their ions as well as for inorganic carbon and ammoniacal nitrogen.

Figure 2.6 Relative errors incurred in the chemical species concentrations at three different pH and ionic strengths when using the simplification of ideal solution vs. non-ideal solution.

Although this example solution appears to be less sensitive to the use of ideal solution simplifications than the above one, again the predicted errors appear as very significant and seem to increase when the pH of the solution increases and with the ionic strength. For low ionic strengths, the incurred errors could be assumed in specific cases but for values of ionic strength above 0.5 M ideal solution simplifications should never be used.

The error in the calculated pH assuming ideal solution (Figure 2.7) is in this case much lower than in the previous case (Figure 2.5). The error could be assumed for all pH values when ionic strength does not exceed 0.1 M and also

could be acceptable at the higher ionic strengths at low pH of 4. However, the simplification of ideal solution does not appear to be tolerable at higher ionic strengths and for neutral or alkaline pH values.

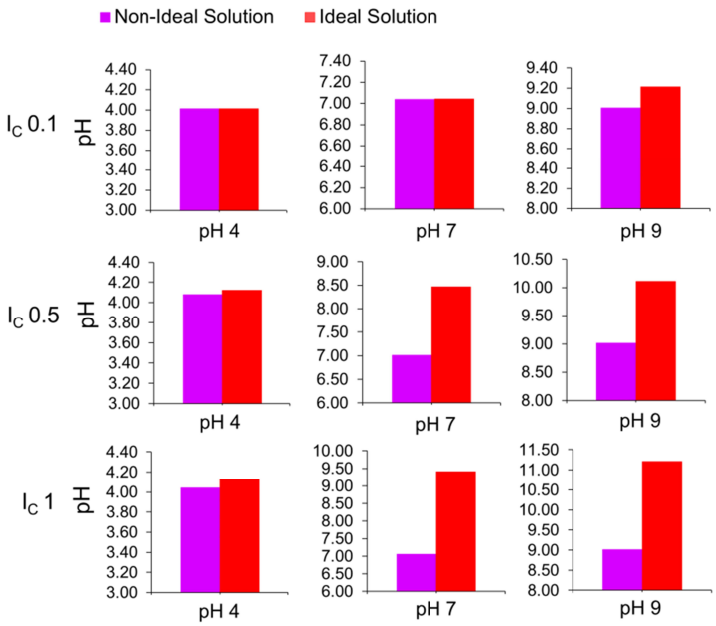

Figure 2.7 Comparison of calculated pH considering ideal solution simplification vs. non-ideal solution at different ionic strength and pH values for the anaerobic digestion media example.

Anaerobic digestion media example with pH experimentally measured

In bioprocess models pH is often considered as a parameter of the model. It could be included in the model as an input, assuming that the pH value does not carry any error (e.g. measured directly in the real process described by the model). In this case, the errors in the calculations of concentrations of soluble chemical components are presumable lower. In Figure 2.8, this is analysed for the example of anaerobic digestion medium.

Figure 2.8 shows that in the case that pH could be included in the model as input, the relative errors incurred with ideal solution are smaller as they are limited only to the species calculation and not to the pH computation itself. The

error becomes important at high values of the ionic strengths and for the most deprotonated forms. For cases with ionic strength as high as 0.5 M it seems however that the solution can still be considered ideal without too large error deviations if the pH is not alkaline. Through this analysis, it becomes clear that the largest relative errors appear for the concentrations of the most deprotonated species, however at non alkaline pH values, the concentrations of these forms are very low, which makes the absolute errors negligible.

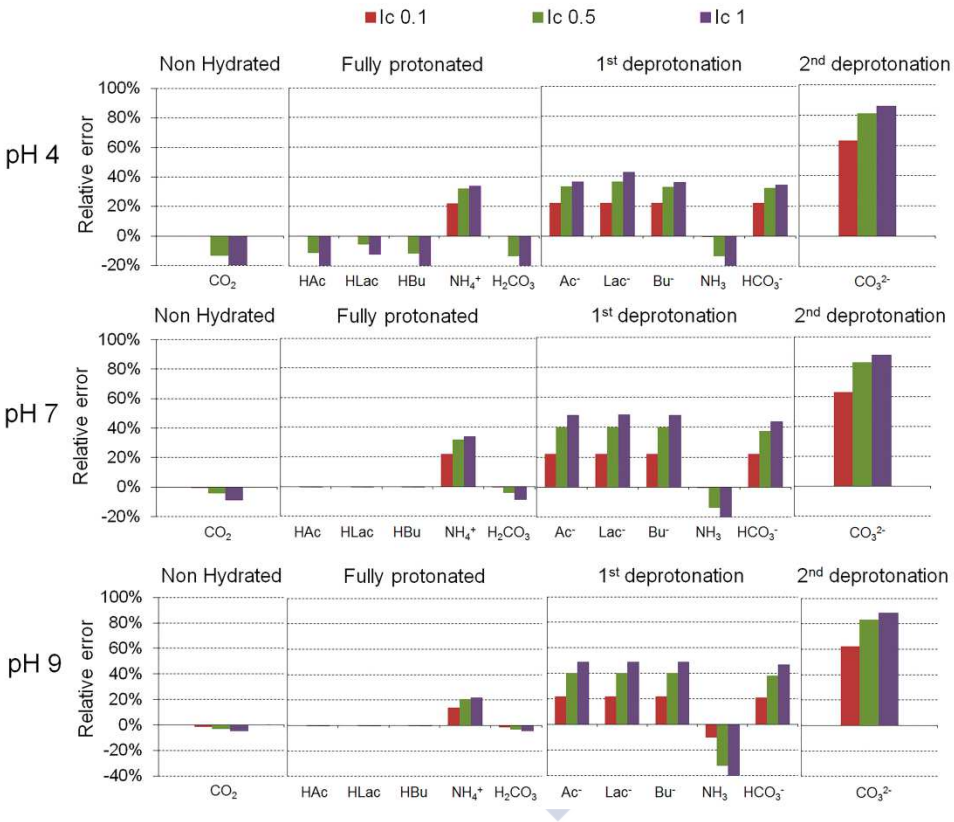

Figure 2.8 Relative errors incurred in the chemical species concentrations at three different ionic strengths and for the case of pH values provided as a measured input when using the simplification of ideal solution vs. non-ideal solution.

2.6 Alkalinity calculations considering ideal and non-ideal solution

It is important to highlight that an accurate description of the physicochemical ionic speciation in solution also affects the predicted alkalinity (total and partial). By comparing calculated alkalinity values considering ideal vs. non-ideal solution, ideal solution brings important errors in (Figure 2.9).

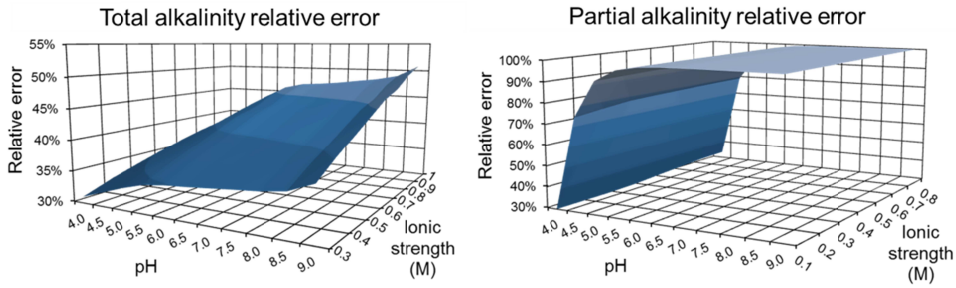

Figure 2.9 Relative errors for partial and total alkalinity considering ideal solution.

Alkalinity is an important parameter typically used in the control of a number of bioprocesses, such as anaerobic digestion [14]. For this reason, even if the errors in the calculated concentrations considering ideal solution could be accepted in some cases (Figure 2.8), if accuracy in alkalinity prediction is required, non-ideality corrections should be necessarily included.

2.7 Ionic strength correction for ideal solution

For the cases in which ideal solution is acceptable to estimate pH and ionic speciation, still the ionic strength of the solution can be approximated by the equation 2.16. Figure 2.10 presents the implicit error incurred when the ionic strength is calculated neglecting its effect on the pH and speciation.

The error on ionic strength presented in Figure 2.10, can be accepted for many applications when the value of the ionic strength solution is lower than 0.1 M. The error would be implicit in the values calculated for the deprotonated forms concentrations and in the alkalinity calculation however, if working at

non-alkaline pH, these differences are normally small and can be accepted always depending on the model application.

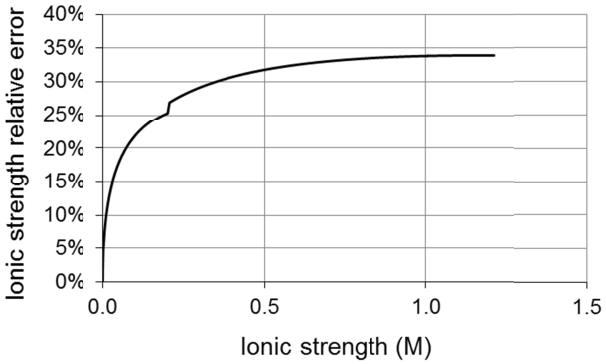

Figure 2.10 Ionic strength relative errors assumed when considering ideal solution for the pH and chemical species concentrations calculations. (The different ionic strengths are obtained assuming different concentrations of undefined single charged anions and cations).

To know the activity coefficients of the chemical species in solution is of importance when the calculation of Gibbs energies is a necessity in the model. However, again is possible to assume ideal solution, to calculate the ionic strength (equation 2.16) and to correct the Gibbs energy calculation accordingly (equation 2.18) [9].

$$\Delta G = \Delta G^{0} + R_{th} \cdot T \cdot \ln \prod_{i} C_{i}^{\nu_i} - 2.303 \cdot R_{th} \cdot T \cdot \left(A \cdot \sum_{i} \nu_i \cdot z_i^{2} \cdot \frac{\sqrt{Ic}}{1 + B \cdot \alpha_i \cdot \sqrt{Ic}} - \dot{B} \cdot I_C \right) \qquad 2.18$$

An example of the error incurred for the calculation of ΔG values if the correction from equation 2.18 is not considered is presented in Figure 2.11 (the graph is symmetric for $\nu_i \cdot z_i^2$ negative values). The error appears as acceptable for applications under low ionic strength. Ionic strength corrections on Gibbs energy calculations appear in any case to be of importance when describing reactions taking place inside a cell in cytoplasmic conditions and/or for cases with reactions close to thermodynamic equilibrium [9].

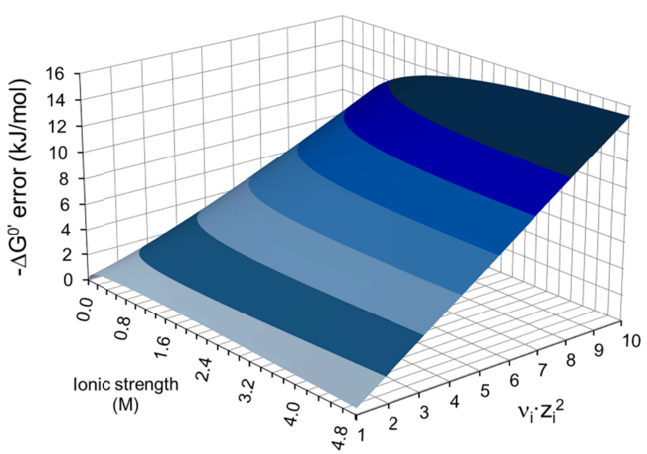

Figure 2.11 Impact of the ionic strength over the ΔG value and function of the term $\nu_i \cdot z_i^2$.

2.8 Conclusions

The fast development of mathematical models for bioprocesses must be accompanied by an accurate description of the physicochemical reactions taking place in these systems. The impact of an accurate description of these reactions is very frequently of comparable or of larger importance than a comprehensive description of the microbial activity.

A detailed mathematical description of the acid-base speciation, physical mechanisms behind precipitation or gas transfer reactions implies implementation and computational costs. It is therefore important to assess previously, based on the intended application, conditions and objectives, what level of accuracy is required. A generalised approach is presented in this work to calculate in full the ionic speciation in terms of concentrations and activities of all chemical species in a solution, as well the ionic strength and the pH of the medium with low implementation and computational efforts. The direct calculation of equilibrium constants from standard Gibbs energy values could also simplify in some cases, the model implementation.

The calculation of activity correction coefficients using B-dot equation is proposed for high ionic strengths, and Davies equation for low. However, the ion size is required for all the molecules in solution if B-dot equation is to be applied. This is not always available and often experimentally fitted, but considering an

average value is acceptable as the error in the activity coefficients appears as constrained to 0.4 units.

Assuming ideal solution in the models has important impacts on pH, chemical species concentrations and alkalinity calculations. It is necessary to consider corrections for non-ideality in solutions with high ionic strength, alkaline pH or when the deprotonated forms play an important role in the system (e.g. when a good description of precipitation processes is needed). In the frequent cases in which pH is measured and can be provided as an input, the errors incurred when assuming ideal solution are smaller as the pH is not affected itself. In these cases and depending on the desired accuracy, ideal solution can be an acceptable approximation.

Therefore, in those applications at not high ionic strength and not very alkaline pH, ideal solution can be assumed thereby simplifying the solution algorithm to a single loop for pH and speciation alone. In these cases the ionic strength can still be approximated with an acceptable error and activity corrections could be applied when the activities of the species w needed (e.g. when calculating Gibbs values).

2.9 References

1. Batstone DJ, Keller J, Angelidaki I, Kalyuzhnyi SV, Pavlostathis SG, et al. (2002) The IWA Anaerobic Digestion Model No 1 (ADM1). *Water Science and Technology* **45**: 65-73.

2. Batstone DJ (2009) Towards a generalised physicochemical modelling framework. *Reviews in Environmental Science and Bio-Technology* **8**: 113-114.

3. Yenigün O, Demirel B (2013) Ammonia inhibition in anaerobic digestion: A review. *Process Biochemistry* **48**: 901-911.

4. Li XZ, Zhao QL (2001) Efficiency of biological treatment affected by high strength of ammonium-nitrogen in leachate and chemical precipitation of ammonium-nitrogen as pretreatment. *Chemosphere* **44**: 37-43.

5. Batstone DJ, Keller J, Steyer JP (2006) A review of ADM1 extensions, applications, and analysis: 2002-2005. *Water Science and Technology* **54**: 1-10.

6. Batstone DJ, Amerlinck Y, Ekama G, Goel R, Grau P, et al. (2012) Towards a generalized physicochemical framework. *Water Science and Technology* **66**: 1147-1161.

7. Wolery TJ (1992) EQ3NR, A Computer Program for Geochemical Aqueous Speciation-Solubility Calculations: Theoretical Manual, User's Guide, and Related Documentation (Version 7.0). Livermore, California: Lawrence Livermore National Laboratory.

8. Rosen C, Vrecko D, Gernaey KV, Pons MN, Jeppsson U (2006) Implementing ADM1 for plant-wide benchmark simulations in Matlab/Simulink. *Water Science and Technology* **54**: 11-19.

9. Maskow T, von Stockar U (2005) How reliable are thermodynamic feasibility statements of biochemical pathways? *Biotechnology and Bioengineering* **92**: 223-230.

10. Bethke CM (1996) Geochemical Reaction Modeling : Concepts and Applications: Oxford University Press.

11. Dowell M, Jarratt P (1972) The "Pegasus" method for computing the root of an equation. *BIT Numerical Mathematics* **12**: 503-508.

12. Noor E, Bar-Even A, Flamholz A, Reznik E, Liebermeister W, et al. (2014) Pathway Thermodynamics Highlights Kinetic Obstacles in Central Metabolism. *PLoS Computational Biology* **10**: e1003483.

13. Ganigue R, Volcke EI, Puig S, Balaguer MD, Colprim J, et al. (2010) Systematic model development for partial nitrification of landfill leachate in a SBR. *Water Science and Technology* **61**: 2199-2210.

14. García-Gen S, Rodríguez J, Lema JM (2014) Optimisation of substrate blends in anaerobic co-digestion using adaptive linear programming. *Bioresource Technology* **173**: 159-167.

USC
UNIVERSIDADE
DE SANTIAGO
DE COMPOSTELA

3

Metabolic energy-based modelling explains product yielding in anaerobic mixed culture fermentations

This chapter has been accepted for publication as:

González-Cabaleiro R, Lema JM, Rodríguez J (2015) Metabolic energy-based modelling explains product yielding in anaerobic mixed culture fermentations. *Plos One*. (Accepted)

Abstract

Fermentation of organic wastes using mixed cultures opens up a promised venue for resources recovery with low operational costs. The use of undefined cultures is technically simple and very effective confronting changes in feed conditions and operative variables. The outcome of these bioprocesses is typically a mixture of carboxylates with intrinsic low value but that within the biorefinery concept are an interesting renewable resource with potential to produce higher valuable chemicals or biofuels. However, the use of mixed cultures still supposes a technological challenge in terms of product yielding optimization due to their unpredictable behaviour. A deeper understanding of the fermentation process involving metabolic and biochemical principles is very necessary to overcome these difficulties.

In this work a novel metabolic energy-based model is presented that accurately predicts for the first time the experimentally observed changes in product spectrum with pH when fermenting glucose. The model predicts the observed shift towards formate production at high pH, accompanied with ethanol and acetate production. Acetate (accompanied with a more reduced product) and butyrate are predicted main products at low pH. The production of propionate between pH 6 and 8 is also predicted. These results are mechanistically explained for the first time considering the impact that variable proton motive potential and active transport energy costs have in terms of energy harvest over different products yielding.

The model results, in line with numerous reported experiments, validate the mechanistic and bioenergetics hypotheses that fermentative mixed cultures products yielding appears to be controlled by the principle of maximum energy harvest and the necessity of balancing the redox equivalents in absence of external electron acceptors.

Table of symbols

References of the main sub-index and super-index used:

ana	*Anabolism*	Gly	*Glycolysis*
Cx	*Carbon of biomass*	out	*Outside the cytoplasm*
d	*Decay*	r	*Reactor*
in	*Inside the cytoplasm*	S	*Substrate*
inf	*Influent of the reactor*	X	*Biomass*
Glu	*Glucose*		

SYMBOL	DEFINITION	UNITS
$\Delta\mu_{H+}$	Proton motive force	kJ/mol_{H+}
$\Delta\mu_{Si}$	Potential associated to a solute transport across the cell membrane	kJ/mol_{Si}
$\Delta\psi$	Membrane potential	V
ΔG	Gibbs energy of a reaction	kJ/mol
ΔG^0	Gibbs energy of a reaction at standard conditions (298.15K, 1 atm, 1M)	kJ/mol
$\Delta G^{0'}$	Gibbs energy of a reaction at standard conditions and pH 7 (298.15K, 1 atm, 1M)	kJ/mol
ΔG_{ATP}	Energy associated to one mol of ATP hydrolysis	kJ/mol_{ATP}
ΔG_{min}	Minimum energy required for a metabolic reaction to occur	kJ/mol
δ_x	Thickness of the cell membrane	m
ν	Stoichiometric coefficient	-
χ_i	Optimized coefficient for predicted microbial activity i	-
$\mathbf{D}_i$	Diffusion coefficient of component i	m^2/h
$C_{eq,i}$	Equilibrium concentration between liquid and gas phase of i component	$mol_{Si}/L{\cdot}h$
$Diff_i$	Coefficient of passive diffusion across of the i component the cell membrane	$L/mol_{Cx}{\cdot}h$

SYMBOL	DEFINITION	UNITS
F	Faraday constant	kC/mol_{e^-}
G_i	Reactor concentration of gasseous i component	mol_{Gi}/L
K_{ATP}	Constant associated to model anabolismrate	$kJ \cdot mol_{Cx}/mol_{Glu} \cdot h$
K_{Na+}	Constant associated to model the sodium pump	-
K_T	Half saturation constant of active transports	mol_{Si}/L
Ks	Half saturation constant of metabolic reactions	mol_{Si}/L
P	Total pressure of the system	atm
Q_{gas}	Gas flow rate out of the reactor	L_{gas}/h
Q_{liq}	Influent and effluent liquid flow rate of the reactor	L_r/h
R_i	Net reaction generation term of component i	$mol_{Si}/L \cdot h$
R_g	Universal gas constant	$L \cdot atm/K \cdot mol$
R_{th}	Universal gas constant	$kJ/K \cdot mol$
$R_{T,i}$	Net transport across the membrane term of component i	$mol_{Si}/L_x \cdot h$
S_{Glu}	Reactor concentration of glucose	mol_{Glu}/L_r
S_i	Reactor concentration of dissolved component i	mol_{Si}/L_r
SRT	Solids retention time	h
T	Temperature	K
V_{gas}	Volume of head space of the reactor	L
V_{liq}	Volume of the liquid inside the reactor	L_r
V_r	Working volume of the reactor	L
V_X	Biomass volume in the reactor	L_x
X	Biomass concentration in the reactor	mol_{Cx}/L_r
a_i	Activity of the i chemical component	mol_{Si}/L
a_x	Specific area of the cell membrane	$m^2/kmol_{Cx}$
f	Factor of thermodynamic feasibility	-
f_{ana}	Factor of energy availability for growth	-

SYMBOL	DEFINITION	UNITS
f_d	Factor of energy scarcity and population decay	-
k_d	Kinetic constant of decay process	h^{-1}
k_La	Coefficient of transference between liquid and gas phases	h^{-1}
m_G	Specific maintenance energy requirement	$kJ/mol_{Cx}·h$
n_{gas-G}	Total gas production rate	mol_{gas}/h
$p_{gas,i}$	Partial pressure of gas i	atm
p_{H2O}	Partial pressure of water vapour	atm
q_S^{cat}	Specific substrate uptake rate for catabolism	$mol_{eD}/mol_{Cx}·h$
q_S^{max}	Maximum specific substrate uptake rate	$mol_{eD}/mol_{Cx}·h$
q_{SGly}	Specific glucose uptake rate	$mol_{Glu}/mol_{Cx}·h$
$q_{r,i}$	Specific uptake rate for the i metabolic reaction	$mol_{Si}/mol_{Cx}·h$
$q_{T,i}$	Active transport rate of i component	$mol_{Si}/mol_{Cx}·h$
$q_{T,i}^{max}$	Maximum active transport rate of i component	$mol_{Si}/mol_{Cx}·h$
r_i	Metabolic reaction rate for i component	$mol_{Si}/ L_x·h$
$r_{Diff,i}$	Passive transport rate for i component	$mol_{Si}/ L_x·h$
$r_{L-G,i}$	Transference rate between liquid and gas phases of the i component	$mol_{Si}/ L_r·h$
$r_{T,i}$	Active transport rate for i component	$mol_{Si}/ L_x·h$
r_y	Proton translocations rate	$mol_{H+}/ L_x·h$
y_i	Number of proton translocations per mol of substrate consumed by the i metabolic reaction	-
z_i	Charge of the i component	-

3.1 Introduction

Carbohydrates anaerobic fermentation towards volatile fatty acids (VFAs) production has an increased interest due to its potential to provide building blocks from wastes towards a plethora of diverse valuable products. These chemical building blocks and complex biofuels [1,2] or bioplastics [3-5] can be obtained from this system accompanied with short biomass production and low operational costs [6-8]. But, despite of its potential interest, significant improvement in the process control is needed towards an important boost of its industrial implementation since the products yielding highly varies with the substrate, inoculum and operational conditions [9,10] with no clarified mechanistic interpretations [11-13].

Fermentations are environments with low energy available where microorganisms behave as highly efficient energy scavengers [14-22]. Mixed culture fermentation (MCF) presents high diversity in catabolic activities which increases the microbial population flexibility, facilitating the overall population survival by maximizing the energy harvest, and confronting successfully environmental changes that energetically constrain the microbial growth.

Previous modelling efforts in literature have attempted to describe product formation in MCF under different pH but have only partly succeeded or simply fell short [23-27]. Since modelling approaches based on constant fermentation reaction stoichiometry are not suitable to accurately describe the changing dependence of product yields with operational conditions [26,28-30], a number of variable stoichiometry models were proposed [31-34]. These models however only achieved limited predictive and explanatory capacity in modelling the observed product shifts as function of changes in the operational conditions [11,35-37]. This, together with the consideration that reproducible experimental products spectra have been obtained under similar operational conditions independently of the microbial inoculum [11], directly supports the hypothesis that biochemical and/or bioenergetics mechanisms play a key role on the observed product yields in MCFs.

Energy-based modelling approaches have been proposed to mechanistically describe the impact of environmental conditions on MCFs catabolic activities by means of bioenergetics [38,39]. These recent models based on bioenergetics considerations did for the first time offer mechanistic insight on the possible

reasons for the specific product yields observed. But did fall short in accurately predict the experimental product formation yields as function of operational conditions beyond very small ranges [24,27], arising from the incompletely defined roles of electron carriers, the use of incomplete metabolic networks and the specific modelling approaches used for the transport processes across the cell membrane. We have identified these three aspects, as the key factors limiting the predictive capacity of the existing energy-based MCFs models which have to be addressed.

In this work, the model developed is applied to the understand of the pH role as operational variable into the product spectrum and this is targeted referring to the most complete experimental work done by Temudo et al. [11], previously performed by Zoetemeyer et al. [35], Horiuchi et al. [36] and Fang and Liu [37] which obtained similar results. The model presented in this study is the first able to accurately describe the pH effect on product formation in MCFs and this is accomplished by directly addressing the above mentioned limitations of previous models.

3.2 Model description

The model proposed, assumes as fundamental hypothesis that the bacteria tend to maximize the energy harvested out of the surrounded system. This energy is later used for maintenance and growth. To maximize this energy, bacteria optimize its metabolic strategy yielding different products out of the available substrates in the system.

The consumption in anaerobic conditions of an easily degradable substrate like glucose in a continuous stirred tank reactor is analysed. A source of nitrogen is added in the reactor and a constant pH is considered. Butyrate, propionate, acetate, ethanol, butanol, lactate, acetone, acetoacetate, butyraldehyde, acetaldehyde, oxalate, malate, succionate and fumarate are the fermentative products considered. The model assumes a single microbial cell able to do all the fermentative metabolic pathways depending on the energy available in the system. The bacteria shift from one metabolic pathway to another towards the maximization of energy harvested for anabolism and maintenance per unit of time. Because our model is built considering that all the energy harvested has its end point in the formation of new phosphate links (to later break them for

maintenance and growth), the maximization of ATP production rate in the catabolic process is used as decision criteria to select between the catabolic pathways.

The model was built in a generalized form, in order to keep the possibility to include new chemical reactions open, and to reduce the number of parameters used. Simplicity and proximity to the basic concepts are always pretended.

Equations of the reactor and physicochemical calculations

The mathematical model developed considered different domains in the continuous stirred tank described. The dynamic equations that constitute the model (differential ordinary equations) are the mass balances of each reactor compartment considered (Figure 3.1).

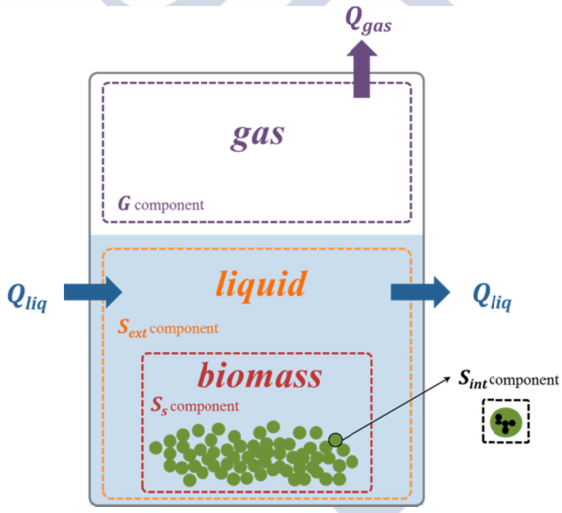

Figure 3.1 Scheme of the reactor sections considered.

The importance of the domains definition resides in the consideration that the processes occurring in each of them are very different which implies the necessity to define different equations. As the chemical reactions occurring are different, also the physicochemical conditions in the domains are different. The biocatalysed reactions only occur inside the cytoplasm of the biomass and latter, the products obtained are extruded to the environment. The intracellular reactions proceed in environmental conditions which are highly different than the

conditions of the surrounded environment; in the cytoplasm, the pH is neutral or close [40] and the ionic strength is higher than in the typical liquid bulk of a reactor because in lower volume higher concentrations of charged molecules are present [41].

Each compartment defined in the model, corresponds to a volume in the reactor: V_r (L_r) the working volume, V_{liq} (L_{liq}) the volume of liquid (working volume subtracting the volume occupied by the biomass), V_x (L_x) the biomass volume, and V_{gas} (L_{gas}) the head space volume.

Intracellular balance (no transportable components, S_i mol_{Si}/L_x):

$$\frac{dS_i}{dt} = R_i \tag{3.1}$$

Intracellular balance (transportable components, S_j mol_{Sj}/L_x):

$$\frac{dS_j}{dt} = R_j + R_{T,j} \tag{3.2}$$

Extracellular balance (S_k, mol_{Sk}/L_{liq}):

$$\frac{dS_k}{dt} = \frac{1}{V_{liq}} \cdot Q_{liq} \cdot (S_{k,inf} - S_k) + R_{T,k} \tag{3.3}$$

Biomass balance (X, mol_{Cx}/L_r):

$$\frac{dX}{dt} = -\frac{X}{SRT} + R_X \tag{3.4}$$

Gas balance (G, mol_{Gl}/L_{gas}):

$$\frac{dG_l}{dt} = -\frac{Q_{gas}}{V_{gas}} \cdot G_l + R_l \tag{3.5}$$

The operational conditions of the reactor simulated in the study are summarised in Table 3.1 where only the external pH is modified function of the case analysed.

Table 3.1 Reactor operational conditions for all simulated case studies

VARIABLE	VALUE	UNITS
V_r (Working Volume)	2	L
V_{gas} (Head space)	1	L
P (Total gas pressure)	1	atm
Q_{liq} (Liquid flow)	0.25	L/h
HRT (Hydraulic retention time)	8	h
Glu_{inf}	0.022	mol/L
NH_4^+-Cl^-_{inf}	0.011	mol/L

To calculate the physicochemical conditions of the liquid bulk intra- and extracellular, an algebraic implicit routine like presented in Chapter 2 is used. Like exposed in Chapter 2, the dynamic variables are defined as the sum of all the species concentrations of the chemical components in solution (all deprotonations plus hydrated and non-hydrated species). In this case, extended Debye-Hückel equations are used for calculating the activity of all the chemical components and non-ideality correction is not applied when calculating the pH of the medium. These simplifications have been made as their impact is not of importance in this model, because not all the intracellular metabolite concentrations are dynamically approximated.

Modelling the dynamics of the reactor, the liquid-to-gas reactions of transference cannot be neglected as they have approximately the same rate as the biological ones [42]. The rate of transport from the liquid to the gas depends on an empirical coefficient of transference between the gas-liquid phases (K_La) that is characteristic of each reactor and of each component considered. In this model this is simplified assuming a value of 15 h^{-1} for the K_La related to all the components considered. Moreover, the rate of transference also depends on the difference between the actual concentration in the liquid phase and the equilibrium concentration, calculated through the Henry constant (K_H) and the gas partial pressure of the component considered inside the reactor, $p_{gas,i}$.

$$C_{eq,i} = K_{H,i} \cdot p_{gas,i} \quad 3.6$$

$$r_{L-G,i} = k_L a \cdot \left(C_i - C_{i,eq} \right) \quad 3.7$$

Fixing a constant total pressure inside the reactor, the calculation of the gas flow comes due to the extra pressure produced by the new gas formed.

$$Q_{gas} = \frac{n_{gas-G} \cdot R_g \cdot T}{P - p_{H_2O}} \quad 3.8$$

$n_{gas\text{-}G}$ is the total sum of all the moles in gas form generated and R_g the universal ideal gas constant with a value of 0.082 atm·L/mol·K. The extra pressure due to the water vapour (p_{H2O}) that is present in the reactor at the operational temperature, is also considered (at 298.15 K, p_{H2O} is $3.12 \cdot 10^{-2}$ atm).

Metabolic network and transport

The main goal of the model is to mechanistically describe the product spectrum shifts and trends experimentally observed in the mixed culture fermentation as function of the environmental conditions fixed in a continuous stirred tank reactor. To achieve this, the model proposed is based on the consideration of only one single hypothetical microbial population capable of performing all of the most important known metabolic fermentation pathways from glucose. This is in line with a similar approach previously proposed [24] neglecting microbial speciation or diversity at this stage. The network of metabolic fermentation reactions used (presented in Figure 3.2) was selected based on widely accepted literature [17,25,43-48] to include the most important and well described pathways towards the major fermentation products typically observed from glucose glycolysis.

Feasible intermediate intracellular metabolites concentrations can be assumed to have to fall between a maximum of 10 mM and a minimum of 1 µM [49] for physiological and kinetic reasons respectively. Then, kinetic limitations can be induced by thermodynamics [21,50] implying unfeasible metabolite concentrations that could bring the pathway to a hold [21]. This is the case when extremely low product concentrations (< 1µM, reduces the kinetics of enzymatic reactions of consumption), or too high substrate concentrations (e.g. > 10mM

incompatible with cell homeostasis) [51,52] are needed for an intermediate reaction to thermodynamically proceed ($\Delta G < 0$).

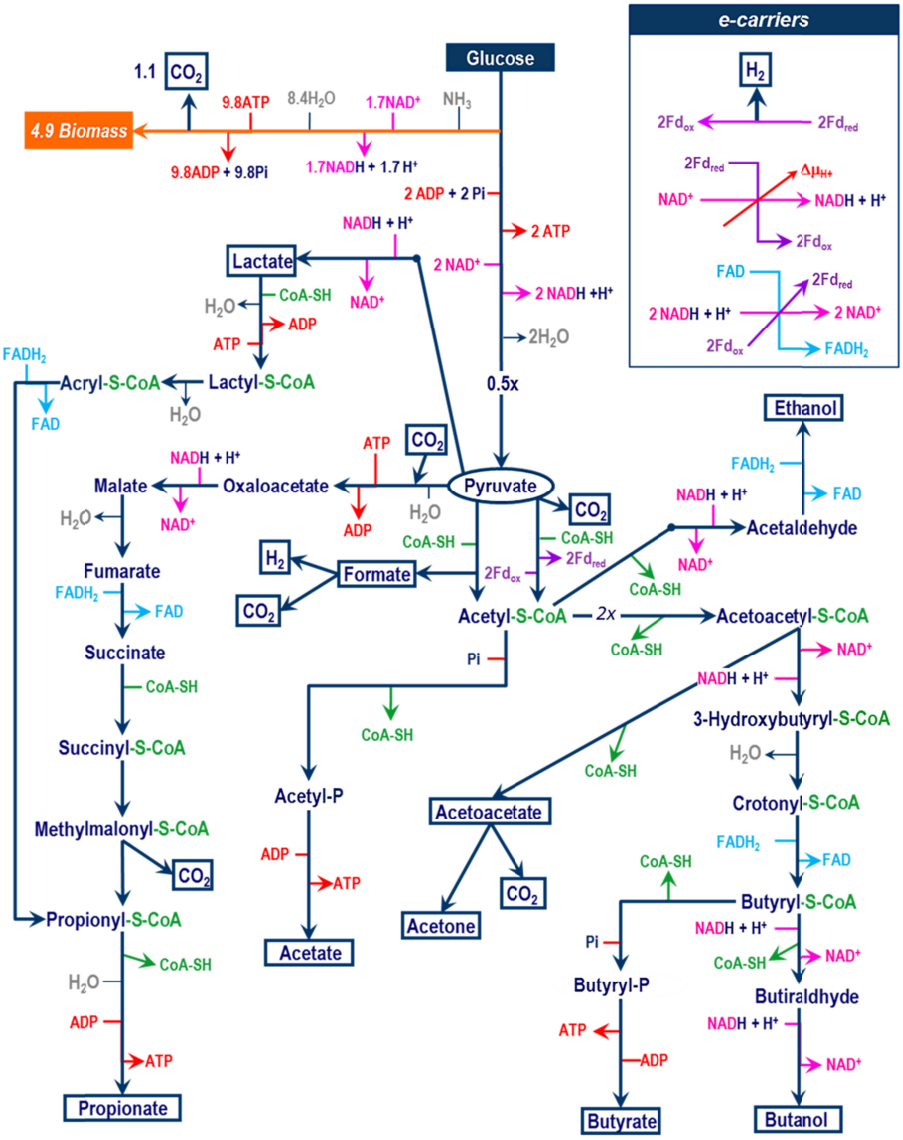

Figure 3.2 Metabolic reaction network of the model for the mixed culture fermentation of glucose.

By conducting a thermodynamic assessment of the metabolic network presented in Figure 3.2, unavoidable energy limitations are not observed as

energy demands of lower than 30 kJ are overcome by reasonable intracellular concentrations [49]. In Figure 3.3, it is detailed that the two reactions with Gibbs energy higher than 30 kJ are fuelled by an ATP hydrolysis.

The concentrations of chemical components in both the intra- (cytoplasmic) and extracellular volume domains, including pH and full ionic speciation are modelled and simulated dynamically. After analysing that no important kinetic bottlenecks seems to be present in the enzymatic reactions of the metabolic network (Figure 3.3), from all the intracellular chemical components shown in Figure 3.2, only those presented in Figure 3.4 have been dynamically modelled with intermediate metabolites concentrations assumed constant. As it is known to occur in living cells, a control system was established to maintain intracellular concentrations and pH within valid homeostasis values for the microorganism [49,51,52]. The model describes the close tied up between bioenergetics [53] and all solute transport across the membrane in line with the chemiosmotic theory.

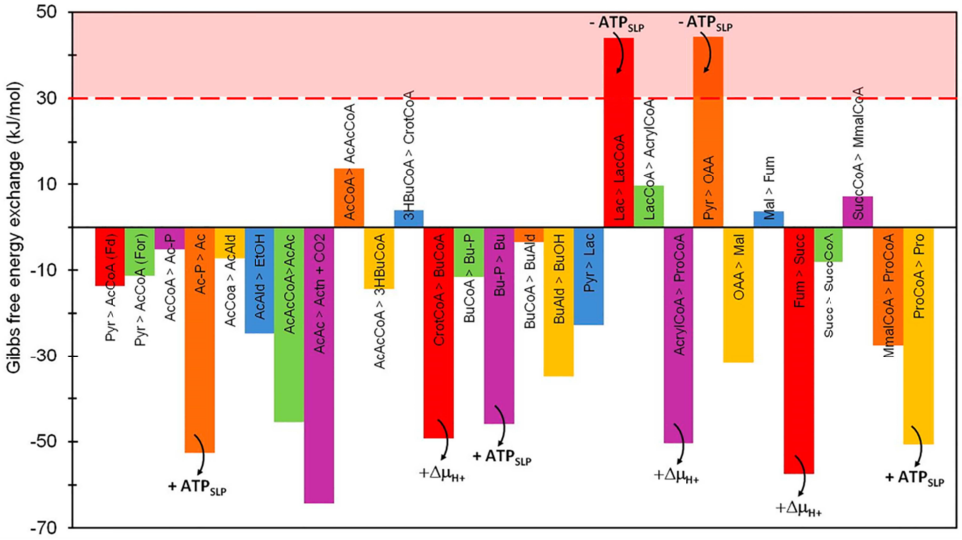

Figure 3.3 Gibbs free energy of central catabolic reactions of the metabolic network considered at 298.15 K, 1 atm, pH 7 and 1 mM concentrations.

The model presented here is, at first sight, similar to flux based analysis (FBA) methodology. But, the optimization strategies widely applied in FBA methods for large metabolic networks [54], do typically use experimentally measured intracellular metabolite concentrations and optimize the metabolic network

towards an objective such that the mass fluxes are predicted. The scope of this work differs from the conventional FBA in that it focuses on describing the microbial ecosystem reaction network interlinked with its environmental reactor conditions, such that a feedback of the reactor conditions impacts and is impacted by the microbial activity. Feedback from the environmental conditions into the network is modelled through mechanisms including transport energetics and maintenance requirements.

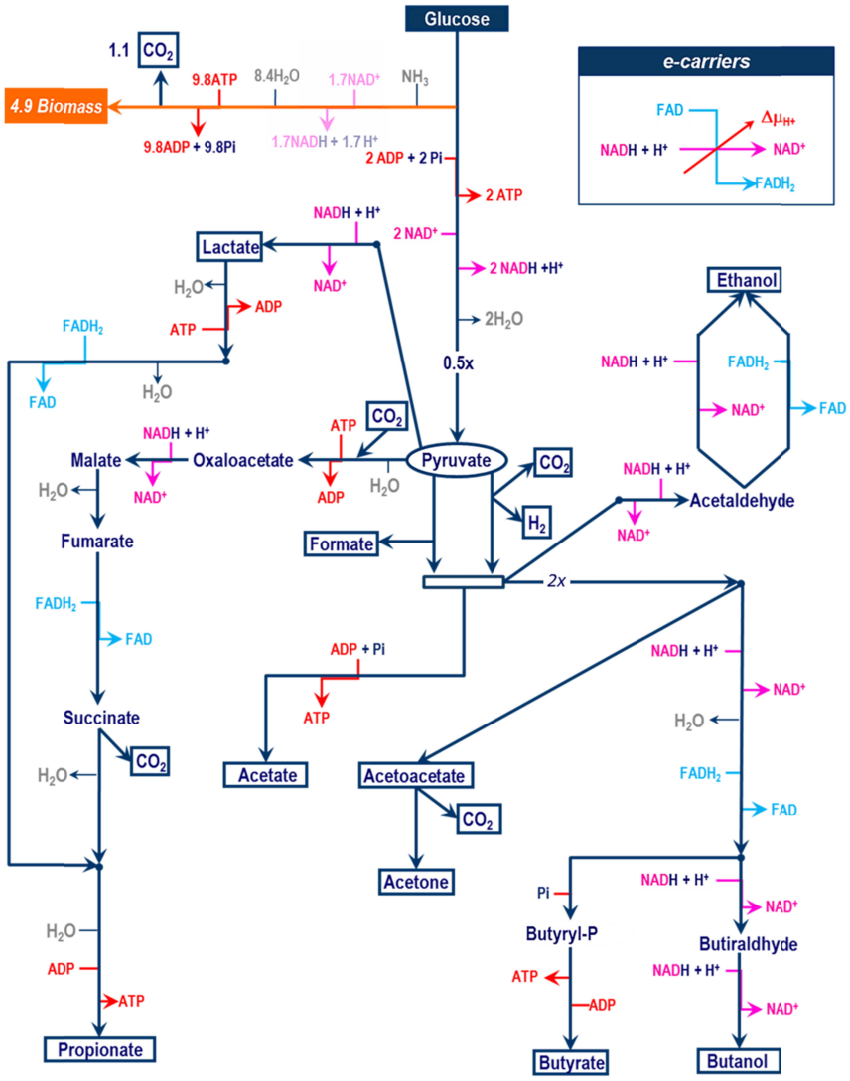

Figure 3.4 Simplified reaction network used for MCF model.

Metabolic energy production

The metabolism of a microbial cell can be described as a system organized in an energy harvesting catabolism coupled to an energy consuming anabolism and maintenance [55]. Cells can harvest catabolic energy through two mechanisms namely substrate level phosphorylation (SLP) and membrane related ion/proton translocations [56]. Both mechanisms end up yielding net ATP production, which is later used for anabolism and cell maintenance. The reaction sites in the fermentation network at which ATP via SLP is produced, are well-known and defined (Figure 3.2). However, energy can be harvested through proton extrusion across the membrane coupled to a less defined group of (or in principle to any) highly exergonic reactions.

The reversible nature of the ATP synthase mechanism [57], allows for the contrary also occurring, fuelling an endergonic reaction coupled with the energy yielding intrusion of a proton (previously extruded concomitantly to ATP consumption). In such cases, energy might be spent by the cell to e.g. avoid a limitation in a specific catabolic pathway of interest [21].

Proton motive force ($\Delta\mu_{H+}$) is commonly defined as energy liberated when a proton enters in the cytoplasm [47] and that energy depends on the membrane potential and on the difference between the concentrations of the solutions separated by the membrane (equation 3.9).

$$\Delta\mu_{H^+} = F\Delta\psi + R_{th}T\cdot\ln 10^{-pH_{in}} / 10^{-pH_{out}} \quad (kJ/mol_{e^-}) \qquad 3.9$$

In equation 3.9, $\Delta\psi$ is defined as $\Delta\psi = \Delta\psi_{in} - \Delta\psi_{out}$, with the inner membrane surface considered negative. $\Delta\psi$ has been reported near to a constant value depending on the microorganism and growth conditions [47]. In this model $\Delta\psi$ is considered constant at 0.2 V and any process increasing $\Delta\psi$ is assumed to be automatically compensated by an ATP coupled decreasing one [47,57]. This, together with the intracellular pH assumed equilibrated at 7 by the sodium pump, $\Delta\mu_{H+}$ any variations are solely considered due to variations on the external pH [58].

Types and role of electron carriers

The availability of different electron carriers with different reductive potentials in the cell increases the energy harvest efficiency from catabolism as the most suitable carrier that can be coupled to the specific reaction according to its redox potential. This has been accounted for in the model and three electron carriers have been considered (Figure 3.5, the potential of each electron carrier is presented according to [59]).

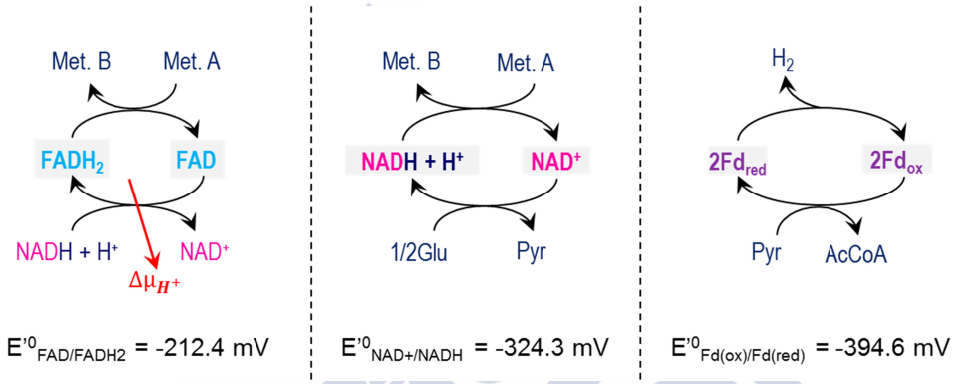

Figure 3.5 Electron carriers as included in the model with their specific reductive potential.

Ferredoxin ($Fd_{ox/red}$), due to its more negative reduction potential, is the only electron carrier considered capable to direct H_2 production [25,32]. Ferredoxin reduction takes place only at pyruvate oxidation to acetyl-CoA (Figure 3.2) and it is assumed simultaneously to its oxidation that yields H_2 (Figure 3.5) and which is consistent with experimental observations [11].

NAD(H) has a less negative reductive potential than ferredoxin and although in previous models NAD(H) was considered an electron carrier capable of direct H_2 production [27], both experimental observations [11] and thermodynamic calculations [25,32] (ΔG^{o1} = +34.9 kJ/mol, for NADH oxidation towards soluble H_2 production) strongly rule out direct H_2 production from this carrier under cytoplasmic conditions [49]. NAD(H) takes part as electron carrier in specific metabolic reactions of the metabolic network (Figure 3.2) and it is balanced as a conserved moiety throughout the overall fermentation network stoichiometry. Although NADP(H) is also known to take part in some of the intracellular

reactions, the small and not well defined differences between NADP(H) and NAD(H) and the difficulty to experimentally differentiate one from the other justify for the consideration of only NAD(H) in the model [60].

FAD(H_2) is the third electron carrier considered in the model and it is associated to the highly exergonic metabolic reactions because of its less negative reduction potential. FAD reduction can be coupled to energy harvest by proton translocation [17]; thus, FAD(H_2) electron carrier plays the role of an intermediate facilitating the coupling of a highly energetic metabolic reaction with the generation of proton motive force described with the oxidation of NADH following the mechanism presented in equations 3.10-3.13 [61-64].

$$Met.A + FADH_2 \rightarrow Met.B + FAD \quad 3.10$$

$$FAD + 2NADH + 2H^+ + 2Fd_{ox} \rightarrow FADH_2 + 2NAD^+ + 2Fd_{red} \quad 3.11$$

$$2\,Fdred + NAD^+ \rightarrow 2\,Fdox + NADH + H^+ + \Delta\mu_{H^+} \quad 3.12$$

$$\text{Total:} \quad Met.A + NADH + H^+ \rightarrow Met.B + 2NAD^+ + \Delta\mu_{H+} \quad 3.13$$

Although Seedorf et al. [61] also suggested the direct production of H_2 instead of one proton translocation in these highly energetic reactions, this was not considered due to the experimental observed 1:1 stoichiometry of H_2 respect to pyruvate oxidation [11]. The same applies to discard the possibility of NAD^+ reduction coupled to the pyruvate oxidation to acetyl-CoA.

In the network of Figure 3.2 we have included $FADH_2$ associated to a proton translocation mediating the reduction of acetaldehyde to ethanol. This has not been reported but it has been found as a necessary mechanism to ensure the prediction of the observed high yield of ethanol production. In the ethanol pathway, the reduction of acetaldehyde to ethanol is typically exergonic (Figure 3.3), but the energy available is not as high as in other reductions associated to $FADH_2$ oxidation. Then, in certain conditions, the available energy is not sufficient to yield a proton translocation ($\Delta\mu_{H+}$). However, reduction of ferredoxin by acetaldehyde has been reported [11,65] thus, a similar electron bifurcation mechanism with $FADH_2$ involved is proposed as possible in the ethanol pathway at conditions of low $\Delta\mu_{H+}$ (Figure 3.4).

In the simplified network of Figure 3.4 only NAD(H) appears as electron carrier modelled dynamically assuming the rest constants according to the exposed in this section. Ferredoxin is assumed instantaneously re-oxidized producing H_2 and FAD(H_2) forms are also equilibrated considering the total sum of transformations of equation 3.13 which shows that in the overall mechanism, only NADH is oxidized.

Kinetic model of the metabolic reactions

Kinetic differences in metabolic reaction rates are expected to be not highly significant due to the nature of the system. The overall process rate is assumed controlled by the glucose uptake rate and glycolysis, which being highly exergonic, is never limited by thermodynamics. Therefore highly general and similar kinetic parameters are assumed across the board for all metabolic routes as they did not impact the predicted product spectrum trends during our preliminary assessment (not shown).

First, the ΔG of each metabolic reaction is calculated using a generalized routine, to check its feasibility. Knowing the stoichiometry of each reaction (ν_i, is the stoichiometry coefficient for each component i of the reaction considered), actual ΔG at each step of simulation time is calculated with the ΔG^o values obtained from literature [56,59,66-68] that have been previously pre-stored in a matrix.

$$\Delta G = \Delta G^0 + R_{th} \cdot T \cdot \ln \prod_i a_i^{\nu_i} \qquad 3.14$$

Depending on its ΔG, the direction of the reaction is fixed through a factor f and considering that the minimum energy necessary to run the reaction (ΔG_{min}) is of -2 kJ/mol (equation 3.15).

$$\begin{aligned} f &= 1 \quad if \quad \Delta G < \Delta G_{min} \\ f &= 0 \quad if \quad \Delta G_{min} < \Delta G < -\Delta G_{min} \\ f &= -1 \quad if \quad \Delta G > -\Delta G_{min} \end{aligned} \qquad 3.15$$

When the reaction is thermodynamically feasible, it is assumed that it can proceed. The rate for all the metabolic reactions is assumed the same, avoiding

enzymatic differences. In this model, the overall process rate is limited to one general maximum corresponding to 3 $mol_{e^-}/mol_{Cx}·h$ transferred in the glycolysis [55] and the only kinetic limitation comes due to glucose scarcity that is modelled through a Monod-like term.

$$q_{SGly} = q_S^{max} \cdot \frac{S_{Glu}}{K_S + S_{Glu}} \quad 3.16$$

In equation 3.16, q_S^{max} has a value of 0.75 $mol_{Glu}/mol_{Cx}·h$, based on the 4 electrons transferred in the glycolysis [46] (2 mol of NAD^+ reduced per mol of glucose) and Ks is $1·10^{-3}$ M. No accumulation of intermediate metabolites is considered and a constant concentration of 7.5 mM assumed for intracellular pyruvate [69]. Thus, kinetics of all the catabolic reactions considered limited only by glucose availability and thermodynamic feasibility, are modelled according equation 3.17 (q_{ri}, $mol_{Si}/mol_{Cx}·h$) where ν_i is the stoichiometry factor between the reaction i and the glycolysis ($mol_{Si}/mol_{Glu}·h$).

$$q_{r,i} = f_i \cdot \nu_i \cdot q_{SGly} \quad 3.17$$

Each substrate consumption yield ($q_{r,i}$) is finally multiplied by the biomass present to calculate the reaction rate (r_i, $mol_{Si}/L_x·h$).

$$r_i = q_{r,i} \cdot X \cdot \frac{V_r}{V_X} \quad 3.18$$

Transport model for solutes across the membrane

Semi-permeable cell membranes in bacteria are known to allow for both, the passive and active transport of solutes. Considering the model focus is on product prediction, active transport of substrates (i.e. glucose) is not described and only products transport is modelled with distinction between uncharged species (free diffusion) and charged (active transport).

Passive transport is modelled considering that the lipid bilayer membrane controls only the cross of charged species but does not act as a barrier for small uncharged species. These species are assumed as freely diffusing through the

membrane with no energy coupling or control from the cell homeostasis (equation 3.19).

$$r_{Diff,i} = Diff_i \cdot \left(S_{i,out} - S_{i,in} \right) \cdot X \cdot \frac{V_r}{V_X} \qquad 3.19$$

The $Diff_i$ term in $L/mol_{Cx} \cdot h$ is calculated according equation 3.20 where $\mathbf{D}_i$ is the diffusion of the chemical component considered in m^2/h, a_x is the superficial area of transport of one mol of biomass m^2/mol_{Cx} and δ_x is the thickness of the membrane, in m.

$$Diff_i = 10^3 \cdot \frac{\mathbf{D}_i \cdot a_x}{\delta_x} \qquad 3.20$$

While the diffusivity parameters ($\mathbf{D}_i$) could be simply estimated according to the measurement of diffusion values in water, a_x values are largely unknown. For this reason, in our model, the differences in diffusion coefficients are neglected accepting that this values are within the same order of magnitude and that the process is highly regulated by the differences in substrates partition coefficients[27] (i.e. acid-base ionic speciation due to different intra- and extracellular pH). This effect is already implemented in the model accurately describing the species deprotonations concentrations in both intra- and extracellular compartments. Therefore, all the $Diff_i$ are assumed equal with a value of 100 $L/ mol_{Cx} \cdot h$ [24,27].

Active transport of charged and/or large molecules that are not freely diffusing through the cell membrane is coupled to metabolic energy exchange which is known to be performed by a diversity of transport proteins (ports) allowing only specific molecules to cross [47]. For the energy exchange, these ports are typically coupled to proton translocations, allowing endergonic transports to be fuelled by proton motive force if needed [70].According to this, the transport of acidic components is modelled as active for their ionized deprotonated species and passive for their uncharged fully protonated species (Figure 3.6). In this scenario, the passive transport term of a product extrusion might follow the same or opposite direction as active transport and therefore decreasing or increasing the active transport energy cost respectively.

Active transport is carried out by enzymatic control like the intracellular metabolic reactions, thus we assumed a similar kinetic expression for all of them. However, active transport is not thermodynamically controlled as energy input is applied if the transport is endergonic. For this reason, the transport is modelled only with a maximum rate equal than the one for glycolysis, and a Monod-like term referred to the intracellular component transported across the membrane.

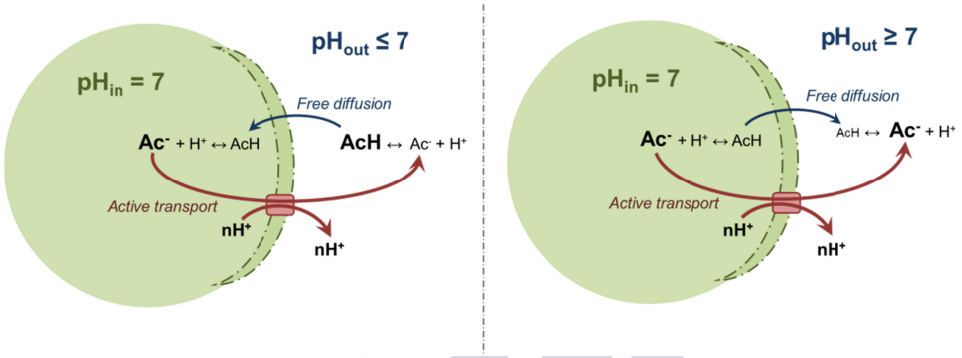

Figure 3.6 Transport model of acidic components across the membrane.

$$q_{T,i} = q_{T,i}^{max} \cdot \frac{S_{T,i}}{K_T + S_{T,i}} \quad 3.21$$

$$r_{T,i} = q_{T,i} \cdot X \cdot \frac{V_r}{V_X} \quad 3.22$$

$q_{T,i}^{max}$ is defined like $q_{T,i}^{max} = \nu_i \cdot q_{SGly}$ referred to the reaction that generates the product transported.

Accumulations higher than 10 mM [49] are considered not physiologically possible so when the intracellular concentrations reach this value, it is assumed that the production is equal to the active transport that reach its maximum value, equation 3.23 (K_T in equation 3.21 has a value of 20 mM for all the active transports described).

$$r_{T,i} = r_i - r_{Diff,i} \quad 3.23$$

Any change in membrane potential associated to the transport of charged species is compensated by the needed proton translocation coupled to ATP hydrolysis. In this way the cell is capable of the maintenance of its homeostasis

and membrane potential. The potential associated to a solute transport across the membrane is calculated by equation 3.24 where z_i is the charge of the solute.

$$\Delta\mu_{Si} = z_i \cdot F\Delta\Psi + RT \cdot \ln\left[S_{i,in}\right] / \left[S_{i,out}\right] \quad 3.24$$

All charged products considered in the fermentation model are negatively charged and their transport outside the cytoplasm leads to a decrease in the potential of the membrane (i.e. first term of equation 3.24) [47]. An equivalent number of protons must be transported to maintain the membrane potential as well as the internal pH (Figure 3.6). Moreover, if the solute is transported against or in favour its chemical gradient across the membrane (i.e. the second term in equation 3.24) this energy might generate or consume additional proton motive force.

Overall, the number of protons (y) needed for transport fuelling (-) or harvested from transport energy surplus (+) are calculated as proposed in the well-known recycling model [71], equation 3.25.

$$y = -\frac{z_i \cdot F \cdot \Delta\Psi + R_{th} \cdot T \cdot \ln\frac{[S_{i,in}]}{[S_{i,out}]}}{\Delta\mu_{H^+}} + z_i \quad 3.25$$

Sodium pump

A specific active transport is done by the cell to equilibrate the intracellular pH as it has to be homeostatically maintained close to neutrality. When it is required, positive charged species (i.e. Na^+, K^+, etc.) are transported inside/outside the cytoplasm, with a proton transported in opposite direction to maintain the membrane potential. To describe the control of the intracellular pH, the model assumes the presence of a sodium pump only (Figure 3.7).

As we are not modelling cases where bacteria are in hypotonic or hypertonic environment, we assume that there is not a limitation or excess of external ions concentrations, which could imply a significant energy variation. Therefore, intracellular and extracellular sodium concentrations in each simulation time step are fixed equal. This simplification is based in the assumption that the cell is transporting the less costly cation to balance its intracellular pH. For this reason, the energetic cost of this transport is expected minimum reaching a chemical

equilibrium between both intra and extracellular compartments. Moreover, intracellular pH in our model is slightly variable because already all the reactions and transports are pH balanced, thus, sodium pump has a low impact as it is only balancing the pH in the transient states when acids intracellular accumulation or depletion occurs.

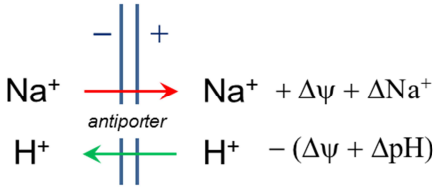

Figure 3. 7 Model of the sodium pump.

Sodium pump is modelled considering a Na^+/H^+ antiporter [47]. It acts as a proportional control action to maintain intracellular pH at 7 (equation 3.26). K_{Na+} has a value of 100 (dimensionless) to buffer the sodium pump effect.

$$q_{Na+} = 1 - \exp\left[K_{Na+}\left(10^{-7} - 10^{-pH_{in}}\right)\right] \quad if \quad pH > 7$$
$$q_{Na+} = 0 \quad if \quad pH = 7 \qquad 3.26$$
$$q_{Na+} = \exp\left[K_{Na+}\left(10^{-pH_{in}} - 10^{-7}\right)\right] - 1 \quad if \quad pH < 7$$

Energy generation through proton translocation

Proton translocations are coupled to active transport but also to the referred reactions where the electron carrier FAD(H) is involved. The translocations produced by a catabolism in active transport or metabolic reactions are computed by the model and the ATP generated or consumed is calculated. For this, first the number of protons translocated per mol of substrate of each reaction is multiplied by the reaction rate. The sum is the total rate of proton translocations (r_y).

$$r_y = \sum_{i=1}^{n} y_i \cdot r_i \qquad 3.27$$

Then, the number of protons produced, are simply translated to ATP generated considering the ATP formation rate according equation 3.28. This ATP rate sums to the rate of ATP formed via SLP.

$$r_{ATP} = r_y \cdot \frac{\Delta\mu_{H+}}{\Delta G_{ATP}} \qquad 3.28$$

Anabolism and decay

Anabolism and decay processes are modelled through overall mass balanced reactions. Equation 3.29 presents the global stoichiometry assumed for anabolism in the model. It is considered that 2 mol of ATP are consumed per mol of biomass formed [72].

$$0.203 \cdot Glu + 0.2 \cdot NH_3 + 1.72 \cdot H_2O + 0.34 \cdot NAD^+ + 2 \cdot ATP \rightarrow \\ \rightarrow 0.22 \cdot CO_2 + 2 \cdot Pi + 2 \cdot ADP + 0.34 \cdot NADH + 2.34 \cdot H^+ + \mathbf{X} \qquad 3.29$$

For decay, the same equation 3.29 is consider multiplied by -1 but due to the favourable growth conditions imposed in the system studied; the microbial decay impact is almost marginal. For simplicity, the NADH re oxidation needed for the anabolic process is neglected. It implies an error of no more of ± 20% in the NADH balance of all the simulations presented, which supposes an underestimation of the rate of pathways that occur with NADH oxidation, but in any case affects to the tendencies predicted over the products spectrum with changes in pH.

Anabolism (from glucose) is modelled limited by substrate and energy availability that comes from catabolism [73-75]. To account for the substrate limitation, Monod kinetic terms are used analogously than for glycolysis (equation 3.16) while for the energy availability the total amount of net ATP generated by catabolism is calculated. The ratio of (ADP·Pi)/ATP concentrations is considered maintained constant at ΔG of -50 kJ/mol for ATP hydrolysis to preserve the cell homeostasis [76]. Part of the overall net ATP generated is allocated to a constant term of maintenance, [77] assumed constant as 4.5 $kJ/mol_{Cx} \cdot h$ [78] and added as another term of ATP consumption. But if

besides this consumption for maintenance, concentrations of ATP increase the energy liberated in its hydrolysis to more than 50 kJ/mol, anabolism proceeds, if the contrary, population decays like described by equation 3.30 where K_{ATP} has an arbitrary value of 5 kJ·mol_{Cx}/mol_{Glu}·h in order to smooth the discontinuity of the function.

$$\begin{aligned} f_{ana} &= \frac{\Delta G_{ATP} - 50}{K_{ATP}}; \quad f_d = 0 \quad if \quad \Delta G_{ATP} > 50 \text{ kJ/mol} \\ f_{ana} &= 0; \quad f_d = 0 \quad if \quad \Delta G_{ATP} = 50 \text{ kJ/mol} \\ f_{ana} &= 0; \quad f_d = \frac{50 - \Delta G_{ATP}}{K_{ATP}} \quad if \quad \Delta G_{ATP} < 50 \text{ kJ/mol} \end{aligned} \qquad 3.30$$

Including the glucose limitation (ammonium is never a limiting reactant in the conditions simulated (Table 3.1)), the anabolism rate is defined like equation 3.31, whereas decay is only defined by energy limitation.

$$r_{ana} = f_{ana} \cdot \frac{S_{Glu}}{K_{Gly} + S_{Glu}} \qquad 3.31$$

Selection of dominant metabolic pathways

The fundamental hypothesis in the model to describe product formation is that the dominant catabolic pathways will be those that return more net energy as ATP and consequently lead to the highest biomass growth. This is estimated by lineal optimization of the catabolic stoichiometry considering the ATP yielded per mol of glucose consumed by each branch of the network presented (Figure 3.2 and 3.4) (χ_i). The optimization is constrained by closing electron balances (as NADH equivalents) and a zero or net HCO_3^- production as it is not fed (Table 3.1) and it acts as substrate in some catabolic reactions (Figure 3.2).

The ATP produced per unit of time is computed for each branch of the metabolic network considering the sum of the ATP produced via SLP plus the ATP produced via proton motive force. In the same way, the NADH oxidized/reduced and HCO_3^- generation/consumption is computed per each metabolic branch. A MATLAB solver for linear programing problems is used to find the stoichiometry between catabolic branches that leads to a maximum ATP production. The inputs

of the solver are the total NADH reduced, the total HCO_3^- and the total ATP produced in each catabolic branch defined.

Example of one catabolic branch:

$$1\ \text{Glucose} + 2\ NAD^+ + 4\ ADP + 4\ Pi \rightarrow$$
$$\rightarrow 2\ \text{NADH} + 2\ H^+ + 2\ \text{Formate} + 2\ \text{Acetic acid} + 4\ \text{ATP}$$

The solver finds, between these catabolic branches a linear combination of χ_i ($\sum_{i=1}^{N}\chi_i = 1$) that makes cero the production/consumption of NADH (maintaining the redox balance of the cytoplasm) and maximizes the ATP production rate (mol_{ATP}/ h).

$$\chi_i = lin\_opt\left(d[\text{NADH}]/dt = 0; d\left[HCO_3^-\right]/dt \geq 0;\ 0 \leq \chi_i \leq 1\right) \quad 3.32$$

3.3 Results

Model simulations were conducted until steady state for an HRT of 8 hours and for pH values between 4 and 8.5 with a resolution of 0.5 pH units. The same carbon source as in Temudo et al. [11], 4 g/L of glucose, was used and ammonium was fed in non-limiting concentrations (Table 3.1).

The experimental observations by Temudo et al. [11] are to our knowledge the only experimental work reporting closed electron and carbon balances (Figure 3.8). In this section, a comparison between these experimental results and the outputs of our model is presented for the major products observed in glucose MCF.

Formate vs H_2

The experimental observations reported [11] indicate that H_2 and CO_2 are predominant at low pH while formate production dominates at higher pH (Figure 3.8). The sum of H_2 and formate yields returning approximately the same as the sum of acetyl-CoA products serves as partial validation of the metabolic network assumed for the model (Figure 3.2). The model simulations results

succeed in predicting these yield trends as experimentally observed (Figures 3.8, 3.9 and 3.10).

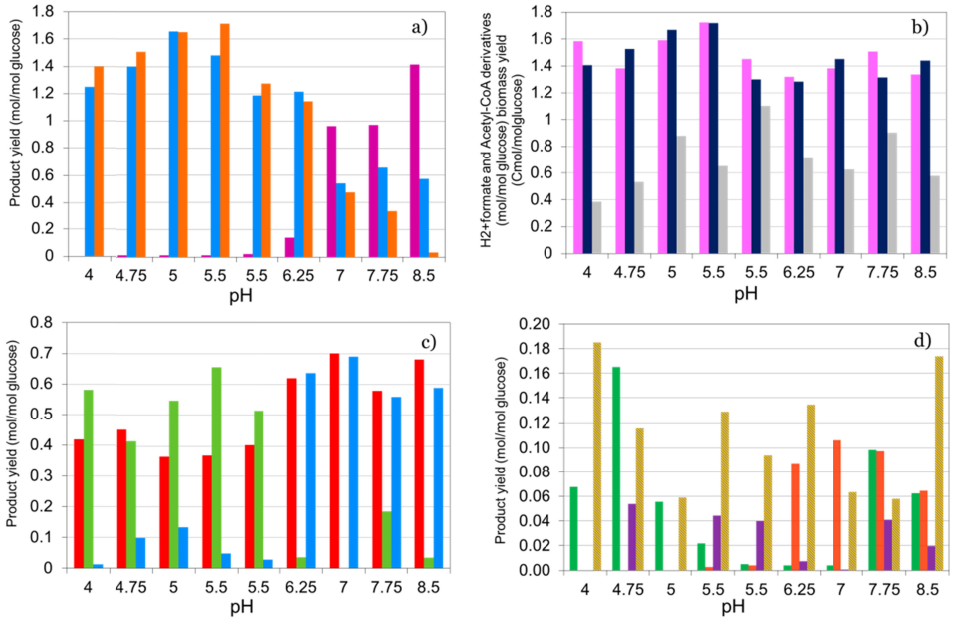

Figure 3.8 Experimental steady state yields as reported by Temudo et al. [11] (at 20 hours of HRT for pH ≤ 5.5 and at 8 hours of HRT for pH ≥ 5.5). a) Influence of pH on formate, CO_2, and H_2 yields per glucose consumed by MCF. Yields of: ■ formate ■ CO_2 (gas and dissolved CO_2 + HCO_3^-) and ■ H_2. b) Influence of pH on acetyl-CoA derivatives, H_2 + formate and biomass yields per glucose consumed by MCF: ■ Total acetyl-CoA derivatives as sum of acetate, acetoacetate, butyrate (x2), butanol (x2), butyraldehide (x2), ethanol and acetaldehyde yields; ■ sum of H_2 and formate yields and ■ biomass yield. c) Influence of pH on major dissolved products yields per glucose consumed: ■ acetate; ■ propionate; ■ butyrate; ■ ethanol and ■ butanol. d) Influence of pH on major dissolved products yields per glucose consumed: of: ■ lactate; ■ succionate; ■ propionate; ■ glycerol.

The energy yields during pyruvate oxidation to acetyl-CoA between H_2 production (through ferredoxin) and formate production (through ferredoxin or direct pyruvate oxidation) are equivalent and no evidence suggests that extracellular pH could have an impact on them [11]. However, the model is successful at predicting the shift from CO_2 + H_2 to formate at high pH (Figure 3.9) being therefore attributed to the extra energy harvested through formate active transport across the membrane at high pH together with the increased energy

costs of transporting HCO_3^- outside the cytoplasm due to higher inorganic carbon solubility when pH increases.

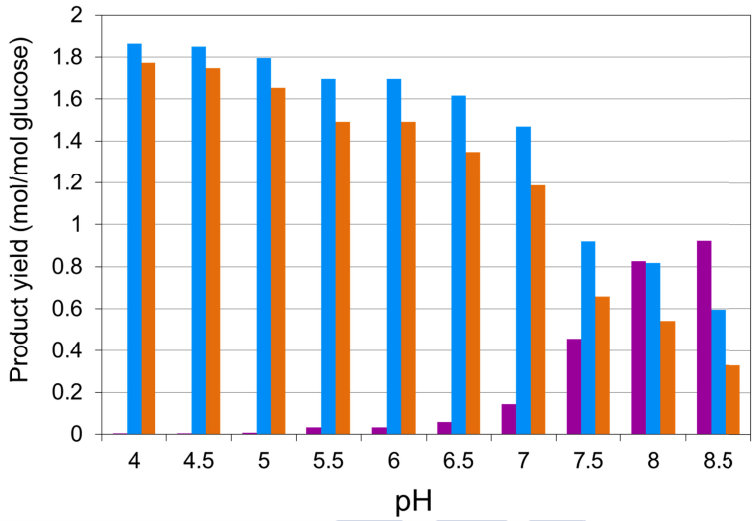

Figure 3.9 Model simulation results on the influence of pH on formate CO_2, and H_2 yields per glucose consumed. Yields of: ■ formate; ■ CO_2 (gas and dissolved CO_2 + HCO_3^-) and ■ H_2. (Compared to the experimental results presented in Figure 3.8.a).

Differences between model predicted higher biomass yields at high pH (Figure 3.10) and experimental observations cannot be clearly attributed. The reduction of HRT at higher pH in the experimental operation by Temudo et al. [11] (Figure 3.8.b) with the associated change in growth rate could be a cause of discrepancy that is not fully described in our model however, they also observed a reduction of the biomass yield referred to the ATP harvested when the external pH is low and the fermentation is yielding butyrate at high concentrations [10,79]. Alternatively, also variations of the internal pH (physiologically feasible between 5.5 to 7 [80]) which are not considered in the model (internal pH is fixed at 7) could account for significant different maintenance energy costs and efficiencies impacting biomass yield values.

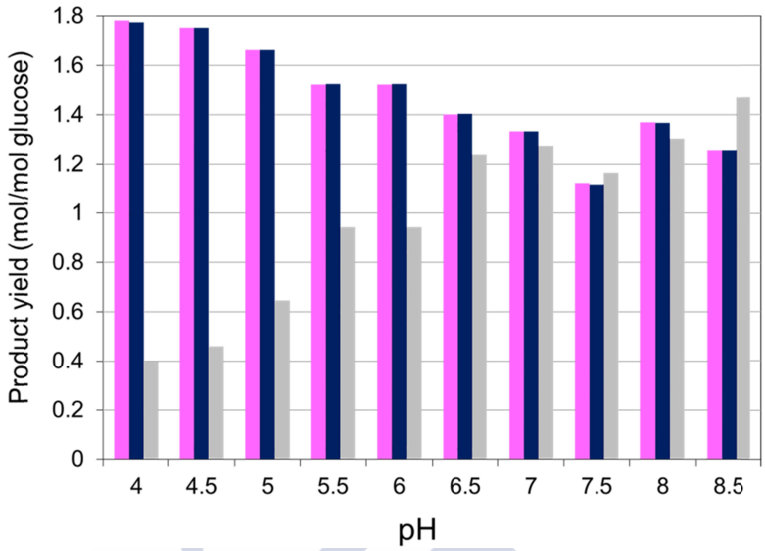

Figure 3.10 Model simulation results on the influence of pH on acetyl-CoA derivatives, H_2 plus formate and biomass yields per glucose consumed. Yields of: ■ Total acetyl-CoA derivatives as sum of acetate, acetoacetate, butyrate (x2), butanol (x2), butyraldehide (x2), ethanol and acetaldehyde yields; ■ sum of H_2 and formate yields and ■ biomass yield. (Compared to the experimental results presented in Figure 8.b).

Product spectrum

In Figure 3.11 the organic products spectrum predicted by the model is presented. As experimentally observed (Figure 3.8.c), acetate and butyrate high concentrations are predicted at low pH whereas a shift from butyrate to ethanol at higher pH is observed.

Fermentation with acetate as only product has not been experimentally reported being its production always accompanied by other more reduced products yielding [81]. The main reason lies in the necessity to oxidize the NADH produced in glycolysis, which, in absence of external electron acceptors (such as O_2, NO_3^-), leads to electrons allocation in reductive fermentation steps. The need for this complete electron balance fully accounted for in the model, is a main constraint during the maximization of ATP production and appears to be in line with the experimental observations.

At low pH, butyrate and acetate are predicted as major products as well as experimentally reported (Figures 3.8.c and 3.11) with presence of other more reduced products. At high pH, butyrate production appears to dramatically diminish and ethanol and acetate are predicted as well as experimentally reported as the major products (Figures 3.8.c and 3.11). This clear shift in products is successfully predicted by the model but at a higher pH than in the observations. The presence of propionate is predicted as secondary reduced product (Figure 3.11) associated to acetate production while is not present in the experimental observations by Temudo et al. [11] where ethanol or glycerol are found in higher concentrations (Figure 3.8.c). However, propionate producers seems to have limited presence in the mixed culture inoculum used by Temudo et al. [11] because in contrary, it has been reported as a major product together with acetate at approximately the same pH than the predicted by the model in the experiments developed by other authors [36,37].

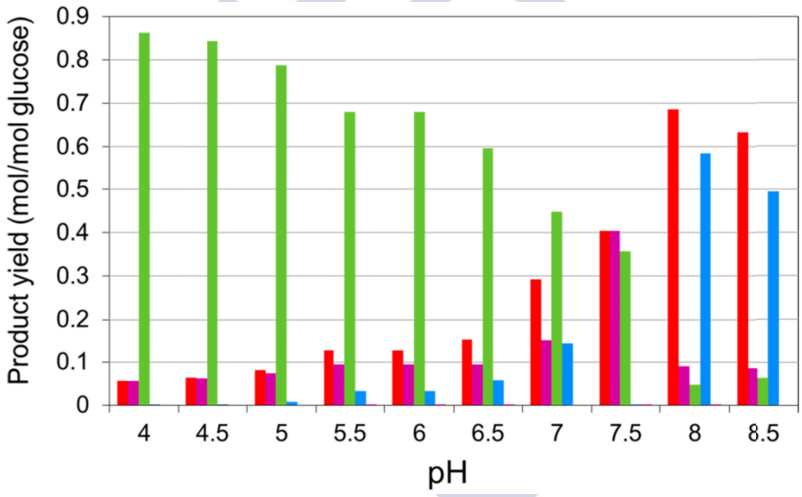

Figure 3.11 Model simulation results on the influence of pH on dissolved products yields per glucose consumed by MCF. Yields of: ■ acetate ■ propionate ■ butyrate and ■ ethanol. (Compared to the experimental results presented in Figure 8.c).

Based on the metabolic network in Figure 3.2 acetate plus ethanol; acetate plus propionate; and butyrate production are the three combinations of catabolic products leading, closed electron balances, to a maximum energy harvest per unit of glucose consumed (one ATP by SLP formation plus the energy of one proton

translocation per unit of glucose). These products are the ones with higher yields predicted by the model as well as experimentally reported [11,36,37].

Considering that $\Delta\mu_{H+}$ is modelled as only depending on external pH, when it is low, ΔpH increases and more energy is needed to translocate one proton across the cell ($\Delta\mu_{H+}$ increases). In ethanol pathway, the energy available during $FADH_2$ mediated acetaldehyde reduction is not as high as that in crotonyl-CoA reduction (part of the butyrate pathway) or that in fumarate or in acryl-CoA reductions (part of the propionate pathways) (Figures 3.2 and 3.4). Therefore, at low pH, no proton translocation is possible when ethanol is yield and butyrate is predicted as major product.

Butyrate production at low pH supposes the less retention of the concomitantly produced inorganic carbon, with its increased transfer as CO_2 to the gas phase. At higher pH however, butyrate production energetic yield decreases as more total inorganic carbon is kept in solution. This favours the propionate pathway energetics, as it does not imply any decarboxylation. Then, at pH range between 6 and 7.5, acetate and propionate together with formate production increases (Figure 3.9 and Figure 3.11).

Ethanol pathway at high external pH (8, 8.5) permits one proton translocation ($\Delta\mu_{H+}$ is low in these conditions) which elevates the capacity of energy harvest by this pathway making together with acetate yielding, its production competitive comparatively to yield butyrate or acetate plus propionate. This comes together with the higher energy available for acidic components transport at high pH, and makes the ethanol production more favourable than propionate in terms of energy yield as formate, which is the strongest acid, is produced in ethanol pathway (Figure 3.2).

Results for minor products

The results obtained for the prediction of minor products concentrations are not very valuable. They do not permit to obtain final conclusions as the model has not enough precision. We include here the comparison between the results obtained for the concentrations of these products by Temudo et al. [11] (Figure 3.8.d) and the results predicted by the model (Figures 3.12 and 3.13).

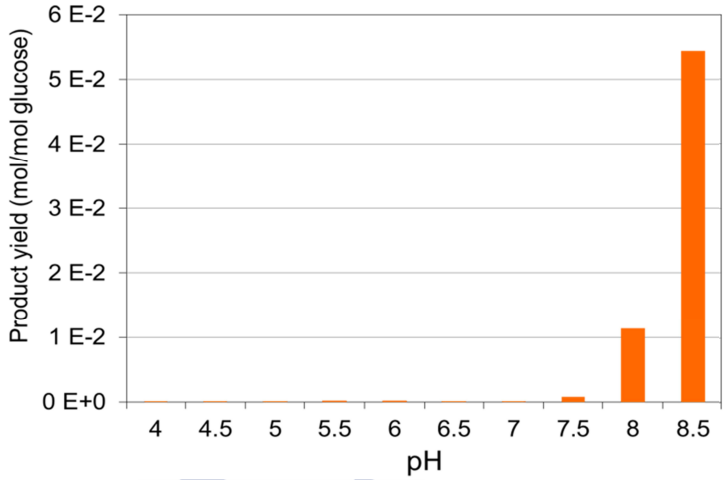

Figure 3.12 Model simulation results on the influence of pH on succionate yield.

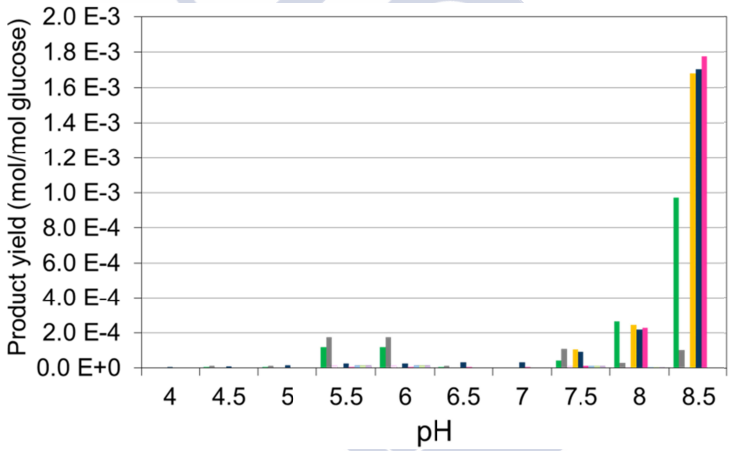

Figure 3.13 Model simulation results on the influence of pH on minor products. Yields of: lactate; acetoacetate; acetone; oxaloacetate; malate; fumarate; acetaldehyde; butyraldehide; butanol.

3. 4 Limitations of the model and opportunities for development

The proposed model provides insights into energetically based mechanisms of the trends and shifts observed on the product spectrum in glucose fermentations; the model has some limitations and areas for further development to be considered including:

1. The numerical accuracy on the prediction of product yields is expected to improve if more kinetic information is incorporated. Currently no specific kinetic information has been modelled for each intracellular reaction as the dynamical description of each of the metabolic fluxes and transports was not targeted as a main objective, the steady state products yield were targeted instead controlled by energetic considerations.

2. Alternative additional fermentation products such as glycerol, currently not included, could potentially have roles in the balancing of electron equivalents (NADH) and could affect the model prediction capacity in some cases.

3. Alternative additional mechanisms of NADH/NAD^+ recovery impacting the electron balances and possibly involving other electron carriers not considered could have significant roles (Temudo et al. [11]).

4. The impact of anabolism and decay on the NADH balance has not been included and only the oxidation or reduction present in catabolism (as included in Figure 3.4) was considered. This possibly implies a slight underestimation of the yields of the more reduced products (since glucose has a slight lower degree of reduction than microbial biomass assumed as $CH_{1.8}O_{0.5}N_{0.2}$).

5. All solutes have been modelled using the same diffusion coefficient through the cell membrane due to the lack of reliable values for many of them. Differences in these coefficients could slightly increase or reduce the predicted product yields under specific operational conditions.

6. Physiological characteristics not considered in the model, such as variable internal pH or variable membrane potential, could lead to changes in the energetics of specific products and therefore their predicted yields by the model.

The current modelling framework as presented, can be adapted to describe the fermentation of other substrates (e.g. xylose or glycerol) by modification of the upper parts of the metabolic network. The model application to the study of more complex substrates (constituted by lipids, carbohydrates or proteins) is however thought to be more troublesome due to the number of additional factors that could deviate from the model assumptions (these include inhibitions or

physicochemical solubility-related factors). Experimentally, when using complex substrates, the control of the products spectrum is difficult, however, mechanistic insights on their fermentation, such as those obtained through in this study with glucose, do contribute towards the overall understanding and accelerate the industrial application of these bioprocesses towards valuable products recovery from wastes. Extensions of the metabolic network to address additional or more complex substrates are not expected to pose major impacts on computational times to solve the model as the already long simulation times required are mainly caused by short integration time steps due to the stiffness of specific variables.

3.5 Conclusions

The model developed, based on the optimization of the ATP production under a detailed metabolic network and with a full account of the electron balances and membrane transport energetics is, to our knowledge, the first mechanistic model succeeding in the prediction of observed shifts in major fermentation products with external pH, including the shift between CO_2/H_2 and formate production.

The breakthrough improvement respect to previous models is attributed to the more comprehensive account for the different electron carriers and their roles, a more complete metabolic reaction network and a detailed modelling of the energetics of solutes transport across the cell membrane. Additional value comes from the minimum parameter fitting needed and the fact that all results obtained are mechanistically related.

Under this approach, mixed culture fermentations, known to take place under strong energy limitation, are treated as networks that optimize the energy harvest rate of the overall mixed microbial population. The model focuses on first principles and on the energetic constrains imposed by the environment and avoids other specific physiological and ecological mechanisms. The results obtained under this modelling approach strongly support the hypothesis that mixed culture microbial ecosystems can be described as highly efficient energy harvesters in which, independently from the microbial community composition, the conditions of maximum energy harvest rate are achieved in the long term.

3.6 References

1. Agler MT, Wrenn BA, Zinder SH, Angenent LT (2011) Waste to bioproduct conversion with undefined mixed cultures: the carboxylate platform. *Trends in biotechnology* **29**: 70-78.

2. Angenent LT, Wrenn BA (2008) Optimizing mixed-culture bioprocessing to convert wastes into bioenergy. In: Press A, editor. Bioenergy. Washington. pp. 181-194.

3. Reis MA, Serafim LS, Lemos PC, Ramos AM, Aguiar FR, et al. (2003) Production of polyhydroxyalkanoates by mixed microbial cultures. *Bioprocess Biosystems Engineering* **25**: 377-385.

4. Angenent LT, Karim K, Al-Dahhan MH, Wrenn BA, Domíguez-Espinosa R (2004) Production of bioenergy and biochemicals from industrial and agricultural wastewater. *Trends in Biotechnology* **22**: 477-485.

5. Kleerebezem R, van Loosdrecht MCM (2007) Mixed culture biotechnology for bioenergy production. *Current Opinion in Biotechnology* **18**: 207-212.

6. Eggeman T, Verser D (2005) Recovery of Organic Acids from Fermentation Broths. In: Davison B, Evans B, Finkelstein M, McMillan J, editors. Twenty-Sixth Symposium on Biotechnology for Fuels and Chemicals: Humana Press. pp. 605-618.

7. Dellomonaco C, Clomburg JM, Miller EN, Gonzalez R (2011) Engineered reversal of the [bgr]-oxidation cycle for the synthesis of fuels and chemicals. *Nature* **476**: 355-359.

8. Singhania RR, Patel AK, Christophe G, Fontanille P, Larroche C (2013) Biological upgrading of volatile fatty acids, key intermediates for the valorization of biowaste through dark anaerobic fermentation. *Bioresource Technology* **145**: 166-174.

9. Lengeler JW, Gerhart D, Schlegel HG, Georg TV (1999) Biology of the Prokariotes; Thieme, editor. Stuttgart.

10. Temudo MF (2008) Directing product formation by mixed culture fermentation. Delft: T. U. Delft. 122 p.

11. Temudo MF, Kleerebezem R, van Loosdrecht MCM (2007) Influence of the pH on (open) Mixed Culture Fermentation of Glucose : A Chemostat Study. *Biotechnology and Bioengineering* **98**: 69-79.

12. Sieuwerts S, de Bok FAM, Hugenholtz J, van Hylckama Vlieg JET (2008) Unraveling Microbial Interactions in Food Fermentations: from Classical to Genomics Approaches. *Applied and Environmental Microbiology* **74**: 4997-5007.

13. Hoelzle RD, Virdis B, Batstone DJ (2014) Regulation mechanisms in mixed and pure culture microbial fermentation. Biotechnology and Bioengineering 111: 2139-2154.

14. Jackson BE, McInerney MJ (2002) Anaerobic microbial metabolism can proceed close to thermodynamic limits. *Nature* **415**: 454-456.

15. Smith DP, McCarty PL (1989) Reduced product formation following perturbation of ethanol- and propionate-fed methanogenic CSTRs. *Biotechnology and Bioengineering* **34**: 885-895.

16. Kohn RA, Boston RC (2000) The role of thermodynamics in controlling rumen metabolism. In: McNamara JP, France J, Beever DE, editors. Modelling nutrient utilization in farm animals: Oxford RU: CAB International. pp. 11-21.

17. Kleerebezem R, Stams AJM (2000) Kinetics of syntrophic cultures: a theoretical treatise on butyrate fermentation. *Biotechnology and Bioengineering* **67**: 529-543.

18. Jin Q, Bethke CM (2007) The thermodynamics and kinetics of microbial metabolism. *American Journal of Science* **307**: 643-677.

19. LaRowe DE, Dale AW, Amend JP, Van Cappellen P (2012) Thermodynamic limitations on microbially catalyzed reaction rates. *Geochimica et Cosmochimica Acta* **90**: 96-109.

20. Vallino JJ (2003) Modeling Microbial Consortiums as Distributed Metabolic Networks. *The Biological Bulletin* **204**: 174-179.

21. González-Cabaleiro R, Lema JM, Rodriguez J, Kleerebezem R (2013) Linking thermodynamics and kinetics to assess pathway reversibility in anaerobic bioprocesses. *Energy and Environmental Science* **6**: 3780-3789.

22. Hoehler TM, Jorgensen BB (2013) Microbial life under extreme energy limitation. *Nature Reviews Microbiology* **11**: 83-94.

23. Mosey FE, Matter O (1983) Mathematical modelling of the anaerobic digestion process: Regulatory mechanisms for the formation of short-chain volatile acids from glucose. *Water Science and Technology* **15**: 209-232.

24. Rodríguez J, Kleerebezem R, Lema JM, van Loosdrecht MCM (2006) Modeling product formation in anaerobic mixed culture fermentations. *Biotechnology and Bioengineering* **93**: 592-606.

25. Kleerebezem R, Rodríguez J, Temudo MF, van Loosdrecht MCM (2008) Modeling mixed culture fermentations; the role of different electron carriers. *Water Science and Technology* **57**: 493-497.

26. Aceves-Lara CA, Latrille E, Bernet N, Buffière P, Steyer JP (2008) A pseudo-stoichiometric dynamic model of anaerobic hydrogen production from molasses. *Water research* **42**: 2539-2550.

27. Zhang F, Zhang Y, Chen M, van Loosdrecht MCM, Zeng RJ (2013) A modified metabolic model for mixed culture fermentation with energy conserving electron bifurcation reaction and metabolite transport energy. *Biotechnology and Bioengineering* **110**: 1884-1894.

28. Kleerebezem R, van Loosdrecht MCM (2006) Critical analysis of some concepts proposed in ADM1. *Water Science and Technology* **54**: 51-57.

29. Gadhamshetty V, Arudchelvam Y, Nirmalakhandan N, Johnson DC (2010) Modeling dark fermentation for biohydrogen production: ADM1-based model vs. Gompertz model. *International Journal of Hydrogen Energy* **35**: 479-490.

30. Batstone DJ, Keller J, Steyer JP (2006) A review of ADM1 extensions, applications, and analysis: 2002-2005. *Water Science and Technology* **54**: 1-10.

31. McCarty PL, Mosey FE (1991) Modelling of anaerobic digestion processes (a discussion of concepts). *Water Science and Technology* **24**: 17-33.

32. Lee H-S, Krajmalinik-Brown R, Zhang H, Rittmann BE (2009) An electron-flow model can predict complex redox reactions in mixed-culture fermentative BioH2: Microbial ecology evidence. *Biotechnology and Bioengineering* **104**: 687-697.

33. Penumathsa BKV, Premier GC, Kyazze G, Dinsdale R, Guwy AJ, et al. (2008) ADM1 can be applied to continuous bio-hydrogen production using a variable stoichiometry approach. *Water Research* **42**: 4379-4385.

34. Wu L, Wang W, van Winden WA, van Gulik WM, Heijnen JJ (2004) A new framework for the estimation of control parameters in metabolic pathways using lin-log kinetics. European *Journal of Biochemistry* **271**: 3348-3359.

35. Zoetemeyer RJ, Vandenheuvel JC, Cohen A (1982) pH influence in acidogenic dissimilation of glucose in an anaerobic digester. *Water Research* **16**: 303-311.

36. Horiuchi JI, Shimizu T, Tada K, Kanno T, Kobayashi M (2002) Selective production of organic acids in anaerobic acid reactor by pH control. *Bioresource Technology* **82**: 209-213.

37. Fang HHP, Liu H (2002) Effect of pH on hydrogen production from glucose by a mixed culture. *Bioresource Technology* **82**: 87-93.

38. Rodríguez J, Lema JM, Kleerebezem R (2008) Energy-based models for environmental biotechnology. *Trends in Biotechnology* **26**: 366-374.

39. Rodríguez J, Premier GC, Guwy AJ, Dinsdale R, Kleerebezem R (2009) Metabolic models to investigate energy limited anaerobic ecosystems. *Water Science and Technology* **60**: 1669-1675.

40. Kashket ER (1987) Bioenergetics of lactic acid bacteria: cytoplasmic pH and osmotolerance. *FEMS Microbiology Letters* **46**: 233-244.

41. Maskow T, von Stockar U (2005) How reliable are thermodynamic feasibility statements of biochemical pathways? *Biotechnology and Bioengineering* **92**: 223-230.

42. Batstone DJ, Keller J, Angelidaki I, Kalyuzhnyi SV, Pavlostathis SG, et al. (2002) The IWA Anaerobic Digestion Model No 1 (ADM1). *Water science and technology* **45**: 65-73.

43. Papoutsakis ET, Meyer CL (1985) Fermentation equations for propionic-acid bacteria and production of assorted oxychemicals from various sugars. *Biotechnology and Bioengineering* **27**: 67-80.

44. Bennett GN, Rudolph FB (1995) The central metabolic pathway from acetyl-CoA to butyryl-CoA in Clostridium acetobutylicum. *FEMS Microbiology Reviews* **17**: 241-249.

45. Schink B (1997) Energetics of syntrophic cooperation in methanogenic degradation *Microbiology and molecular biology reviews* **61**: 262-280.

46. Kanehisa M, Goto S (2000) KEGG: kyoto encyclopedia of genes and genomes. *Nucleic Acids Research* **28**: 27-30.

47. White D (2007) The physiology and biochemistry of prokaryotes. New York: Oxford University Press. 628 p.

48. Schomburg I, Chang A, Placzek S, Söhngen C, Rother M, et al. (2013) BRENDA in 2013: integrated reactions, kinetic data, enzyme function data, improved disease classification: new options and contents in BRENDA. *Nucleic Acids Research* **41**: D764-D772.

49. Bar-Even A, Flamholz A, Noor E, Milo R (2012) Thermodynamic constraints shape the structure of carbon fixation pathways. *Biochimica et Biophysica Acta (BBA) – Bioenergetics* **1817**: 1646-1659.

50. Noor E, Bar-Even A, Flamholz A, Reznik E, Liebermeister W, et al. (2014) Pathway Thermodynamics Highlights Kinetic Obstacles in Central Metabolism. *PLoS Computational Biology* **10**: e1003483.

51. Bar-Even A, Noor E, Flamholz A, Buescher JM, Milo R (2011) Hydrophobicity and charge shape cellular metabolite concentrations. *PLoS Computational Biology* **7**: e1002166.

52. Bennett BD, Kimball EH, Gao M, Osterhout R, Van Dien SJ, et al. (2009) Absolute metabolite concentrations and implied enzyme active site occupancy in Escherichia coli. *Nature Chemical Biology* **5**: 593-599.

53. Mitchell P (1961) Coupling of phosphorylation to electron and hydrogen transfer by a chemi-osmotic type of mechanism. *Nature* **191**: 144-148.

54. Orth JD, Thiele I, Palsson BØ (2010) What is flux balance analysis? *Nature Biotechnology* **28**: 245-248.

55. Heijnen JJ, Kleerebezem R (2010) Bioenergetics of microbial growth. Encyclopedia of Industrial Biotechnology: Bioprocess, Bioseparation and Cell Technology. pp. 1-24.

56. Thauer RK, Jungermann K, Decker K (1977) Energy conservation in chemotrophic anaerobic bacteria. *Bacteriological Reviews* **41**: 809.

57. Elston T, Wang H, Oster G (1998) Energy transduction in ATP synthase. *Nature* **391**: 510-513.

58. ten Brink B, Otto R, Hansen UP, Konings WN (1985) Energy recycling by lactate efflux in growing and nongrowing cells of Streptococcus cremoris. *Journal of bacteriology* **162**: 383-390.

59. Flamholz A, Noor E, Bar-Even A, Milo R (2012) eQuilibrator--the biochemical thermodynamics calculator. *Nucleic Acids Research* **40**: D770-D775.

60. Canelas AB, van Gulik WM, Heijnen JJ (2008) Determination of the cytosolic free NAD/NADH ratio in Saccharomyces cerevisiae under steady-state and highly dynamic conditions. *Biotechnology and Bioengineering* **100**: 734-743.

61. Seedorf H, Fricke WF, Veith B, Brüggemann H, Liesegang H, et al. (2008) The genome of Clostridium kluyveri, a strict anaerobe with unique metabolic features. *Proceedings of the National Academy of Sciences of the United States of America* **105**: 2128-2133.

62. Huang H, Wang S, Moll J, Thauer RK (2012) Electron bifurcation involved in the energy metabolism of the acetogenic bacterium Moorella thermoacetica growing on glucose or H_2 plus CO2. *Journal of bacteriology* **194**: 3689-3699.

63. Sapra R, Bagramyan K, Adams MWW (2003) A simple energy-conserving system: proton reduction coupled to proton translocation. *Proceedings of the National Academy of Sciences of the United States of America* **100**: 7545-7550.

64. Chowdhury NP, Mowafy AM, Demmer JK, Upadhyay V, Koelzer S, et al. (2014) Studies on the mechanism of electron bifurcation catalyzed by electron transferring flavoprotein (Etf) and butyryl-CoA dehydrogenase (Bcd) of Acidaminococcus fermentans. *Journal Biological Chemistry* **289**: 5145-5157.

65. Brill WJ, Wolfe RS (1965) Ferredoxin reduction by acetaldehyde. *Federation Proceedings* **24**: 233-236.

66. Alberty RA (2006) Biochemical Thermodynamics: Applications of Mathematica. Hoboken: Wiley.

67. Alberty RA (2010) Biochemical thermodynamics and rapid-equilibrium enzyme kinetics. *The Journal of Physical Chemistry B* **114**: 17003-17012.

68. Hanselmann KW (1991) Microbial energetics applied to waste repositories. *Experientia* **47**: 645-687.

69. Yang Y-T, Bennett GN, San K-Y (2001) The Effects of Feed and Intracellular Pyruvate Levels on the Redistribution of Metabolic Fluxes in Escherichia coli. *Metabolic Engineering* **3**: 115-123.

70. Konings W, Lolkema J, Poolman B (1995) The generation of metabolic energy by solute transport. *Archives of Microbiology* **164**: 235-242.

71. Otto R, Sonnenberg AS, Veldkamp H, Konings WN (1980) Generation of an electrochemical proton gradient in Streptococcus cremoris by lactate efflux. *Proceedings of the National Academy of Sciences of the United States of America* **77**: 5502-5506.

72. Tobajas M, Garcia-calvo E (1999) Determination of biomass yield for growth of Candida utilis on glucose : Black box and metabolic descriptions. *World Journal of Microbiology and Biotechnolog* **15**: 431-438.

73. von Stockar U, Maskow T, Liu J, Marison IW, Patiño R (2006) Thermodynamics of microbial growth and metabolism: An analysis of the current situation. *Journal of Biotechnology* **121**: 517-533.

74. Kleerebezem R, van Loosdrecht MCM (2010) A Generalized Method for Thermodynamic State Analysis of Environmental Systems. *Critical Reviews in Environmental Science and Technology* **40**: 1-54.

75. Russell JB, Cook GM (1995) Energetics of bacterial growth: balance of anabolic and catabolic reactions. *Microbiology Reviews* **59**: 48-62.

76. Toei M, Gerle C, Nakano M, Tani K, Gyobu N, et al. (2007) Dodecamer rotor ring defines H+/ATP ratio for ATP synthesis of prokaryotic V-ATPase from Thermus thermophilus. *Proceedings of the National Academy of Sciences* **104**: 20256-20261.

77. Pirt SJ (1965) The maintenance energy of bacteria in growing cultures. *Proceedings of the Royal Society of London B Biological Sciences* **163**: 224-231.

78. Tijhuis L, van Loosdrecht MCM, Heijnen JJ (1993) A thermodynamically based correlation for maintenance Gibbs energy requirements in aerobic and anaerobic chemotrophic growth. *Biotechnology and Bioengineering* **42**: 509-519.

79. Temudo MF, Muyzer G, Kleerebezem R, van Loosdrecht MC (2008) Diversity of microbial communities in open mixed culture fermentations: impact of the pH and carbon source. *Applied Microbiology and Biotechnology* **80**: 1121-1130.

80. Diez-Gonzalez F, Russell JB (1997) The ability of Escherichia coli 0157 : H7 to decrease its intracellular pH and resist the toxicity of acetic acid. *Microbiology* **143**: 1175-1180.

81. Stams AJM (1994) Metabolic interactions between anaerobic bacteria in methanogenic environments. *Antonie van Leeuwenhoek Journal of Microbiology* **66**: 271-294.

USC
UNIVERSIDADE
DE SANTIAGO
DE COMPOSTELA

4

Linking thermodynamics and kinetics to assess pathway reversibility in anaerobic bioprocesses

This chapter has been published as:

González-Cabaleiro R, Lema JM, Rodríguez J, Kleerebezem R (2013) Linking thermodynamics and kinetics to assess pathway reversibility in anaerobic bioprocesses. *Energy and Environmental Science* **6**: 3780-3789.

Abstract

The on-going research towards sustainable fuel production entails the improvement of the microbial catalysts involved. The possible reversibility of specific anaerobic catabolic reactions opens up a range of possibilities for the development of novel reductive bioprocesses. These reductive biohydrogenation pathways enable production of high energy density chemicals of interest as biofuels such as alcohols and long chain fatty acids. Anaerobic bioprocesses take place in energy scarcity conditions due to the absence of strong electron acceptors such as oxygen, and provide metabolic pathways towards these energy dense (reduced) chemicals. Metabolic reactions are running very close to thermodynamic equilibrium with minimum energy dissipation consequently, environmental changes in products and substrates concentrations can easily reverse the driving force of the chemical reaction catalysed. The objective of this work is to investigate the potential reversibility of specific anaerobic pathways of interest. The thermodynamics of the different steps in biochemical pathways are analysed and combined with assumptions concerning kinetic and physiological constraints to evaluate if pathways are potentially reversible by imposing changes in process conditions. The results suggest that (i) in homoacetogenesis may operate in both reductive and oxidative directions depending on the hydrogen partial pressure in the system, (ii) acetate reduction to butyrate with hydrogen is not feasible, but no biochemical bottlenecks are apparent in butyrate production from acetate with ethanol or lactate as electron donors; (iii) the reduction of short chain to longer chain fatty acids with ethanol as electron donor appears thermodynamically and kinetically feasible; (iv) alcohol production from the corresponding fatty acids (e.g. ethanol from acetate) was found to require proton translocations at specific sites in the biochemical pathways in order to compensate for the ATP required for phosphatation of acetate and to enable energy harvesting. Overall, the methodology proposed here allows for analysing the potential reversibility of catabolic pathways and therewith contributes to the development of efficient and reliable anaerobic bioprocesses for the production of biofuels and chemicals.

4.1 Introduction

Anaerobic oxidative reactions when operating in the opposite (reductive) direction can typically result in the production of high energy density chemicals of interest such as hydrogen, alcohols and long chain fatty acid molecules [1]. In addition, the hydrophobicity of reduced end products tends to increase compared to that of the substrate, simplifying product purification through phase separation (gas or solid). Therewith the reversibility of catabolic pathways could be potentially exploited to favour reductive pathways that yield end-products with higher energy density and lower solubility enabling product separation[2-5] as well as the formation of longer hydrophobic carbon chains through condensation reactions [1,6-11]. In this manner, alcohols, medium and long chain fatty acids (MCFAs and LCFAs), could be produced from volatile fatty acids (VFAs) by e.g. increasing the hydrogen partial pressure or through addition of one or more electron donors, pushing reaction driving forces towards the reductive direction.

Lee and Zinder [12] reported the first example of a bacterial strain capable to reverse its metabolism when the ambient conditions change. *Thermacetogenium phaeum* is a homoacetogen growing on carbon dioxide reduction to acetate with molecular hydrogen as electron donor, but it can also grows on acetate oxidation if molecular hydrogen partial pressure is low. The short lag times reported for the microbe to change its metabolism as well as the enzymatic activities measured, strongly suggested that the same (reverted) metabolic pathway was used in both directions. This implies a highly efficient energy harvest by a highly flexible microorganism, working close to thermodynamic equilibrium and switching its metabolism in response to a change in environmental substrate and product concentrations [13-15]. However, the way *Thermacetogenium phaeum* strain is able to harvest energy for its anabolism, still remains as an open question as no ATP gain through substrate level phosphorylation (SLP) is reported through either pathway directions the homoacetogenic or acetate oxidation [14,16].

Microbial metabolism energetics can be simply described in terms of energy production in catabolism (ΔG_{cat}), energy consumption for anabolism (growth) and maintenance purposes (ΔG_m) [17]. Metabolism furthermore requires the dissipation of some energy (ΔG_{dis}) in order to proceed. ΔG_{dis} represents the actual thermodynamic driving force of microbial metabolism in a given direction [18]. In

order to connect catabolism and anabolism the cells use energy conservation mechanisms. In anaerobic fermentations energy can be harvested directly through substrate level phosphorylation, or indirectly by generating an electrochemical (proton) gradient across the cytoplasmic membrane according to the chemiosmotic theory [19-21].

The translocation of protons across the cell membrane takes place in catabolism when some enzymes catalysing highly exergonic redox reactions are capable of coupling the electron transfer to the translocation (extrusion) of protons across the cytoplasmic membrane. The resulting proton motive force can be used to form ATP. Indeed, the opposite is also possible with endergonic reactions being enabled by coupling to proton translocations (intrusion) to provide the energy required. Proton translocations can also take place coupled with the transport of solutes across the membrane [19] as well investing or harvesting energy.

The energy required to extrude one proton across the cytoplasmic membrane ($\Delta\mu_{H+}$) constitutes the minimum energy quantum that can be harvested by the cell in the form of ATP via *ATPase* [20,22]. Its value is variable (i.e. different conditions, different microorganisms) but it has been proposed to amount approximately 1/3 of the energy liberated in ATP hydrolysis under normal growth conditions i.e. -15, -20 kJ/mol [18,23-25]. Thus, 3 protons are assumed as equivalent to one ATP [26].

The efficiency of the energy harvesting mechanisms of the cell gain importance in anaerobic fermentations. The inherent energy scarcity in anaerobic fermentative systems forces microorganisms to become highly efficient energy scavengers [13,27,28] and the need to harvest most of the available energy implies that metabolic reactions must proceed very close to thermodynamic equilibrium (i.e. keeping energy dissipation at a minimum, $\Delta G_{dis} \approx 0$ kJ/mol) [18,27,29,30].

In these low ΔG scenarios changes in reactants and products concentrations can reverse the driving force of catabolic reactions [31-33]. This potential reversibility of specific anaerobic catabolic reactions opens up a range of possibilities for the development of novel reductive bioprocesses [34] which appear as promising avenues to produce high energy density products of interest as biofuels [1-11,35,36].

In this work a rigorous method focusing on the thermodynamic analysis of several catabolic pathways, based on quasi equilibrium calculations, is presented. This method is used to assess the feasibility of reverting specific anaerobic pathways of interest and whether bacteria are capable of harvesting energy enough for growth and maintenance through these catabolic processes. Upper and lower limit metabolite concentrations (thermodynamically and kinetically/physiologically feasible) are analysed by estimating the intermediate metabolite concentrations, assessing the feasible kinetic limits of several metabolic pathways of interest.

Firstly, we focus on the homoacetogenesis vs. acetate oxidation (case shown by Lee and Zinder [12]) and on how the available energy can be harvested by the cell to survive. Carbon dioxide reduction is of great high interest towards production of biofuel or chemicals with high selectivity when using synthesis gas as a low cost substrate [37,38].

Secondly, the anaerobic butyrate oxidation, previously studied by Kleerebezem and Stams [18], is confronted with acetate reduction to butyrate. The energetics of acetate reduction and its limitations are studied using three different electron donors namely H_2, ethanol and lactate. Acetate reduction could be a key step to open a pathway towards the production of high density energy products like it was proposed firstly by Smith and McCarty [35,36]. Butyrate production could be extended towards increase the carbon chain length to the production of medium chain fatty acids (MCFAs) like caprilate and caproate [1,2,6,8,9]. In line with this, we focus our interest on the complete chain from carbon dioxide reduction to MCFAs.

Thirdly, we conducted a thermodynamic analysis of the limitations of alcohol production as biochemical reduction of their corresponding volatile fatty acids (VFAs). VFA reduction was experimentally reported in Steinbusch et al. [4]. Our study will focus on the physiological options for the cell to harvest energy from these reactions. VFAs reduction opens the possibility to obtain higher energy density products in fermentative processes as well the possibility of diversification of substrates for alcohol production [4].

4.2 Methodology

Quasi-equilibrium thermodynamic calculations

The actual Gibbs free energy exchange (or driving force) of any chemical reaction can be calculated as a function of the Gibbs free energy exchange at a standard reference state (ΔG^o) (25 °C, 1 atm, 1 M) and activities (a_i) of reactants and products relative to the reference state analogously as presented in Chapter 3.

$$\Delta G = \Delta G^0 + R_{th} \cdot T \cdot \ln \prod_i a_i^{\nu_i} \quad \text{with} \quad a_i = \gamma_i \cdot C_i \qquad 4.1$$

We assume in all the cases that activities are equal to concentrations neglecting ionic strengths, assuming activity coefficients equal to 1.

In pathways with very small driving forces, (i.e. running in quasi equilibrium conditions), changes in reactant and/or product activities can change the sign of the ΔG and therewith the direction of the reaction.

In this study we estimate the metabolite concentrations in a catabolic pathway assuming thermodynamic equilibrium for the individual steps ($\Delta G = 0$). Since the ΔG of the overall catabolic reaction is favourable, reaction steps need to be identified where either Gibbs energy is dissipated or used for proton translocation and therewith energy harvesting. Herewith thermodynamic equilibrium of the overall pathway is introduced and all metabolite concentrations can be estimated. Additional assumptions and generalizations that were included are outlined in the next sections.

At all the cases an intracellular pH of 7 and a temperature of 25 °C were assumed. Values for the standard Gibbs energies of formation are available [19,39-44].

Limit metabolite concentrations and conserved moieties

The assumption of thermodynamic equilibrium enables the calculation of intermediate metabolite concentrations. Very low metabolite concentrations are likely to impose kinetic limitations in the metabolic pathway consequently actual

concentrations inside the cell are typically constrained (by enzyme kinetics, cell volume and solubility). According to this we assume in this study that limit concentrations below 1 μM will kinetically disable the reaction in the cell, and concentrations bigger than 10 mM are not physiologically feasible [33,45,46].

In addition, microbial cells contain specific molecules/groups required by the metabolism (such as -CoA, -THF, -P_i, NAD(P)x, FADx) which total concentrations are presumed to remain constant inside the cell (conserved moieties [47]). This implies that there is a limited availability of those functional groups/metabolites and that not only thermodynamics but also total availability of conserved moieties has an impact on the intermediate concentrations calculated for a given pathway.

Assumptions and justification

The total concentrations for the conserved moieties assumed in this study are presented in Table 4.1. The value for the total THF is estimated equal to the total CoA. Its value appears as not having significant impact on the studied pathways feasibility according to the sensitivity analysis presented in section 4.4.

Table 4.1 Total intracellular conserved moiety concentrations assumed in this study (free form plus all the metabolites linked to these functional groups).

CONSERVED MOIETY	TOTAL CONCENTRATION (mM)
-CoA_{Total}	10 [18]
-$Phosphate_{Total}$	20 [18]
-THF_{Total}	10

The total concentration of electron carrier conserved moieties, such as NAD(P)x and FADx are also assumed constant. However it is only their ratio between oxidized and reduced species that affects energetic calculations. In this study, we assume them in equilibrium with the H_2 partial pressure [48] not analysing differences between electron carriers potentials and not limiting the possible feasible ratios between reduced and oxidised forms (in any metabolic process studied is glycolysis present, thus the limitation for NADH/NAD^+ ratio presented in Chapter 1 cannot be considered here). Higher H_2 partial pressures (P_{H_2}) (that could be considered as undefined reducing power equivalents) will

favour the reductive direction of pathways and allow for higher limit equilibrium concentrations of the intermediate metabolite products.

A set of possible electron carriers mechanisms (coupled to redox reactions) is assumed, simplifying in some cases respect to the mechanisms found in the literature [49,50] and only considering one electron carrier involved in the reaction (not considering chains of electron transfer reactions). The simplification is justified assuming that the expected impact of including the alternative detailed chain mechanisms for electron carrying is negligible. This is due to the fact that reactions in these energy limited pathways must proceed very close to thermodynamic equilibrium, no more energy could be expend on other biochemical mechanisms, and the use of one mechanism or another becomes a question of efficiency in the electron transport chain process unlikely to affect significantly any other relevant aspect of the reaction outcome.

In this study the analysis of metabolic pathways under thermodynamic equilibrium could reveal kinetic bottlenecks due to very unfeasibly low required limit intermediate concentrations. This does not occur in cases of very favourable pathways where very high calculated limit equilibrium concentrations of a metabolite can be overcome by energy dissipation allowing feasible actual metabolite concentrations. In addition, the energy dissipated in highly favoured reactions can help promote other less favoured reactions, allowing the whole pathway to proceed (e.g. occupying less -CoA and increasing the availability of its free form, CoASH, to drive other reactions).

The energy conservation mechanisms in the cell allow for the energy gained in catabolism to be invested in anabolism or, alternatively to fuel other not energetically favourable intermediate reactions such as certain catabolic pathway steps (e.g. through activation with ATP hydrolysis or translocation of one or more protons across the membrane, $\Delta\mu_{H+}$). So, $\Delta\mu_{H+}$ is assumed as the minimum usable energy quantum for the cell but its amount of energy associated is still an open question as a number of microbial strains in syntrophic cooperation have been shown to survive in conditions extremely close to thermodynamic equilibrium, with very low energy available [24,30].

Indeed, proton motive force $\Delta\mu_{H+}$ has been observed to vary with external conditions, increasing or decreasing the energy to translocate one proton by changes in the membrane potential [51-53] and even using only ΔpH as driving

force [51]. In any case, the value of $\Delta\mu_{H+}$ must be maintained in order to preserve cell homeostasis [54].

Likewise, wide ranges of values for ATP hydrolysis synthesis energy have been reported in the literature [29,55-58]. The *ATPase* system allows for the interchange of ATP energy with proton motive force $\Delta\mu_{H+}$ maintaining a certain concentration of ATP such that cells minimise energy losses (as part of cell homeostasis) enabling survival under energy scarce conditions [55].

In this study, a constant membrane potential of 0.2 V [59] value is used and a constant energy for ATP hydrolysis of 50 kJ/mol. Consequently $\Delta\mu_{H+}$ is close to 1/3 of the energy liberated in ATP hydrolysis without ΔpH. The consideration of keeping constant a $\Delta\mu_{H+}$ value related with the ATP hydrolysis value seems consistent in order to assess the feasibility of the pathways.

Calculation method of the conserved moieties concentrations

The limits in total intracellular concentrations of conserved moieties affect the equilibrium-based metabolite concentration calculations. This is due to the fact that conserved moieties forms have to must be allocated among several intermediate metabolites (e.g. all X-CoA and X-THF intermediate metabolites) without exceeding the total amount available inside the cell (e.g. of total -CoA or total -THF).

In order to solve the system for quasi equilibrium and limitation of conserved moieties, their free concentrations are used as variable through an iterative procedure.

Initially, the total concentration of the conserved moieties are assumed in their free forms (i.e. CoASH, THF) and the concentrations of all intermediate metabolites are calculated based on the ΔG proposed for each reaction. The new total concentration of all the conserved moieties forms is compared with the maximum and the excess subtracted from the free form before the calculation process is repeated until the convergence.

Variables selection for the cases studied

The conditions considered for each pathway, were chosen, fixing the energy available in the system to run the analysed catabolic process. The pH and temperature were considered at 7 and 298.15 K respectively in all the analysed processes (Table 4.2).

The intracellular pH is assumed to be 7. Considering only the energetics associated to the metabolic pathway, a change in the external pH has a similar impact than an increase or decrease in the concentration of products and reactants, increasing or decreasing the total energy available in the system for the metabolic process. Even though, it implies a more important impact on the $\Delta\mu_{H+}$ value.

Table 4.2 Conditions (the same for all case studies).

VARIABLE	VALUE	UNIT
pH_{intrac}	7.00	-
pH_{extrac}	7.00	-
T	298.15	K
ΔG_{ATP}	50.00	kJ/mol
$\Delta\Psi$	-0.2	V

Changes in temperature can also have impacts in the feasibility of the process that could be evaluated under this framework. However, additional thermodynamic information is needed in order to do the calculations.

As a variable in each pathway, the concentration of e-donor in the system was chosen since it generates an impact in the intermediate metabolite concentrations. Other external metabolites concentrations (i.e. final products and reactants of the pathway) were fixed as constants because they have usually less impact over the relative intermediate concentrations of the metabolites inside the cell. Thus, a change on their concentration would increase or decrease the energy available in the system to run the process but would not reveal possible kinetic bottlenecks.

The final products and reactants were in all the cases chosen with the objective to maximise the production of the desire final product, keeping the energy available close to the limits of feasibility.

Calculation method of the intermediate metabolites concentrations

Under all the considerations exposed, the energy released is estimated for all the reactions of all the pathways studied. In the majority of the reactions, we assume equilibrium (as a measurement of the limit of all the metabolite concentrations), but when it is necessary and available, energy dissipation is also possible and considered. Besides, in some metabolic reactions coupling with a proton translocation is also considered. In these cases, the necessary energy for the translocation is included in the calculation.

Therefore, fixing the substrates and products concentrations for the total pathway, all the information is available to estimate the intermediate metabolites concentrations. The calculation process drifts from the first reaction of the pathway to the last with only one unknown present for each reaction, solved using equation 4.1.

4.3 Results

Homoacetogenesis reversibility

Lee and Zinder [12] first reported homoacetogenesis reversibility. Only by introducing an elevated hydrogen partial pressure in the system, it changed from an acetate oxidizing system to a CO_2 reducing system. The absence of a lag phase in the change of the direction of the reaction catalysed, suggest that the same pathway is involved in both reductive and oxidative directions.

Since no net ATP gain is attained via SLP in either direction of the homoacetogenesis (Figure 4.1), the cells should harvest their energy through $\Delta\mu_{H+}$ energy recovery coupled steps. Hattori [15] suggested that $\Delta\mu_{H+}$ energy recovery only takes place at the CO oxidation in the oxidative direction and, in reductive direction, the *methylene-THF reductase* is the enzyme considered most probably coupled with the proton translocation. To analyse the energy requirements of the

pathway in both directions, oxidative and reductive, all the metabolite concentrations were calculated considering thermodynamic equilibrium and energy recovery only at the sites indicated by Hattori [15] (Figures 4.2.a and 4.3.a). Our analysis indicates that energy can be harvested as suggested, but also energy investment is needed as $\Delta\mu_{H+}$ in order to avoid the formation of kinetic bottlenecks that would block the pathway even at low P_{H2} (Figures 4.2.b and 4.3.b).

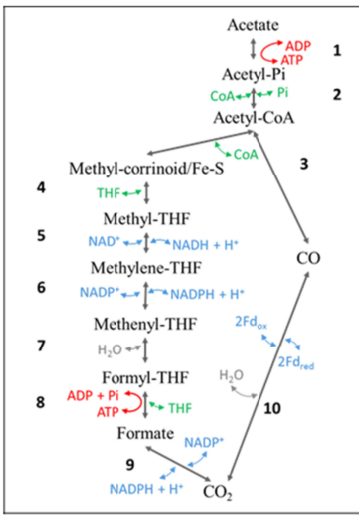

Nº	ΔG⁰ (kJ/mol)
1	-0.80
2	5.03
3+4	63.46[a]
5	61.95
6	4.90
7	43.95
8	8.40
9	-21.50
10	38.92
Total	55.05

Figure 4.1 Considered metabolic pathway for oxidation/reduction of acetic acid and standard Gibbs energy values for each metabolic step.

When thermodynamic equilibrium is considered for all the metabolic reactions in the oxidative direction (Figure 4.2.a), unfeasible limit forced metabolite concentrations were predicted, above or below the feasible limits assumed (10 mM and 1 µM respectively). At lower P_{H2}, more energy is available to run the complete pathway, however if energy is not recovered or dissipated at specific sites of the pathway, the calculated equilibrium concentrations of certain metabolites would have to reach even higher concentrations (CO concentrations in Figure 4.2.a) or lower concentrations (Methyl-THF concentration in Figure 4.2.a) making the catabolic pathway more difficult.

The reaction catalysed by *methylene-THF reductase* enzyme (from methyl-THF to methylene-THF) is largely endergonic (ΔG^o = 61.95 kJ/mol). Consequently, the concentrations of methylene-THF would have to be very low

rendering the pathway kinetically unfeasible if no energy is invested in this step. However, as suggested by Hattori [15], this enzymatic reaction is likely to be coupled to membrane proton translocation and energy harvesting when the pathway runs in the reductive direction. Assuming that the metabolic mechanism is the same in both directions of the pathway, energy investment in the form of $\Delta\mu_{H+}$ is proposed for the oxidative direction, in order to run the pathway without kinetic bottlenecks (Figure 4.2.b). In addition, if it is available in the system, more energy could be invested in the catabolic process since some reactions in the pathway remain highly exergonic. These reactions could dissipate some energy avoiding bottlenecks otherwise occurring under thermodynamic equilibrium.

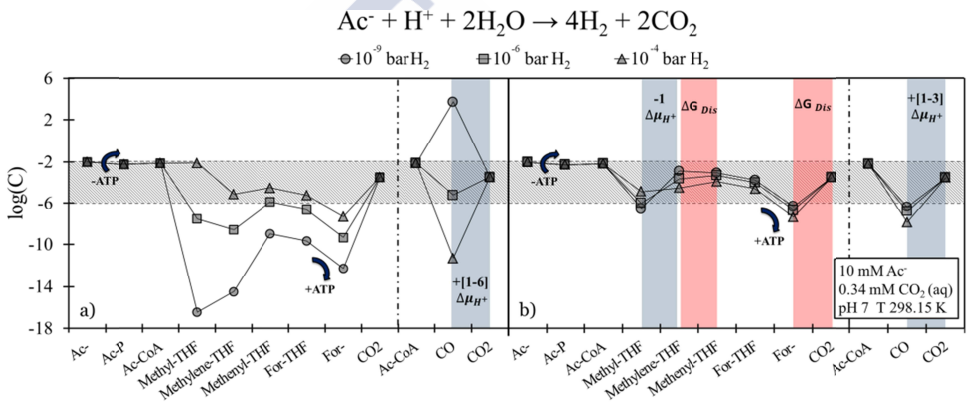

Figure 4.2 Limit (quasi equilibrium) metabolite concentrations (C, mol/L) of the acetate oxidation pathway under different P_{H2} (ΔG_{cat} values for the three lines at increasing P_{H2} are -121.89, -53.40 and -7.73 kJ/mol). a) Without energy dissipation and only $\Delta\mu_{H+}$ energy recovery at the CO oxidation site, kinetically unfeasible (too low or high) concentrations of metabolites (e.g. Methyl-THF, For⁻, CO) disable the pathway. b) With energy dissipation and $\Delta\mu_{H+}$ energy investment (-) at the Methyl-THF oxidation site, kinetically feasible concentrations of metabolites enable the pathway.

The Gibbs energy change of the catabolism decreases at increasing values for P_{H2}. At low P_{H2} (10^{-9} and 10^{-6} bar) the total energy available (ΔG_{cat} = -121.89 and -53.40 kJ/reaction) is sufficient for net translocation of at least one proton for energy harvesting while the remaining energy can be dissipated. However at higher P_{H2} (10^{-4} bar) the catabolic energy available (ΔG_{cat} = -7.73 kJ/reaction) is not sufficient. The one proton extruded during CO oxidation needs to be invested in Methyl-THF conversion and net no energy is harvested. In addition, at high

P_{H2}, very low metabolite concentrations (i.e. For$^-$, CO concentrations) are estimated suggesting kinetic bottlenecks.

If the pathway is analysed in the opposite direction (CO_2 reduction), energy as $\Delta\mu_{H+}$ can be recovered at the *methylene-THF reductase* enzyme site and energy investment is now needed instead of recovered at the CO oxidation step (Figure 4.3.a).

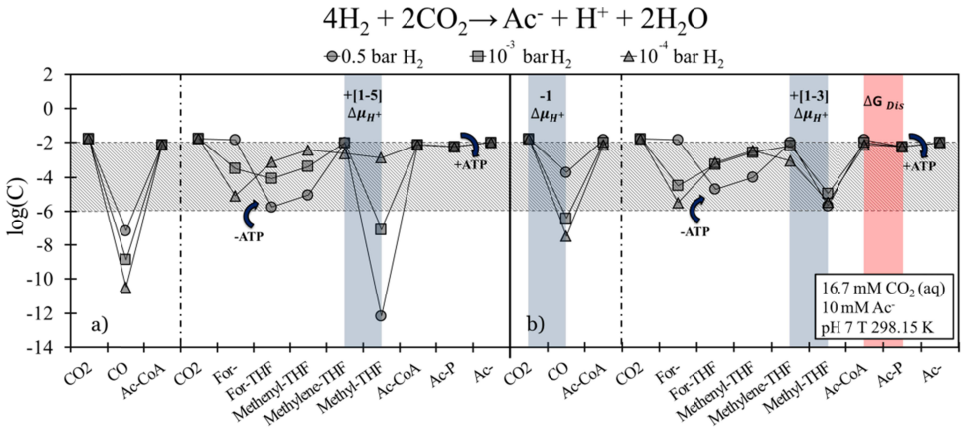

Figure 4.3 Limit (quasi equilibrium) metabolite concentrations (C, mol/L) of the homoacetogenesis pathway under different P_{H2} (ΔG_{cat} values for the three lines at decreasing P_{H2} are -96.11, -34.49 and -11.66 kJ/mol). a) Without energy dissipation and only $\Delta\mu_{H+}$ energy recovery (+) at the methylene-THF reduction site, kinetically unfeasible (too low) concentrations of metabolites (e.g. Methyl-THF, CO) disable the pathway. b) With energy dissipation, $\Delta\mu_{H+}$ energy recovery (+) at the methylene-THF reduction site and $\Delta\mu_{H+}$ energy investment (-) at the CO_2 reduction site, kinetically feasible concentrations of metabolites enable the pathway.

In this case, $\Delta\mu_{H+}$ energy investment and energy dissipation are also necessary in specific steps in order to avoid kinetic bottlenecks (Figure 4.3.b). Similarly as it was shown in the acetate oxidation study, the decrease of the total energy available (ΔG_{cat}) at decreasing P_{H2} values leads to a situation where no net energy harvesting is possible due to the impossibility of at least one proton translocation to yield energy for anabolism and growth (Figure 4.3.b).

In order for the cell to grow and the maintenance to proceed, the net total energy gained from catabolism must income at least the minimum energy

necessary to translocate one proton ($\Delta\mu_{H+}$); otherwise the cell would not survive. But the minimum energy needed to survive running the process, will be in part determined by the capacity of the cell to modify its $\Delta\mu_{H+}$ according the conditions of the system.

Summarizing this analysis, we propose that the homoacetogenesis pathway may very well be fully reversible, provided that energy harvesting sites and energy investment sites in the pathway are switched. Using $\Delta\mu_{H+}$ to harvest energy for anabolism or using $\Delta\mu_{H+}$ in order to drive unfavourable reactions provides the cell the required flexibility to reverse its catabolic pathway when exposed to different environmental conditions.

The minimum energy to run the pathway should be the $\Delta\mu_{H+}$ fixed by the cell, and together with some energy dissipation, the enzymatic kinetics would not be constrained.

Based on this analysis, the reported reversible homoacetogenesis appears feasible. Proton motive force energy coupling is necessary in order to make key unfavourable reaction steps run in both oxidative and reductive directions, allowing the microorganism to survive under a broader spectrum of conditions. This analysis sustains our initial assumption that pathway reversibility is biochemically and bioenergetically possible [14-16].

Acetate reduction pathways

Building up on a previous theoretical study [18] and in order to explore the possibilities for carbon chain elongation towards higher energy density products, the reversibility of butyrate oxidation to acetate is studied (Figure 4.4).

Figure 4.5.a illustrates how the pathway on butyrate oxidation to acetate remains feasible at a wide range of P_{H_2}. The overall reaction including the gain of one full ATP via SLP would be endergonic under the considered conditions [18] however part of the energy is re-invested through proton translocations to enable the overall reaction. This reinvestment takes place at the highly endergonic step of butyryl-CoA oxidation to crotonyl-CoA (Figure 4.5.a).

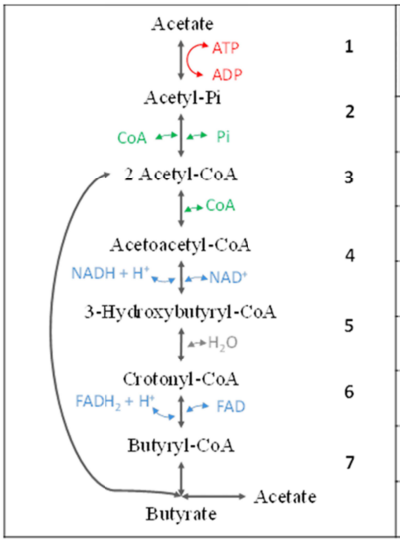

Nº	ΔG^0 (kJ/mol)
1	-0.8
2	5.03
3	27.1
4	-61.53
5	1.72
6	-115.7
7	4.93
Total	-80.02

Figure 4.4 Considered metabolic pathway for oxidation of butyric acid to acetic or reversed and standard Gibbs energy values for each metabolic step.

In addition to the circa 2/3 of the energy from ATP hydrolysis reinvested in the pathway, energy must be dissipated at the exergonic step of acetoacetyl-CoA dissociation [18] to avoid a kinetic bottleneck formed if only thermodynamic equilibrium is considered (Figure 4.5.a). The circa 2/3 ATP reinvested plus the dissipated energy needed to allow the pathway to run imply that the net energy gain is less than one $\Delta\mu_{H+}$. The total catabolic energy available (ΔG_{cat}) in the butyrate oxidation decreases at higher P_{H2}, suggesting that in these cases it might not be possible avoid the acetoacetyl-CoA kinetic bottleneck by energy dissipation.

The reverse study of this pathway (acetate reduction to butyrate) is presented in Figure 4.5.b. A kinetic limitation arises with unfeasibly low acetoacetyl-CoA concentration required by the condensation reaction of two acetyl-CoA (Figure 4.5.b) which remains highly endergonic (ΔG^o = 27.1 kJ/mol) even at high P_{H2} values implying that the reductive process would be difficult to proceed.

Therefore, Figure 4.5 illustrates how pathways running very close to thermodynamic equilibrium might be non-reversible. This is caused by the fact that $\Delta\mu_{H+}$ coupling might be possible only at specific sites (in this case, only at crotonyl-CoA reduction to butyryl-CoA) and the limited availability of conserved moieties can block one of the two directions of the pathway.

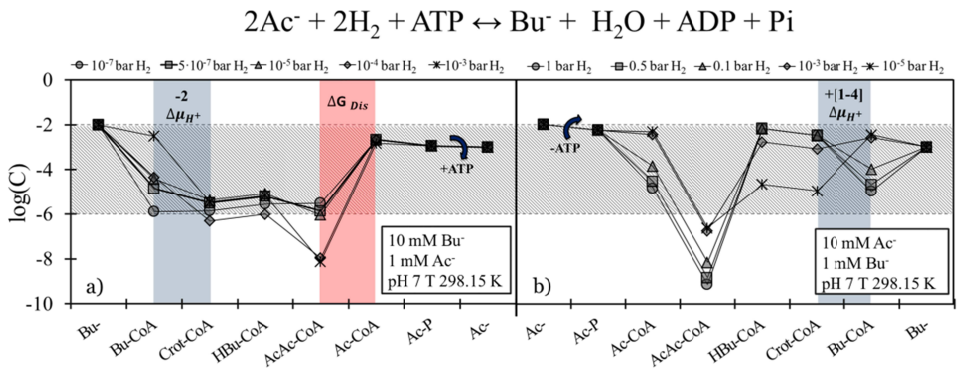

Figure 4.5 Limit (quasi equilibrium) metabolite concentrations (C, mol/L) under different P_{H2} for butyrate oxidation to acetate and acetate reduction butyrate pathways. a) Butyrate oxidation limit concentrations remain within feasible ranges and $\Delta\mu_{H+}$ energy is recovered (ATP) for a wide range of P_{H2} (ΔG_{cat} values, including ATP production, for the five lines at increasing P_{H2} are 45.48, 53.46, 56.89, 68.30 and 79.72 kJ/mol) b) The acetate reduction pathway however, suffers from a clear kinetic bottleneck in the acetyl-CoA condensation step even at the highest P_{H2}, disabling the pathway (ΔG_{cat} values, including ATP hydrolysis, for the five lines at decreasing P_{H2} are -92.51, -89.07, -81.09, -58.26 and -35.57 kJ/mol).

Despite the results above, acetate reductive pathways have been reported experimentally with electron donors like ethanol and H_2 [8,9]. In fact, the analysis of the acetate reduction pathway to butyrate with ethanol as electron donor (Figure 4.6) does not actually lead to kinetic limitations such as described for the hydrogen case (Figure 4.7). In addition $\Delta\mu_{H+}$ energy can even be harvested (Figure 4.7.a). Similar results are achieved when lactate is the electron donor (Figure 4.7.b).

These results confirm the biochemical and thermodynamic feasibility of acetate reduction with electron donors other than H_2. The production of butyrate and caproate has been also reported with H_2 fed as sole electron donor [8] but under those conditions ethanol was always detected. We propose that acetate reduction to butyrate with H_2 as electron donor (Figure 4.5.b) involves initial reduction of acetate to ethanol, and subsequent butyrate and caproate production from acetate with ethanol as electron donor as presented in Figure 4.7.

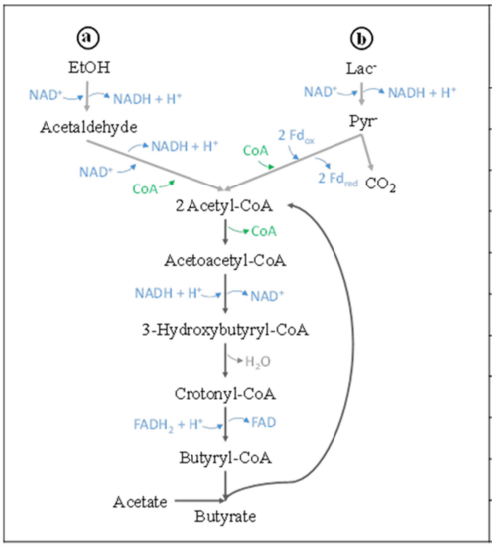

N°	ΔG^0 (kJ/mol)
1	63.68
2	65.01
3	25.58
4	20.32
5	27.1
6	-61.53
7	1.72
8	-115.7
9	4.93
Total for EtOH	-38.65
Total for Lac-	-96.95

Figure 4.6 Considered metabolic pathway for reduction of acetic acid to butyric acid using ethanol or lactate as electron donor and standard Gibbs energy values for each metabolic step.

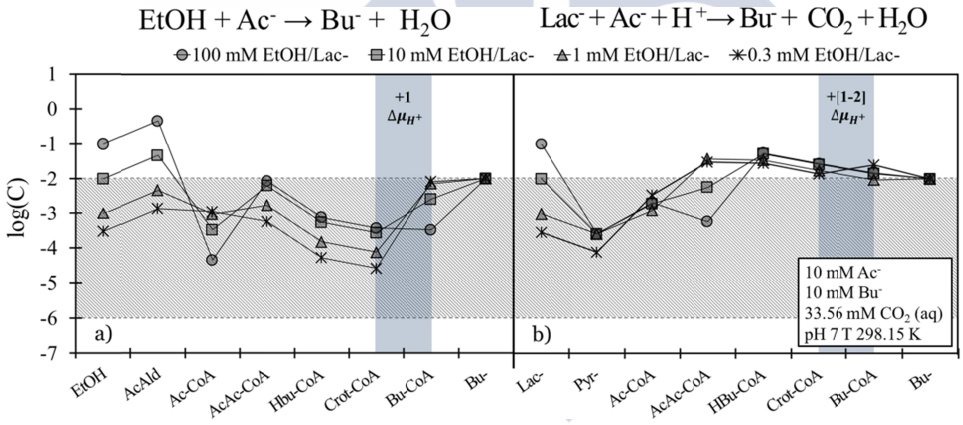

Figure 4.7 Limit (quasi equilibrium) metabolites concentrations (C, mol/L) for acetate reduction to butyrate with ethanol (a) (ΔG_{cat} values for the four lines at decreasing ethanol concentrations are -32.94, -27.23, -21.53 and -18.54 kJ/mol) and lactate (b) (ΔG_{cat} values for the four lines at decreasing lactate concentrations are -41.59, -35.88, -30.17 and -27.19 kJ/mol) as electron donor. Both pathways remain feasible under different concentrations of e-donors.

The use of ethanol as electron donor enables the production of longer chain fatty acids such as caproate from acetate [1,2] through the extended butyrate production pathway as suggested by Seedorf et al. [49] for *Clostridium kluyveri* (Figure 4.8). The further extension of the carbon chain does not only imply energy cost to the cell [11] but can theoretically yield useful energy in the form of additional $\Delta\mu_{H+}$ (Figure 4.9).

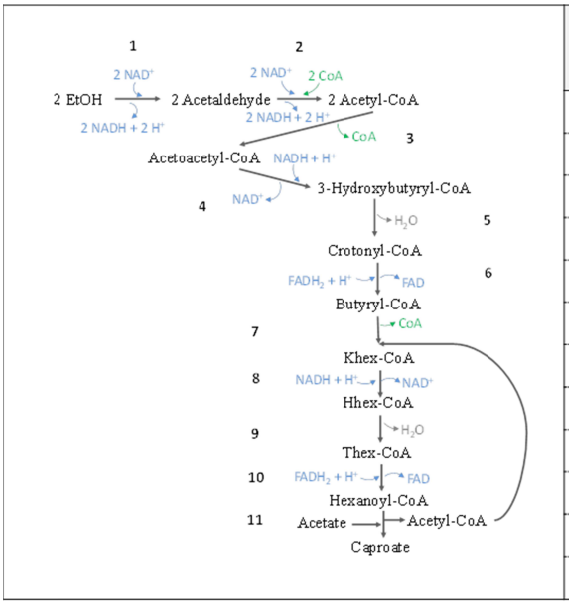

Nº	ΔG^0 (kJ/mol)
1	63.68
2	25.58
3	27.1
4	-61.53
5	1.72
6	-115.7
7	27.1
8	-60.23
9	4.02
10	-118.4
11	8.85
Total	-77.41

Figure 4.8 Considered metabolic pathway for caproate production from ethanol and standard Gibbs energy values for each metabolic step.

Caproate production has been reported using ethanol and butyrate as substrates [10]. This involves the ethanol oxidation to acetate and later combination with butyrate for caproate production. This route, technically more interesting due to the lower requirement of ethanol compared to the butyrate elongation with acetate (which requires two mol of ethanol per mol of caproate), appears perfectly feasible (Figure 4.10). As well, the possibility of caproate production directly from ethanol as single substrate is analysed (Figure 4.11) and in this case the process allows for more energy harvesting for growth and maintenance. This route for caproate production includes ethanol oxidation to acetic acid, which is later used in the butyrate elongation.

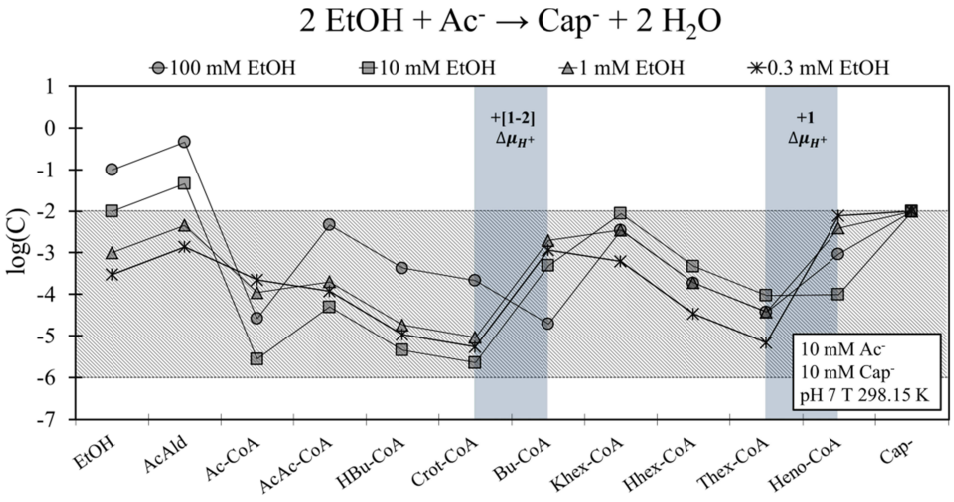

Figure 4.9 Limit (quasi equilibrium) metabolites concentrations (C, mol/L) for acetate reduction to caproate with ethanol as electron donor. The pathway remains feasible under different concentrations of e-donor (ΔG_{cat} values for the four lines at decreasing ethanol concentrations are -65.99, -54.58, -43.16 and -37.19 kJ/mol).

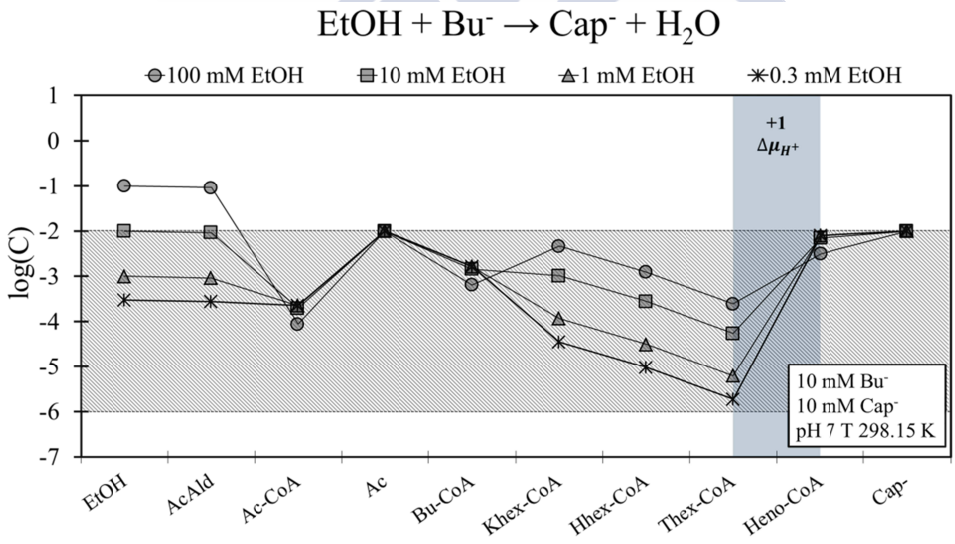

Figure 4.10 Limit (quasi equilibrium) metabolites concentrations (C, mol/L) for caproate production using ethanol and butyrate as substrates. The pathway remains feasible under different concentrations of e-donor (ΔG_{cat} values for the four lines at decreasing ethanol concentrations are -33.05, -27.34, -21.63 and -18.65 kJ/mol).

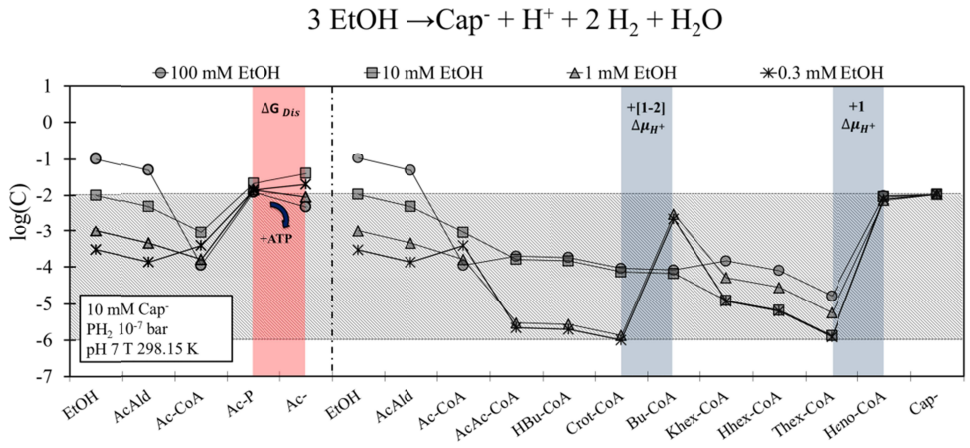

Figure 4.11 Limit (quasi equilibrium) metabolites concentrations (C, mol/L) for caproate production using only ethanol as substrate. The pathway remains feasible under different concentrations of e-donor (ΔG_{cat} values for the four lines at decreasing ethanol concentrations are -142.04, -124.92, -107.80 and -98.84 kJ/mol).

Alcohol production through reduction of volatile fatty acid

Acetate, butyrate and propionate reduction to their corresponding alcohols using H_2 as electron donor was first reported by Steinbusch et al. [4] working with a mixed culture. The low VFA reduction yield observed was allegedly attributed to competition with the more favourable methanogenesis for the electron equivalents. The metabolic pathways for the three VFAs reduction into their respective alcohols are very similar, following analogous steps. The study of acetate reduction to ethanol is presented here (Figure 4.12).

In this pathway, acetate activation is reported to take place through the hydrolysis of one ATP [59,60] (Figure 4.12) but in order for the pathway to yield a net energy gain to the cell, a minimum of one net proton translocation should be obtained. This implies that the amount of energy recovered from the remaining steps of the pathway should be the energy of one ATP (to recover the invested ATP for acetate activation) plus at least one additional $\Delta\mu_{H+}$. Despite this pathway is not known to have any step coupled to proton translocation neither to ATP formation via SLP [59,60], possible energy recovery mechanisms based on those two mechanisms can be proposed.

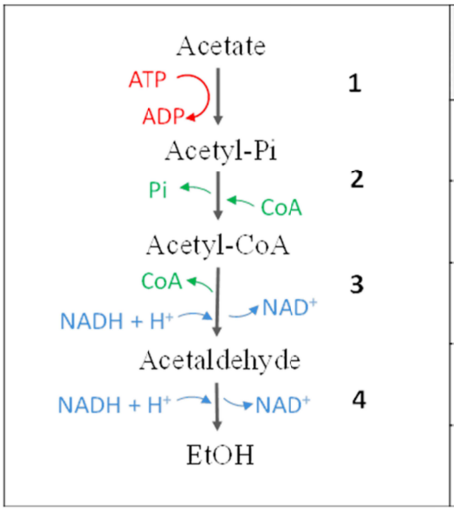

N°	ΔG^0 (kJ/mol)
1	-0.8
2	5.03
3	-25.58
4	-63.68
Total	-41.43

Figure 4.12 Considered metabolic pathway for acetic acid reduction to ethanol and standard Gibbs energy values for each metabolic step.

A first possibility could be coupling of acetate uptake and ethanol extrusion with the translocation of a total of four protons (Figure 4.13.a). However this would require physiologically and chemically unfeasible concentration gradients for both acetate and ethanol.

A second alternative could be the translocation of one single proton on acetate uptake together with the formation of one ATP via SLP at the acetyl-Pi to acetyl-CoA step (Figure 4.13.b) where a phosphate molecule is liberated. This however would force the maximum concentration of acetyl-CoA to unfeasibly low values for the reaction to proceed further, kinetically blocking the subsequent steps.

These two options suggest that feasible alternatives must be based on proton translocations coupled not only to solute transport but also to redox reaction steps. The reduction step from acetaldehyde to ethanol happens to be the most energetic step if acetaldehyde concentration is to remain above feasibility limits allowing in theory for the translocation of up to three protons. In addition, the reduction of acetyl-CoA would allow for the translocation of one more proton.

According to this we consider in Figure 4.13.c the possibility that both acetate uptake and acetyl-CoA reduction could be coupled to the translocation of one

proton each and the reduction of acetaldehyde coupled to the translocation of two additional protons. This scheme would imply however a relatively low (though feasible) concentration of intracellular acetate.

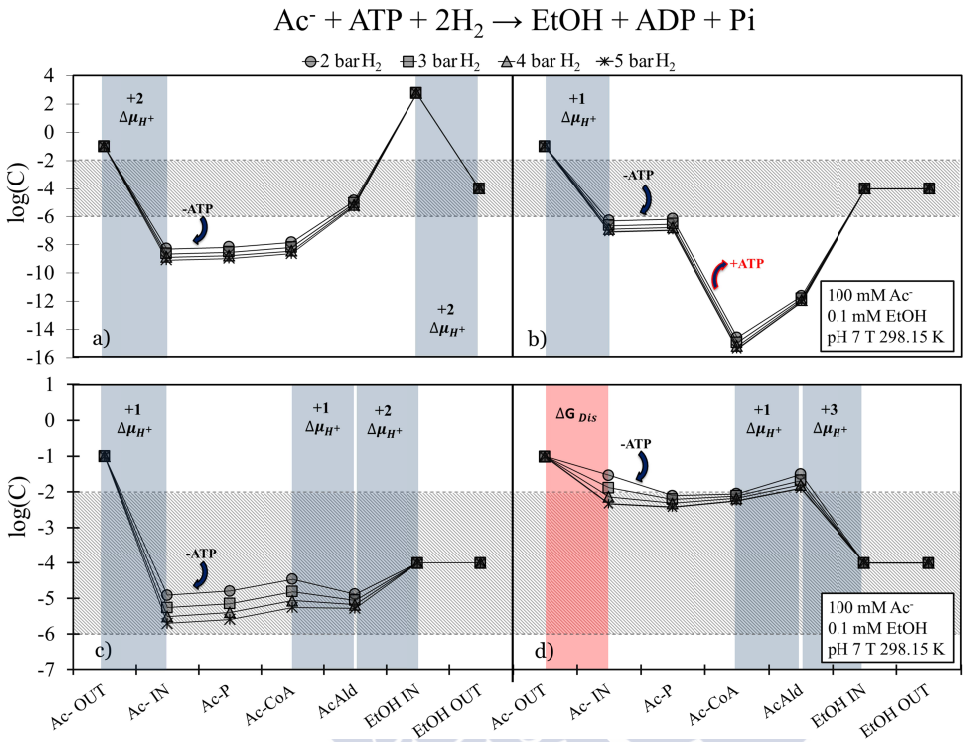

Figure 4.13 Limit (quasi equilibrium) metabolites concentrations (C, mol/L) for acetate reduction to ethanol under different P_{H2} (ΔG_{cat} values for the four lines at increasing P_{H2} are -30.11, -32.12, -33.55 and -34.65 kJ/mol). Unfeasible energy recovery alternatives: a) Proton translocations at the substrate and product transport sites requiring unfeasible concentration gradients and b) recovery of ATP via SLP requiring unfeasibly low metabolite concentrations. Feasible energy recovery alternatives: c) Proton translocations at the substrate transport site and at two reduction sites and d) Proton translocations at the reduction sites only.

If no proton translocation is coupled to acetate uptake, another option could be considered. One and three protons could be coupled to acetyl-CoA and acetaldehyde reductions respectively (Figure 4.13.d). This mechanism would allow higher metabolite concentrations within the cell all the way through the pathway.

Alternatively, a third feasible possibility could be considered assuming that the reduction of the NAD^+ to recover NADH could be coupled with 2 proton translocations across the membrane. The NADH recovery could occur with the electron transfer between a second electron carrier or with H_2 consumption. In this case, the total of the energy of 4 proton translocations could be harvested per mol of ethanol produced. This option appears also feasible (Figure 4.14) and does not imply that the acetyl-CoA and acetaldehyde reductions should have activity in the membrane. Moreover, proton translocations in electron changes between NAD^+ and NADPH were already pointed out as coupled with proton translocations in previous studies [61].

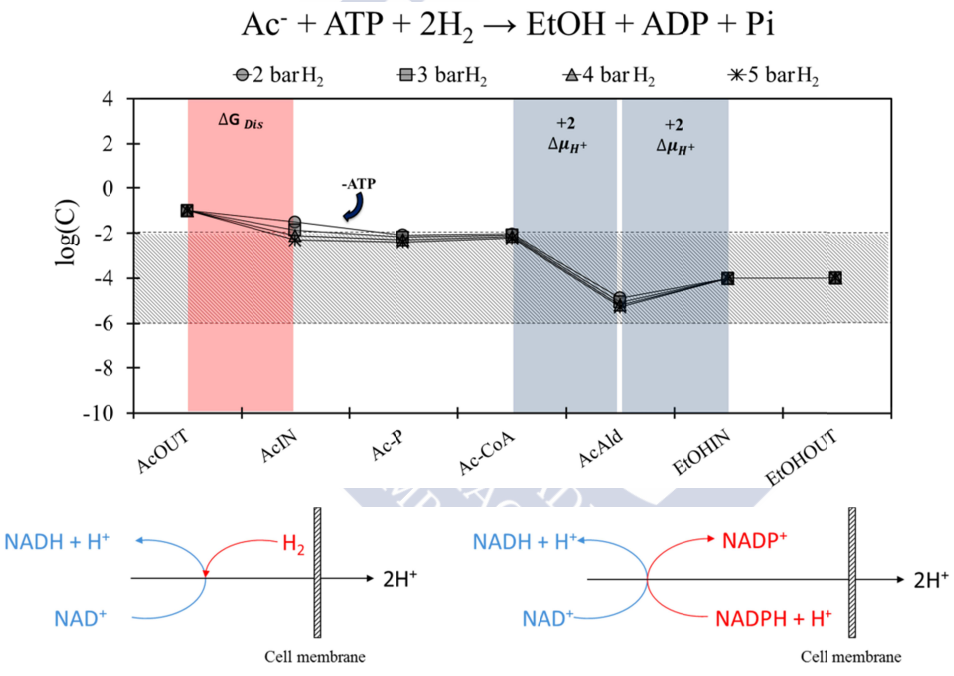

Figure 4.14 Limit (quasi equilibrium) metabolites concentrations (C, mol/L) for ethanol production with acetate reduction showing a feasible energy recovery alternative considering the NADH recovery coupled with two proton translocations across the membrane. (ΔG_{cat} values for the four lines at increasing P_{H2} are -30.11, -32.12, -33.55 and -34.65 kJ/mol).

In conclusion, the analysis presented with acetate reduction to ethanol, suggests that further study on the energy coupling mechanisms of specific redox reaction steps would be beneficial. Moreover, because the energy is clearly limited

in this pathway, a highly efficient performance of the *ATPase* enzymatic group is expected (minimizing the energy dissipation/loss) otherwise, the pathway could become unfeasible.

Typical operation under acidic pH (in order to inhibit methanogenesis) such as by Steinbusch et al. [4] (pH 5) implies that the reduction of VFAs (acidic components) to alcohols (non-acidic components) becomes thermodynamically more favourable and lower P_{H2} would be needed to enable these catabolic pathways. However, an external acidic pH will affect to the $\Delta\mu_{H+}$ value, but the homeostatic control of the membrane potential could offset the pH effect allowing the cell to survive under those conditions.

4.4 Sensitive analyses for the assumptions considered

Total conserved moieties concentrations

The values for the -CoA and -Pi total concentrations inside the cell are obtained from Kleerebezem and Stams [18] but -THF total concentration estimation was not found in any reference. Figure 4.15 illustrates that the impact of assuming different total concentration values of THF within a reasonable range is not very significant for the purpose of this study.

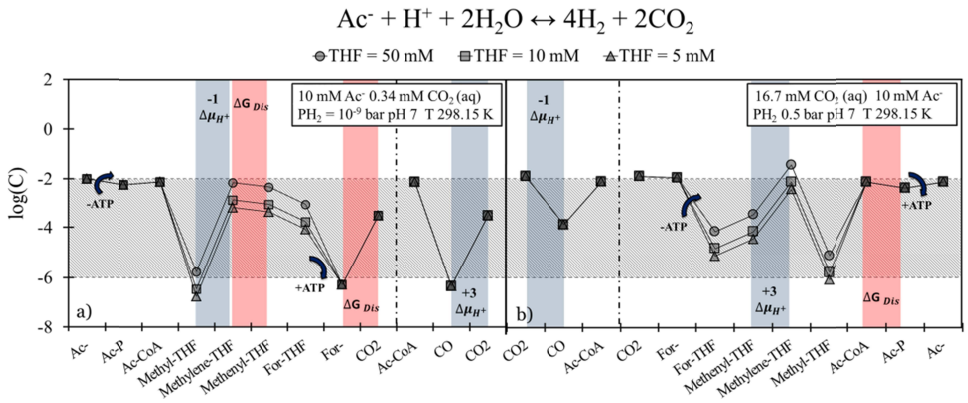

Figure 4.15 Limit (quasi equilibrium) metabolites concentrations (C, mol/L) for acetate oxidation (a) and CO_2 reduction (b) considering different total THF concentrations.

Energy value of $\Delta\mu_{H+}$

In this study we use a constant electrical potential gradient ($\Delta\psi$) across the membrane of -200 mV and we assume no ΔpH considering in all the cases studied, a pH 7 inside and outside the cell compartment (Table 4.2). However, it is known that the membrane potential could vary depending on the conditions or species involved [52]. As well, some of the processes studied might be running under different pH, fact that might affect to the $\Delta\mu_{H+}$ value, equation 4.2 [4,10].

$$\Delta\mu_{H+} = -F\cdot\Delta\Psi + R\cdot T\cdot \ln\frac{H^+_{out}}{H^+_{in}} \qquad 4.2$$

In the processes running under energy scarcity conditions, the $\Delta\mu_{H+}$ value should be optimized with the homeostasis of the cell in order to survive. Indeed, if lower $\Delta\mu_{H+}$ values are considered, in some cases higher efficiency harvesting energy could be achieved allowing the cell to survive. An example on the effect of lowering $\Delta\mu_{H+}$ for acetate reduction to butyrate using ethanol as electron donor is presented (Figure 4.16).

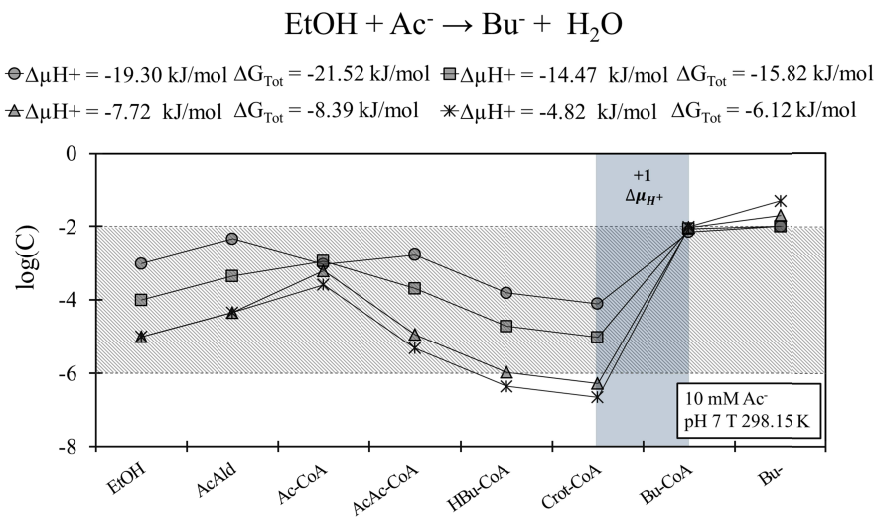

Figure 4.16 Limit (quasi equilibrium) metabolites concentrations (C, mol/L) for acetate reduction to butyrate using ethanol as electron donor considering different proton motive forces ($\Delta\mu_{H+}$). The $\Delta\mu_{H+}$ value optimization allows the cell to survive under lower energy available.

The $\Delta\mu_{H+}$ value optimisation could allow the cell to survive in lower energy available conditions like it is presented in Figure 4.16 but also it could increase the energy harvested for anabolism and maintenance as exposed in Figure 4.17. The pH inside the cell is considered to be approximately constant around 7 but outside it could be different. Changes in the external pH could increase or decrease the total energy available in the system to run a specific process, but it has more impact in the intermediate metabolite concentrations due to the generation of a ΔpH gradient that affects the $\Delta\mu_{H+}$ value.

Agler et al. [10] produced caproate with ethanol under pH 5.5. An analysis of the pathway considering external acidic pH demonstrates how the pathway keeps feasible even if the potential of the membrane does not change ($\Delta\psi$ = -200 mV) (Figure 4.18).

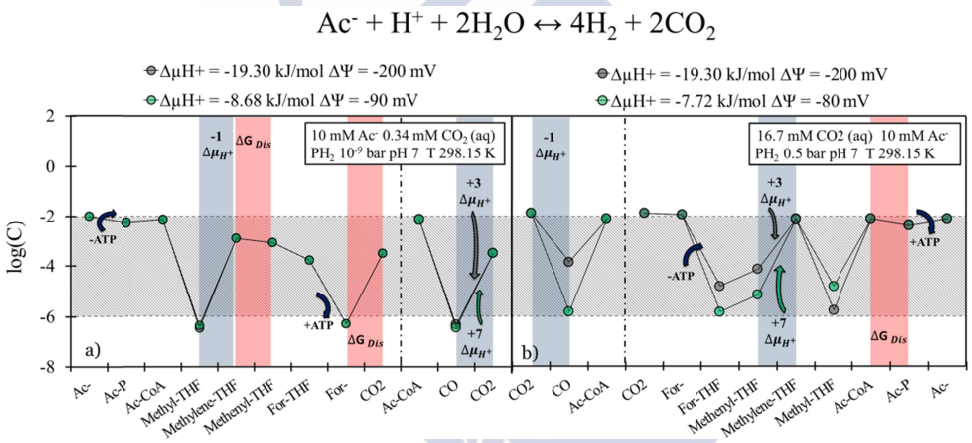

Figure 4.17 Limit (quasi equilibrium) metabolites concentrations (C, mol/L) for (a) acetate oxidation and for (b) CO_2 reduction considering optimised proton motive forces ($\Delta\mu_{H+}$) allowing the cell to harvest more energy per mol of product.

Nonetheless, as it was presented in Figure 4.16 and in Figure 4.17 the membrane potential could change, increasing the energy harvested to allow the cell to survive under energy scarcer conditions and reducing the minimum amount of energy needed to survive. Even, in some cases the change of the membrane potential could be a key factor to make a pathway feasible (Figure 4.19). Alcohol production runs experimentally under lower pH than 7 [4] but when we analyse the pathway, a different potential gradient across the

membrane than -200 mV seems to be needed in order to make the pathway feasible in acidic conditions (Figure 4.19).

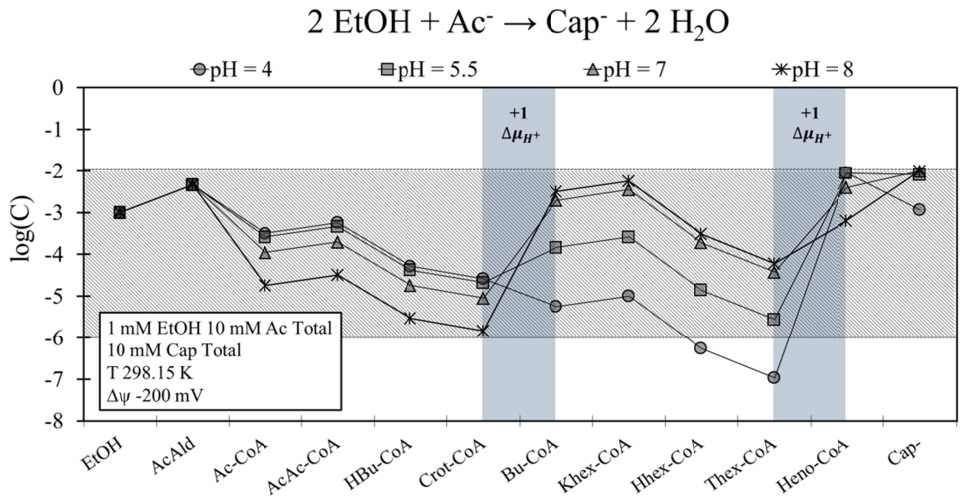

Figure 4.18 Limit (quasi equilibrium) metabolites concentrations (C, mol/L) for acetate reduction to caproate using ethanol as electron donor and considering different ΔpH.

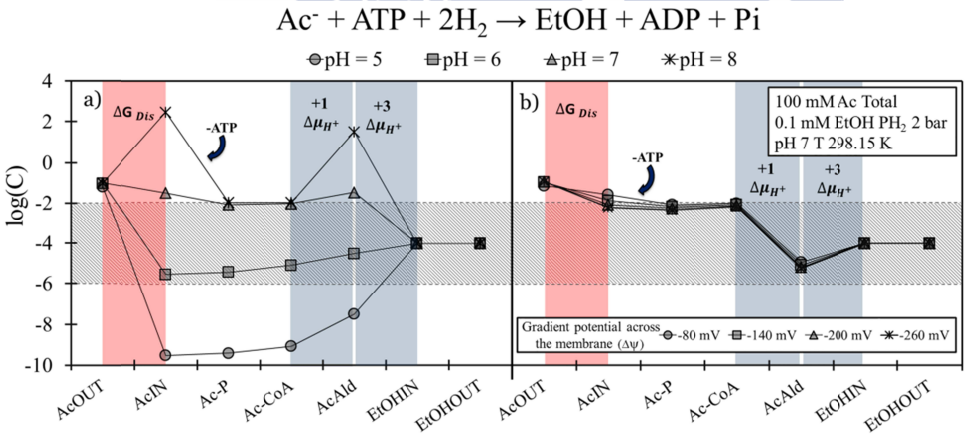

Figure 4.19 Limit (quasi equilibrium) metabolites concentrations (C, mol/L) for acetate reduction to ethanol considering different ΔpH at (a) the same membrane potential in all the cases and (b) with optimized membrane potential.

4.5 Conclusions

With this work is presented a theoretical framework for metabolic flux analysis based on quasi thermodynamic equilibrium calculations and limiting concentrations of conserved moieties to study several anaerobic pathways. The main conclusions of this work are:

1. The reversibility of homoacetogenesis, as reported in literature, appears to require reversible proton translocation mechanisms as well as Gibbs energy dissipation at specific intermediate reaction steps in order to obtain realistic metabolite concentrations. The energy recovery and investment sites appear to be the same in both reductive and oxidative pathways but in opposite directions.

2. The energy dissipation required for butyrate oxidation to acetate suggests that a net amount of less than one $\Delta\mu_{H+}$ energy for anabolism is harvested (1 ATP minus 2 $\Delta\mu_{H+}$ invested minus dissipated energy).

3. Acetate reduction to butyrate with H_2 as electron donor seems not feasible due to the kinetically unfeasible low acetoacetyl-CoA concentration required by thermodynamics.

4. The experimentally reported acetate reduction with ethanol or lactate as electron donors is shown in this study to be thermodynamically and kinetically feasible.

5. Reduction of VFAs into longer chain fatty acids with ethanol as electron donor appears as very thermodynamically and kinetically feasible.

6. Ethanol production from acetate appears to require $\Delta\mu_{H+}$ energy generation coupled to redox reactions in order for the cell to obtain net energy for growth and compensate for the ATP invested on phosphatation of acetate. The active transport of solutes across the membrane could also be coupled with $\Delta\mu_{H+}$ to be used further in anabolism and maintenance.

The data of all the figures of this chapter is publicly available in the supplementary information of the article:

R. González-Cabaleiro, J. M. Lema, J. Rodríguez, R. Kleerebezem (2013) Linking thermodynamics and kinetics to assess pathway reversibility in anaerobic bioprocesses. *Energy and Environmental Science* **6**: 3780-3789

4.6 References

1. Grootscholten TIM, Steinbusch KJJ, Hamelers HVM, Buisman CJN (2013) Chain elongation of acetate and ethanol in an upflow anaerobic filter for high rate MCFA production. *Bioresource Technology* **135**: 440-445.

2. Angenent LT, Karim K, Al-Dahhan MH, Wrenn BA, Domíguez-Espinosa R (2004) Production of bioenergy and biochemicals from industrial and agricultural wastewater. *Trends in Biotechnology* **22**: 477-485.

3. Agler MT, Wrenn BA, Zinder SH, Angenent LT (2011) Waste to bioproduct conversion with undefined mixed cultures: the carboxylate platform. *Trends in Biotechnology* **29**: 70-78.

4. Steinbusch KJJ, Hamelers HVM, Buisman CJN (2008) Alcohol production through volatile fatty acids reduction with hydrogen as electron donor by mixed cultures. *Water Research* **42**: 4059-4066.

5. Steinbusch KJJ, Arvaniti E, Hamelers HVM, Buisman CJN (2009) Selective inhibition of methanogenesis to enhance ethanol and n-butyrate production through acetate reduction in mixed culture fermentation. *Bioresource Technology* 100: 3261-3267.

6. Grootscholten TIM, Steinbusch KJJ, Hamelers HVM, Buisman CJN (2013) High rate heptanoate production from propionate and ethanol using chain elongation. *Bioresource Technology* **136**: 715-718.

7. Dellomonaco C, Clomburg JM, Miller EN, Gonzalez R (2011) Engineered reversal of the [bgr]-oxidation cycle for the synthesis of fuels and chemicals. *Nature* **476**: 355-359.

8. Steinbusch KJJ, Hamelers HVM, Plugge CM, Buisman CJN (2011) Biological formation of caproate and caprylate from acetate: fuel and chemical production from low grade biomass. *Energy and Environmental Science* **4**: 216-224.

9. Grootscholten TIM, Kinsky dal Borgo F, Hamelers HVM, Buisman CJN (2013) Promoting chain elongation in mixed culture acidification reactors by addition of ethanol. *Biomass and Bioenergy* **48**: 10-16.

10. Agler MT, Spirito CM, Usack JG, Werner JJ, Angenent LT (2012) Chain elongation with reactor microbiomes: upgrading dilute ethanol to medium-chain carboxylates. *Energy and Environmental Science* **5**: 8189-8192.

11. Ding HB, Tan GY, Wang JY (2010) Caproate formation in mixed-culture fermentative hydrogen production. *Bioresource Technology* **101**: 9550-9559.

12. Lee MJ, Zinder SH (1988) Isolation and Characterization of a Thermophilic Bacterium Which Oxidizes Acetate in Syntrophic Association with a Methanogen and Which Grows Acetogenically on H_2-CO_2. *Applied and Environmental Microbiology* **54**: 124-129.

13. Schink B (1997) Energetics of syntrophic cooperation in methanogenic degradation *Microbiology and Molecular Biology Reviews* **61**: 262-280.

14. Hattori S, Galushko AS, Kamagata Y, Schink B (2005) Operation of the CO dehydrogenase/acetyl coenzyme A pathway in both acetate oxidation and acetate formation by the syntrophically acetate-oxidizing bacterium Thermacetogenium phaeum. *Journal of Bacteriology* **187**: 3471-3476.

15. Hattori S (2008) Syntrophic acetate-oxidizing microbes in methanogenic environments. *Microbes and Environments* **23**: 118-127.

16. Hattori S, Kamagata Y, Hanada S, Shoun H (2000) Thermacetogenium phaeum gen. nov., sp. nov., a strictly anaerobic, thermophilic, syntrophic acetate-oxidizing bacterium. *International Journal of Systematic and Evolutionary Microbiology* **50**: 1601-1609.

17. Heijnen JJ, Romein B (1995) Derivation of kinetic equations for growth on single substrates based on general properties of a simple metabolic network. *Biotechnology Progress* **11**: 712-716.

18. Kleerebezem R, Stams AJM (2000) Kinetics of syntrophic cultures: a theoretical treatise on butyrate fermentation. *Biotechnology and Bioengineering* **67**: 529-543.

19. Thauer RK, Jungermann K, Decker K (1977) Energy conservation in chemotrophic anaerobic bacteria. *Bacteriological Reviews* **41**: 809.

20. Mitchell P (1979) Keilin's respiratory chain concept and its chemiosmotic consequences. *Science* **206**: 1148-1159.

21. LaRowe DE, Dale AW, Amend JP, Van Cappellen P (2012) Thermodynamic limitations on microbially catalyzed reaction rates. *Geochimica et Cosmochimica Acta* **90**: 96-109.

22. Sapra R, Bagramyan K, Adams MWW (2003) A simple energy-conserving system: proton reduction coupled to proton translocation. *Proceedings of the National Academy of Sciences of the United States of America* **100**: 7545-7550.

23. Schink B, Thauer RK (1988) Energetics of syntrophic methane formation and the influence of aggregation. In: Lettinga G, Zehnder AJB, Grotenhuis JTC, Hulshoff Pol LW, editors. Granular anaerobic sludge; microbiology and technology. Wageningen: Pudoc. pp. 5-17.

24. Hoehler TM (2004) Biological energy requirements as quantitative boundary conditions for life in the subsurface. *Geobiology* **2**: 205-215.

25. von Ballmoos C, Wiedenmann A, Dimroth P (2009) Essentials for ATP synthesis by F1F0 ATP synthases. *Annual Review of Biochemistry* **78**: 649-672.

26. Rodríguez J, Kleerebezem R, Lema JM, van Loosdrecht MCM (2006) Modeling product formation in anaerobic mixed culture fermentations. *Biotechnology and Bioengineering* **93**: 592-606.

27. Stams AJM (1994) Metabolic interactions between anaerobic bacteria in methanogenic environments. *Antonie van Leeuwenhoek Journal of Microbiology* **66**: 271-294.

28. Hoehler TM, Jorgensen BB (2013) Microbial life under extreme energy limitation. *Nature Reviews Microbiology* **11**: 83-94.

29. Jackson BE, McInerney MJ (2002) Anaerobic microbial metabolism can proceed close to thermodynamic limits. *Nature* **415**: 454-456.

30. Rodríguez J, Lema JM, Kleerebezem R (2008) Energy-based models for environmental biotechnology. *Trends in Biotechnology* **26**: 366-374.

31. Siegrist H, Renggli D, Gujer W (1993) Mathematical modelling of anaerobic mesophilic sewage sludge treatment. *Water Science and Technology* **27**: 25-36.

32. Warikoo V, McInerney MJ, Robinson JA, Suflita JM (1996) Interspecies acetate transfer influences the extent of anaerobic benzoate degradation by syntrophic consortia. *Applied Environmental Microbiology* **62**: 26-32.

33. Bar-Even A, Flamholz A, Noor E, Milo R (2012) Thermodynamic constraints shape the structure of carbon fixation pathways. *Biochimica et Biophysica Acta (BBA) – Bioenergetics* **1817**: 1646-1659.

34. Fischer CR, Klein-Marcuschamer D, Stephanopoulos G (2008) Selection and optimization of microbial hosts for biofuels production. *Metabolic Engineering* **10**: 295-304.

35. Smith DP, McCarty PL (1989) Energetic and rate effects on methanogenesis of ethanol and propionate in perturbed CSTRs. *Biotechnology and Bioengineering* **34**: 39-54.

36. Smith DP, McCarty PL (1989) Reduced product formation following perturbation of ethanol- and propionate-fed methanogenic CSTRs. *Biotechnology and Bioengineering* **34**: 885-895.

37. Younesi H, Najafpour G, Mohamed AR (2005) Ethanol and acetate production from synthesis gas via fermentation processes using anaerobic bacterium, Clostridium ljungdahlii. *Biochemical Engineering Journal* **27**: 110-119.

38. Mohammadi M, Najafpour GD, Younesi H, Lahijani P, Uzir MH, et al. (2011) Bioconversion of synthesis gas to second generation biofuels: A review. *Renewable and Sustainable Energy Reviews* **15**: 4255-4273.

39. Hanselmann KW (1991) Microbial energetics applied to waste repositories. *Experientia* **47**: 645-687.

40. Diekert G, Wohlfarth G (1994) Metabolism of homocetogens. *Antonie Van Leeuwenhoek* **66**: 209-221.

41. Alberty RA (2006) Biochemical Thermodynamics: Applications of Mathematica. Hoboken: Wiley.

42. Heijnen JJ (2001) Stoichiometry and kinetics of microbial growth from a thermodynamic perspective. In: Ratledge C, Kristiansen B, editors. Basic biotechnology. Second Edi ed. Cambridge: Cambridge University Press.

43. Stephanopoulos G, Aristidou AA, Nielsen J (1998) Metabolic Engineering: Principles and Methodologies. San Diego, California: Academic Press. 725 p.

44. Noor E, Bar-Even A, Flamholz A, Lubling Y, Davidi D, et al. (2012) An integrated open framework for thermodynamics of reactions that combines accuracy and coverage. *Bioinformatics* **28**: 2037-2044.

45. Bar-Even A, Noor E, Flamholz A, Buescher JM, Milo R (2011) Hydrophobicity and Charge Shape Cellular Metabolite Concentrations. *PLoS Computational Biology* **7**: e1002166.

46. Bennett BD, Kimball EH, Gao M, Osterhout R, Van Dien SJ, et al. (2009) Absolute metabolite concentrations and implied enzyme active site occupancy in Escherichia coli. *Nature Chemical Biology* **5**: 593-599.

47. Reich JG, Selkov EE (1981) Energy metabolism of the cell: a theoretical treatise. New York: Academic Press London.

48. Mosey FE, Matter O (1983) Mathematical modelling of the anaerobic digestion process: Regulatory mechanisms for the formation of short-chain volatile acids from glucose. *Water Science and Technology* **15**: 209-232.

49. Seedorf H, Fricke WF, Veith B, Brüggemann H, Liesegang H, et al. (2008) The genome of Clostridium kluyveri, a strict anaerobe with unique metabolic features. *Proceedings of the National Academy of Sciences of the United States of America* **105**: 2128-2133.

50. Wang S, Huang H, Moll J, Thauer RK (2010) NADP+ reduction with reduced ferredoxin and NADP+ reduction with NADH are coupled via an electron-bifurcating enzyme complex in Clostridium kluyveri. *Journal of Bacteriology* **192**: 5115-5123.

51. Daniels L, Sparling R, Sprott GD (1984) The bioenergetics of methanogenesis. *Biochimica et Biophysca Acta* **768**: 113-163.

52. Kadenbach B (2003) Intrinsic and extrinsic uncoupling of oxidative phosphorylation. *Biochimica et Biophysca Acta* **1604**: 77-94.

53. Dimroth P, von Ballmoos C, Meier T, Kaim G (2003) Electrical power fuels rotary ATP synthase. *Structure* **11**: 1469-1473.

54. Stoner CD (1992) An investigation of the relationships between rate and driving force in simple uncatalysed and enzyme-catalysed reactions with applications of the findings to chemiosmotic reactions. *Biochemical Journal* **283**: 541-552.

55. Toei M, Gerle C, Nakano M, Tani K, Gyobu N, et al. (2007) Dodecamer rotor ring defines H+/ATP ratio for ATP synthesis of prokaryotic V-ATPase from Thermus thermophilus. *Proceedings of the National Academy of Sciences* **104**: 20256-20261.

56. Bethke CM, Sanford RA, Kirk MF, Jin Q, Flynn TM (2011) The thermodynamic ladder in geomicrobiology. *American Journal of Science* **311**: 183-210.

57. Larowe DE, Helgeson HC (2007) Quantifying the energetics of metabolic reactions in diverse biogeochemical systems: electron flow and ATP synthesis. *Geobiology* **5**: 153-168.

58. Tran QH, Unden G (1998) Changes in the proton potential and the cellular energetics of Escherichia coli during growth by aerobic and anaerobic respiration or by fermentation. *European Journal of Biochemistry* **251**: 538-543.

59. White D (2007) The physiology and biochemistry of prokaryotes. New York: Oxford University Press. 628 p.

60. Kanehisa M, Goto S (2000) KEGG: kyoto encyclopedia of genes and genomes. *Nucleic Acids Research* **28**: 27-30.

61. Huang H, Wang S, Moll J, Thauer RK (2012) Electron bifurcation involved in the energy metabolism of the acetogenic bacterium Moorella thermoacetica growing on glucose or H_2 plus CO2. *Journal of bacteriology* **194**: 3689-3699.

USC
UNIVERSIDADE
DE SANTIAGO
DE COMPOSTELA

5

Microbial catabolic activities are naturally selected by metabolic energy harvest rate

This chapter has been accepted for publication as:

González-Cabaleiro R, Ofiteru ID, Lema JM, Rodríguez J (2015) Microbial catabolic activities are naturally selected by metabolic energy harvest rate. *ISME Journal*. (Accepted)

Abstract

The fundamental trade-off between yield and rate of energy harvest per unit of substrate has been largely discussed as a main characteristic for microbial established cooperation or competition. In this study, this point is addressed by developing a generalized model that simulates competition between existing and not experimentally reported microbial catabolic activities defined only based on well-known biochemical pathways. No specific microbial physiological adaptations are considered, growth yield is calculated coupled to catabolism energetics and a common maximum biomass specific catabolism rate (expressed as electron transfer rate) is assumed for all microbial groups. Under this approach, successful microbial metabolisms are predicted in line with experimental observations under the hypothesis of maximum energy harvest rate.

Two microbial ecosystems, typically found in wastewater treatment plants, are simulated, namely: (i) the anaerobic fermentation of glucose and (ii) the oxidation and reduction of nitrogen under aerobic autotrophic (nitrification) and anoxic hetero- and autotrophic (denitrification) conditions. The experimentally observed cross feeding in glucose fermentation, through multiple intermediate fermentation pathways, towards ultimately methane and carbon dioxide is predicted. Analogously, two-stage nitrification (by ammonium and nitrite oxidizers) is predicted as prevailing over nitrification in one-stage. Conversely, denitrification is predicted in one-stage (by denitrifiers) as well as *anammox* process (anaerobic ammonium oxidation). The model results suggest that these observations are a direct consequence of the different energy yields per electron transferred at the different steps of the pathways. Overall our results theoretically support the hypothesis that successful microbial catabolic activities are selected by an overall maximum energy harvest rate.

Table of symbols

References of the main sub-index and super-index used:

ana	*Anabolism*	e	*Electron*
cat	*Catabolism*	eD	*Electron donor*
met	*Metabolism*	S	*Substrate*
C	*Carbon*	X	*Biomass*

SYMBOL	DEFINITION	UNITS
ΔG	Gibbs energy of a reaction	kJ/mol
ΔG^0	Gibbs energy of a reaction at standard conditions (298.15K, 1 atm, 1M)	kJ/mol
$\Delta G^{0'}$	Gibbs energy of a reaction at standard conditions and pH 7 (298.15K, 1 atm, 1M)	kJ/mol
ΔG_{cat}	Catabolic reaction energy per mol of electron donor consumed	kJ/mol_{eD}
ΔG_{ana}	Anabolic reaction energy per mol of biomass formed	kJ/mol_{Cx}
ΔG_{dis}	Energy dissipated per mol of biomass formed	kJ/mol_{Cx}
δ_x	Thickness of the cell membrane	m
γ	Oxidation state of a component	$mol_e/mol_{(C)}$
λ_{cat}	Times that the catabolic reaction need to run per unit of biomass formed (inverse of maximum growth yield)	mol_{eD}/mol_{Cx}
μ	Specific biomass growth	$mol_{Cx}/mol_{Cx}{\cdot}h$
ν	Stoichiometric coefficient	-
$\mathbf{D}_i$	Diffusion coefficient of component i	m^2/h
E_{cat}	Energy harvested through a catabolic activity in the system conditions and per mol of biomass	$kJ/mol_{Cx}{\cdot}h$
G_i	Partial pressure of component i in the gas phase	bar_i
K_{Hyd}	Kinetic constant of death biomass hydrolysis	h^{-1}
Ks_i	Half saturation constant of substrate i	mol_{Si}/L

SYMBOL	DEFINITION	UNITS
Ne	Number of electrons transferred per mol of electron donor substrate in the catabolism	mol_e/mol_{eD}
NoC	Carbon chain length of the carbon source substrate	∅
P	Total pressure of the system	atm
P_{H2}	Hidrogen partial pressure	atm
Q_{gas}	Gas flow rate out of the reactor	L_{gas}/h
Q_{liq}	Influent and effluent liquid flow rate of the reactor	L/h
R_i	Net reaction generation term of component i	$mol_{Si}/L{\cdot}h$
R_g	Universal gas constant	L·atm/K·mol
R_{th}	Universal gas constant	kJ/K·mol
S_i	Reactor concentration of dissolved component i	mol_{Si}/L
S_{lim}	Reactor concentration of limiting substrate in a reaction	mol_{Slim}/L
SRT	Solids retention time	h
T	Temperature	K
V_{gas}	Volume of head space of the reactor	L
V_r	Working volume of the reactor	L
X_i	Reactor concentration of solid (biomass) component i	mol_{Cx}/L
X_d	Reactor concentration of dead biomass	mol_{Cx}/L
Y_{XS}^{max}	Theoretical maximum biomass growth yield	mol_{Cx}/mol_{eD}
a_i	Activity of the chemical component i	mol_{Si}/L
a_x	Specific area of the cell membrane	$m^2/kmol_{Cx}$
b	Specific biomass decay rate	$mol_{Cx}/mol_{Cx}{\cdot}h$
k_d	Kinetic constant of decay process	h^{-1}
m_G	Specific maintenance energy requirement	$kJ/mol_{Cx}{\cdot}h$
m_S^{req}	Specific substrate consumption required for maintenance	$mol_{eD}/mol_{Cx}{\cdot}h$
$n_{gas\text{-}G}$	Total gas production rate	mol_{gas}/h
q_S^{cat}	Specific substrate uptake rate for catabolism	$mol_{eD}/mol_{Cx}{\cdot}h$

SYMBOL	DEFINITION	UNITS
q_S^{max}	Maximum specific substrate uptake rate	$mol_{eD}/mol_{Cx}{\cdot}h$
q_{STr}^{max}	Maximum specific substrate transport rate across the cell membrane	$mol_{Si}/mol_{Cx}{\cdot}h$
q_S^{met}	Specific substrate uptake rate for growth metabolism	$mol_{eD}/mol_{Cx}{\cdot}h$
r_{cat}	Substrate uptake rate for catabolism	$mol_{eD}/\ L{\cdot}h$
r_d	Biomass decay rate	$mol_{Cx}/\ L{\cdot}h$
r_{Hyd}	Dead biomass hydrolysis rate	$mol_{Cx}/L{\cdot}h$
r_{met}	Substrate uptake rate for growth metabolism	$mol_{Cx}/\ L{\cdot}h$

5.1 Introduction

According to the second law of thermodynamics, systems with a high degree of organization are maintained by the input of external energy. Microorganisms, like other living systems, can be described as open systems exchanging material and energy with their surroundings [1]. They obtain the required chemical energy input by the transformation from high- into low-energy content chemical components [2,3].

Evidence suggests that the successful microbial metabolic strategies which still survive today in natural ecosystems could constitute the most efficient forms of energy harvest developed over millions of years of evolution [4-7]. Successful microbial groups, when competing in energy limited environments, consume the available energy and might prevent less efficient groups to thrive. This competition can be considered as a natural selection towards the most efficient microbial strategies and drives adaptation in energy limited environments as well as improvements in the biochemical energy harvest mechanisms [8,9], pursuing the minimization of energy losses [10,11].

In natural ecosystems, a microorganism capable of harvesting more energy per unit of substrate consumed (i.e. higher ATP yield) appears, in principle, as in competitive advantage. But in systems where substrate availability is the limiting factor, a microorganism capable of harvesting more energy per unit of time (i.e. higher ATP rate) could overcome the previous one [12]. Longer catabolic pathways favour higher yields by harvesting more energy per mol of substrate while shorter pathway metabolisms can achieve faster specific uptake turnover rates. This makes not always clear whether a system would evolve towards a maximization of the growth yield or growth rate.

This trade-off between yield and rate of energy harvest is believed to be a key factor for ecological interactions. Cooperation, selfishness, altruism and competition have been widely observed in microbial ecosystems [8,9,13,14]. In particular, syntrophic relations between species have been strongly hypothesized as predecessor stages for a later evolved endosymbiosis which ended up in the formation of new species [4,15-17].

In this study we propose that the success of certain experimentally observed microbial metabolisms and syntrophic relationships over others (theoretically

possible but never experimentally found to be conducted by one single cell) might be determined by bioenergetic considerations. For this purpose an energy-based model has been developed, which includes thermodynamic information (potential energy harvested from a specific catabolism) and kinetic information (related to catabolic pathway length and substrate availability), to study the competition between different proposed microbial metabolisms. The catabolic activities are limited to known enzymatic reactions and carried out by cells with no specific adaptations to the environment. The model aims at describing not only the growth of the different microbial groups considered, but also the impact of their activities in the environment (i.e. changes in the media chemical concentrations) such that syntrophic relationships between microorganisms in the ecosystem might emerge or be limited.

5.2 Model description

In order to test the hypothesis of bioenergetics as main selector for the success of specific microbial metabolisms, an energy-based model [18] has been developed to be applied to specific microbial ecosystems hypothesized in this study. The model simulates the activity of simple microbial groups (non-adapted in terms of specific advantages to any environment) carrying out different specific catabolic processes defined as combinations of well-known biochemical reactions present in microorganisms.

Generalized metabolism stoichiometry (growth yield) from bioenergetics

Microorganisms must survive with the energy they harvest (typically as ATP) from the total available in the overall catabolism reactions, ΔG_{cat}. Part of this energy must be invested in maintenance and the rest is available to drive growth through anabolic reactions. Catabolism is here defined as a chemical reaction which converts substrates (S) into lower energy products (P), and anabolism as the process that converts a carbon source (C_S) and a nitrogen source (N_S) into cells biomass (C_X) with energy consumption (equation 5.1).

$$\text{CATABOLISM:} \quad 1\cdot eD + \nu i\cdot Si + \ldots \rightarrow \nu j\cdot Pj + \nu k\cdot Pk + \ldots \quad \Delta G_{cat}\ kJ/mol_{eD}$$

$$\text{ANABOLISM:} \quad \nu c\cdot CS + \nu n\cdot NS + \nu i\cdot Si + \ldots \rightarrow 1\cdot C_X + \nu j\cdot Pj + \Delta G_{ana}\ kJ/mol_{Cx} \qquad 5.1$$

Catabolism and anabolism are described as two mass-balanced independent processes only linked by the energy exchange through the production and consumption of ATP. Both processes are quantitatively coupled by the number of times that catabolism needs to run to yield the necessary energy to form one C-mol of biomass λ_{cat} (mol_{eD}/mol_{Cx}) [19]. Under this approach, if catabolism and anabolism reactions are known, the overall metabolism becomes a function of λ_{cat} (Met = Ana + λ_{cat} Cat).

The ΔG of each anabolic and catabolic reaction is calculated using a generalized routine. Given the stoichiometry of each reaction, actual ΔG at each step of simulation time are calculated from the ΔG^o values obtained from literature [20-24] and pre-stored in a matrix.

$$\Delta G = \Delta G^0 + R_{th}\cdot T\cdot \ln \prod_i a_i^{\nu_i} \qquad 5.2$$

Neglecting the ionic strength effect and assuming an activity coefficient of one, the Gibbs energy is directly calculated from the actual concentrations in each step of simulation.

Not all the energy harvested through catabolism can be available for growth as part must be dissipated mainly during anabolism (ΔG_{dis}, kJ/mol_{Cx}). The energy dissipated has been previously estimated based on the carbon source molecule size and degree of reduction [25,26]. This approach allows for the overall metabolism to be estimated by means of an energy balance to the system [1,27] equation 5.3, in which the energy dissipated in catabolism is negligible respect to anabolism, based on the much lower number of reactions and minimised energy losses in catabolic reactions (microorganisms are able to survive in systems even with strong energy limitations [10,28]). The inverse of λ_{cat} is analogous to the maximum growth yield if the electron donor for anabolism and catabolism are different (Y_{XS}^{max}, mol_{Cx}/mol_{eD}) [19] (equation 5.4).

$$\Delta G_{cat} \cdot \lambda_{cat} + \Delta G_{ana} + \Delta G_{dis} = 0 \quad 5.3$$

$$1/\lambda_{cat} = \frac{\Delta G_{cat}}{-(\Delta G_{ana} + \Delta G_{dis})} \quad 5.4$$

This generalized approach allows for the overall metabolism stoichiometry and yield to be described as a sole function of bioenergetics (ΔG_{cat}, ΔG_{ana} and ΔG_{dis}) for any postulated microbial metabolism. As an illustrative example, the metabolism of a microorganism catalysing glucose fermentation to acetic acid is analysed with this methodology below.

Generalized calculation of microbial metabolism stoichiometry: Example

CATABOLISM: $\text{Glucose} + 2\cdot H_2O \rightarrow 2\cdot\text{Acetate} + 2\cdot CO_2 + 4\cdot H_2 + 2\cdot H^+$

ANABOLISM: $0.175\cdot\text{Glucose} + 0.2\cdot NH_4^+ \rightarrow 1\cdot X + 0.05\cdot CO_2 + 0.45\cdot H_2O + 0.2\ H^+$

With a pH of 7, a concentration of 10 mM for soluble components and biomass and 0.1 bar of H_2 and CO_2 gases, the ΔG for catabolism is -261.56 kJ/mol_{Glu}, and the ΔG for anabolism -18.57 kJ/mol_{Cx}. The generalized cell mass formula $CH_{1.8}O_{0.5}N_{0.2}$ is used [29].

The dissipation energy required for anabolism is approximated according the equation given by the *Gibbs dissipation method* [25,26] which considers the carbon chain length (NoC) and the oxidation state of the carbon source (γ).

$$\Delta G_{dis} = 200 + 18\cdot(6 - \text{NoC})^{1.8} + \exp^{(3.6+0.4\cdot\text{NoC})\cdot\left[(-0.2-\gamma)^2\right]^{0.16}} \quad 5.5$$

In this case for glucose as electron donor, ΔG_{dis} = 236.05 kJ/mol_{Cx}

The inverse of λ_{cat} is calculated through the energy balance.

$$1/\lambda_{cat} = \frac{\Delta G_{cat}}{-(\Delta G_{ana} + \Delta G_{dis})} = 1.20\ mol_{Cx}/mol_{Glucose} \quad 5.6$$

The metabolism is calculated as the correlation between anabolism and catabolism using λ_{cat} (equation 5.3).

Metabolism:

$$1.0064\ Glu + 0.2000 \cdot NH_4^+ + 1.2129\ H_2O \rightarrow$$
$$\rightarrow 1 \cdot X + 1.6629 \cdot Ac^- + 1.8629 \cdot H^+ + 3.3258 \cdot H_2 + 1.7129 \cdot CO_2$$

Generalized kinetics from maximum electron transfer in the catabolism

The reported attempts to estimate the rate of microbial growth from bioenergetics (e.g. using an approximation of the energy dissipation in the catabolic pathway) have not been fully successful [30,31]. Growth rate has, however, been considered as limited by the length of the pathway by relating the need for higher enzyme concentrations with higher energy consumptions [8] or directly by relating the growth rate with the number of reaction steps required in the catabolism [32].

Experimental evidences of a maximum specific rate of electron transport in the catabolism (referred to enzymatically catalysed oxidations or reductions) have been reported and used in similar models [33,34]. In this work the number of electrons transferred has been used as the general representative measure of catabolic activity and a constant maximum value (3 $mol_{e^-}/mol_{Cx} \cdot h$) adopted across the board for all microbial activities considered. This has been implemented in the form of a specific maximum substrate uptake rate (q_S^{max}, $mol_{eD}/mol_{Cx} \cdot h$) using equation 5.7 [19], in which Ne (mol_{e^-}/mol_{eD}) is the number of electrons transfers attributed throughout a catabolism per mol of the electron donor substrate.

$$q_S^{max} = \frac{3}{Ne} \qquad 5.7$$

In addition to the above q_S^{max}, the metabolic rate depends also on the availability of the limiting substrate. Monod-like saturation terms (equation 5.8), as commonly used in microbial kinetic models, are adopted. The minimum among all substrate saturation terms (i.e. the limiting substrate) (S_{lim}) is defining the metabolic rate (equation 5.8).

$$q_S^{(.)} = q_S^{max} \cdot \frac{S_{lim}}{K_{S_{lim}} + S_{lim}} \qquad 5.8$$

Monod half saturation values (Ks) are typically obtained experimentally [19] and no general agreement on their mechanistic interpretation has been achieved [35–37]. For the purpose of this model, a general theoretical approach was proposed based only on the relative differences between the diffusivities of the different substrates (which implies no differences in the Ks values for the species competing for the same substrate), to estimate Ks values of both the existing and postulated microbial metabolic activities. In this manner, Ks values are related only with the substrates ability to cross the membrane and uncoupling them with the cell metabolism.

At low concentrations, transport of substrates is assumed controlled by molecular diffusion through the cell membrane (equation 5.9). Ks values are according to equation 5.10.

$$S_i << K_{Si} \Rightarrow q_{Si} \cong q_{Si,Tr}^{max} \cdot \frac{S_i}{K_{S_i}} \cong \frac{\mathbf{D}_i \cdot a_X}{\delta_X} \cdot \left(S_{i,ext} - S_{i,int} \right) \quad 5.9$$

$$S_{i,int} \cong 0 \Rightarrow K_{Si} \cong \frac{q_{S_i,Tr}^{max} \cdot \delta_X}{\mathbf{D}_i \cdot a_X} \quad 5.10$$

Where $\mathbf{D}_i$ is the diffusivity of the substrate i in water (m^2/h) [38]; a_x the specific cell area ($m^2/kmol_{Cx}$) and δ_x the thickness of the transport layer assumed as the membrane cell thickness (m). All cells are assumed equal in size and spherical with typical values of 1 μm of diameter and 0.05 μm of wall thickness. No general differences are considered in transport abilities between all postulated cells. Therefore transporters are assumed the same for all microorganisms (this eliminates any transport related advantage to specific microorganisms), assuming a maximum transport rate ($q_{Si,Tr}^{max}$) of 1.0 $mol_{Si}/mol_{Cx} \cdot h$ for all cases.

The main goal of the Ks implementation is to maintain a working realistic dynamics of the microbial ecosystem while avoiding much interference with the bioenergetics hypothesis subject of the study. It is important to highlight that all microorganisms are modelled as non-specialized to any particular environment and as physiologically non-differentiated, being also equally efficient in harvesting the energy from their catabolic activities. Experimentally observed physiological differences among microbial species leading to differences in the parameters describing their kinetics can be attributed to later evolutionary adaptations and specialisations of species conducting a catabolic activity. Considering that this

modelling approach addresses the competition between microbial activities, these specific adaptation differences cannot be and are not considered. In the model presented, microbial groups compete based on energetic considerations.

For this reason, the same values for q_S^{max} and for Ks are applied to all the microbial activities considered in the model. The uncertainty and impact of the numerical values used, due to the limited experimental information available, was assessed with a sensitivity analysis for both Ks and q_S^{max} values presented at section 5.5.

Calculation of Ne

In order to estimate the number of electrons transfers involved in each specific catabolism considered, metabolic pathways were analysed. Figures 5.1 and 5.2 present the pathways considered for all the cases presented in the main manuscript. For the non-experimentally observed metabolisms, the same biochemistry than in those observed is assumed for the individual pathway steps. The details of mechanisms which define each pathway step were obtained from literature [28,39,40].

The electrons transferred in each step of the pathways presented in Figures 5.1 and 5.2 could come associated with the reduction or oxidation of any specific electron carrier that in last term comes related to a reduction of O_2, an oxidation of H_2 or other electron donor.

Generalized maintenance estimation

In living cells, a fraction of the catabolic energy harvested must be diverted from growth to maintenance purposes, thus, decreasing the observed growth yield. Maintenance energy (m_G, $kJ/mol_{Cx}{\cdot}h$) is assumed only temperature dependent and constant per mass of cells and per time, neglecting any other physiological aspects as in the rest of the model. A constant value of 4.5 $kJ/mol_{Cx}{\cdot}h$ is assumed for m_G of all the functional groups considered [19]. Maintenance energy requirements can be also expressed in terms of a specific substrate consumption rate (m_S^{req}, $mol_{eD}/mol_{Cx}{\cdot}h$) (equation 5.11) representing the consumption of substrate that is required for maintenance of the microbial population and not allocated for growth purposes.

$$m_S^{req} = \frac{m_G}{-\Delta G_{cat}} \qquad 5.11$$

When the energy is not enough to maintain the microbial population the decay starts. Death biomass is assumed to be hydrolysed to glucose or acetate equivalents and ammonium in order to serve as substrate for other cells in the system.

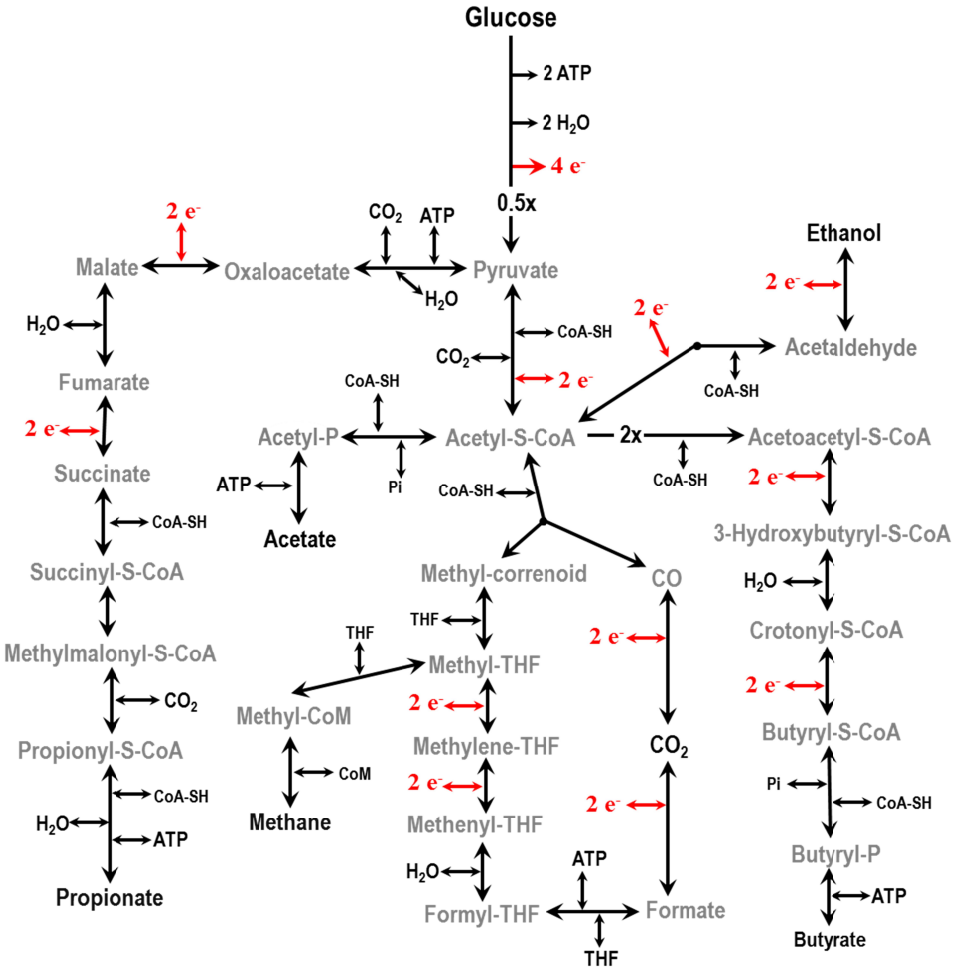

Figure 5. 1 Possible pathways considered for glucose anaerobic fermentation with detailed account of the number of electron transfers involved

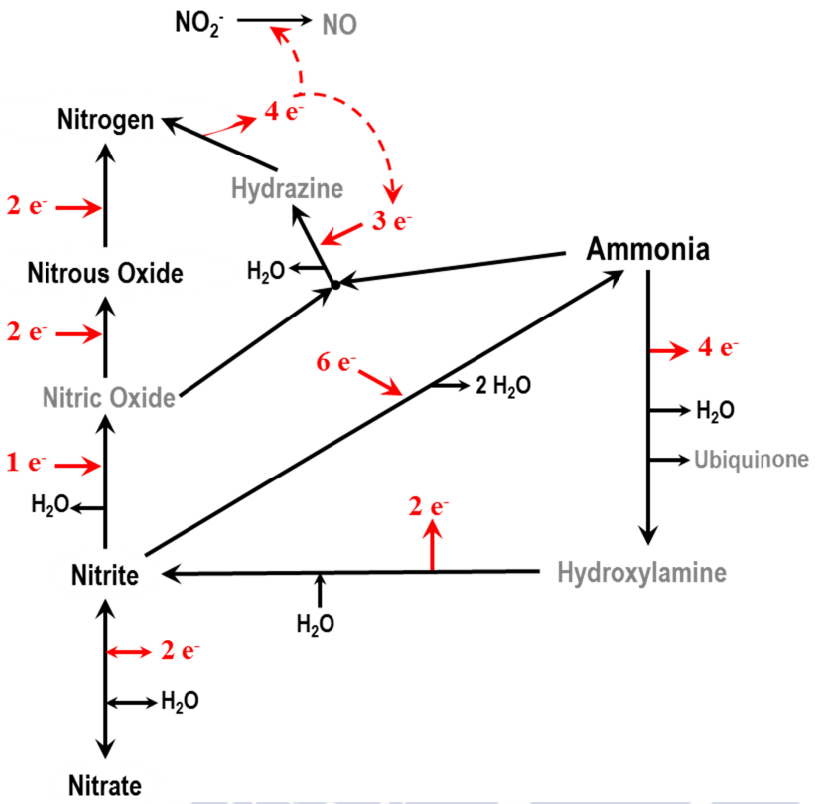

Figure 5.2 Possible pathways considered for nitrogen oxidation-reduction with detailed account of the number of electron transfers involved.

Kinetics of microbial growth and decay

Although the specific microbial growth rate of each postulated microbial group (μ, h^{-1}) is determined by the total energy harvest rate from its specific catabolism (E_{cat}, $kJ/mol_{Cx}{\cdot}h$) (equation 5.12), not all the energy harvested can be used for growth. As the maintenance energy is required to sustain the population (m_G, $kJ/mol_{Cx}{\cdot}h$), reducing the actual growth yield.

The actual Gibbs energy change of each catabolic reaction (ΔG_{cat}), function of the concentrations of the chemical components in the system, is precisely computed at each simulation time step and the specific catabolic energy harvest rate calculated according to equation 5.12.

$$E_{cat} = q_S^{cat} \cdot (-\Delta G_{cat}) \qquad 5.12$$

With this approach three possible modes of the microbial growth are presented.

Positive net growth

It occurs when the rate of energy harvest exceeds that required for the maintenance of the existing cell population (equation 5.13). Here substrate uptake goes to both growth and catabolism purposes.

$$\mu = Y_{XS}^{max} \cdot \left(q_S^{met} - m_S^{req} \right); \quad if \quad E_{cat} > m_G \left(i.e. q_S^{cat} > m_S^{req} \right) \qquad 5.13$$

q_S^{met} kinetics (equation 5.8) includes anabolism related possible limiting substrates (e.g. N source).

Zero net growth

It occurs when the energy available exactly meets the requirements for maintenance of the existing cell population. In this mode, no net growth or decay takes place, only substrate consumption in order to provide the necessary energy for maintenance of the microbial population.

Negative net growth (decay)

It occurs when the energy available is not sufficient to meet the maintenance requirements of the existing cell population. A net decay rate is modelled as proportional to the energy shortage with respect to that required for maintenance. This process is defined as converting active biomass into death biomass (X_d), equation 5.14. In this and in the previous zero net growth mode, substrate uptake goes only to catabolism (q_S^{cat}).

$$\mu = -k_d \cdot \left(m_S^{req} - q_S^{cat} \right) / m_S^{req}; \quad if \quad E_{cat} < m_G \left(i.e.\ q_S^{cat} < m_S^{req} \right) \qquad 5.14$$

In equation 5.14, k_d is the decay kinetic parameter, which value is assumed of $8.33 \cdot 10^{-4}\ h^{-1}$ for all postulated microorganisms [41] and q_S^{cat} kinetics (equation 5.8) includes only catabolism related possible limiting substrates as no cell growth occurs in this scenario.

Dead biomass is assumed as biodegradable and hydrolysed into glucose or acetate equivalents in a first order kinetics (equation 5.15) as commonly found in literature [41].

$$r_{Hyd} = K_{Hyd} \cdot X_d \qquad 5.15$$

K_{Hyd} is the first order constant for death biomass hydrolysis with a value of 0.01 h^{-1} and is considered equal for all the microorganisms considered [41].

The reactive terms presented are calculated by comparing between the specific rate of energy harvested by the catabolism ($E_{cat} = q_S^{cat} \cdot (-\Delta G_{cat})$ $kJ/mol_{Cx} \cdot h$) and the energy needed for the maintenance of the population (m_G). Equation 5.16 summarizes the three different scenarios depending on the available energy. A rate of catabolism in order to satisfy the maintenance of the population, a rate of metabolism to compute the growth of the population with the energy available, and a rate of decay (biomass which is converted to death biomass) proportional to the lack of energy for the maintenance of the whole population are calculated.

$$\begin{cases} r_{cat} = m_S^{req} \cdot X; \quad r_{met} = \left(q_S^{met} - m_S^{req} \right) \cdot X; \quad r_d = 0; & if \quad E_{cat} \geq m_G \\ r_{cat} = m_S^{req} \cdot X; \quad r_{met} = 0; \quad r_d = 0; & if \quad E_{cat} = m_G \\ r_{cat} = q_S^{cat} \cdot X \quad r_{met} = 0; \quad r_d = -k_d \cdot X \left(m_S^{req} - q_S^{cat} \right) / m_S^{req}; \\ \qquad r_{Hyd} = K_{Hyd} \cdot X_d & if \quad E_{cat} \leq m_G \end{cases} \qquad 5.16$$

In equation 5.16 α is the stoichiometric coefficient accompanying the electron donor in the metabolic equation (λ_{cat} when the electron donor for anabolism and catabolism are different).

In overall, the consumption or generation of any component in the model is approximated summing the contributions of catabolic and metabolic processes, hydrolysis and decay (equation 5.17).

$$R_i = \sum_{j=1}^{N} \nu_{met,i,j} \times r_{met,j} + \sum_{j=1}^{N} \nu_{cat,i,j} \times r_{cat,j} + \sum_{j=1}^{N} \nu_{dec,i,j} \times r_{dec,j} + \sum_{j=1}^{N} \nu_{Hyd,i,j} \times r_{Hyd,j} \qquad 5.17$$

Mass balances for each phase of the reactor

Mass balances in each phase of the perfectly mixed vessel, are expressed as differential ordinary equations to describe the dynamic changes of all state variables (liquid compounds and biomass concentrations, and gas components partial pressure) at each time step. Equations 5.17, 5.18 and 5.19 are used for the mass balances of the dissolved, solid and gas phase components. The consumption/generation terms vector (R_i), are calculated according to equation 5.17, and included in the mass balance differential equations.

1. Liquid phase (Si, mol/L)

A constant influent flow rate (Q_{liq} of 0.125 L/h) and working volume (V_r of 1L) are used that corresponds to a hydraulic retention time (HRT) of 8 hours.

$$\frac{dS_i}{dt} = \frac{1}{V_r} \cdot Q_{liq} \left(S_{i,inf} - S_i \right) + R_i \qquad 5.18$$

In equation 5.18 $S_{i,inf}$ is the influent concentration of component i and S_i its concentration in the reactor bulk. The calculation of the concentrations of all chemical species is addressed like in previous chapters and it is calculated fixing the pH of the bulk according the conditions of each simulation.

2. Solid phase (Xj, mol/L)

A long solids retention time (SRT) (for the suspended microorganisms) is used in the system to be able to simulate higher controlled microbial densities inside the reactor. In real industrial systems SRT is typically controlled by solid retention mechanisms such as recirculation, membranes, biofilms etc. Long (30 days) SRT values were used in all simulations in order to ensure even the slowest microbial activities have the option to thrive.

$$\frac{dX_j}{dt} = -\frac{X_j}{SRT} + R_j \qquad 5.19$$

In equation 5.19 no influent microbial biomass is fed and X is the concentration of the microbial species j in the reactor bulk.

3. Gas phase (Gk, bar)

Gas flow rate is modelled assuming a constant pressure and a head space volume (V_g) of 1 L. Equilibrium gas-liquid is assumed as by law of Henry.

$$\frac{dG_k}{dt} = -\frac{1}{V_{gas}} \cdot Q_{gas} \cdot G_k + R_k \qquad 5.20$$

The gas flow out of the system is calculated according equation 5.21 where $n_{gas\text{-}G}$, is the molar flow of gas transferred (calculated from the generation term of gas produced or consumed coming as per equation 5.17) to the gas phase.

$$Q_{gas} = \frac{n_{gas-G} \cdot R_g \cdot T}{P} \qquad 5.21$$

In this case, the gas-liquid transfer dynamics are not modelled like in Chapter 3 and it is assumed complete equilibrium. The production of gas components is assumed directly as gas, neglecting any step of transfer from dissolved to gas phase. Only the liquid concentrations are calculated through law of Henry in order to compute any uptake kinetic limitations associated to gaseous substrates (equation 5.8).

5.3 Results and discussion

The model as described above was applied to the simulation of two microbial ecosystems under different environmental conditions. Firstly, the anaerobic fermentation of glucose at pH 7 and at pH 5 with controlled hydrogen partial pressure is studied. Secondly, the aerobic autotrophic oxidation of inorganic nitrogen compounds and the reduction of nitrogen oxides with and without organic carbon source are studied. Table 5.1 presents the environmental conditions fixed for each microbial ecosystem analysed.

Table 5.1 Reactor operational conditions simulated for the two different microbial ecosystems analysed.

ANFER: Anaerobic fermentation of glucose to CH_4 production.

ANFERH_2: Acidogenic anaerobic fermentation of glucose with H_2 fixed.

AUTNOX: Aerobic autotrophic inorganic nitrogen compounds oxidation.

HETNRED: Heterotrophic reduction of nitrogen oxides.

AUTNRED: Autotrophic reduction of nitrogen oxides.

PARAMETER (UNIT)	ANFER	ANFERH_2	AUTNOX	HETNRED	AUTNRED
Temperature (K)	298.15		298.15		
pH (-)	7	5	7		
SRT (h)	720		720		
HRT (h)	8		8		
P (atm)	1	2	1		
P_{H2} (atm)	Not fixed	1	0		
Dissolved O_2 conc. (mM)	0		0.52	0	
Dissolved CO_2 conc. (mM)	Not fixed		5	Not fixed	5
Influent glucose conc. (mM)	15		0		
Influent acetic acid conc. (mM)	0		0	30	0
Influent NH_4^+ conc. (mM)	5		15	30	30
Influent NO_3^- conc. (mM)	0		0	15	
Influent NO_2^- conc. (mM)	0		0	15	

The list of potential catabolic activities considered in each microbial ecosystem, including both reported and postulated are presented in Tables 5.2 and 5.3. The considered hypothetical catabolic activities never observed in nature consist only of possible combinations of other observed ones; therefore activities involving unknown biochemistry have not been included. For the anabolic reaction, the same electron donor as in catabolism is taken as carbon or nitrogen source when it contains carbon or nitrogen respectively. Alternatively, CO_2 is considered as carbon source and NH_4^+ as the nitrogen source.

All the simulation case studies are started with equal concentrations of all microbial groups. A continuous stirred tank reactor (CSTR) model with high solids retention time (average cell age, SRT) was selected to describe the hydrodynamics of the process. The CSTR system selection was considered that analogous systems are frequently found in nature and in most wastewater treatment plants.

Anaerobic fermentation of glucose

Anaerobic digestion is a well-established process widely used in waste and wastewater treatment due to its potential as biogas producer [42]. In anaerobic digesters the importance of an efficient syntrophic cooperation between different bacteria and archaea, fermenting glucose to methane and carbon dioxide, is well-known [43,44]. This microbial ecosystem was selected to investigate, among other questions, whether, under this approach, a hypothetic microorganism capable of producing methane directly from glucose would be competitive over the experimentally reported volatile fatty acids (VFAs) synthesizers in synergy with methane producing archaea. Methanogens have been reported to possess the biochemical mechanisms to metabolize carbohydrates [45,46] however; there is no experimental evidence of any microorganism producing methane directly from a carbohydrate as substrate [44].

The anaerobic glucose fermenting microbial ecosystem studied is defined by also initially considering the presence of microorganisms that hypothetically would be able to completely convert glucose or different VFAs and ethanol to CH_4 and CO_2 or H_2 and CO_2 in addition to those well-known that convert glucose or VFAs and ethanol first to acetate and then to CH_4, CO_2 and H_2 (Table 5.2).

Table 5.2 Catabolic reactions considered in the glucose anaerobic fermentation microbial ecosystem.

ANAEROBIC FERMENTATION OF GLUCOSE				
X_i	CATABOLISM REACTION	Ne mol_{e^-}/mol_{eD}	ΔG^{o1} (*) kJ/mol_{eD}	$\Delta G^{o1}/e^-$ kJ/mol_{e^-}
1	$C_6H_{12}O_6 + 2H_2O \rightarrow 2C_2H_3O_2^- + 2CO_2 + 4H_2 + 2H^+$	8	-215.90	-26.99
2	$C_6H_{12}O_6 \rightarrow C_4H_7O_2^- + 2CO_2 + 2H_2 + H^+$	12	-264.10	-22.01
3	$C_6H_{12}O_6 + 2H_2 \rightarrow 2C_3H_5O_2 + 2H^+ + 2H_2O$	12	-359.25	-29.94
4	$C_6H_{12}O_6 \rightarrow 2C_2H_6O + 2CO_2$	16	-235.00	-14.69
5	$C_2H_3O_2^- + H^+ \rightarrow CH_4 + CO_2$	2	-35.78	-17.89
6	$C_2H_3O_2^- + H^+ + 2H_2O \rightarrow 2CO_2 + 4H_2$	8	95.02	11.88
7	$\frac{1}{2}CO_2 + H_2 \rightarrow \frac{1}{4}C_2H_3O_2^- + \frac{1}{4}H^+ + \frac{1}{2}H_2O$	2	-23.76	-11.88
8	$H_2 + \frac{1}{4}CO_2 \rightarrow \frac{1}{4}CH_4 + \frac{1}{2}H_2O$	2	-32.70	-16.35
9	$C_4H_7O_2^- + 2H_2O \rightarrow 2C_2H_3O_2^- + H^+ + 2H_2$	4	48.20	12.05
10	$C_3H_5O_2^- + 2H_2O \rightarrow C_2H_3O_2^- + 3H_2 + CO_2$	6	71.68	11.95
11	$C_2H_6O + H_2O \rightarrow C_2H_3O_2^- + H^+ + 2H_2$	4	9.55	2.39
12	$C_6H_{12}O_6 + 6H_2O \rightarrow 6CO_2 + 12H_2$	24	-25.85	-1.08
13	$C_6H_{12}O_6 + 2H_2O \rightarrow 2CH_4 + 4CO_2 + 4H_2$	12	-287.46	-17.97
14	$C_6H_{12}O_6 \rightarrow 3C_2H_3O_2^- + 3H^+$	16	-310.92	-19.43
15	$C_6H_{12}O_6 \rightarrow 3CH_4 + 3CO_2$	20	-418.26	-20.91
16	$C_4H_7O_2^- + H^+ + 6H_2O \rightarrow 4CO_2 + 10H_2$	20	238.25	11.91
17	$C_4H_7O_2^- + H^+ + 2H_2O \rightarrow 2CH_4 + 2CO_2 + 2H_2$	8	-23.36	-1.95
18	$C_3H_5O_2^- + H^+ + 4H_2O \rightarrow 3CO_2 + 7H_2$	14	166.70	11.91
19	$C_3H_5O_2^- + H^+ + 2H_2O \rightarrow CH_4 + 2CO_2 + 3H_2$	8	35.90	3.59
20	$C_2H_6O + 3H_2O \rightarrow 2CO_2 + 6H_2$	12	104.57	8.71
21	$C_2H_6O + H_2O \rightarrow CH_4 + CO_2 + 2H_2$	6	-26.23	-3.28

(*)Considering pH 7 and 298.15K. Liquid concentrations 1M and 1 bar for gas components (CH_4, CO_2 and H_2).

Two operational conditions were simulated: i) Anaerobic fermentation of glucose towards methane production and ii) Non-methanogenic fermentation of glucose at controlled hydrogen partial pressure (Table 5.1). The latter is an operation mode of current interest in process development towards the production of higher energy density liquid products from VFAs [28].

Glucose fermentation to methane.

The model simulations (Figure 5.3.a) predict acetate producers (X_1) and acetate consumers to methane (X_5) as the dominant activities at steady state in line with the experimental observation. These results can be explained because X_1 catabolism involves a smaller quantity of metabolic labour (measured in this model as number of electrons transferred, Ne) than other glucose consuming metabolisms (Table 5.2) and that translates into a higher maximum specific substrate uptake rate (q_S^{max}, equation 5.7). Acetate production catabolism appears as one of the largest energy harvesters per mol of electron transferred (Figure 5.3.b, left axis) advantage that allows this catabolism to dominate over the others under these specific conditions.

Simultaneously to this, acetate consuming methanogenesis performed by X_5 appear to obtain a very low energy yield from acetate to methane, but it is the large availability of the substrate combined with a high maximum specific uptake rate due to the very low metabolic labour involved (Ne = 2, Table 5.2) what allows this catabolic activity to also succeed in parallel with acetate producers.

The synergy established between acetate producers and consumers in this system constitutes a division of labour revealed as beneficial for both. The first provides substrate for the second which in turn, increases the energy available for the first (ΔG_{cat}) by removing the reaction product. This collaborative work does not imply a higher total energy yield per unit of substrate over the whole pathway but it does achieve a higher overall energy harvest rate.

The existing trade-off between yield and rate in energy harvest, promotes the abundance of species that consume glucose to produce VFAs in this system. This analysis presents a mechanism for the reasons why a possible microorganism capable of harvesting more overall energy per mol of glucose (by complete conversion into CH_4 and CO_2) may not actually have an overall competitive advantage compared with other organisms converting glucose to only VFAs. The

additional energy gained by the final steps of the full pathway would not compensate for the lower metabolic rate associated to the longer metabolic pathway.

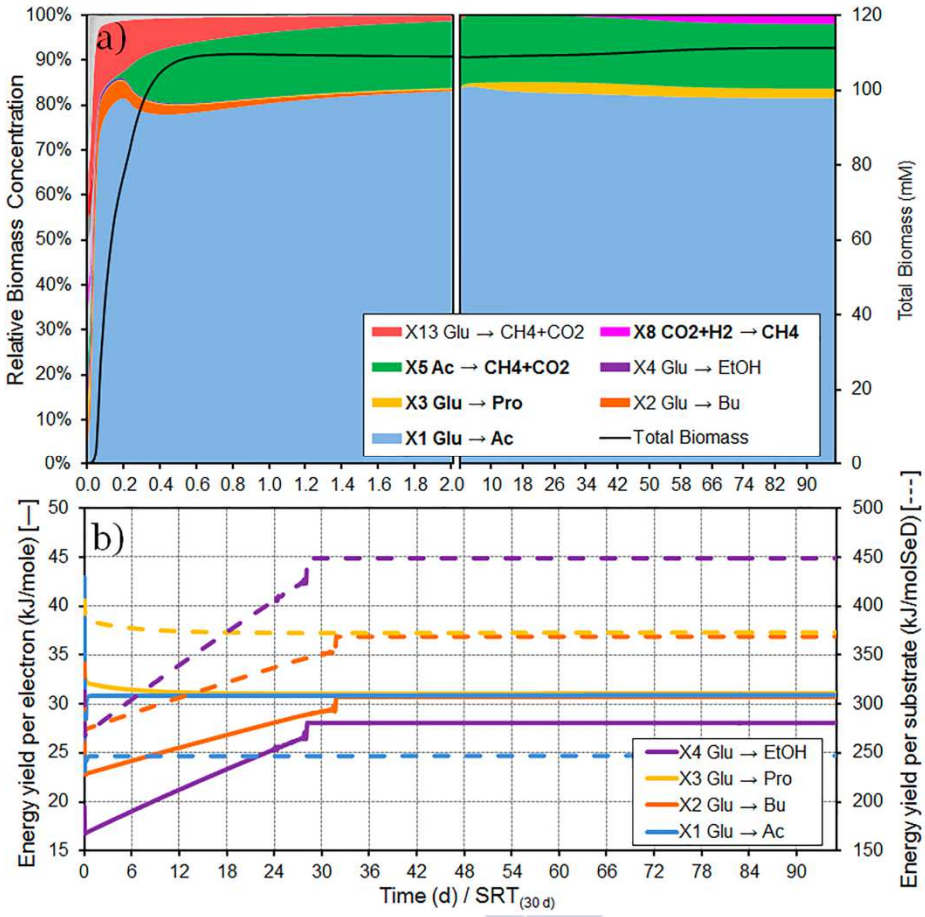

Figure 5.3 Simulated dynamics of the microbial ecosystem during anaerobic fermentation of glucose to CH_4. a) Evolution of the microbial population in total biomass and relative abundance terms. b) Catabolic energy yield per mol of electron transferred throughout the catabolic reaction (solid line) and catabolic energy yield per mol of substrate (dashed line).

Non-methanogenic glucose fermentation at high H_2.

Acidogenic fermentation of glucose by mixed anaerobic cultures is a process well-known to display a large diversity of products [47]. Our approach provides a

possible explanation to this observation. The diverse catabolic pathways in anaerobic glucose fermentation have indeed very similar values of energy yield per electron mol (i.e. acetate X_1, butyrate X_2, propionic X_3 and ethanol X_4 producers, Figure 5.3.b and Figure 5.4.b), which implies that small changes in environmental conditions (concentrations), can easily lead to shifts between the most successful catabolic activities. This, together with the need to allocate electron equivalents into products in a system with no external electron acceptors available, presents a possible explanation for the variability and diversity of products typically observed in these fermentation systems.

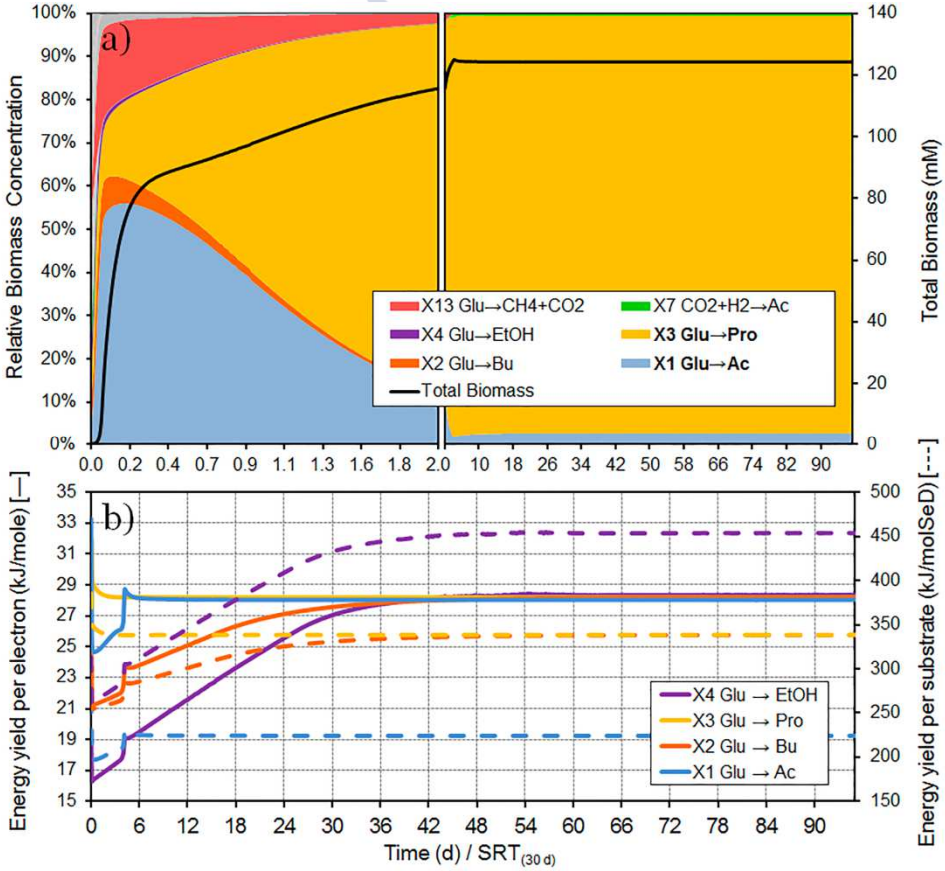

Figure 5.4 Simulated dynamics of the microbial ecosystem during anaerobic fermentation of glucose at acidic pH and constant high P_{H2}. a) Evolution of the microbial population in total biomass and relative abundance terms. b) Catabolic energy yield per mol of electron transferred throughout the catabolic reaction (solid line) and catabolic energy yield per mol of substrate (dashed line).

In order to test this and in the context of interest in the production of reduced products (propionic or butyric acids and ethanol) for biorefinery applications, the impact of high hydrogen pressure in the non-methanogenic fermentation of glucose was simulated. A simulation case study at constant fixed P_{H_2} of 1 atm (and a total pressure of 2 atm) and pH 5 was conducted (Table 5.1). For the sole purpose to isolate the intended effects, in this simulation, CH_4, CO_2 and H_2 producers (X_5, X_6 and X_8, typically archaea) were manually removed from the ecosystem (as they are fully inhibited in acidogenic fermentation at low pH). Simulation results are shown in Figure 5.4.

The high P_{H_2} value allowed the hydrogen consuming propionate producers (X_3) to overcome other microbial groups that had initially higher growth rates (such as acetic acid producers, X_1). This is caused by the energetic shift that increases the catabolic available energy for X_3 due to the higher P_{H_2}, and that therefore also directs the product formation of the ecosystem towards more reduced products.

Inorganic nitrogen oxidation-reduction

The second microbial ecosystem studied in this work is that performing the conversions from the nitrogen cycle metabolism consisting of the oxidation and reduction of inorganic nitrogen compounds. Winogradsky, 1890, did first report about two microbial groups (AOB and NOB) working in syntrophic cooperation on the oxidation of ammonia. The reasons behind nitrification taking place in two stages have been an old question addressed by the kinetic theory of the optimal pathway length [32]. Authors such as Costa et al. [32] have hypothesized the possible existence of strains capable of performing complete nitrification in one-stage. However to date, no microorganisms capable of performing complete nitrification have been reported, fact that has been addressed by [49] based on the presence of some limitations of physiological nature.

The nitrogen oxidation-reduction microbial ecosystem studied is defined by initially considering the presence of microorganisms that hypothetically could conduct aerobic autotrophic nitrification as well as anoxic hetero- and autotrophic nitrogen oxides reduction reactions (Table 5.3). Both reported and hypothetical not observed catabolic activities are included based only on combinations of known feasible biochemical reactions.

Table 5.3 Catabolic reactions considered in the inorganic nitrogen oxidation-reduction microbial ecosystem.

NITROGEN OXIDATION AND REDUCTION				
X_i	CATABOLISM REACTION	Ne mol_{e^-}/mol_{eD}	$\Delta G^{01(*)}$ kJ/mol_{eD}	$\Delta G^{01}/e^-$ kJ/mol_{e^-}
1	$NH_4^+ + 1.5O_2 \rightarrow NO_2^- + 2H^+ + H_2O$	6	-269.90	-44.98
2	$NO_2^- + ½\ O_2 \rightarrow NO_3^-$	2	-76.50	-38.25
3	$NH_4^+ + 2O_2 \rightarrow NO_3^- + 2H^+ + H_2O$	8	-346.40	-43.30
4	$C_2H_3O_2^- + 8/5NO_3^- + 13/5H^+ \rightarrow 4/5N_2 + 2CO_2 + + 14/5H_2O$	8	-805.60	-100.70
5	$C_2H_3O_2^- + 8/3\ NO_2^- + 11/3\ H^+ \rightarrow 4/3N_2 + 2CO_2 + + 10/3H_2O$	8	-977.50	-122.19
6	$C_2H_3O_2^- + 2NO_3^- + 3H^+ \rightarrow N_2O + 2CO_2 + 3H_2O$	8	-689.40	-86.18
7	$C_2H_3O_2^- + 4NO_2^- + 5H^+ \rightarrow 2N_2O + 2CO_2 + 4H_2O$	8	-831.00	-103.88
8	$C_2H_3O_2^- + 4N_2O + H^+ \rightarrow 4N_2 + 2CO_2 + 2H_2O$	8	-1270.50	-158.81
9	$C_2H_3O_2^- + 4NO_3^- + H^+ \rightarrow 4NO_2^- + 2CO_2 + 2H_2O$	8	-547.70	-68.46
10	$C_2H_3O_2^- + NO_3^- + 3H^+ \rightarrow NH_4^+ + 2CO_2 + H_2O$	8	-507.30	-63.41
11	$C_2H_3O_2^- + 4/3NO_2^- + 11/3H^+ \rightarrow 4/3NH_4^+ + 2CO_2 + + 2/3H_2O$	8	-493.80	-61.73
12	$NH_4^+ + NO_2^- \rightarrow N_2 + 2H_2O$	4	-362.80	-90.70

(*) Considering pH 7 and 298.15K. Liquid concentrations 1M and 1 bar for gas components (N_2, N_2O, CO_2).

The operational and environmental conditions applied to this ecosystem are detailed in Table 5.1. This ecosystem is also simulated for a CSTR at high SRT. Organic and inorganic carbon supply as well as oxygen presence are adjusted to evaluate three possible scenarios namely i) autotrophic aerobic, ii) heterotrophic anaerobic and iii) autotrophic anaerobic ecosystems. The simulation results are presented in Figure 5.5 for the autotrophic aerobic case and in Figure 5.6 for both the heterotrophic and autotrophic anaerobic cases.

Autotrophic aerobic nitrogen ecosystem.

Under aerobic conditions only X_1, X_2 and X_3, (i.e., the aerobic autotrophic metabolic activities) have the necessary substrates to thrive and the others quickly decrease(Figure 5.5).

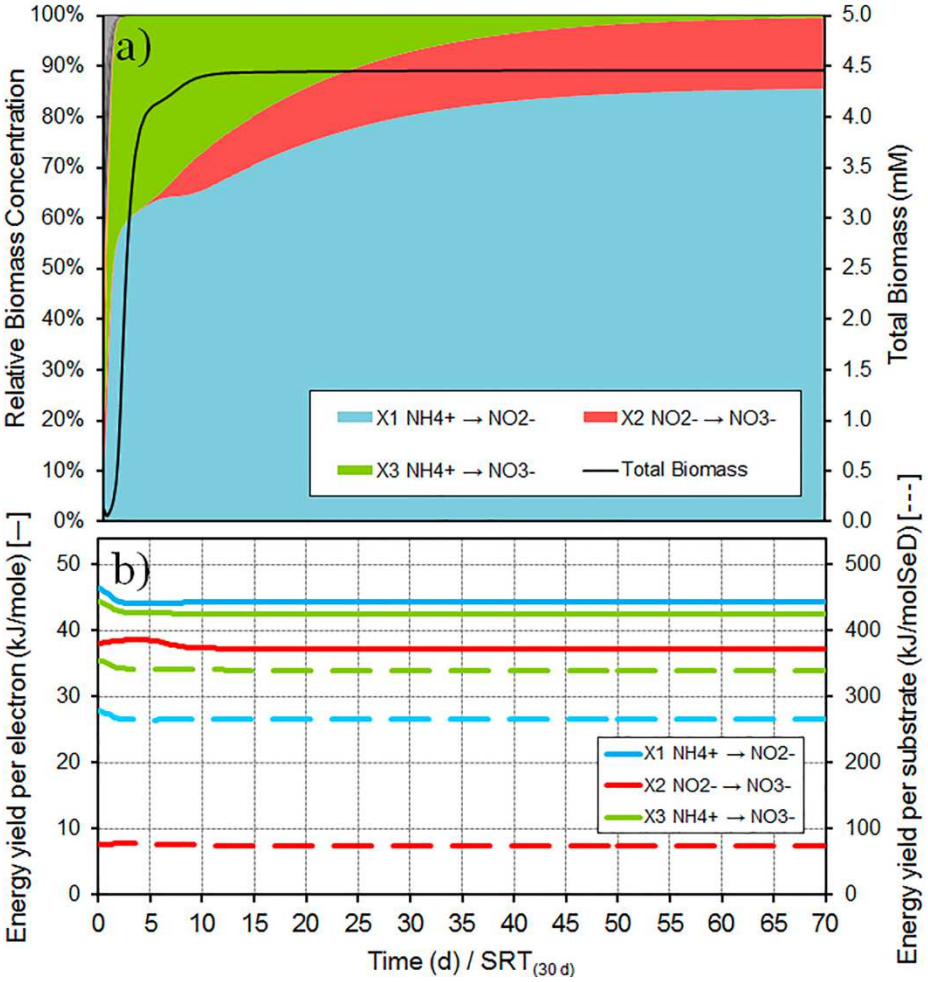

Figure 5.5 Simulated dynamics of the microbial ecosystem during autotrophic nitrogen oxidation a) Evolution of the microbial population in total biomass and relative abundance terms. b) Catabolic energy yield per mol of electron transferred throughout the catabolic reaction (solid line) and catabolic energy yield per mol of substrate (dashed line).

When looking at the complete nitrification (X_3), although the total energy yield per unit of substrate is higher (Figure 5.5.b), the energy yield per electron is lower than that of the partial nitrifiers to nitrite (X_1). The initially high concentration of ammonium allows for the presence of both partial (X_1) and complete (X_3) nitrifiers (Figure 5.5.a). However as the ammonium concentration decreases over time, the energy yield gained by the one-step nitrifiers (X_3) becomes diminished in a larger extent than that of the partial nitrifiers (X_1). This is due to the later benefiting from the activity of nitrite oxidizers (X_2), which by removing their reaction product (NO_2^-) allow them to maintain a high energy yield to outcompete the complete nitrifiers (X_3) in the long run.

Nitrite oxidizers (X_2) become, together with ammonium oxidizers (X_1), the dominant microbial activities in the long term; this is despite their lower yield and partly due to the absence of any other competitors for nitrite in the system. The synergism between the two catabolic activities, analogous to the case of the anaerobic glucose fermentation system, leads to a higher overall energy harvest rate than the one-step nitrification. In both cases, the same overall energy yield per unit of substrate is obtained but, again, this occurs at a higher rate if the process is conducted by two separated microbial groups.

Since these results are completely in line with the experimental observation of the well-known ammonium oxidizing bacteria (AOB) and nitrite oxidizing bacteria (NOB), a possible explanation of the absence of competitive advantage for a microorganism in developing the complete nitrification in one step is hereby provided based on the energetic considerations.

Heterotrophic and autotrophic anaerobic nitrogen ecosystems.

In order to explore the system behaviour under anaerobic conditions (Table 5.3) with an eye in denitrification, a case study is simulated with a mixture of nitrogen compounds (NH_4^+, NO_2^- and NO_3^-) with roles in denitrification, fed to the reactor (Table 5.1). Both heterotrophic (with acetate as carbon source) and autotrophic (with HCO_3^- as carbon source) conditions are studied. Simulations were run first with an acetate feed to allow for heterotrophic growth and after steady state was reached, the feed of acetate ceased and a constant concentration of CO_2 was maintained for autotrophic growth conditions.

Heterotrophic denitrification activities from both NO_3^- (X_4) and NO_2^- (X_5) are predicted as prevailing metabolisms in line with experimental observations [50], both displaying similar growth rates and yields. Other postulated metabolisms, such as the two-stage heterotrophic denitrification through N_2O (X_6, X_7, and X_8), and dissimilatory nitrite and nitrate reductions (X_9, X_{10} and X_{11}) are however not predicted as successful in the system (Figure 5.6.a).

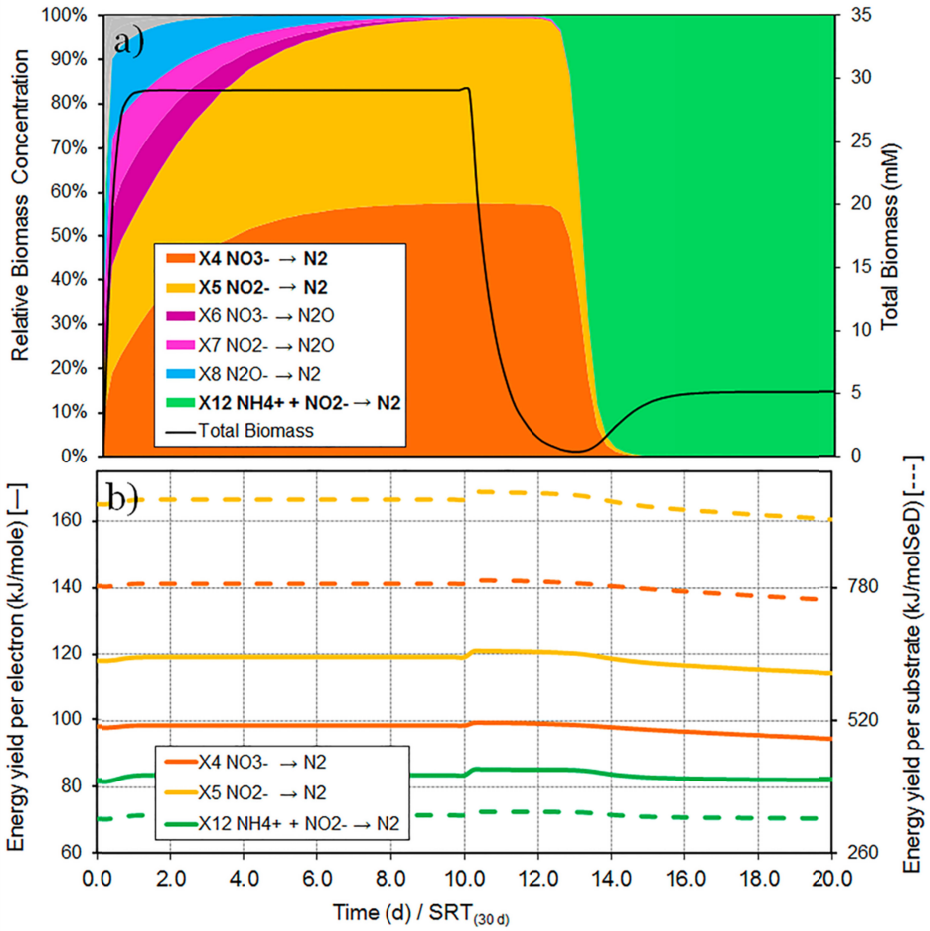

Figure 5.6 Simulated dynamics of the microbial ecosystem during nitrogen reduction a) Evolution of the microbial population in total biomass and relative abundance terms. b) Catabolic energy yield per mol of electron transferred throughout the catabolic reaction (solid line) and catabolic energy yield per mol of substrate (dashed line).

The energy available in NO_x reduction to N_2O (X_6 and X_7) is smaller compared to the reduction to N_2 (X_4 and X_5, Table 5.3) while the same amount of electrons are transferred in the process. This explains why denitrification stopping in N_2O appears as not favoured in our simulations (Figure 5.6.a). However, NO_x reduction to N_2O has been repeatedly reported associated to a competition between the enzymes involved in the four reductive steps of complete denitrification under specific environmental conditions such as limitation in the carbon and nitrogen ratio or at low ranges of pH [51-53]. These very specific biochemical limitations are out of the scope of our modelling approach and for this, the presence of N_2O denitrification cannot be predicted.

Dissimilatory nitrite and nitrate reductions are also not predicted as successful metabolisms (even if NH_4^+ feeding is stopped, data not shown) despite the fact that they have been reported where electron donors other than organic matter (e.g. H_2S, [54]) and/or specific environmental conditions [55] are present.

Finally, in the absence of organic carbon source, autotrophic anaerobic ammonium oxidizers (*anammox*, X_{12}) are predicted as successful dominant catabolic activity (Figure 5.6.a). This occurs despite the higher energy yields of other denitrification routes (Figure 5.6.b) and it is attributed to the environmental conditions of limited organic carbon source that allow anaerobic ammonium oxidizers to appear [56].

5.4 Shorter pathway lengths and cross feeding prevail under decreasing average energy yield per electron

Two-stages autotrophic nitrification as opposite to one-stage heterotrophic denitrification are both predicted by the modelling approach and experimentally observed. An analysis of the energy yields per electron provides a plausible explanation of these observations. Unlike the similar analysis by Costa et al. [32], any physiological aspects of ATP production are excluded and the total Gibbs energy available of each catabolic process is directly used together with an account of the number of electron transfers in each pathway. The relationship between energy and pathway length is illustrated in Figure 5.7 by comparing the average Gibbs energy yields per electron transferred with the yields per mol of substrate for the pathways studied above (standard conditions and pH 7 considered).

The overall analysis of the modelling results suggests that the lengths of the successful pathways predicted above and experimentally reported appear to be defined by the maximum energy harvest rate (which is also affected by the environmental conditions). Stepwise processes appear as more favourable when pathways have decreasing average energy yields per electron transferred (Figure 5.7.b) while direct longer pathway conversions are favoured at increasing average energy yields instead (Figure 5.7.c).

Nevertheless, this analysis could be generalized (Figure 5.8). The maximum average energy harvested per electron mol corresponds always to the optimum length of a metabolic pathway at which the specific growth rate would become maximum. When the dependence between ΔG_{cat} and electrons transported is linear (Figure 5.8.a, red lines) shorter or longer pathways are not clearly favoured. If the dependence is above linear (Figure 5.8.a, green lines), a maximum energy yield ($\Delta G_{cat}/e^-$, dot line) appears associated with shorter pathways. Longer pathways are favoured when the dependence of the catabolic energy with the number of electrons is under linear (Figure 5.8.a, blue lines).

In many pathways, however, the relationship between the number of electrons transferred and the catabolic energy yield might not be monotonous as in Figure 5.8.a and a maximum energy per electron transferred could also appear in a specific middle point of the catabolic pathway as illustrated in Figure 5.8.b. In this case, a division of labour is expected. According to the theoretical example of Figure 5.8.b, one microorganism is expected to conduct the first part of the pathway alone (involving around 7 electrons in this example). Other microorganisms would consume the product and continue the metabolic pathway establishing a synergy with the first microorganism. This synergy, as presented in our model predictions, would raise the overall growth yield of both species, increasing their dominance over other metabolic strategies.

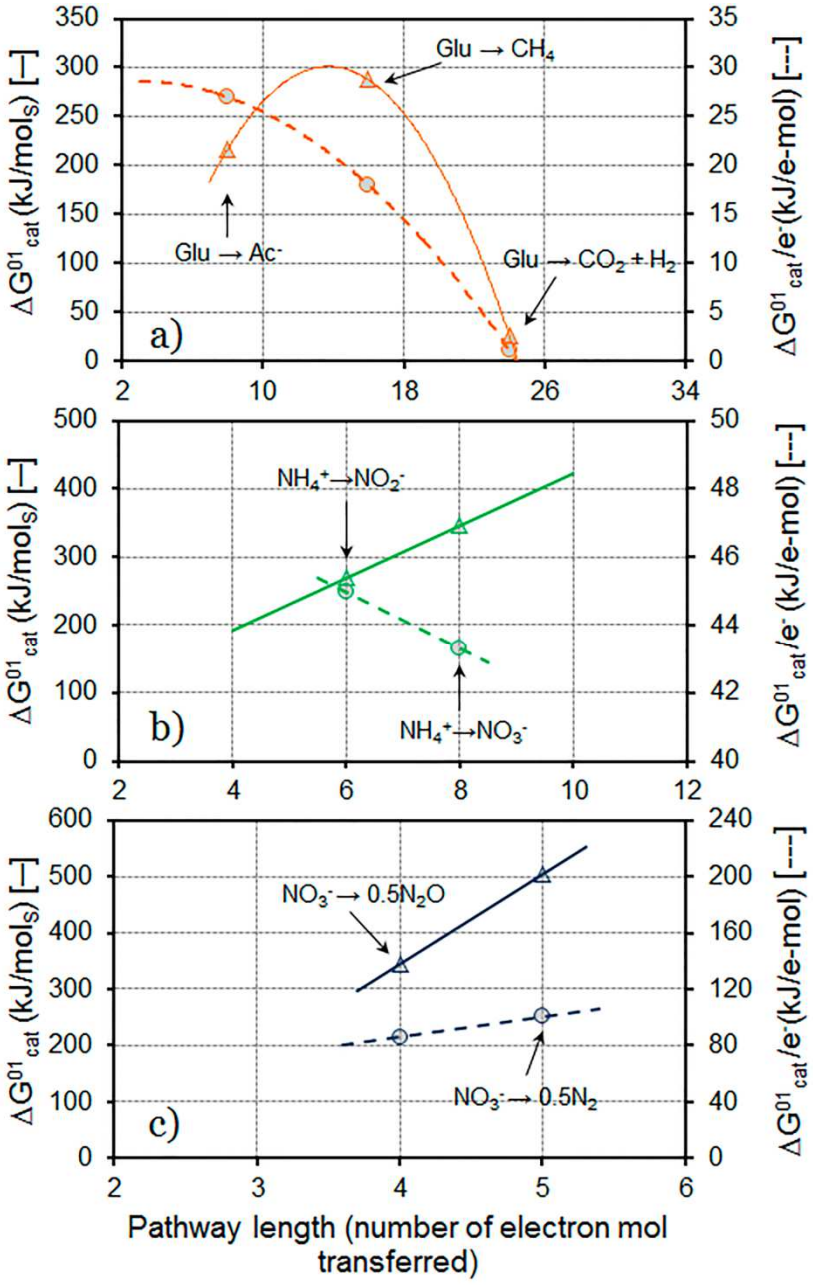

Figure 5.7 Theoretical energy yield per mol of substrate (triangles) and per mol of electron transferred (circles) respect to pathway length for (a) glucose fermentation; (b) nitrification and (c) denitrification. (ΔG^{01} values are presented in Table 5.2 and Table 5.3; for denitrification case ΔG^{01} is referred per mol of NO_3^-).

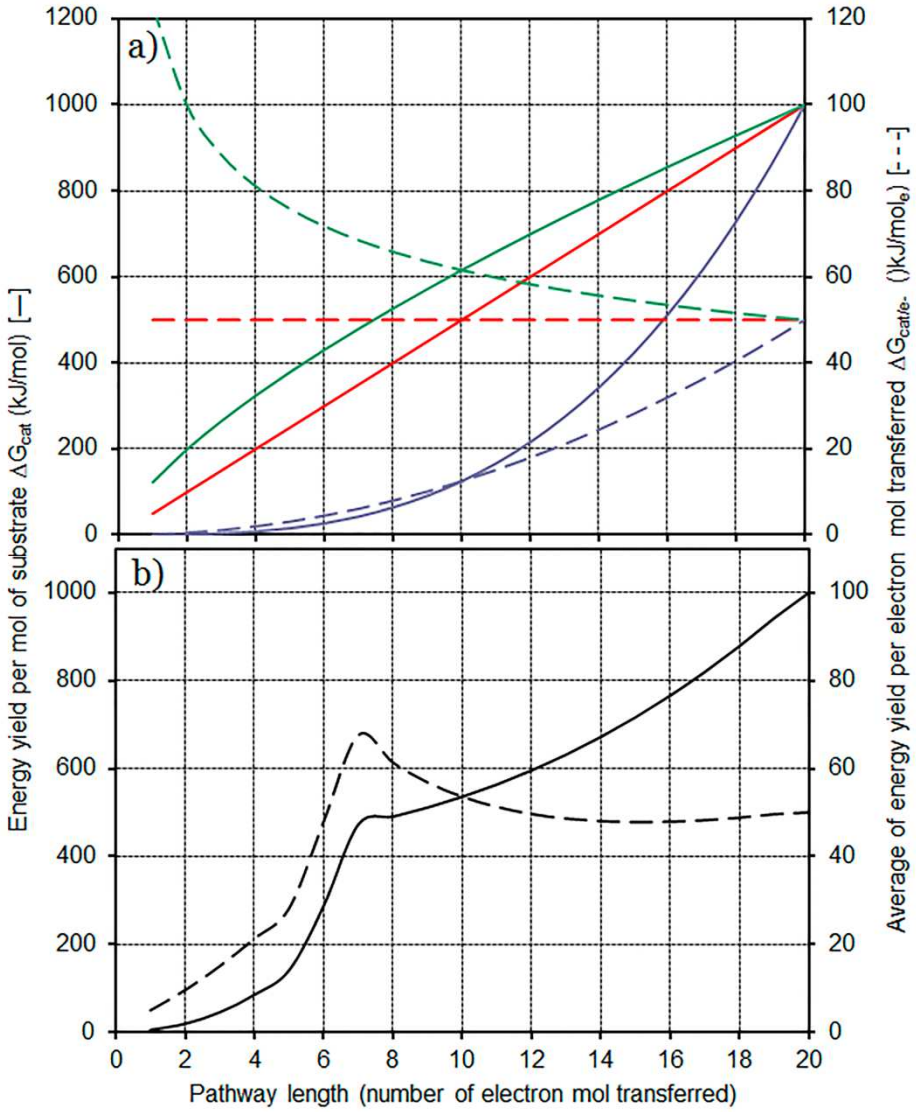

Figure 5.8 Theoretical average energy yields per substrate mol (solid line) and per electron transferred (dashed line) as function of the pathway length for hypothetic catabolic pathways. a) Decreasing (green), constant (red) and increasing (blue) average energy yields per electron. b) Case at which an optimum point for pathway length arises is in the middle of the pathway potentially leading to a division of pathway labour.

5.5 Sensitivity analysis for q_s^{max} and Ks

The values considered for q_s^{max} and Ks are applied to all the microbial activities considered in the model as physiological adaptive differences between microbial species experimentally observed are not considered in the hypothetical approach of this work. However, there is weak or null experimental validation for these actual values and therefore a sensitivity analysis is provided.

In this analysis, the value of q_s^{max} is modified in terms of the number of electrons transferred maintaining it constant for all the microorganisms as a surrogate measure of maximum metabolic activity rate. In regards to the Ks, the same modification is done keeping it constant for all the microbial groups.

The sensitivity analysis confirms the negligible impact of the actual numeric values for q_s^{max} or Ks (if kept above biomass washout/decay values) on the conclusions of this work (Figures 5.9-5.16). The impact of the values used is limited to changes in the predicted relative abundances among successful microorganisms due to the faster or slower kinetics of the microbial activities in the continuous reactor under fixed hydraulic and biomass retention times. However, this analysis graphically shows that the values chosen for q_s^{max} and Ks for the cases in the main manuscript are not hiding the microbial synergies established in the different ecosystems considered.

Anaerobic fermentation of glucose

In Figure 5.9 note that for the very slow kinetics (q_s^{max} = 0.5 $mol_{e^-}/X \cdot h$) most biomasses are washed out of the reactor, X_1 as it is the strain growing the most in the ecosystem, is still partly surviving. When q_s^{max} is set high, the presence of these other microorganisms, successful but in low abundances, appear in the graphs (X_3, X_5 and X_8). When $q_s^{max} \geq 6$ $mol_{e^-}/X \cdot h$ the very high rate of X_1 does not allow for the presence of X_3 competing for glucose in these conditions as X_3 harvest lower energy per mol of glucose, and X_8 increases its abundance as the higher activity of the other microorganisms implies higher concentrations of its substrates (CO_2 and H_2) in the reactor. In all the cases, same syntrophisms are predicted. These changes in the relative abundance of the different catabolic activities do not alter the conclusions presented in simulated case studies and

manuscript. Only the successful activities appear even at very different q_S^{max} values.

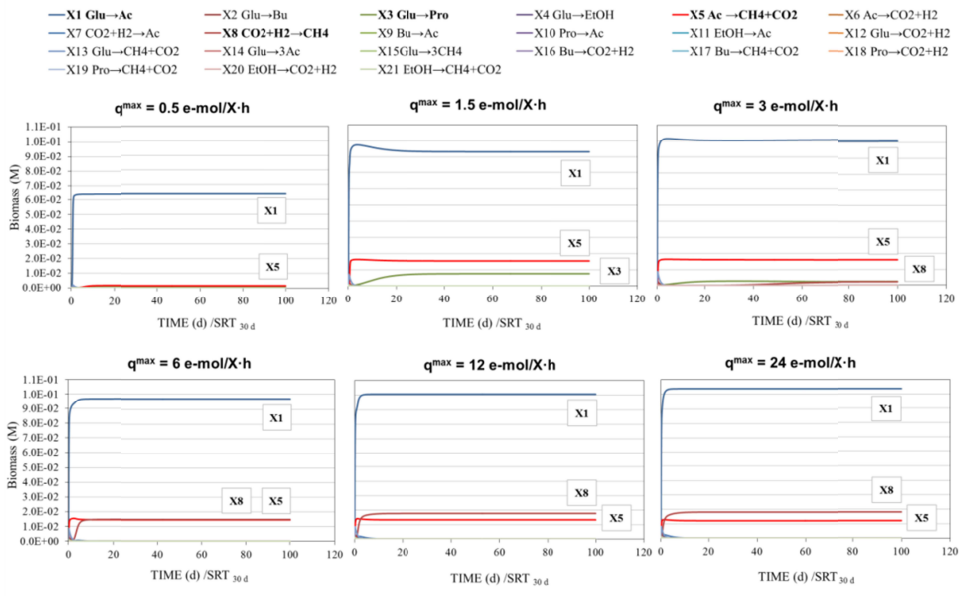

Figure 5.9 Sensitivity analysis for q_S^{max} in the case of anaerobic fermentation of glucose.

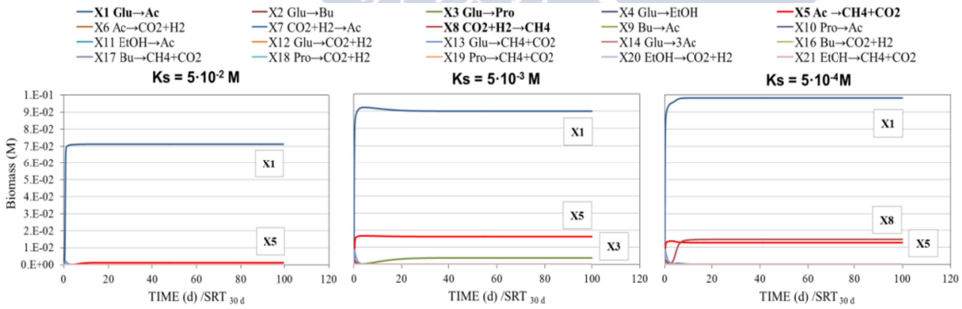

Figure 5.10 Sensitivity analysis for Ks in the case of anaerobic fermentation of glucose.

In Figure 5.10 is observed that changes in Ks have a similar effect over the whole ecosystem than changes in q_S^{max}. Low Ks values imply a faster kinetics for all the microorganisms and high Ks low substrate consumption rate. High Ks ($Ks = 5 \cdot 10^{-2}$ M) leads to a low abundance of microorganisms in the reactor and to

only X_1 surviving at steady state, however, very low Ks (Ks = $5 \cdot 10^{-4}$ M) makes that even the slower but successful activities (like X_8) are present in the reactor with higher abundance. Similar trends are observed for acidogenic glucose fermentation (Figures 5.11 and 5.12), nitrification (Figures 5.13 and 5.14) and denitrification systems (Figures 5.15 and 5.16).

Acidogenic fermentation of glucose at high H_2 partial pressure

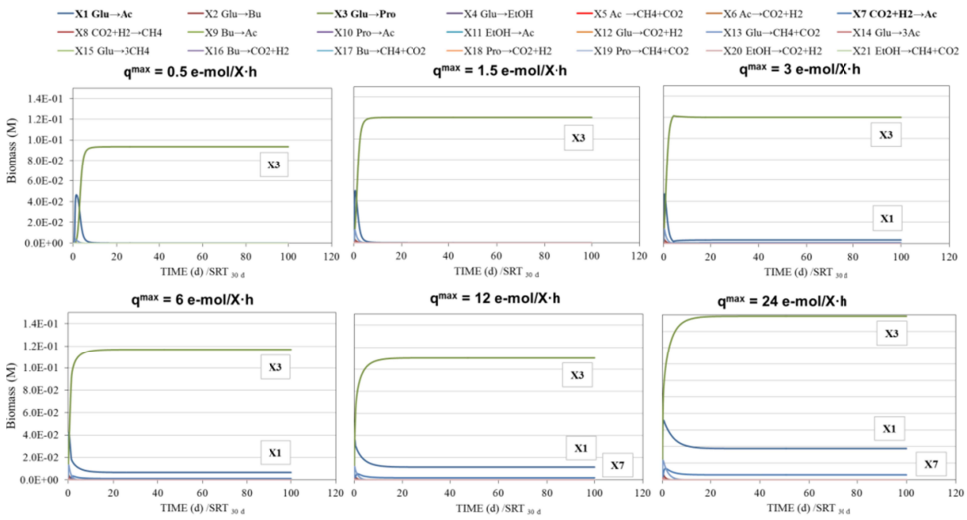

Figure 5.11 Sensitivity analysis for q^{max} in the case of acidogenic fermentation of glucose at high H_2 partial pressure.

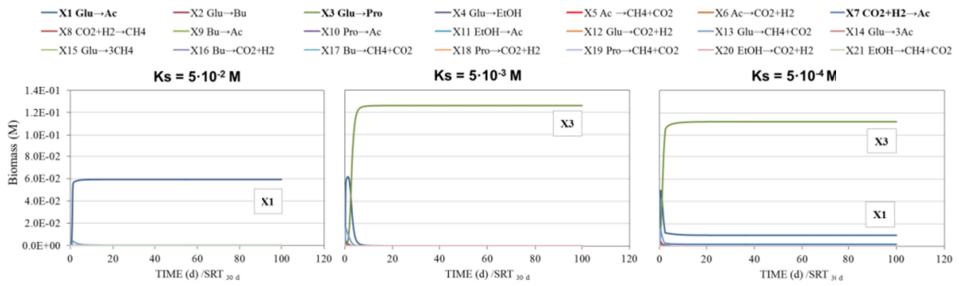

Figure 5.12 Sensitivity analysis for Ks in the case of acidogenic fermentation of glucose at high H_2 partial pressure.

Nitrification system

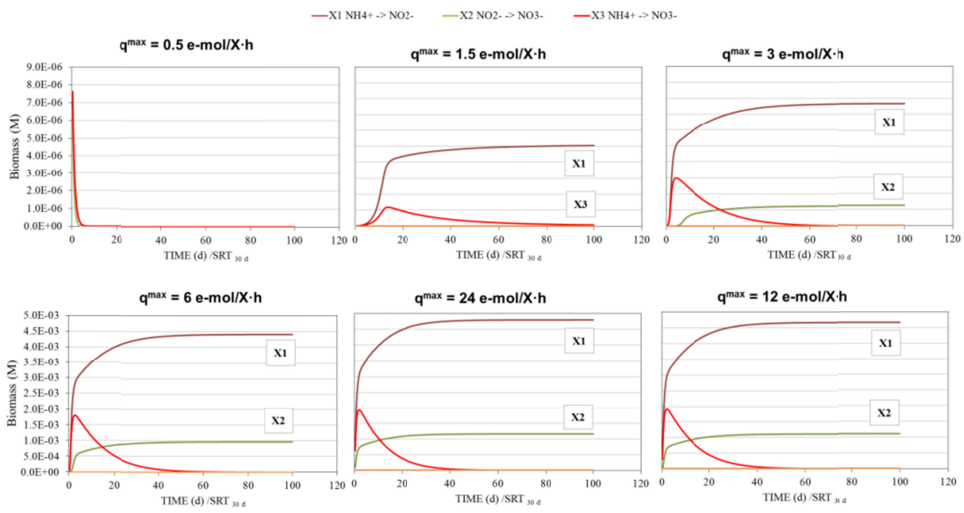

Figure 5.13 Sensitivity analysis for q^{max} in the case of nitrification

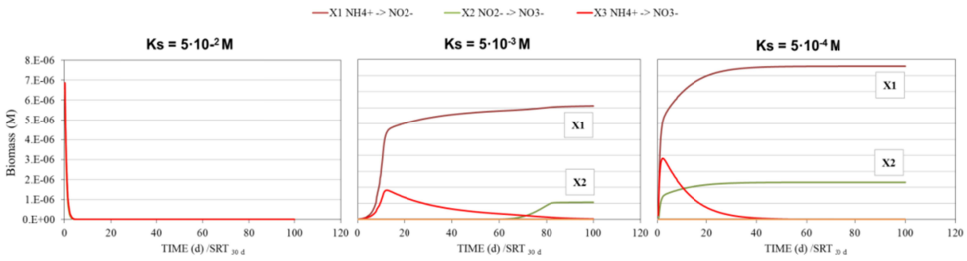

Figure 5.14 Sensitivity analysis for Ks in the case of nitrification

Denitrification system

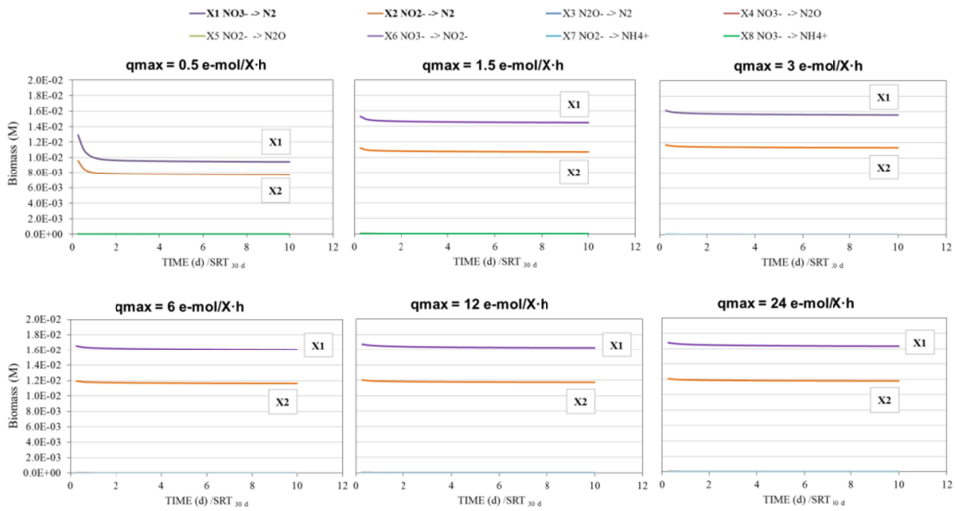

Figure 5.15 Sensitivity analysis for q^{max} in the case of denitrification

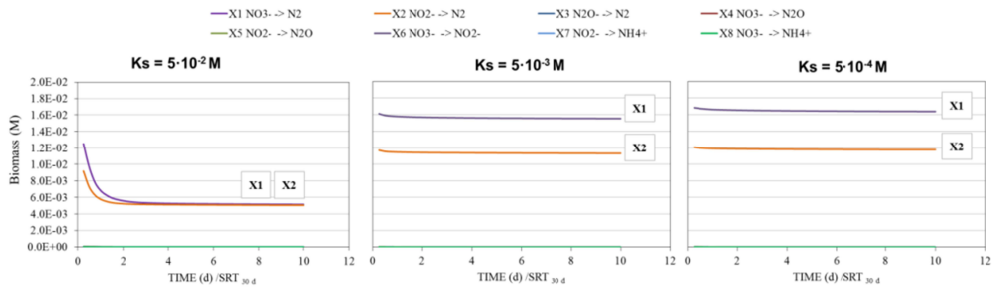

Figure 5.16 Sensitivity analysis for Ks in the case of denitrification

5.6 Conclusions

Through a modelling approach based on the available energy in catabolic reactions and using the number of electron transfers in a pathway as measure of maximum specific metabolic rate, the success of specific microbial catabolic activities as well as syntrophic relations can be predicted in good agreement with experimental observations. The modelling approach provides mechanistic hypotheses, on the basis of the bioenergetics considerations, for the reasons behind the success of certain microbial activities in nature versus others.

The analyses are developed by comparing metabolic activities conducted by non-adapted microbial groups, competing under the same conditions for the available energy. Non-differentiated enzymatic rates are assumed by considering the same q_s^{max} per electron for all microbial groups (equation 5.7). Similarly, non-differentiated substrate transport capacities are assumed for Ks calculations by considering the same cell shape and size. These generalised parameter values attempt to reflect the modelling of non-specifically adapted microorganisms, using very limited empirical information. The q_s^{max} and Ks parameters, for which arguably different numerical values could be used, do not appear to affect the results and conclusions obtained, which are very much in line with the experimentally observed microbial activities. However, it is important to highlight that at the core of the modelling approach presented is the assumption that all the non-adapted microbial groups have non-differentiated physiological characteristics (i.e. the same maximum specific rates, half saturation kinetic constants controlled by transport kinetics, cell shape and size, equal maintenance and decay kinetics, fully efficient catabolic energy harvest) and that the hypotheses resulting from this study must be interpreted with this limitations in consideration.

During the simulation of a glucose anaerobic fermentation ecosystem, a multistage microbial conversion from glucose to methane (involving VFAs producers in synergy with methanogens) is predicted as successful versus a single stage microbial conversion. This is a direct consequence of the higher energy yield per electron in the conversion of glucose to VFAs respect to that of VFAs to methane. In addition, the very similar energy harvest rates displayed by several of the alternative conversions of glucose to VFAs and alcohols potentially explain the

variability and diversity of catabolic products observed in (non-methanogenic) glucose fermentation ecosystems under different operational conditions.

Analogously, during the simulation of the nitrogen oxidation-reduction ecosystem, the autotrophic ammonium oxidation in two-stages (involving AOB in synergy with NOB) is predicted as favoured versus a single stage microbial conversion from ammonium to nitrate. This is a direct consequence of the mutually beneficial syntrophic relation between AOB and NOB described by the dynamic model simulations presented. The syntrophic AOB-NOB cooperation is analogous to that existing between acetate producers and consumers in the glucose fermentation case capable of overcoming a hypothetical one-stage nitrification alternative.

The above pathway partitions are not predicted however during the simulation of heterotrophic denitrification (NO_x reduction), again in line with experimental observations. This is attributed to the lower energy per electron involved in NO_2^- or NO_3^- reduction to N_2O than that from N_2O to N_2, leading to an optimum one-stage denitrification to achieve a maximum energy harvest rate.

Overall the modelling approach provides energy-based mechanistic interpretations to experimental observations, supporting a hypothesis of maximum energy harvest rate as main selective pressure in some microbial ecosystems.

The dynamic simulation of the hypothetic competition between non-specialised proposed and experimentally observed microbial activities suggests that the evolutionary adaptation of microorganisms towards specific successful catabolic activities is determined by the maximum energy harvest rate under the given environmental conditions. The dynamic model is capable of describing the interdependences between the energy available in the system the environmental conditions and the activity of the microorganisms present, which dynamically affect one another.

Given these results we advocate for the study of microbial ecosystems as highly efficient energy harvesters and postulate that the quest for energy might have promoted synergetic cooperation between microorganisms and also possibly directed subsequent steps in the evolutionary course towards more complex micro- and macro-organisms.

5.7 References

1. von Stockar U, Maskow T, Liu J, Marison IW, Patiño R. (2006) Thermodynamics of microbial growth and metabolism: an analysis of the current situation. *Journal of Biotechnology* **121**: 517-33.
2. Morowitz HJ. (1968) Energy Flow in Biology. Academic P. Academic Press, editor. New York.
3. Westerhoff H V, Winder C, Messiha H, Simeonidis E, Adamczyk M, Verma M, et al. (2009) Systems Biology: The elements and principles of Life. *FEBS Lett. Federation of European Biochemical Societies* **583**: 3882-3890.
4. Lane N, Martin W. (2010) The energetics of genome complexity. *Nature* **467**: 929–34.
5. Lane N, Martin WF, Raven JA, Allen JF. (2013) Energy, genes and evolution: introduction to an evolutionary synthesis. *Philosophical Transactions of the Royal Society of London B Biological Science* **368**: 20120253.
6. Vallino JJ. (2003) Modeling microbial consortiums as distributed metabolic networks. *Biological Bulletin* **204**: 174–9.
7. Pascal R, Boiteau L. (2011) Energy flows, metabolism and translation. *Philosophical Transactions of the Royal Society of London B Biological Science* **366**: 2949–58.
8. Pfeiffer T, Bonhoeffer S. (2004) Evolution of cross-feeding in microbial populations. *The American Naturalist* **163**: E126–35.
9. Pfeiffer T, Schuster S, Bonhoeffer S. (2001) Cooperation and competition in the evolution of ATP-producing pathways. *Science* **292**: 504–7.
10. Jackson BE, McInerney MJ. (2002) Anaerobic microbial metabolism can proceed close to thermodynamic limits. *Nature* **415**: 454–6.
11. Hoehler TM, Jørgensen BB. (2013) Microbial life under extreme energy limitation. *Nature Reviews Microbiology* **11**: 83–94.
12. Schuster S, Pfeiffer T, Fell DA. (2008) Is maximization of molar yield in metabolic networks favoured by evolution? *Journal of Theoretical Biology* **252**: 497–504.
13. MacLean RC. (2008) The tragedy of the commons in microbial populations: insights from theoretical, comparative and experimental studies. *Heredity* **100**: 233–9.
14. Kreft JU, Bonhoeffer S. (2005) The evolution of groups of cooperating bacteria and the growth rate versus yield trade-off. *Microbiology* **151**: 637–41.
15. Stams AJM, Plugge CM. (2009) Electron transfer in syntrophic communities of anaerobic bacteria and archaea. *Nature Reviews Microbiology* **7**: 568–577.
16. López-García P, Moreira D. (1999) Metabolic symbiosis at the origin of eukaryotes. *Trends Biochemical Sciences* **24**: 88–93.
17. Margulis L, Chapman MJ. (1996) Endosymbioses: cyclical and permanent in evolution. *Trends in Microbiology* **6**: 342–5; discussion 345–6.
18. Rodríguez J, Lema JM, Kleerebezem R. (2008) Energy-based models for environmental biotechnology. *Trends in Biotechnology* **26**: 366–74.
19. Heijnen JJ, Kleerebezem R. (2010) Bioenergetics of microbial growth. Encyclopedia of Industrial Biotechnology: Bioprocess, Bioseparation and Cell Technology pp. 1–24.

20. Thauer RK, Jungermann K, Decker K. (1977) Energy conservation in chemotrophic anaerobic bacteria. *Bacteriological Reviews* **41**: 100–180.

21. Hanselmann KW. (1991) Microbial energetics applied to waste repositories. *Experientia* **47**: 645-687.

22. Diekert G, Wohlfarth G. (1994) Metabolism of homocetogens. *Antonie Van Leeuwenhoek* **66**: 209-21.

23. Alberty RA. (2006) Standard molar entropies, standard entropies of formation, and standard transformed entropies of formation in the thermodynamics of enzyme-catalyzed reactions. *Journal of Chemical Thermodynamics* **38**: 396–404.

24. Flamholz A, Noor E, Bar-Even A, Milo R. (2012) eQuilibrator-the biochemical thermodynamics calculator. *Nucleic Acids Research* **40**: D770–5.

25. Heijnen JJ, Van Dijken JP. (1992) In search of a thermodynamic description of biomass yields for the chemotrophic growth of microorganisms. *Biotechnology and Bioengineering* **39**: 833-58.

26. Heijnen JJ, van Loosdrecht MCM, Tijhuis L. (1992) A Black Box Mathematical Model to Calculate Auto- and Heterot rophic Biomass Yields Based on Gibbs Energy Dissipation. *Biotechnology and Bioengineering* **40**: 1139–1154.

27. Kleerebezem R, van Loosdrecht MCM. (2010) A Generalized Method for Thermodynamic State Analysis of Environmental Systems. *Critical Reviews in Environ Scice and Technology* **40**: 1-54.

28. González-Cabaleiro R, Lema JM, Rodríguez J, Kleerebezem R. (2013) Linking thermodynamics and kinetics to assess pathway reversibility in anaerobic bioprocesses. *Energy and Environmental Science* **6**: 3780–3789.

29. Roels JA. (1983) Energetics and kinetics in biotechnology. Elsevier B. Elsevier Biomedical Press, editor. New York.

30. Waddell TG, Repovic P, Meldndez-Hevia E, Heinrich R, Montero F. (1999) Optimization of glycolysis : new discussions. *Biochemical Education* **27**: 12–13.

31. Manchester K. (2000) Optimization of energy coupling: what is all the argument about? *Biochemical Education* **28**: 18–19.

32. Costa E, Pérez J, Kreft JU. (2006) Why is metabolic labour divided in nitrification? *Trends in Microbiology* **14**: 213–9.

33. Andersen KB, von Meyenburg K. (1980) Are growth rates of Escherichia coli in batch cultures limited by respiration? *Journal of Bacteriology* **144**: 114–23.

34. van De Leemput IA, Veraart AJ, Dakos V, Klein JJM De, Strous M, Scheffer M. (2011) *Predicting microbial nitrogen pathways from basic principles*. *Environmental Microbiology* **13**: 1477–1487.

35. Liu Y. (2007) Overview of some theoretical approaches for derivation of the Monod equation. *Applied Microbiology and Biotechnology* **73**: 1241–50.

36. Wang X, Mann CJ, Bai Y, Ni L, Weiner H. (1998) Molecular cloning, characterization, and potential roles of cytosolic and mitochondrial aldehyde dehydrogenases in ethanol metabolism in Saccharomyces cerevisiae. *Journal of Bacteriology* **180**: 822–30.

37. Snoep JL, Mrwebi M, Schuurmans JM, Rohwer JM, Teixeira de Mattos MJ. (2009) Control of specific growth rate in Saccharomyces cerevisiae. *Microbiology* **155**: 1699–707.

38. Lundblad RL, MacDonald FM. (2010) Handbook of Biochemistry and Molecular Biology, Fourth Edition. Lundblad R. L. MFM, editor. CRC Press.

39. Kanehisa M, Goto S. (2000) KEGG: kyoto encyclopedia of genes and genomes. *Nucleic Acids Research* **28**: 27–30.

40. Kartal B, Maalcke WJ, de Almeida NM, Cirpus I, Gloerich J, Geerts W, et al. (2011) Molecular mechanism of anaerobic ammonium oxidation. *Nature* **479**: 127–30.

41. Batstone DJ, Keller J, Angelidaki I, Kalyuzhnyi S V, Pavlostathis SG, Rozzi A, et al. (2002) The IWA Anaerobic Digestion Model No 1 (ADM1). *Water Science and Technology* **45**: 65-73.

42. Appels L, Baeyens J, Degrève J, Dewil R. (2008) Principles and potential of the anaerobic digestion of waste-activated sludge. *Progress in Energy Combustion Science* **34**: 755–781.

43. Schink B, Stams AJM. (2006) Syntrophism among Prokaryotes. The Prokaryotes, Vol 2. pp. 309-335.

44. Schink B. (1997) Energetics of syntrophic cooperation in methanogenic degradation. *Microbiology and Molecular Biology Reviews* **61**: 262–280.

45. Murray PA., Zinder SH. (1987) Polysaccharide reserve material in the acetotrophic methanogen, Methanosarcina thermophila strain TM-1: accumulation and mobilization. *Archives of Microbiology* **147**: 109–116.

46. König H, Nusser E, Stetter KO. (1985) Glycogen in Methanolobus and Methanococcus. *FEMS Microbiology Letters* **28**: 265–269.

47. Temudo MF, Kleerebezem R, van Loosdrecht MCM (2007) Influence of the pH on (Open) Mixed Culture Fermentation of Glucose : A Chemostat Study. *Biotechnology and Bioengineering*. **98**: 69–79.

48. Winogradsky S. (1890) Sur les organismes de la nitrification. *Comptes rendus l'Académie des Sciences* **110**: 1013–1016.

49. Pérez J, Costa E, Kreft JU. (2009) Conditions for partial nitrification in biofilm reactors and a kinetic explanation. *Biotechnology and Bioengineering* **103**: 282–95.

50. Ruiz G, Jeison D, Rubilar O, Ciudad G, Chamy R. (2006) Nitrification-denitrification via nitrite accumulation for nitrogen removal from wastewaters. *Bioresource Technology* **97**: 330-5.

51. Pan Y, Ni B-J, Bond PL, Ye L, Yuan Z. (2013) Electron competition among nitrogen oxides reduction during methanol-utilizing denitrification in wastewater treatment. *Water Research* **47**: 3273–81.

52. Pan Y, Ni B-J, Yuan Z. (2013) Modeling electron competition among nitrogen oxides reduction and N2O accumulation in denitrification. *Environmental Science and Technology* **47**: 11083-11091.

53. Pan Y, Ye L, Ni B-J, Yuan Z. (2012) Effect of pH on N2O reduction and accumulation during denitrification by methanol utilizing denitrifiers. *Water Research* **46**: 4832–40.

54. An S, Gardner W. (2002) Dissimilatory nitrate reduction to ammonium (DNRA) as a nitrogen link, versus denitrification as a sink in a shallow estuary (Laguna Madre/Baffin Bay, Texas). *Marine Ecology Progress Serires*. **237**: 41–50.

55. Roberts KL, Kessler AJ, Grace MR, Cook PLM. (2014) Increased rates of dissimilatory nitrate reduction to ammonium (DNRA) under oxic conditions in a periodically hypoxic estuary. *Geochimica et Cosmochimica Acta* **133**: 313–324.

56. van de Graaf AA, de Bruijn P, Robertson LA, Jetten MSM, Kuenen JG. (1996) Autotrophic growth of anaerobic ammonium-oxidizing micro-organisms in a fluidized bed reactor. *Microbiology* **142**: 2187-2196.

USC
UNIVERSIDADE
DE SANTIAGO
DE COMPOSTELA

6

Discussion and general conclusions

6.1 Environmental selection

Environmental conditions limit the survival of any living organism constraining its possibilities to grow and to survive. The survival of a microbial species within an ecosystem comes largely determined by the energy available in the system and by the mechanisms that the organism possesses to harvest it. Metabolic reactions are catalysed by microorganisms pursuing the objective of energy harvest and building blocks for growing (i.e. C-source, N-source and/or others). When a metabolic activity is successful, a microbial species can thrive and even dominate an ecological niche leading to a change in the environment around.

Back in the 1930s, Professor Bass Becking hypothesized that microbial life worldwide spread implies that most microbial species would be present in most niches at least in a latent condition [1]. Considering that the confirmation of the presence of latent microbial species below the given lowest limits of detection is not possible, the hypothesis has at first, a difficult direct confirmation. Today, it is considered proven that bacterial undefined cultures containing large numbers of species, have also high functional redundancy [2]. This implies that, even if not all possible species would be present in a set ecological niche, we would expect that almost all possible microbial activities would have a chance to appear. Therefore, the expected successful microorganisms are those that catalyse the reactions that lead to a faster energy harvest (Chapter 3 and Chapter 5).

The successful microorganisms will, in principle, grow more and may restrain with their activity the possibility of other microorganisms to survive (e.g. by consuming the available substrates). The importance of avoiding fixed snapshot approaches must be highlighted; instead, dynamic descriptions of the environmental interactions with the microbial ecosystem must be used. The environmental conditions limit the microbial functionalities while the microbial activity modifies the environmental conditions, all in interaction with the physicochemical processes concomitantly taking place (Figure 6.1). Dynamic models have been shown necessary if these interactions between microbial activities and the environment are to be described correctly (Chapter 3 and Chapter 5).

Microbial ecosystems that are limited in energy availability are, arguably, subjected to stronger selective pressures [3] because under those conditions only

a limited number of metabolic activities are capable of maintaining a microbial population and changes in those conditions may have a major impact on that capacity. In these systems, a predicted environmental selection can be used as an engineering tool to establish those operational conditions that select and favour those microbial activities of interest for the bioprocess at hand. The detailed understanding on the impact of environmental conditions over the microbial activity pretends to elucidate what the optimal conditions are to maximise the yield of a desired product or products pursued (Chapter 3). If sufficiently high efficiencies are achieved, numerous direct industrial applications are possible, especially for processes aiming at the recovery of valuable products from complex wastes (Chapter 1) [4].

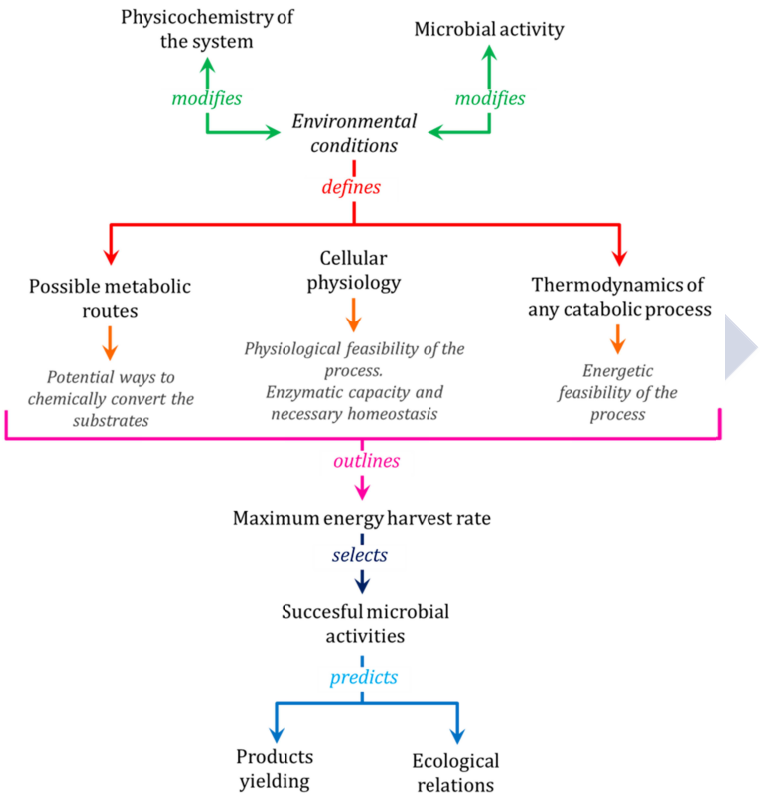

Figure 6.1 Environmental conditions select successful metabolic routes. Analysing the bioenergetics fluxes of the possible metabolic routes in any ecological niche and tacking in account the cellular physiological limitations is possible to predict the most probable activity of an undefined culture constrained by the energy available.

6.2 Bioenergetics analysis

In order to quantify the impact of the environmental conditions over the microbial functionalities, a bioenergetics analysis approach has been applied successfully throughout this thesis in order to study in detail the metabolic fluxes of specific catabolic reactions (Chapter 4) and also overall microbial activities (Chapter 5).

In an undefined mixed culture it is highly difficult to relate microbial functionality with microbial community composition due to the large number of species typically present and to their metabolic redundancy [5]. In this work, bioenergetics has been demonstrated as a powerful tool to justify the presence of specific microbial activities. The analysis of the energetics fluxes establishes feasible limits for catabolic reactions and explains the need for possible syntrophic interactions (Chapter 5) as well as the impossibility of survival of one species when another is not present in the system.

A bioenergetics analysis can also be used for a preliminary assessment of the feasibility of a specific application. Throughout thermodynamic calculations the feasibility of a process under given environmental conditions can be tested together with the possibilities of other processes taking place alongside. Bioenergetics calculations could serve as preliminary analysis tools for the set-up of an experiment, reducing uncertainty in the system and increasing the chances for a successful operation.

6.3 Undefined mixed cultures: Conclusions about microbial ecology

The presence of multiple different microbial species running different catabolic reactions increases the flexibility that a microbial community has to degrade different types of substrates. Given the competition of these microorganisms for the resources available, the evolution of the microbial population towards higher robustness of the system is expected [6,7]. But, although the use of mixed cultures is essential to be able to treat complex and variable substrates, and the operational costs are smaller, the control of these systems remains complex. The information available related with the mechanisms that govern these microbial

processes is limited, which affects our capacity to predict the responses of the system.

Through the bioenergetics analysis developed, it was observed how in energy scarcity conditions, environmental selection in mixed culture appears as highly important. The hypothesis that successful activities are the ones harvesting highest amounts of energy per time appears to be strongly supported by the work developed (Chapter 3 and Chapter 5). Our results support that the microbial community seems to evolve towards a maximum energy harvest from the environment, limited by the physiological mechanisms of the cell and the available metabolic routes. It is worth noting that a maximum energy harvest for growth is also implying a maximum of entropy in the system [8].

Our results also emphasize how in environmental energy limited conditions, different parallel routes successfully and simultaneously appear to compete in a given ecological niche, and that all of them are bioenergetically comparable i.e. all of them harvest almost the same amount of energy per unit of time. This has been clearly observed when analysing mixed culture fermentations in Chapter 3 and Chapter 5. The results from Chapter 3 indicate how the mayor products observed in an anaerobic fermentation of glucose are able to harvest very similar amounts of energy and how the shift between products occurs with variations of only a few kilojoules per mol of substrate harvested by the cell. In Chapter 5, in which the number of the metabolic steps necessary to conduct a specific pathway determines the maximum rate of the process, very similar amounts of energy harvested per unit of substrate and time are obtained when glucose is fermented (Figure 6.2). This supports the hypothesis that the presence of different possible metabolic activities, with very similar energy harvest might increase the flexibility of the microbial community and increase the chances of survival of the community. Under energy scarcity, if the environmental conditions change, the microbial population could shift towards the catalysis of alternative metabolic routes that would yield approximately the same energy for growth and that more favoured under the changed environmental conditions.

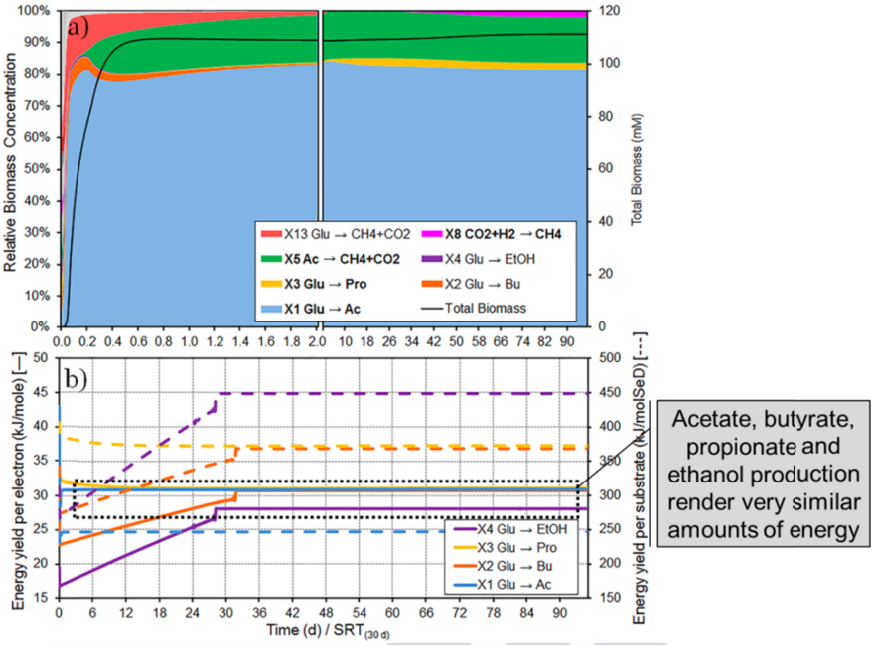

Figure 6.2 Different pathways for glucose fermentation have similar energy harvest yields.

6.4 Highly efficient energy scavengers

The microbial efficiency in terms of energy harvest gains importance in conditions of energy scarcity. Under these conditions, the microorganisms must become highly efficient in catalysing reactions as close to thermodynamic equilibrium as possible in order to minimise the energy losses. It has been proven that in order to survive they can harvest energy even at lower than 20 kJ of energy available per mol of substrate degraded [9,10]. In many cases, the energy harvested through catabolism must be invested to avoid thermodynamic limitations in subsequent metabolic steps (Figure 6.3) thus reducing further the energy available for growth and maintenance (Chapter 4). Taking into account those calculations, Figure 6.3 is obtained assuming ideal thermodynamic equilibrium in all steps, it is clear that the energy harvested per unit of substrate degraded is severely restricted.

In numerous cases, the energy harvested through catabolism corresponds merely to the equivalent to one proton translocation (Chapter 4). This implicitly reveals that the dissipation of a few kilojoules in any catabolic pathway could

imply the difference between the decay and survival of a microbial population. This, points out how the enzymatic mechanisms that catalyse the reactions appear to dissipate very small amounts of energy and how the ATP energy synthesis (used in anabolism) as well as the proton motive force must be finely balanced for the same reasons [11].

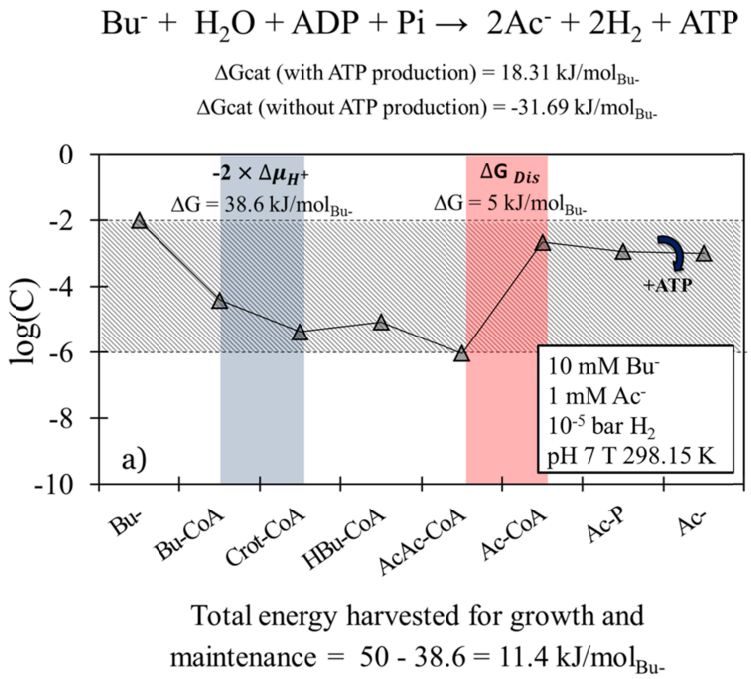

Figure 6.3 Very limited energy is harvested for growth and maintenance during the catalysis of butyrate oxidation to acetic acid.

The efficiency in energy harvest is also presented in Chapter 5 as a plausible explanation for the existence of some syntrophic relations. Our results indicated how the division of pathway labour observed in certain niches favours the rate in energy harvest. Instead of only one microbial species catalysing a lengthy pathway of many metabolic steps, two or more specie could catalyse the process in steps. With this division of labour even if a lower energy yield per substrate is obtained by each individual species, overall they are increasing their rates of energy harvest. In global, the microbial community increases the energy harvest rate from the environment. In these specific cases reported, the division of labour favours both microbial groups as the activity of one microorganism favours the

activity of its partner by changing the environmental conditions (e.g. consuming the product of the activity of the microbial partner).

6.5 On the importance of accurately describing physicochemical processes

When the environmental conditions are key factor to predict the behaviour of a microbial ecosystem, the description of the physicochemical processes concomitantly taking place becomes highly important. A good description of precipitation or gas-liquid transfer processes comes with an obligated detailed description of the liquid phase (Chapter 2). But an increment in the accuracy of describing the physicochemistry of the liquid solution is not always easy to achieve. Even if highly accurate complex models, such as Pitzer equations, can be used, they require of many parameters not always available [12].

Although acid-base physicochemical processes are well-known, their impact is in many cases erroneously neglected. Their mathematical description has not evolved at the same pace as other microbiological phenomena in bioprocess models towards a detailed and closed framework [13]. To achieve a reliable description of any bioprocess it is essential to reach to an optimum compromise in the complexity level to accurately describe the physicochemistry. In Chapter 2 possible indicators to determine on the adequate level of complexity are presented.

6.6 Common limitations and uncertainties related to the models developed

Bioenergetics can be a powerful tool to analyse the detailed steps of the metabolic fluxes and the impact of environmental conditions over the microbial functionality. However important uncertainties remain and must be taken into account related with the concentrations of the intermediate metabolites, the Gibbs energy values, etc. The mathematical models presented (Chapters 3, 4 and 5) are fed with the biochemical information available but show high number of uncertainties and low experimental support.

Metabolic pathways

More detailed information about the metabolic pathways carried out by the microorganisms could lead to more accurate conclusions by the bioenergetics-based analysis. Even considering that different literature references and data bases [14] make available updated information on metabolic pathways, the uncertainty when selecting the metabolic routes to consider in a model is important. In numerous occasions a route presents more than one reaction possible and specific steps such as whether a coenzyme or an ATP is consumed or released are not always clear. Uncertainties exist also related with the specific reactive ionic species (1^{st}, 2^{nd} or *n*, deprotonation) that is actually transformed by the enzyme catalysing a metabolic step.

Electron carriers

Uncertainties are also involved during the analysis of oxidative or reductive metabolic steps in which the reduction or oxidation of another molecule is involved. Typically these molecules are conserved moieties (molecules that never cross the cell wall) and that are often referred to as electron carriers. These electron carriers have different ratios of concentrations between the oxidized and the reduced forms (not always known) and different Gibbs energies. This implies that the energy needed for each reductive or oxidative step is different depending on which electron carrier is involved and this, in numerous cases, is related with the capacity of energy harvesting by the cell. It is not always clear when a microorganism uses one or another electron carrier and this can have a direct impact on bioenergetics calculations.

Proton pump coupling

Proton pump is related with the highly energetic reactions involved in the metabolic process. In the glucose fermentation model (Chapter 3), it was assumed as coupled with FAD reduction, as it is the electron carrier with higher redox potential. However, the proton coupling in a metabolic route is not always clear and uncertainties are often found about the step where it is occurring.

Moreover, to carry active transport across the cellular membrane, proton pump coupling is often necessary to invest or harvest the energy involved. This

mechanism is however not fully described yet. The recycling model is typically used to describe this energy coupling [15] assuming that the transport coupled to proton pump occurs close to the thermodynamic equilibrium. With this model, the calculation of energy harvested or consumed is direct, but this theory has not been fully validated as it is built up on limited experimental values obtained from lactic acid active transport across cell membrane [16].

ATP yield for growth

The amount of ATP required for the generation of one unit of new biomass is also not fully known as the complete anabolism is complex and involves multiples stages where consumption of ATP takes place.

Stouthamer 1973 [17] related ATP costs for growth process with the different carbon sources synthetized, the necessity of transport across the membrane and other metabolic mechanisms of energy consumption. The Gibbs energy dissipation method used by Heijnen estimates the coupling between catabolism and anabolism by also relating the energetic requirements of the anabolism with the carbon source used [18]. Other methods [19] also consider that the differences in the ATP yield are mainly due to the necessary metabolic steps to process different carbon sources. Although, none of this approximations seems to present strong experimental support and it is not clear whether ATP yields vary or not with the microbial species considered.

Intermediate metabolite concentrations

The analysis of the bioenergetics of any bioprocess including the study of the metabolic steps required can be valuable as kinetic limitations not firstly expected and observed experimentally could be in this way explained. To study the intracellular bioenergetics it is however necessary to know the intracellular concentrations or at least, their ranges. A feasible intracellular range between 1 μM to 10 mM has been considered because it has been reported as the physiological range to, on one end, avoid instability in the cytoplasm (i.e. elevated ionic strengths) and on the other to enable the enzymatic catalysis kinetics [20-22]. The combined analysis of kinetic limitations in relation with the

thermodynamic ones to allow maintaining the intracellular concentrations in the feasible range has been proven of interest.

Moreover, in many cases, the cytoplasm present compartments in which different concentrations of conserve moieties are kept to preserve the thermodynamic feasibility of a specific the metabolic route [23]. Existing knowledge on these aspects is currently very limited and the determination of intermediate metabolites concentrations difficult. The thermodynamics analysis of a process using the available information can however bring insights about the possible cytoplasmic compartmentalisation, intermediate metabolites concentrations or on the most likely electron carriers ratios between oxidative and reductive forms as well as about other conservative moieties.

Thermodynamic calculations

$$\Delta G = \Delta G^0 + R_{th} \cdot T \cdot \ln \prod_i a_i^{v_i} \qquad 6.1$$

The Gibbs energy exchange of any reaction is calculated through equation 6.1 where R_{th} is the universal constant in kJ/mol·K, T the temperature in Kelvin and a_i refers to the activities of products and substrates. To apply this equation the Gibbs standard value of the reaction (ΔG^o) is required. This value can be calculated through the standard Gibbs values of all reactants involved which are found in literature. Some uncertainty is added due to the slight differences in reported Gibbs energy values between different data bases [24-29].

Concentrations instead of activities can be used to approximate ΔG values avoiding the correction for non-ideality. But in many environments, this correction could be highly important to predict the feasibility of a reaction, especially when it is close to thermodynamic equilibrium and occurring within the cytoplasm of a cell with high ionic strength [30] (Chapter 2). To consider non-ideal solution, a well described phisicochemistry in the liquid bulk medium in which the microbial activity takes place is necessary. Moreover pH, ionic strengths and calculation of all chemical species concentrations (i.e. hydrolysed forms and deprotonations) affect Gibbs calculations.

6.7 General conclusions

The present Thesis, in which the bioenergetics of different bioprocesses has been analysed, brings conclusions and hypotheses towards the understanding of the ecological relations in microbial cultures and on their capacity to survive under energy scarcity. The work also contributes to the advance in control and improvement on efficiency of those bioprocesses which use undefined microbial cultures. Environmental selection has been proposed to explain the product output obtained in well-known bioprocesses (such as anaerobic fermentations) as well as to understand microbial ecological interactions. The work developed strongly suggests that the selection of a product in a fermentation using mixed cultures is deterministically possible by changing the operational conditions under the proposed mechanisms (Chapter 3); that it is possible by changing the operational conditions, to revert typical oxidative fermentative processes towards the reductive direction while involving the same enzymatic mechanisms in both directions (Chapter 4);and that the selection of microbial activities and syntrophisms established in a mixed culture seems to maximize the energy harvest rate (Chapter 5).

The following are the main general conclusions of this Thesis:

I) On the prediction of the product spectrum during glucose anaerobic fermentation

1. The model developed, based on the optimization of the ATP production with a full account of the electron balances and membrane transport energetics is the first mechanistic model succeeding in the prediction of observed shifts in major fermentation products with external pH:

   a. Butyrate is the major product at low pH together with acetate and propionate production.

   b. At intermediate pH, a decrease in butyrate is observed with an increase in acetate and propionate production

   c. At highly alkaline pH, ethanol and acetate are predicted as preferred products.

d. A shift between hydrogen and formate is predicted and experimentally observed when pH is increased. The modelling proposed clearly explains that this observation is due to the higher solubility of inorganic carbon on water at alkaline pH.

2. The results obtained under this modelling approach strongly support the hypothesis that mixed culture microbial ecosystems can be described as highly efficient energy harvesters in which, independently from the microbial community composition, the conditions of maximum energy harvest rate are achieved in the long term.

II) On the reversibility of anaerobic fermentation pathways from oxidative to reductive direction

1. The reversibility of homoacetogenesis, as reported in literature, appears to require reversible proton translocation mechanisms as well as Gibbs energy dissipation at specific intermediate reaction steps in order to perform within feasible metabolite concentrations. The energy recovery and investment sites appear to be the same in both reductive and oxidative pathways but running in opposite direction.

2. The energy dissipation required for butyrate oxidation to acetate suggests that a net amount of less than one $\Delta\mu_{H+}$ energy for anabolism is harvested (1 ATP minus 2 $\Delta\mu_{H+}$ invested minus dissipated energy).

3. Acetate reduction to butyrate with hydrogen as electron donor appears as not possible due to the kinetically unfeasible low acetoacetyl-CoA concentration required by thermodynamics.

4. The experimentally reported acetate reduction with ethanol or lactate as electron donors is shown in this study to be thermodynamically and kinetically feasible.

5. The reduction of VFAs into longer chain fatty acids with ethanol as electron donor appears as highly feasible both thermodynamically and kinetically.

6. Ethanol production from acetate appears to require $\Delta\mu_{H+}$ energy generation coupled to redox reactions in order for the cell to obtain net energy for growth

and to compensate for the ATP invested on the phosphatation of acetate. The active transport of solutes across the membrane could also be coupled with $\Delta\mu_{H+}$ to be used further in anabolism and maintenance.

III) On the competition and syntrophic relations between microbial groups in mixed cultures

1. Through a modelling approach based on the available energy in catabolic reactions and using the number of electron transfers in a pathway as measure of maximum specific metabolic rate, the success of specific microbial catabolic activities as well as syntrophic relations can be predicted in good agreement with experimental observations.

2. During the simulation of a glucose anaerobic fermentation ecosystem, a multistage microbial conversion from glucose to methane (involving VFAs producers in synergy with methanogens) is predicted as successful versus a single stage microbial conversion. This is a direct consequence of the higher energy yield per electron in the conversion of glucose to VFAs respect to that of VFAs to methane.

3. The very similar energy harvest rates displayed by several of the alternative conversions of glucose to VFAs and alcohols potentially explain the variability and diversity of catabolic products observed in (non-methanogenic) glucose fermentation ecosystems under different operational conditions.

4. During the simulation of a nitrogen oxidation-reduction microbial ecosystem, the autotrophic ammonium oxidation in two-stages (involving AOB in synergy with NOB) is predicted as favoured versus a single stage microbial conversion from ammonium to nitrate. This is a direct consequence of the mutually beneficial syntrophic relation between AOB and NOB described by the dynamic model simulations presented.

5. Simulation of heterotrophic denitrification (NO_x reduction), predicts denitrification occurring in only one step, again in line with experimental observations. This is attributed to the lower energy per electron involved in NO_2^- or NO_3^- reduction to N_2O than that from N_2O to N_2, leading to an optimum one-stage denitrification to achieve a maximum energy harvest rate.

6. Overall the modelling approach provides energy-based mechanistic interpretations to experimental observations, supporting the hypothesis of maximum energy harvest rate as main selective pressure in some microbial ecosystems. This suggests that the evolutionary adaptation of microorganisms towards specific successful catabolic activities is determined by the maximum energy harvest rate under the given environmental conditions.

7. The dynamic model is capable of describing the interdependences between the energy available in the system the environmental conditions and the activity of the microorganisms present, which dynamically affect one another.

6. 8 References

1. de Wit R, Bouvier T (2006) 'Everything is everywhere, but, the environment selects'; what did Baas Becking and Beijerinck really say? *Environmental microbiology* **8**: 755-758.

2. Wellnitz T, Poff NL (2001) Functional redundancy in heterogeneous environments: implications for conservation. *Ecology Letters* **4**: 177-179.

3. Rodríguez J, Lema JM, Kleerebezem R (2008) Energy-based models for environmental biotechnology. *Trends in Biotechnology* **26**: 366-374.

4. Agler MT, Wrenn BA, Zinder SH, Angenent LT (2011) Waste to bioproduct conversion with undefined mixed cultures: the carboxylate platform. *Trends in Biotechnology* **29**: 70-78.

5. Carballa M, Regueiro L, Lema JM (2015) Microbial management of anaerobic digestion: exploiting the microbiome-functionality nexus. *Current Opinion in Biotechnology* **33**: 103-111.

6. Kleerebezem R, van Loosdrecht MCM (2007) Mixed culture biotechnology for bioenergy production. *Current Opinion in Biotechnology* **18**: 207-212.

7. Angenent LT, Wrenn BA (2008) Optimizing mixed-culture bioprocessing to convert wastes into bioenergy. In: Press A, editor. Bioenergy. Washington. pp. 181-194.

8. Schrödinger E (1944) What is life? The physical aspect of the living cell; Press CU, editor.

9. Jackson BE, McInerney MJ (2002) Anaerobic microbial metabolism can proceed close to thermodynamic limits. *Nature* **415**: 454-456.

10. Kleerebezem R, Stams AJM (2000) Kinetics of syntrophic cultures: a theoretical treatise on butyrate fermentation. *Biotechnology and Bioengineering* **67**: 529-543.

11. Sapra R, Bagramyan K, Adams MWW (2003) A simple energy-conserving system: proton reduction coupled to proton translocation. *Proceedings of the National Academy of Sciences of the United States of America* **100**: 7545-7550.

12. Wolery TJ (1992) EQ3NR, A Computer Program for Geochemical Aqueous Speciation-Solubility Calculations: Theoretical Manual, User's Guide, and Related Documentation (Version 7.0). Livermore, California: Lawrence Livermore National Laboratory.

13. Batstone DJ, Amerlinck Y, Ekama G, Goel R, Grau P, et al. (2012) Towards a generalized physicochemical framework. *Water Science and Technology* **66**: 1147-1161.

14. Kanehisa M, Goto S (2000) KEGG: kyoto encyclopedia of genes and genomes. *Nucleic Acids research* **28**: 27-30.

15. Otto R, Sonnenberg AS, Veldkamp H, Konings WN (1980) Generation of an electrochemical proton gradient in Streptococcus cremoris by lactate efflux. *Proceedings of the National Academy of Sciences of the United States of America* **77**: 5502-5506.

16. ten Brink B, Otto R, Hansen UP, Konings WN (1985) Energy recycling by lactate efflux in growing and nongrowing cells of Streptococcus cremoris. *Journal of Bacteriology* **162**: 383-390.

17. Stouthamer AH (1973) A theoretical study on the amount of ATP required for synthesis of microbial cell material. *Antonie Leeuwenhoek* **39**: 545-565.

18. Kleerebezem R, van Loosdrecht MCM (2010) A Generalized Method for Thermodynamic State Analysis of Environmental Systems. *Critical Reviews in Environmental Science and Technology* **40**: 1-54.

19. Tobajas M, Garcia-calvo E (1999) Determination of biomass yield for growth of Candida utilis on glucose : Black box and metabolic descriptions. *World Journal of Microbiology and Biotechnology* **15**: 431-438.

20. Noor E, Bar-Even A, Flamholz A, Reznik E, Liebermeister W, et al. (2014) Pathway Thermodynamics Highlights Kinetic Obstacles in Central Metabolism. *PLoS Computational Biology* **10**: e1003483.

21. Bar-Even A, Noor E, Flamholz A, Buescher JM, Milo R (2011) Hydrophobicity and Charge Shape Cellular Metabolite Concentrations. *PLoS Computational Biology* **7**: e1002166.

22. Bennett BD, Kimball EH, Gao M, Osterhout R, Dien SJV, et al. (2009) Absolute metabolite concentrations and implied enzyme active site occupancy in Escherichia coli. *Nature Chemical Biology* **5** 593-599.

23. Canelas AB, van Gulik WM, Heijnen JJ (2008) Determination of the cytosolic free NAD/NADH ratio in Saccharomyces cerevisiae under steady-state and highly dynamic conditions. *Biotechnology and Bioengineering* **100**: 734-743.

24. Alberty RA (2006) Biochemical Thermodynamics: Applications of Mathematica. Hoboken: Wiley.

25. Flamholz A, Noor E, Bar-Even A, Milo R (2012) eQuilibrator-the biochemical thermodynamics calculator. *Nucleic Acids Research* **40**: D770-D775.

26. Hanselmann KW (1991) Microbial energetics applied to waste repositories. *Experientia* **47**: 645-687.

27. Diekert G, Wohlfarth G (1994) Metabolism of homocetogens. *Antonie Van Leeuwenhoek* **66**: 209-221.

28. Heijnen JJ (2001) Stoichiometry and kinetics of microbial growth from a thermodynamic perspective. In: Ratledge C, Kristiansen B, editors. Basic biotechnology. Second Edi ed. Cambridge: Cambridge University Press.

29. Stephanopoulos G, Aristidou AA, Nielsen J (1998) Metabolic Engineering: Principles and Methodologies. San Diego, California: Academic Press. 725 p.

30. Maskow T, von Stockar U (2005) How reliable are thermodynamic feasibility statements of biochemical pathways? *Biotechnology and Bioengineering* **92**: 223-230.

List of publications

Journal publications

González-Cabaleiro R, Lema JM, Rodríguez J, Kleerebezem R (2013) Linking thermodynamics and kinetics to assess pathway reversibility in anaerobic bioprocesses. *Energy and Environmental Science* **6**: 3780-3789.

González-Cabaleiro R, Ofiteru ID, Lema JM, Rodríguez J (2015) Microbial catabolic activities are naturally selected by metabolic energy harvest rate. *ISME Journal*. (Accepted).

González-Cabaleiro R, Lema JM, Rodríguez J (2015) Metabolic energy-based modelling explains product yielding in anaerobic mixed culture fermentations. *Plos One*. (Accepted).

Tolutola O, González-Cabaleiro R, Ahmad, F, Rodríguez, J A generalized Excel/C-Simulink architecture for enhanced bioprocess model implementation and simulation. *Water Science and Technology*. (Submitted).

Conference papers

Oral contributions

González-Cabaleiro R, Lema JM, Rodríguez J, Kleerebezem R (June 2013) Linking thermodynamics and kinetics to assess pathway reversibility in anaerobic bioprocesses. 13th World Congress on Anaerobic Digestion. Santiago de Compostela, Spain. *Awarded as best oral contribution of the conference.*

González-Cabaleiro R, Ofiteru ID, Lema JM, Rodríguez J (July 2014) Microbial energy harvesting rate explains the success of specific strains and metabolisms in mixed culture fermentation. IWA International Workshop on Resource Recovery from Wastewater/Bio-solids. Harbin, China.

González-Cabaleiro R, Ofiteru ID, Lema JM, Rodríguez J (November 2014) Can bioenergetics tell us more about microbial ecosystems activity than community identity? Workshop on Engineering and Control of Natural and Synthetic Microbial Communities. Isaac Newton Institute. Cambridge, United Kingdom.

Poster

González-Cabaleiro R, Lema JM, Rodríguez J (June 2013) Generalised acid-base calculation method for aqueous systems. 13th World Congress on Anaerobic Digestion. Santiago de Compostela, Spain.

González-Cabaleiro R, Sharma M, Sarma PM, Lema JM, Rodríguez J (June 2013) Bioelectrochemical reduction of VFAs into alcohols in a microbial electrolysis cell. 13th World Congress on Anaerobic Digestion. Santiago de Compostela, Spain.

USC
UNIVERSIDADE
DE SANTIAGO
DE COMPOSTELA